Connexin43 behaviour in cardiac myocytes exposed to ischaemia and hypoxia

by

Thomas Clarke

A thesis submitted in candidature for the degree of
Philosophiae Doctor

Cardiff University

March 2007

ProQuest LLC
789 East Eisenhower Parkway
P.O. Box 1346
Ann Arbor, MI 48106-1346

Dedicated to Laura

Acknowledgements

I would like to express my great thanks to Prof. W. Howard Evans for his excellent supervision, patience and guidance throughout the course of this study.

I also wish to thank Dr Patricia E. M. Martin, who has been invaluable for her technical expertise in the laboratory and for being a never ending source of ideas and support.

Special thanks to Dr Chris George for the continued advice and helpful discussions regarding molecular biology methodology and thanks to Dr Jørgen Petersen of Zealand Pharma for valuable guidance regarding rotigaptide (ZP123).

A big thank you to everyone in the Wales Heart Research Institute and The Department of Medical Biochemistry, and to those with whom I shared the lab: Karolina, Jon, Raul, Sadie, Dafydd, Oli, Lowri, Vandana and Pete who made my time in Cardiff so enjoyable.

Thanks to the British Heart Foundation for their financial support towards the studies.

A special thanks to Dr Wade and all the doctors and nursing staff for making sure I could write this thesis up after my illness.

Also, Thanks to my dad Roger for helping with the printing of this thesis.

I'd like to thank my family who have always been a great support, and finally a huge thanks to my wife, Laura for her unfailing patience, love and support.

Publications

Thomas C. Clarke, Dafydd Thomas, Jørgen S. Petersen, W. Howard Evans, Patricia E.M. Martin. The antiarrhythmic peptide rotigaptide (ZP123) increases gap junction intercellular communication in cardiac myocytes and HeLa cells expressing connexin 43. British Journal of Pharmacology, 2006 March; 147(5): 486-95.

Thomas C. Clarke, Oliver J.S. Williams, Patricia E.M. Martin & W. Howard Evans. ATP release by cardiac myocytes in ischaemia. Inhibition by a connexin mimetic and enhancement by an antiarrhythmic peptide. American Journal of Physiology, (Submitted December 2006).

Abstracts

Thomas C. Clarke, Oliver J.S. Williams, Patricia E.M. Martin & W. Howard Evans. ATP release by cardiomyocytes in ischaemia or hypoxia and its blockage by connexin hemichannel inhibitors. A key cardiac vasodilation mechanism? Abstract. International Gap Junction Conference, Whistler, Canada (2005).

Thomas C. Clarke, Dafydd Thomas, Patricia E.M. Martin, W. Howard Evans. Effects of an antiarrhythmic drug and ischaemia on cardiac myocyte connexins. Abstract. UK Gap junction meeting, Wales Heart Research Institute (2004).

Summary

In coronary heart disease, the blood supply to the myocardium is insufficient for its needs and leads to cardiac ischaemia, which is often accompanied by the onset of lethal cardiac arrhythmias. Electrical communication between cardiac myocytes occurs across gap junctions located in intercalated discs. Gap junctions are specialised structures of the plasma membrane which facilitate direct and rapid communication between adjacent cells. Connexin 43 (Cx43) is the most widely expressed of the connexin family and is the main connexin in the heart. A cardiac ischaemia model system was developed to study the various aspects of cardiac myocyte biology.

Simulated ischaemia caused neonatal cardiac myocytes to cease synchronous contractions after 3-4 hours and was accompanied by the reversible dephosphorylation of Cx43 after 5 hours. Cx43 dephosphorylation was then reversed by reoxygenating the cells for 30 minutes. In hypoxia the myocytes continued to beat and Cx43 remained phosphorylated.

Rotigaptide, an antiarrhythmic peptide with protracted action, increased intercellular dye transfer in cardiac myocytes, atrial HL-1 cells and HeLa cells expressing Cx43. The communication-modifying effect of rotigaptide was confined to cells expressing Cx43 since the peptide had no effect on dye transfer in HeLa cells expressing Cx32 and Cx26. Rotigaptide had little effect on cell beating rate or Cx43 expression. Phosphorylation of Cx43 in normoxic and ischaemic cells was also unaffected.

Simulated ischaemia induced cardiac myocytes to release a peak of ATP after 80 minutes that was blocked by the connexin mimetic peptide GAP 26 and the gap junction inhibitor 18-α glyccyrrhetinic acid. This suggested that the release of ATP occurred through connexin hemichannels (CxHcs). The rotigaptide analogue AAP10 increased the transient peak of ATP release caused by ischaemia.

The model developed has provided a platform to study the effects of simulated ischaemia on Cx43 dependent functions in the heart. Rotigaptide and AAP10 emerge as novel peptides with therapeutic potential for treating heart arrhythmias.

Contents

Chapter 2: General materials and methods

Abbreviations

18αGA	18-α-glycyrrhetinic acid
18βGA	18-β-glycyrrhetinic acid
μg	microgram
μl	microlitre
μm	micrometer
μM	micromolar
AAP10	Antiarrhythmic peptide 10
ATP	5'-adenosine trisphosphate
bp	base pair(s)
bpm	beats per minute
BSA	bovine serum albumin
C-terminus	carboxyl (COOH) terminus
Ca^{2+}	Calcium ions
cAMP	Cyclic adenosine 5'-monophosphate
cDMEM	complete DMEM
cDNA	complementary DNA
CFP	cyan fluorescent protein
cGMP	Cyclic guanosine 5'-monophosphate
CIAP	calf intestinal alkaline phosphatase
CK1	Creatine kinase 1
CMTX	Charcot Marie Tooth X-linked neuropathy
Cx	connexin
CxHc(s)	connexin hemichannel(s); connexon(s)
Cyclin B/$p34^{cdc2}$	Cyclin B/$p34^{cdc2}$ kinase
Da	Dalton
dH_2O	distilled H_2O
DMEM	Dulbecco's modified Eagles medium
DMSO	dimethyl sulphoxide
DNA	deoxyribonucleic acid
DNase	deoxyribonuclease
dNTP	equimolar mix of dATP, dCTP, dGTP, dTTP
DsRedFP	DsRed fluorescent protein

E. coli	*Escherichia coli*
ECL	enhanced chemilumenescence
EDTA	ethylenediaminetetraaceticacid
EGTA	ethyleneglycolbis-(β-aminoethylether)-N,N,N',N' tetraaceticacid
ER	endoplasmic reticulum
ERGIC	endoplasmic reticulum/Golgi intermediate compartment
ERK	Externally regulated kinases
FACS	Fluorescence-activated cell sorter
Fmoc	9-fluorenylmethyl carbamate
FRET	Fluorescence resonance energy transfer
FSH	Follicle stimulating hormone
GFP	green fluorescent protein
GJ	gap junctions
hr(s)	hour(s)
Hepes	N-2 hydroxyethylpiperazine-N'-2-ethanesulphonic acid
HPLC	High pressure liquid chromatography
HRP	horse-radish peroxidase
Ig	immunoglobulin
IP_3	Inositol 1,4,5-triphosphate
kDa	kilodalton
LB	Luria-Bertani medium
LY	Lucifer yellow
M	molar
MALDI-TOF	Matrix-assisted laser desorption/ionisation-time of flight
MCS	multiple cloning site
mg	milligram(s)
min(s)	minute(s)
ml	millilitre(s)
mM	millimolar
MAP-K	Mitogen activated protein kinase
mRNA	messenger RNA
nm	nonometre(s)
nM	nanomolar

NP	Non-phosphorylated
N-terminus	amino (NH_2) terminus
OD	optical density
ODDD	oculodentodigital dysplasia
$Pp60^{src}$	Cytoplasmic tyrosine-specific protein kinase
P	Phosphorylated
PAGE	polyacrylamide gel electrophoresis
PBS	phosphate-buffered saline
PCR	polymerase chain reaction
PDI	protein disulphide isomerase
PKA	Protein kinase A (cAMP-dependant kinase)
PKC	Protein kinase C
PKG	Protein kinase G
PM	plasma membrane
pS	picoSimens
RI	refractive index
RNA	ribonucleic acid
Rotigaptide	Zealand Pharma compound 123 (Rotigaptide); an antiarrhythmic peptide
rpm	revolutions per minute
SD	standard deviation
SDS	sodium dodecyl sulphate
sec(s)	second(s)
SEM	standard error of the mean
Taq	*Thermus aquaticus*
TAE	Tris-acetate-EDTA buffer
TBS	Tris buffered saline
TBS-T	Tris buffered saline with Tween-20
TCA	trichloroacetic acid
TEA	triethanolamine
TEMED	N,N,N',N', tetramethylethylethylenediamine
Tm	melting temperature
TM	transmembrane domain
TPA	(12-tetradecanoylphorbol-13-acetate)

Tris	tris(hydroxymethyl)aminomethane
UV	ultraviolet
V	volt
v/v	volume to volume
WT	wild-type
w/v	weight to volume
YFP	yellow fluorescent protein
ZP123	see Rotigaptide

Chapter 1

General Introduction

1.1 Intercellular communication

There has always been the question of how complex organisms coordinate the activity of the many different cells constituting tissues and organs. The release of chemical factors and hormones provided an explanation for some of the observed cooperative behaviour of cells. However, it is evident that cells have mechanisms that allow direct communication with their neighbours. Gap junctions ensure the intercellular communication that operates at regions of cell contact and adhesion. The gap junction is a specialised structure of the plasma membrane which facilitates direct and rapid communication between adjacent cells. These junctions are ubiquitous in vertebrates and perform a variety of functions in different tissues. Gap junctions provide a regulated pathway linking the cytoplasms of attached cells, ensuring integration of metabolic activities and creating a network of directly communicating cell assemblies. Gap junctions can facilitate electrical coupling, calcium wave spread or the passage of small signalling or biochemical molecules.

1.1.1 The structure of gap junctions

Gap junctions were first described as plasma membrane areas that were closely apposed with a distinct 2-4 nm gap (Revel & Karnovsky 1967). The presence of gap junctions in the form of hexagonally packed subunits was first shown between the plasma membranes of Mauthner cells of goldfish brain (Robertson et al., 1963). Similar structures were found in rat liver plasma membrane by thin-section electron microscopy (Benedetti & Emmelot 1965; Revel & Karnovsky 1967). Revel and Karnovsky saw that their objects of interest were "cell junctions in which there is a minute gap between the external leaflets." They showed that these junctions were present in non-neuronal tissues such as liver and heart. Soon afterwards, they

published an abstract in which they first referred to the structures as gap junctions, an oxymoron that has stuck ever since.

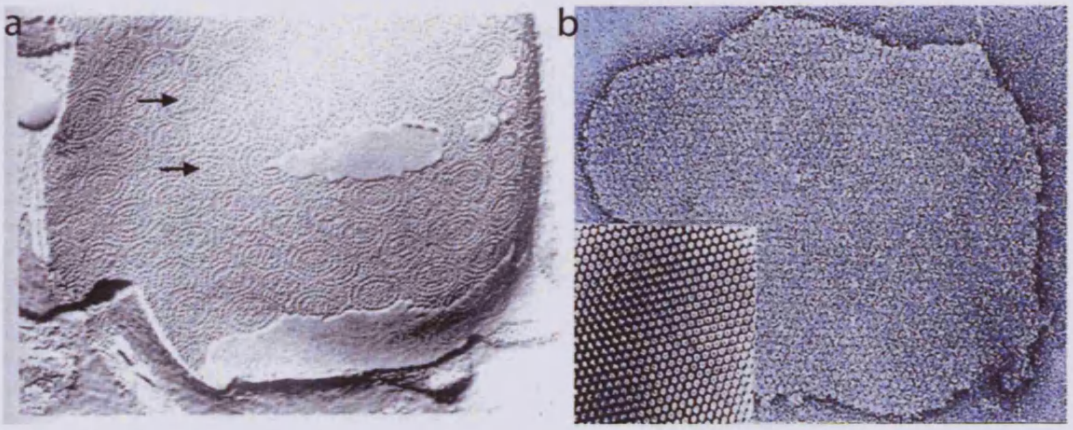

Figure 1.1: Electron micrographs of gap junctions
a) Electron micrograph of rat heart gap junctions after splitting through the bilayer by freeze-fracture. The concentric flower-like depressions are thought to correspond to connexons (hemichannels). Magnification x 117 000. Reproduced from Shibata, Kyushu University, Japan.
b) Gap junction plaque isolated from rat liver, viewed en-face by electron microscopy after negative staining with sodium silicatungstate showing the characteristic hexagonal lattice of subunits. The inset illustrates an unstained junction optically filtered image that shows the crystalline hexameric subunits. Magnification x 220 000. Reproduced from unpublished data WH Evans.

Later studies by Goodenough & Revel (1970) used negative staining and freeze-fracture electron microscopy to show that these structures comprised packed arrays of numerous intra-membrane particles. It was confirmed by X-ray diffraction techniques that these particles were comprised of a pair of apposed hexameric protein structures (one provided by each apposing cell). These component structures of gap junctions were subsequently known as connexons and later CxHcs (the term used in this thesis), and demonstrated a tilt of up to 20°-30° (Makowski et al., 1977). Gap junctions are formed by protein sub-units that have subsequently been named connexins (Cx) (Beyer et al., 1987). When gap junctions form the CxHcs interlock with apposing CxHcs from the adjacent cell as they are skewed by 10° (Baker et al., 1985).

Electron crystallography techniques have produced a slightly higher resolution of the gap junction structure (Perkins et al., 1998). It was later shown that each CxHc tilts at 30° thereby allowing interdigitation and docking of the two apposed connexons when gap junctions form. Electron cryomicroscopy has been employed to examine a recombinant form of Cx43 with the intracellular carboxyl terminus removed (Unger et al., 1997) and it appears that this truncation does not modify substantially channel structure (Sosinsky & Nicholson 2005). These studies have produced a widely accepted three-dimensional structure (Figure 1.2) with a 7Å resolution that demonstrated that the gap junction is comprised of interlocking CxHcs that are tilted and skewed within the plasma membrane as previously shown and arranged around a central pore diameter present in each CxHc. The central pore is predominantly formed from alpha helix structures contributed in the main by the third transmembrane domain of the constituent connexin (Unger et al., 1997). Other approaches such as cysteine scanning mutagenesis revealed that parts of the first transmembrane domain are accessible from the extracellular space and therefore are part of the channel pore lining, (Zhou et al., 1997) and also the flux limiting or narrow part of the channel. (Hu & Dahl 1999; Fleishman et al., 2006). Alterations in calcium concentrations have been shown to induce further tilting of the connexin subunits within the connexon; indeed, such a conformational change was proposed to alter channel permeability (Unwin & Ennis 1984).

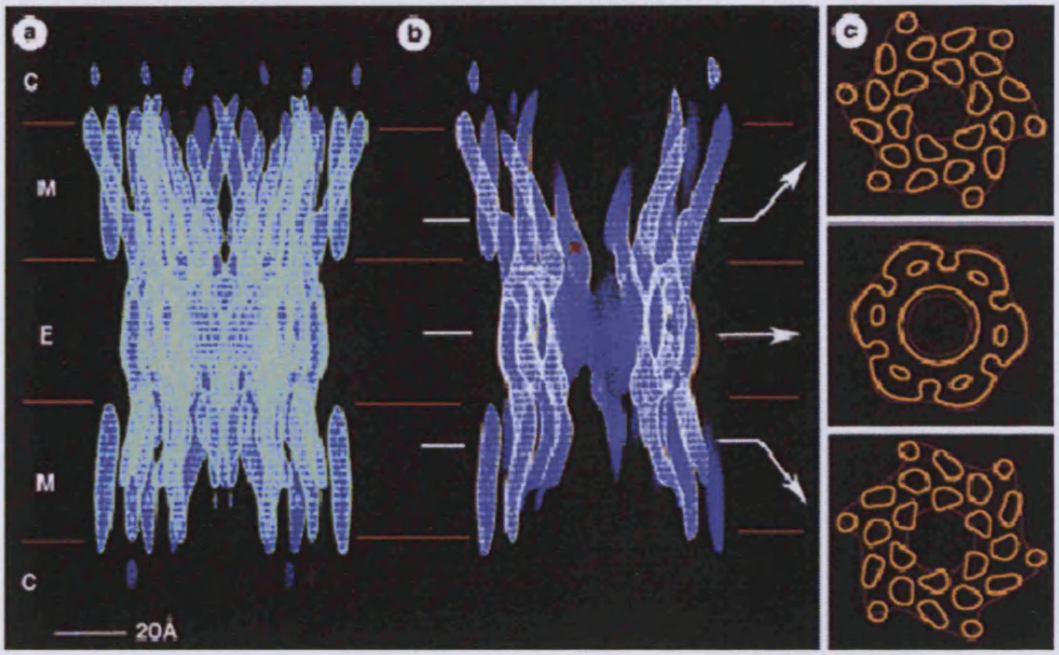

Figure 1.2: A 3D density map showing the molecular organization of a recombinant gap junction channel.
a) A full side view of the channel is shown, and (b) the density has been cropped to show the channel interior. The approximate boundaries for the membrane bilayers "M", extracellular gap "E", and the cytoplasmic space "C" are indicated. The red asterisk in (b) marks the narrowest part of the channel where the aqueous pore is ~15Å in diameter. The white arrows identify the locations of the cross sections shown in (c), are parallel to the membrane bilayers. The red contours indicate data to a resolution of 15 Å and define the boundary of the connexon. The yellow contours include data to a resolution of 7.5 Å. The roughly circular shape of these contours within the hydrophobic region of the bilayers is consistent with 24 transmembrane helices per connexon. Reproduced from Unger et al., 1999.

1.1.2 Connexin protein structure and topography

Hydropathy plots of connexin linear sequences suggest the presence of four regions with high hydrophobicity usually signifying membrane spanning domains, and hydrophilic regions forming two extracellular loops and the carboxyl tail (Figure 1.3) (Paul 1986). Circular dichroism studies suggested that the protein is 60% alpha-helix (Cascio et al., 1990; Unger et al., 1997). Proteolytic studies and application of a range of site-specific anti-peptide antibodies confirmed that the amino and carboxyl termini of connexins are located intracellularly (Milks et al., 1988; Zimmer et al., 1987). The

two extracellular loops contain three cysteine residues in a characteristically conserved sequence (CX_6CX_5C in E1; CX_4CX_5C in E2), with perhaps just one exception to these sequences in Cx31 (Hoh et al., 1991). These cysteine residues form intramolecular disulphide bonds linking the two extracellular loops of connexin32 (Rahman & Evans 1991). Mutations in these crucial cysteine-flanking regions generally abolish the ability of the connexin to form functional gap junction channels (Foote et al., 1998). The intracellular amino terminus is similar in length in all connexins. The major difference between all connexins is in the intracellular loop and carboxyl tail with both regions in some connexins varying in length and/or sequence.

Twenty or more connexin isoforms have been identified by genomic screening especially in humans and mice (Willecke et al., 2002). As the human and mouse genomes are now known, it seems unlikely that many new mammalian connexin isoforms will be discovered. The connexin isoforms show approximately 40% sequence homology with the main amino acid differences in the C-terminal tail.

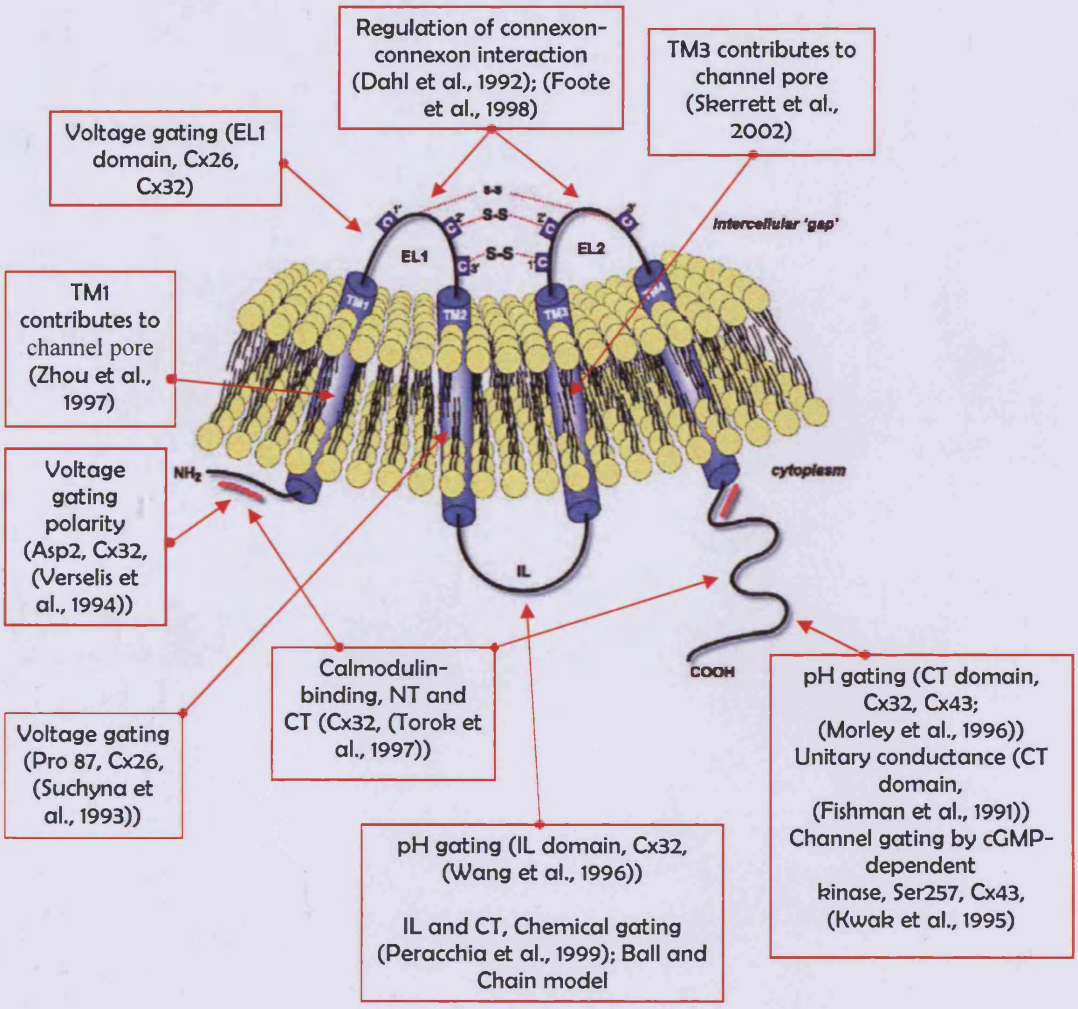

Figure 1.3: Topological representation of connexin in the membrane.
Hydropathy plots predict four membrane spanning regions (M1-M4), two extracellular loops (EL1 and EL2) and three cytoplasmic portions, the amino-terminal and carboxyl-terminal domains and central intracellular loop (IL). The putative role of different domains is inferred from the results of structure/function studies with specific point mutations and chimeras with swapped domains.

Gap junction channels made up from different connexin isoforms (Figure 1.4) have distinct properties with differing conductance, differing gating properties and different expression levels in various cell types (Elfgang et al., 1995). Combined with the structural diversity, it suggests that gap junction channels fulfil and coordinate the different roles required for programmes of cellular differentiation (Willecke et al., 2002).

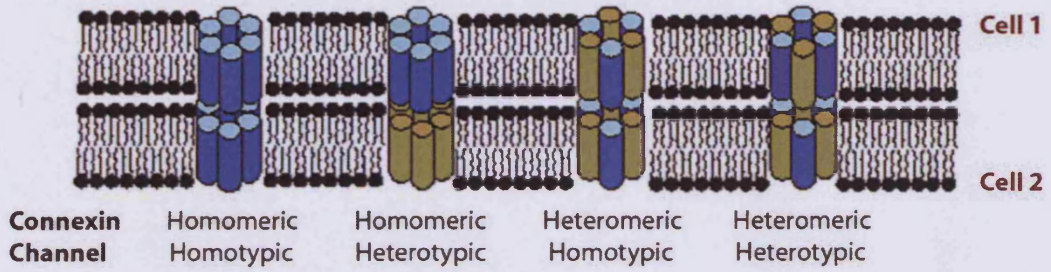

Figure 1.4: Diagram illustrating possible arrangements of connexins in gap junction channels.
Six connexin subunits (blue or green) can form connexons in various configurations. Connexons may be homomeric (composed of six identical subunits) or heteromeric (composed of more than one connexin species). CxHcs from neighbouring cells associate end to end to form a gap junction channel. The channel may be homotypic (if connexons are identical) or heterotypic (if two connexons are different). For example, a cell expressing two types of connexins allows 196 different combinations resulting in a possible variation in gap junction channel selectivity.

1.1.3 Connexin protein nomenclature

An early nomenclature used to describe gap junctions was based on their functional and evolutionary characteristics with connexins described as either α, β or γ. Also at this time, a nomenclature based on molecular weight was also widely used with each connexin described by its apparent or predicted molecular weight. For example Cx32 has a predicted molecular weight from the cDNA of approximately 32kD. Minor variation in apparent molecular weight may occur when the proteins are run on SDS gels. However, connexins in different species are functionally and biologically similar but have slightly different molecular mass, due for example to conservative amino acid substitutions. For example, mouse Cx32 is 32,003Da and the human equivalent is 32,024Da. Given these slight variations and the increasing laboratory use of mouse genetic models, many have argued that the classification should be mainly based on mouse proteins. However, others argued in favour of a purely biochemical classification or one based on the human connexin proteins. A group of

cell biologists in the gap junction field has accepted a nomenclature that reaches a compromise. In this nomenclature the name of the connexin is made up of a prefix letter denoting the species, for example "m" or "h" for mouse or human respectively. This is followed by "Cx" and then by the molecular weight in kDa. For example hCx43 is human connexin 43 and in the heart, mCx30.2 is homologous to hCx31.9 (Bukauskas et al., 2006). There is also a further nomenclature based on the genetics of connexins and is known as the "Gja/Gjb" system and has been adopted by the NCBI (National Centre for Biotechnology Information), but it is not so widely used as the "Cx" nomenclature outside the genetic community. Using the genetic nomenclature Cx43 is GJA1, Cx32 is GJB1 and Cx26 is GJB2.

1.1.4 The Functions of Gap junctions

Gap junctions facilitate electrical communication between cells, as demonstrated in the cardiovascular and nervous system. Gap junctions also allow for the transmission of biochemical messengers in both excitable and non-excitable tissues. For example, using a model in which cardiac myocytes were coupled to ovarian granulosa cells, it was concluded that cAMP diffused across the gap junction (Lawrence et al., 1978). To establish the extent to which cells are functionally coupled and therefore biochemically connected by gap junctions, the technique of dye transfer has been used extensively (Elfgang et al., 1995; Martin et al., 2001). This involves the injection of small fluorescent dyes, especially Lucifer yellow into cells to determine if the dye passes into the neighbouring cells (Stewart 1981). Dye transfer studies have been used to determine any size or charge discrimination of the channel illustrating that molecules within a range of 0.2-1.0kD can pass through the gap junction channel. These investigations were performed mainly on HeLa cells expressing gap junction

channels constructed from various recombinant connexin isoforms, mainly Cx43, Cx32 and Cx26 (Cao et al., 1998; Elfgang et al., 1995; Nicholson et al., 2000).

Fluorescent calcium sensitive dyes in conjunction with ever advancing live-cell imaging technology have revealed that gap junctions have a more direct intercellular signalling role. Intercellular signalling, reflected by changes in intracellular calcium levels, is demonstrated by rapid and direct propagation to neighbouring cells via gap junction channels (Giaume & Venance 1998; Sanderson et al., 1994). Confluent monolayers of HeLa cells expressing recombinant connexins labelled with GFP (green fluorescent protein) were studied to show increases in intracellular calcium levels and especially Ca^{2+} wave transmission by gap junctions (Figure 1.5) (Paemeleire et al., 2000). Intercellular calcium wave propagation can be initiated by chemical, electrical and mechanical stimulation (Isakson et al., 2001). The use of caged IP_3 has also provided investigators with a non-invasive route to induce calcium wave changes resulting in their propagation through gap junctions (Leybaert & Sanderson 2001). In another study by Paemeleire et al. (2000), the calcium distribution was monitored following its release from the intracellular stores in HeLa cells expressing GFP labelled connexins. The calcium wave approaches the gap junction plaque and then instantly appears from the same fluorescently labelled gap junction plaque in the neighbouring cell, as shown in figure 1.5 (panels B2-B4) (Paemeleire et al., 2000). It has been proposed that calcium actually passes through the gap junction (Saez et al., 1989). However, on the contrary, it has long been accepted that high levels of calcium cause gap junctions to close (Rose & Loewenstein 1976). Alternatively, it has been suggested that IP_3 passes across gap

junctions, as in epithelial cells, with IP_3 subsequently inducing the spread of calcium waves (Boitano et al., 1992).

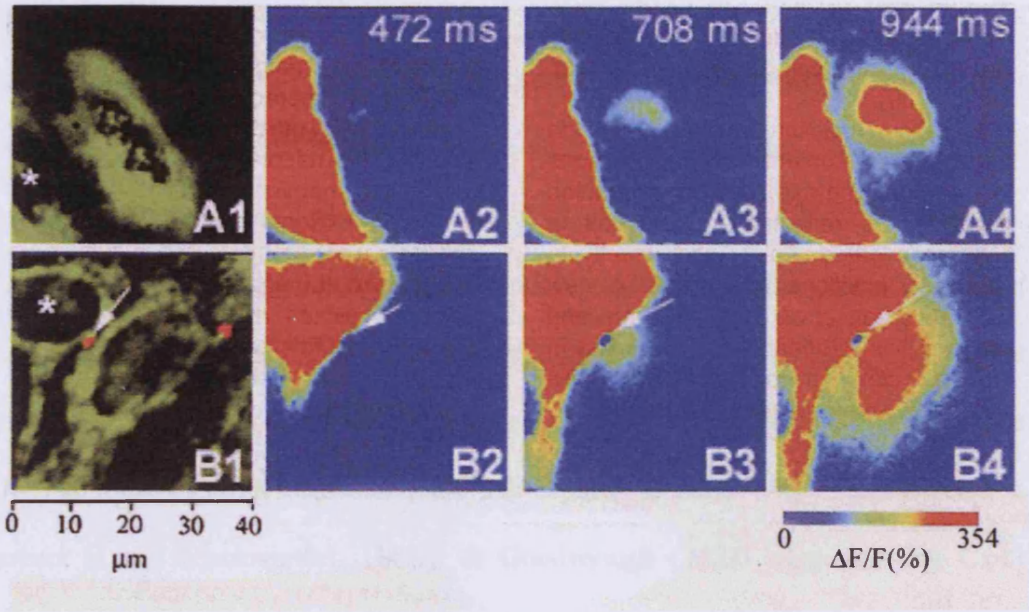

Figure 1.5: Intercellular calcium signalling
Calcium Waves transmitted between contacting HeLa cells by two routes; In A, the spread of the calcium wave in HeLa cells lacking gap junctions occurs by the release of ATP, thus providing an extracellular route. In B, the HeLa cells express fluorescent Cx43 GFP (white arrows) and the spread of the calcium wave occurs via a fluorescent gap junction to a neighbouring cell. This occurred in the presence of apyrase to prevent ATP acting as a mediator. A1 and B1 show the distribution of the endoplasmic reticulum using ER-tracker fluorescence (green). Changes of fluo-3 fluorescence at 488nm excitation, corresponding to changes in [Ca2+]I, are represented in pseudocolour, according to the scale bar. Reproduced from Evans and Martin, 2002.

1.1.5 The biogenesis of gap junctions

The majority of membrane proteins have a half life of around 24 hours. In contrast, connexin proteins have rapid turnovers with half lives of 2-5 hours (Laird 2006). Connexin turnover and trafficking can be influenced by several factors, including cAMP and growth factors (Paulson et al., 2000). Biogenesis of a functional gap junction unit involves a series of events.

CxHcs are delivered to the plasma membrane by vesicular trafficking from the endoplasmic reticulum via the Golgi; the classical secretory pathway. Monomeric connexins are synthesized by membrane bound ribosomes and inserted into the endoplasmic reticulum, achieving the correct membrane topology. Vesicular trafficking then delivers the protein to the Golgi apparatus. However, unlike most other membrane proteins, connexins are not glycosylated during transit through the Golgi owing to the luminal topographical orientation of the amino acid residues that are often glycosylated. The oligomerisation of connexins into hexameric CxHcs proceeds stepwise via association into dimeric and tetrameric connexin intermediates (Ahmad et al., 2001). However, the sub-cellular location where oligomerisation occurs is still controversial. Musil & Goodenough (1993) suggested that Cx43 oligomerisation was delayed until the proteins had entered the distal regions of the Golgi, a result that contradicted the traditional view that membrane proteins are folded and oligomerised once inserted into the ER (Hurtley & Helenius 1989). However, more recent reports have shown that connexin oligomerisation is a sequential event, starting in the ER or the endoplasmic-Golgi-intermediate compartment (ERGIC) and has been completed by arrival at the Golgi (Diez et al., 1999; Falk et al., 1997; George et al., 1999).

A further important aspect of gap junction biogenesis is the evidence that more than one pathway for the delivery of specific connexins to the plasma membrane may exist. An alternative pathway for Cx26 gap junctions has been described suggesting the existence of a Golgi independent mechanism of biogenesis. Brefeldin A, a fungal derived agent that disrupts the Golgi, inhibited Cx32 and Cx43 trafficking to gap junctions but not Cx26 (Martin et al., 2001). This alternative pathway can also be

induced by lowering the temperature of the cell cultures by 15°C (George et al., 1999). By contrast, Cx26 trafficking was blocked by nocodazole, a drug that disassembles microtubules, whereas Cx32 and Cx43 trafficking were relatively unaffected (Martin et al., 2001). Cx43 interacts with tubulin but the short C-terminus of Cx26 precludes this interaction (Giepmans 2004). Earlier studies using subcellular fractionation approaches to separate the membrane components of the secretory pathway had also suggested that Cx26 had more than one trafficking pathway (Diez et al., 1999; George et al., 1998). The first transmembrane domain has emerged as having an important role in determining the trafficking route and post translational insertion into membranes of Cx26 and Cx32. A single site amino acid mutation was introduced into the first transmembrane domain, but not the fourth transmembrane domain, in Cx32 so that it resembled amino acid sequences in Cx26. This single site mutation resulted in the post translational behaviour of Cx26 as well as Brefeldin A insensitivity being conferred to the modified Cx32 (Martin et al., 2001).

The use of fluorescent reporter tags attached to the carboxyl tail of connexins has enabled the intracellular trafficking and life cycle of gap junctions to be studied in live cells and in real time. Despite approximately doubling the molecular mass of the protein, the addition of fluorescent proteins to connexins has been shown not to alter trafficking characteristics significantly (Bukauskas et al., 2000; Martin et al., 1998; Paemeleire et al., 2000). The Golgi is an important transit organelle for the intracellular movement of Cx43 as its disruption by Brefeldin A arrested the delivery to the plasma membrane (George et al., 1999; Laird et al., 1995). Connexin trafficking is also influenced in various but often critical ways by the cytoskeletal network (Giepmans et al., 2001; Johnson et al., 2002; Martin et al., 2001). Connexins

are trafficked in highly mobile vesicles of 0.5μm diameter to the plasma membrane (Jordan et al., 1999; Lauf et al., 2002). CxHcs are inserted over a large area of the plasma membrane and diffuse laterally, attaching as CxHcs to the periphery of gap junction plaques (Gaietta et al., 2002).

The assembly and degradation of gap junctions is a dynamic process, with new channels added continuously to the edge of the gap junction plaque and "older" paired CxHcs are removed from central regions of the plaque (Gaietta et al., 2002; Lauf et al., 2002). The breakdown of connexins occurs by lysosomal or proteosomal degradation, pathways which are ubiquitin-dependent (Laing et al., 1997; Rutz & Hulser 2001). Endosomes have been implicated in the transfer of connexins from the plasma membrane to lysosomes (Pol et al., 1997), but there is also evidence suggesting that gap junction plaques can be internalised in their entirety by autophagy (Jordan et al., 2001).

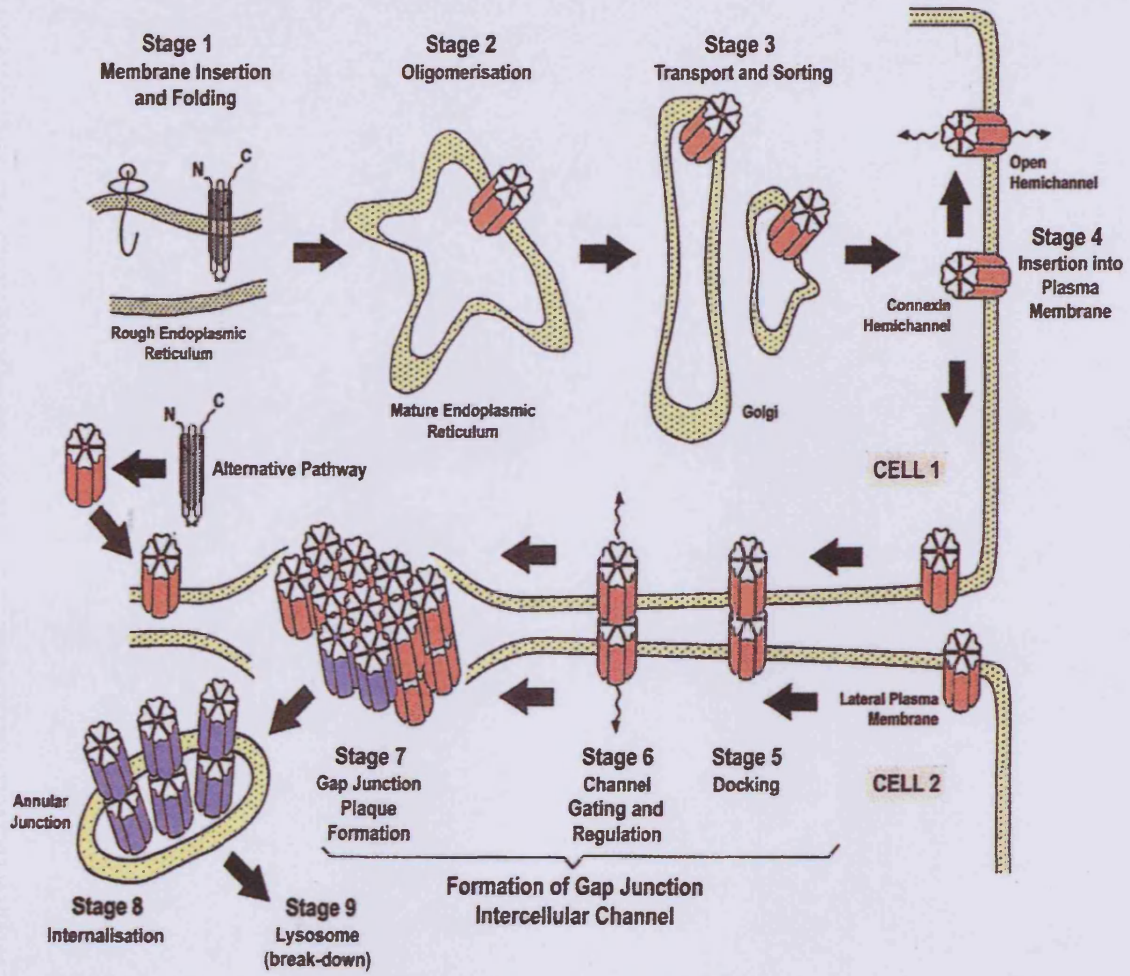

Figure 1.6: The biogenesis and degradation of gap junctions.
Diagrammatic representation of the classical biogenetic pathway by which connexins inserted into the rough endoplasmic reticulum form CxHcs that dock at specific parts of the plasma membrane to form gap junction channels. Portions from the centre of gap junction plaques (blue units) form autophagosomes consisting of paired CxHcs packed into vesicles sometimes referred to as annular gap junctions. Much remains to be learnt about the mechanism resulting in the rapid breakdown of gap junctions. Reproduced from Evans et al., 2006.

1.1.6 Gap junction channel gating

Gap junction channels are gated by pH (a decrease) (Figure 1.7) (Ek-Vitorin et al., 1996) and voltage (a change in potential difference between cells) (Qu & Dahl 2002). Connexins with short intracellular carboxyl tails, e.g. Cx26, or mutant connexins with truncated tails, do not display pH gating, but their gating is restored by addition of peptide sequences from the carboxyl tail projecting into the cell cytoplasm (Morley et

al., 1996). These observations suggest that the mechanism responsible for pH gating is an intramolecular interaction between carboxyl tail and intracellular loop, i.e. a "ball and chain" mechanism. Voltage gating appears to occur via a different gating mechanism and is thought to involve the following regions: the amino terminus, the first transmembrane domain and the first extracellular loop (Pfahnl & Dahl 1998; Verselis et al., 1994). Voltage gating has been proposed to change the selectivity of channels to allow propagation of electrical impulses but preventing larger signalling molecules proceeding through the channel (Qu & Dahl 2002). This mechanism allows electrical synchronisation of cells, while restricting the flow of second messengers and metabolites (such as ATP). This mechanism of gating could be utilised to prevent the loss of important molecules (i.e. ATP) from healthy cells to adjacent damaged cells, such as may occur during ischaemia and reperfusion.

An additional mechanism for regulating the permeability or selectivity of gap junctions could be the formation heteromeric or heterotypic channels composed of different connexin isoforms (Figure 1.4). Cx40 and Cx43 heteromeric channels display a variety of permeability traits whilst heterotypic channels exhibit different conductance states and dye permeability depending on the composition of each CxHc unit (Cottrell & Burt 2001; Cottrell et al., 2002). The permeability of heterotypic Cx40-Cx43 channels show an intermediate permeability rather than an unique permeability (Valiunas et al., 2002).

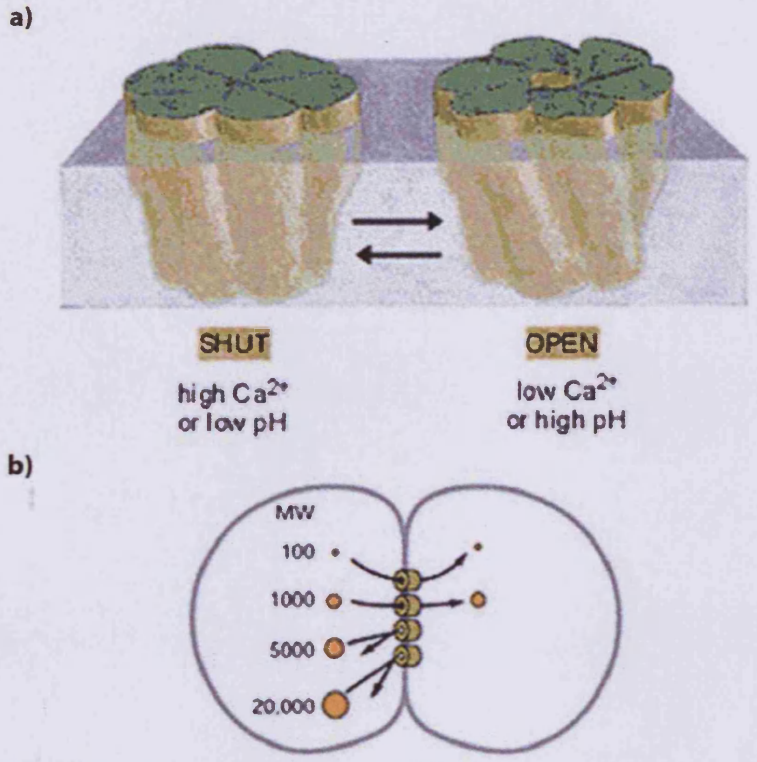

Figure 1.7: Channel gating and permeability
a) A representation of the conformational change in the channel leading to closure by reduction in the central pore, and b) a diagram illustrating size selectivity of connexin-based channels allowing permeation by molecules up to a molecular weight of 1000Da.

1.1.7 Pannexins and Innexins

The pannexins and innexins are two families of proteins that are also capable of forming gap junction channels. The pannexins share little homology to connexins and are expressed in vertebrates as well as invertebrates (Litvin et al., 2006). To date, three pannexin proteins have been identified in rodents and humans: Panx1, Panx2 and Panx3 (Baranova et al., 2004). Panx1 is expressed in multiple organs of rodents and humans, including the nervous system. Panx2 expression is observed in many organ systems of mice and rats but is limited to the nervous system in humans, while Panx3 has been found in the skin of rats (Bruzzone et al., 2003). Channels constructed of pannexin proteins share many similarities with connexin channels, such

as the propagation of Ca^{2+} waves by glial cells and the synchronisation of hippocampal and cortex brain cells (Litvin et al., 2006).

The innexins are the gap junction forming proteins of invertebrates and were originally characterized as "gap junction communication channels" in the arthropod (Adams et al., 2000) and the nematode *Caenorhabditis elegans* (C.elegans sequencing consortium 1998). More recently, innexin homologues have been identified in representatives of the other major invertebrate phyla (Phelan 2005). The Drosophila fly genome currently has 8 identified innexin genes (Stebbings et al., 2002) and the worm has 25 genes (Starich et al., 2001).

1.2 Connexin hemichannels (CxHcs)

CxHcs (also referred to as connexons) were long thought to be mere structural intermediates of gap junctions, but have now emerged as channels by which cells can regulate the release of various signalling molecules (John et al., 2003; Stout et al., 2004). Studies on lens Cx46 expressed in *Xenopus* oocytes revealed that CxHcs had high unitary conductance (300pS) and a large permeability, especially to cations. CxHcs were closed during high external H^+ and Ca^{2+} levels, but were opened by low extracellular Ca^{2+} (Ebihara et al., 1999; Ebihara & Steiner 1993). Another study on horizontal cell dendrites of skate retina showed that CxHc (constructed of Cx35) regulate transmitter binding to cone receptors (Malchow et al., 1993). Further research has examined other vertebrate connexins, including zebra-fish Cx35, chicken Cx56 and Cx45.6, and showed that these CxHcs also opened when exposed to low-Ca^{2+} or Mg^{2+} (Ebihara et al., 1999; 2003; Puljung et al., 2004; Ripps et al., 2004; Srinivas et al., 2005; Valiunas et al., 2000; 2004). Small fluorescent dyes (e.g.

propidium iodide) have also been used to detect open CxHcs since they are taken up by these channels (De Vuyst et al., 2006; Li et al., 1996).

CxHcs are functionally altered by genetic mutations. For example, mutations in the C-terminus of Cx32 that are linked to CMTX (Charcot-Marie-Tooth X-linked disease), caused the dysfunctional CxHcs to become leaky (Castro et al., 1999; Liang et al., 2005). Cx43Hcs containing six different single amino acid mutations produced changes in the entry of dye through the channels, and are linked to oculodentodigital dysplasia – a development disorder with craniofacial and limb disorders (Flenniken et al., 2005; Lai et al., 2006). These mutations are discussed in greater detail in section 1.5.

1.2.1 CxHc properties

Many of the properties of CxHcs are similar to those of entire gap junction channels, especially their permeabilities (Harris 2001; Verselis et al., 2000). However, there are slight structural differences to the extracellular domains of free CxHcs, as revealed by atomic-force microscopy (Thimm et al., 2005). Other reports suggest that CxHcs are arranged in a less ordered fashion within the cell membrane and partition into lipid rafts (Locke et al., 2005; Tillman & Cascio 2003).

In physiological environments, CxHc are maintained in a closed conformation (Figure 1.8d), but when extracellular Ca^{2+} concentration is lowered, they change to an open conformation with pore diameter increasing from 1.8 (closed) to 2.8nm (open) (Thimm et al., 2005). It has been suggested that the hydrophobic extracellular domains are important regions in the regulation of the Ca^{2+}-dependent conformational

changes that are illustrated diagrammatically in Figure 1.8 (Gomez-Hernandez et al., 2003). Owing to the easier accessibility of CxHcs relative to gap junctions, it has been possible to study closely the nature of the amino acid sequence lining the channels, by techniques such as SCAM (substitute cysteine accessibility mutagenesis) (Kronengold et al., 2003). Current thinking is that the first extracellular loop contributes to the extracellular end of the CxHc pore, the second transmembrane domain to the transmembrane part of the channel and the amino terminal and/or part of the intracellular loop, at the cytoplasmic end of the pore (Gomez-Hernandez et al., 2003; Kronengold et al., 2003). A Ca^{2+} binding site has also been detected on the extracellular aspect of CxHcs (Gomez-Hernandez et al., 2003).

1.2.2 Regulation of CxHcs

CxHcs located in the plasma membrane are opened by specific stimuli, such as low extracellular Ca^{2+}, membrane depolarisation, mechanical membrane stress and metabolic inhibition (Evans et al., 2006). It has been observed universally that CxHcs are modulated by extracellular Ca^{2+}, as zero or low extracellular Ca^{2+} environments have been used as a common experimental strategy to activate their opening (Contreras et al., 2003; Quist et al., 2000). Additional studies have revealed that other extracellular ions also influence CxHc opening, such as Mg^{2+}, non physiological bivalent ions like Ba^{2+} and Sr^{2+} (Contreras et al., 2003), univalent cations such as Na^{+} (Kondo et al., 2000; Srinivas et al., 2006) and anions like Cl^{-} (Kondo et al., 2000). Depolarisation is another stimulus that opens CxHcs, with cells being depolarised by several methods including point mechanical stimulation (Bao et al., 2004; Romanello et al., 2003), sheer stress (Cherian et al., 2005), negative pressure by patch pipette (Bao et al., 2004) and changes in osmolarity (Quist et al., 2000). CxHcs in heart cells

must have regulation mechanism to limit the passage of Ca^{2+} when the cells are depolarised during the heart beat. CxHcs composed of Cx26, Cx30, Cx32, Cx35, Cx37, Cx38, Cx43, Cx44, Cx46, Cx50 and Cx56 open when exposed to one or more of the several experimental conditions mentioned above (Harris 2001; Saez et al., 2005). CxHcs can be influenced by additional factors, such as pH (intra- and extra-cellular) (Harris 2001), redox status (Contreras et al., 2002) and phosphorylation status (King & Lampe 2005; Solan & Lampe 2005). It has been demonstrated that ATP is released by cells through CxHcs (Cotrina et al., 1998; Gomes et al., 2005; Stout et al., 2002). This phenomenon is discussed in greater detail in chapter 5 of this thesis, especially its specific blockage by connexin mimetic peptides. Further studies have revealed that other small metabolites that can function as biochemical messengers also pass through CxHcs, such as glutamate released by astrocytes (Parpura et al., 2004; Ye et al., 2003), prostaglandins released from osteoclasts (Bruzzone et al., 2001; Cherian et al., 2005) and NAD+ released by fibroblasts (Bruzzone et al., 2001).

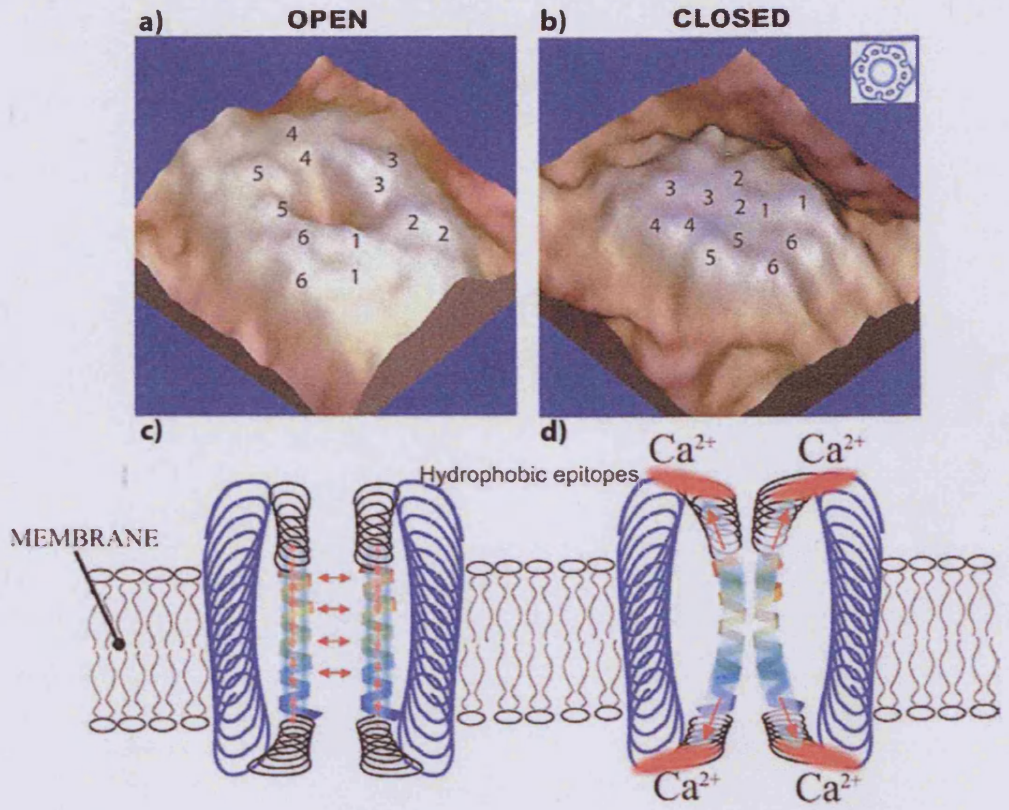

Figure 1.8: Diagram illustrating the CxHc Ca^{2+}-sensitive gating of CxHcs analysed by atomic-force microscopy.
The top two images show high resolution three-dimensional height images of the extracellular face of (a) an open CxHc, imaged in nominally Ca^{2+}-free buffer and (b) a closed CxHc imaged in the presence of 1.8 mM [Ca^{2+}]. The two putative extracellular loops for each of the six connexin subunits forming a hemichannel are denoted by the numbers *1–6*. *The model shown in c* and *d* is a mechanism of channel closing; when the tertiary structure of the open connexon (*c*) is unbalanced by the Ca^{2+} absorbed on the extramembranous surface, the refolding of the E1 and E2 loops hides the hydrophobic domains and at the same time closes the channel (d). Modified from Thimms et al., 2005 and Evans et al., 2006.

1.3 Gap junction regulation by phosphorylation

Connexins are phosphorylated by multiple protein kinases, and dephosphorylated by phosphatases, and these post-translational modifications form a widespread mechanism for functional modification of connexin based channels. Phosphorylation of connexin channels leads to a broad range of effects, including stabilisation of open or closed states as well as changing the kinetics of the transition between states.

The majority of connexins are phosphoproteins, with Cx31, Cx32, Cx37, Cx40, Cx43, Cx45, Cx46, Cx50 and Cx56 shown to be subject to phosphorylation by changes in electrophorectic mobility and ^{32}P incorporation (Lampe & Lau 2000; Saez et al., 1998). The only connexin that is not phosphorylated is Cx26 (Traub et al., 1989), which is most likely due to the shortness of its C-terminus, leaving only a few amino acids free to interact with cytoplasmic signalling elements. Since Cx26 is assembled into functional gap junction channels, it is clear that phosphorylation is not a general prerequisite for channel function. Indeed, Cx43 with truncated carboxyl tails has been shown to form functional channels (Fishman et al., 1991; George et al., 1999), and restoration of the carboxyl tail resulted in the return of certain functional modifications, including v-Src tyrosine kinase activity and cytoplasmic acidification (Calero et al., 1998). In summary, the carboxyl tail thus appears to be the primary target for phosphorylation of connexins.

Activation of cAMP-dependent protein kinase (PKA) is associated with an increase in gap-junctional conductance in several cell types that express Cx32 and Cx40 (Chanson et al., 1996; van Rijen et al., 2000). Cx32 is phosphorylated by PKA and protein kinase C (PKC) at S233 (Saez et al., 1990). Epidermal growth factor and Ca^{2+}/calmodulin-dependent kinase II both phosphorylate Cx32 (Diez et al., 1998; Saez et al., 1990). Phosphorylation of Cx45 has been shown to modulate channel conductance (van Veen et al., 2000). In another study, the last 26 amino acids (involving nine serine residues) were either deleted or substituted (by glycine or alanine), resulted in a 90% reduction in phosphorylation and loss of communication between cells (Hertlein et al., 1998). In the vertebrate lens, Cx46 and Cx50 gap

junctions have been demonstrated to change communication properties with changes in phosphorylation status that is modulated by various protein kinases including casein kinase I and II, and PKC (Berthoud et al., 2000; Cheng & Louis 2001; Yin et al., 2001).

1.3.1 Cx43 Phosphorylation

Cx43 has an extended (156 amino acid) carboxyl tail projecting into the cytoplasm that undergoes extensive phosphorylation during its assembly into gap junctions (Figure 1.9). Phosphorylation of Cx43 can influence gap-junctional communication in both a positive and negative manner (Berthoud et al., 1992; Musil et al., 1990). Cx43 phosphorylation occurs primarily on multiple serine residues located on the carboxyl tail and is mediated by several protein kinases, including, PKA and PKC as discussed above and below. In addition, Cx43 has been shown to be a substrate for src- family protein kinases (Lin et al., 2001), mitogen-activated protein kinase (MAP-K) (Warn-Cramer et al., 1996), p34 kinase (Lampe et al., 1998) and casein kinase 1 (Cooper & Lampe 2002) as shown in Table 1.1. The carboxyl tail of Cx43 contains 21 serine residues and the amino tail contains 2 serine residues, with the known phosphorylation sites indicated in Figure 1.9. Cx43 usually exists in a highly phosphorylated state in cardiac myocytes in vivo and in culture (Kwak et al., 1999; Laird et al., 1991; Lau et al., 1991).

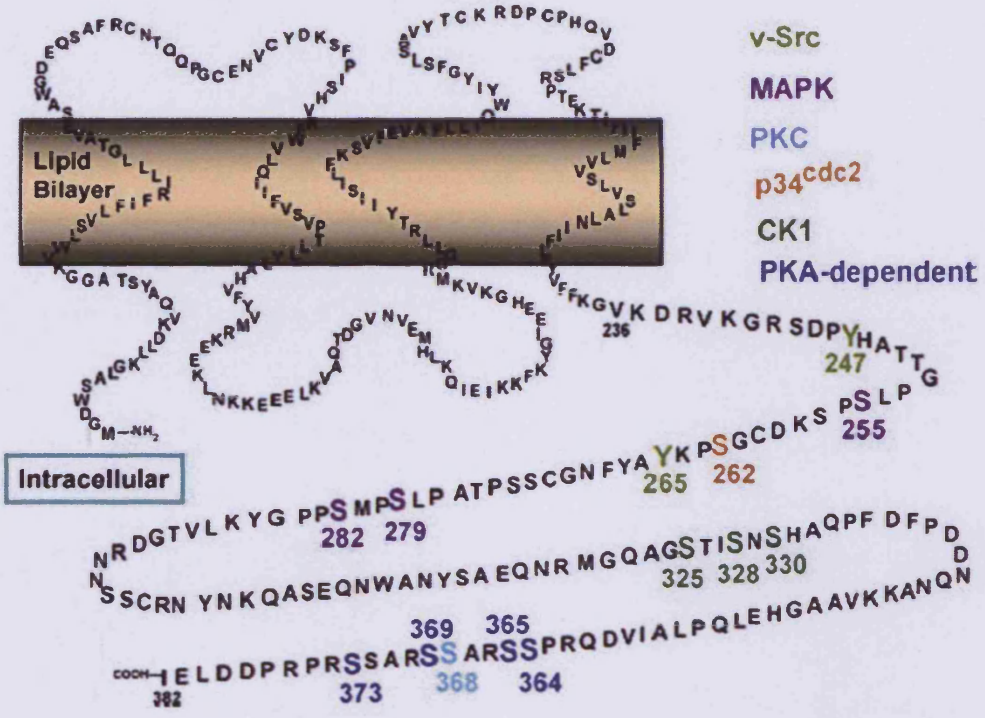

Figure 1.9: The phosphorylation sites of Cx43
Known phosphorylation sites on Cx43 targeted by different protein kinases. For explanation of abbreviations, see main text and abbreviations list. Reproduced from Lampe & Lau 2004.

Electrophysiological studies in cardiac myocytes have shown that non-phosphorylated and phosphorylated Cx43 gives rise to channels that have different unitary conductances. Electrophoresis of phosphorylated Cx43 resulted in bands between 43-45 kDa, which gave channels with a unitary conductance of around 60-70pS. In contrast, Cx43 treated with alkaline phosphatase produced a single band at 41 kDa after electrophoresis, and channels with conductance of 90-100pS (Moreno et al., 1994). Cx43 channel conductance in fibroblasts was altered from approximately 100pS to 45pS when phosphorylated at S368 by PKC, a change not seen in channels formed by mutated Cx43 (S368A) (Lampe et al., 2000). A recent study by Ek-Vitorin et al. (2006) demonstrated that the selective permeability of Cx43 gap junctions is

modulated by PKC dependent phosphorylation of S368, treatment with, a PKC inhibitor reduced phosphorylation at S368, dye transfer and the prevalence lower conducting Cx43 channels (55-70pS). Cx43 phosphorylated at S368 showed enhanced expression in ischemic hearts and was observed to reside at the intercalated disks (Ek-Vitorin et al., 2006).

Residue phosphorylated	Kinase or signaling pathway responsible
Y247	$pp60^{src}$
S255	MAP-K and cyclin B/$p34^{cdc2}$
S262	Cyclin B/$p34^{cdc2}$
Y265	$pp60^{src}$
S279	MAP-K
S282	MAP-K
S325	CK1
S328	CK1
S330	CK1
S364	PKA or PKA-dependent kinases
S365	FSH stimulation (PKA?)
S368	PKC
S369	FSH stimulation (PKA?)
S373	FSH stimulation (PKA?)

Table 1.1
Protein Kinases that phosphorylate Cx43 and their sites of action. Table modified from Lampe and Lau, 2004.

PKC activation results in the phosphorylation of Cx43 at S368 (Lampe et al., 2000) and S372 (Saez et al., 1997). In neonatal cardiac myocytes, TPA (12-tetradecanoylphorbol-13-acetate) a PKC activator, induced increased PKC phosphorylation of Cx43, and resulted in increased gap-junctional conduction (Kwak et al., 1995) or no change (Spray & Burt 1990). However, increased Cx43 phosphorylation due to PKC activation causing decreased gap-junctional communication has been observed in several cell types and has been linked to enhanced tumourigenesis (Berthoud et al., 1992; Brissette et al., 1991; Reynhout et

al., 1992). The reasons for these differences in observed PKC activity caused by TPA could be due to several factors, including cell type and the different isoforms of PKC present, the state of Cx43 phosphorylation when exposed to TPA as well as differences in experimental techniques. An interesting observation in TPA treated cardiac myocytes was that despite overall gap-junctional conduction increasing, the lower conduction state of Cx43 channels (50pS rather than 100pS) was favoured and dye transfer between cells was reduced (Kwak et al., 1995).

Specific isoforms of PKC have been the focus of a few studies in the gap junction field. In cardiac myocytes PKCα and PKCε were associated with Cx43 (Bowling et al., 2001) and in fibroblasts inhibition of gap-junctional communication was dependent to varying extents on PKC α, β and δ (Cruciani et al., 2001). In lens epithelial cells, plasma membrane Cx43 was reduced and it co-immunoprecipitated with PKCγ following TPA treatment (Wagner et al., 2002). Cardiac myocyte gap-junctional permeability was reduced and Cx43 phosphorylation increased by fibroblast growth factor-2, and was associated with Cx43 colocalising with PKCε (Doble et al., 2000). As different cells express distinct PKC isotypes, it is undoubtedly necessary to examine the actual sites of phosphorylation on Cx43's carboxyl tail in order to elucidate consequences of these phosphorylation events (Axelsen et al., 2006).

Increased levels of cAMP are associated with elevated levels of Cx43 phosphorylation and gap-junctional communication (Darrow et al., 1995), as well as an increase in size, number and assembly of gap junctions (Atkinson et al., 1995; Paulson et al., 2000), enhancements that appear to be PKA mediated (Paulson et al., 2000). The

S364 site on the carboxyl tail of Cx43 appears to be an important phosphorylation site for cAMP enhanced gap junction assembly (TenBroek et al., 2001). Despite this, PKA interacts with Cx43 weakly compared to PKC or MAP kinase, leaving the possibility that PKA could phosphorylate S364 indirectly by activating an additional kinase, or that it directly phosphorylates the site inefficiently thereby indicating an advantage of Cx43 being a poor substrate (Shah et al., 2002). A further study using a Cx43 mutant (S364P) has shown alteration in the sensitivity of Cx43 pH gating in Xenopus oocytes (Ek-Vitorin et al., 1996). Clearly, the phosphorylation of Cx43 is an extremely complex process that appears to vary between different cells. Consensus on the relationship between phosphorylation and channel gating is difficult to decipher.

1.4 The pharmacology of cardiovascular gap junctions

There are many agents, both intrinsic and extrinsic, that modulate connexin-based communication. Some pharmacological substances alter channel opening and closing, while others affect the synthesis or expression of connexin channels. Many cations, including H^+, Na^+, Ca^{2+} and Mg^{2+} have been shown to influence gap junction channels and CxHcs, usually exerting their effects directly and causing a reduction in communication (Firek & Weingart 1995). The effects of Ca^{2+} on CxHcs have already been discussed in detail in 1.2.2.

1.4.1 Pharmacological closure of cardiovascular gap junctions

Traditionally, lipophilic agents such as heptanol and octanol have been used as gap uncouplers to inhibit intercellular communication (Evans & Boitano 2001). More recently, fatty acids such as palmitoleic acid, oleic acid and arachidonic acid have

been used at μM concentrations to inhibit gap-junctional communication (Dhein et al., 1999; Hirschi et al., 1993; Schmilinsky-Fluri et al., 1997). The mechanism of action is thought to be due to the incorporation of these agents into the lipid bilayer of the plasma membrane causing a reversible impairment of the gap junction channel pore (Takens-Kwak et al., 1992). Some anesthetics are thought to have a similar mechanism of action. For example, halothane caused a 90% reduction in junctional conductance in rat neonatal cardiac myocytes (Burt & Spray 1989). However, their specificity towards connexin channels relative to other membrane channels can be questioned.

The glycyrrhizic compounds derived from liquorice root are inhibitors of connexin-channel communication, and include 18αGA (Figure 1.10), 18βGA and carbenoxolone. 18αGA has been used to inhibit gap-junctional communication at 50μM (Taylor et al., 2001) and 18βGA at 5μM (Allen et al., 2002). The mechanism and specificity by which glycyrrhetinic acids inhibit connexin communication is not fully understood but it has been suggested that changes in phosphorylation status could be involved as Cx43 is dephosphorylated by 18αGA in HeLa cells (Clarke et al., 2006).

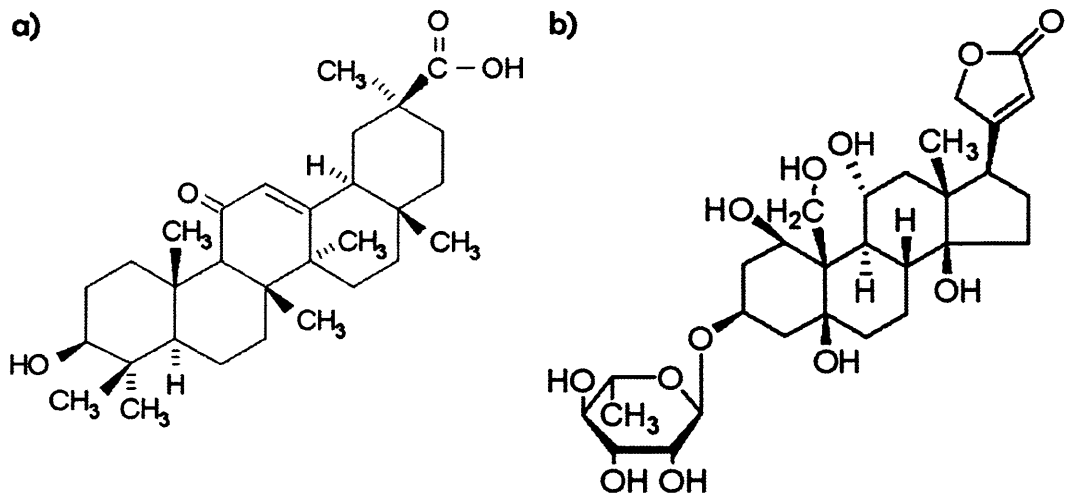

Figure 1.10
The Chemical structures of a) the gap junction inhibitor 18-α-glycyrrhetinic acid (18αGA) and b) the cardiac glycoside ouabain.

The cardiac glycoside group of compounds (digoxin or digitoxin, ouabain and strophanthidin) act by inhibiting the action of the Na^+/K^+-ATPase exchanger, which causes an increase in intracellular Ca^{2+}. In an early study, ouabain decreased conduction velocity in bovine heart (Weingart 1977), while strophanthidin and ouabain caused cellular uncoupling in guinea pig ventricle (De Mello 1976; Weingart & Maurer 1987). More recent investigations have shown that ouabain exerts a biphasic effect, where initially gap-junctional communication is decreased followed by a reduced connexin expression (Martin et al., 2004). It is likely that these uncoupling events contribute to the antiarrhythmic action of the cardiac glycosides.

Connexin mimetic peptides are short peptides corresponding to extracellular loop sequences of connexins, initially Cx32, that delayed the onset of synchronous beating of isolated cells aggregating into contracting myo-balls (Warner et al., 1995). These peptides were later modified to correspond to extracellular loop sequences in Cx43 and were shown to block the gap junctions connecting vascular smooth muscle cells and endothelial cells (Chaytor et al., 1997; 1998). Gap 26 is a short peptide sequence

targeted against the first extracellular loop of Cx43 (VCYDKSFPISHVR). A similar connexin mimetic peptide, GAP 27 (SRPTEKTIFII) corresponds to the second extra cellular loop, and has been extensively used and has been shown to be equally as effective (Chaytor et al., 1999). The peptides have also been modified to act on Cx40 channels.

A number of other agents can be used to regulate the closure of gap junction channels by activating protein kinases and thereby altering the phosphorylation state of the connexins in the channel. Such agents are listed in table 1.2 and include noradrenaline, angiotensin II, phorbal esters such as TPA.

	Class	Agents	Proposed mechanism
Agents that close gap junctions	Ions	H^+, Na^+, Ca^{++}, Mg^{++}	direct effects?
	Lipophilic agents and fatty acids	heptanol, octanol arachidonic acid, oleic acid, palmitoleic acid, decanoic acid, myristoleic acid	incorporation?
	Glycyrrhizic acid metabolites	18-α-glycyrrhetinic acid, 18-β-glycyrrhetinic acid, carbenoxolone	phosphorylation?, aggregation of Cx-subunits?
	Receptor ligands	carbachol (M-cholinoceptor), noradrenaline (α-adrenoceptor), FGF-2, angiotensin-II (AT1 receptor), Atrial natriuretic factor ANF, VEGF	cGMP/PKG, PKC, PKCε, PKC?, cGMP/PKG, ERK
	Dephosphorylating agents	2,3 butandione monoxime	unknown mechanism
	Narcotics	halothane, ethrane, isoflurane	incorporation?
	Phorbol esters	12-O-tetradecanoylphorbol-13-acetate, (TPA)	activation of PKC[a], /Ca^{++}?
	PKC inhibitors	staurosporine	inhibition of PKC[a]
	Metabolites	ATP-decrease, Diacylglycerol/ 1-oleoyl-2-acetyl-sn-glycerol	dephosphorylation, unknown mechanism/disturbance of the lipid bilayer?
	Eicosanoids	11,12-epoxyeicosatrienoic acid (late effect) thromboxane A2	ERK1/2, unknown mechanism
	Fenamates	meclofenamic acid, niflumic acid, flufenamic acid	unknown mechanism
	IP_3-receptor blocker	2-aminoethoxydiphenyl borate	unknown mechanism
	Weak organic acids	acetic acid, propionic acid	H^+
	Cannabinoids	Δ^9-tetrahydrocannabinol	ERK1/2
	Cardiac glycosides	strophanthidin, ouabain	elevation of $[Ca^{2+}]_i$
Agents that enhance gap junction activity	cAMP-enhancing drugs	cAMP, forskolin, isoprenaline	PKA
	Antiarrhythmic drugs	Tedisamil	PKA
	Antiarrhythmic peptides	AAPnat, AAP10, cAAP10RG, HPP-5, ZP123	PKCα, ?PKC
	Eicosanoids	11,12-epoxyeicosatrienoic acid, (early effect)	PKA
	Phorbol ester	TPA	PKC
	Unsaturated fatty acids	eicosapentaenoic acid	inhibition of tyrosine, kinase, (only after hypoxia),
	Receptor ligands	5-hydroxytryptamine	unknown mechanism
	PDE inhibitor	isobutyrylmethylxanthine	cAMP/PKA

[a] Probably depending on the isoform of PKC.

Table 1.2
Agents that act upon cardiovascular gap junctions. Table modified from Dhein, 2004.

1.4.2 Pharmacological manipulation of cardiovascular gap junctions

There are far fewer substances that act on connexin channels thereby enhancing their function than those decreasing their activity, and these are summarised in table 1.2. However, great interest has been shown in agents that enhance cell coupling as this could be advantageous in situations such as in ischaemia-reperfusion, where agents

could act antiarrhythmically. Agents such as forskolin and isoprenaline have been shown to activate PKA, which can lead to increased coupling between cardiac myocytes (De Mello 1991), or they may have no effect on coupling (Kwak & Jongsma 1996), as explained in 1.3.1.

A naturally occurring antiarrhythmic peptide was identified in bovine atria that improved the synchronous contraction of cultured myocardial cell clusters (Aonuma et al., 1980). The hexapeptide, designated AAP_{nat}, has a sequence of H_2N-Gly-Pro-4Hyp-Gly-Ala-Gly-COOH (Aonuma et al., 1982). AAP_{nat} was detected in heart, kidney and blood of rats at concentrations of 203pmol/g, 165pmol/g-1 and 3.8pmol/ml respectively (Kohama et al., 1985). Using mouse models, arrhythmias induced by $CaCl_2$ (Kohama et al., 1987), aconitine (Aonuma et al., 1983) and ouabain were all reduced upon addition of AAP_{nat}, but epinephrine-induced arrhythmias were unaffected . Derivatives of AAP_{nat} such as HPP-5 (N-3-(4-hydroxyphenyl) propionyl-Pro-Hyp-Gly-Ala-Gly) (Aonuma et al., 1980) and the synthetic derivative AAP10 (H_2N-Gly-Ala-Gly-Hyp-Pro-Tyr-$CONH_2$) (Muller et al., 1997) have also shown antiarrhythmic actions. AAP10 is semicyclic in structure and binds to a membrane protein/receptor (Grover & Dhein 2001). All AAPs have been shown to activate PKC (Dhein et al., 2003). The action of AAP10 was inhibited by GDP-β-S, PKC inhibitors and a specific inhibitor of PKCα (CGP54345), which indicates that AAP10 acts via a G-protein which activates PKCα causing Cx43 phosphorylation and thereby improves gap-junctional conductance (Muller et al., 1997; Weng et al., 2002).

1.5 Diseases caused by gap junction abnormalities

Gap junctions are present in all nucleated cells, with the exception of adult striated muscle and sperm, and it is no surprise that abnormalities of connexins cause a wide range of diseases in many tissues and organs throughout the body (Evans & Martin 2002). The majority of diseases described to date relate to single gene defects, which indicates that disease processes could involve polygenic abnormalities affecting structure, expression or trafficking of the gap junction forming proteins, the connexins. A summary of human diseases associated with connexin gene abnormalities and for comparison phenotypic abnormalities identified in mice with connexin abnormalities is shown in Table 1.3.

Mouse connexin	Cell and tissues with major expression levels	Phenotype(s) of Cx-deficient mice	Human hereditary disease(s)	Human connexin
	n.s.	n.s.	n.s.	hCx25
mCx26	breast, skin, cochlea, liver, placenta	lethal on ED11	sensorineural hearing loss, palmoplantar hyperkeratosis	hCx26
mCx29	myelinated cells	n.s.	n.s.	hCx30.2
mCx30	skin, brain, cochlea	hearing impairment	nonsyndromic hearing loss, hydrotic ectodermal dysplasia hair loss, nail defects and often mental deficiency	hCx30
mCx30.2	n.s.	n.s.	n.s.	hCx31.9
mCx30.3	skin	n.s.	erythrokeratoderma variabilis	hCx30.3
mCx31	skin, cochlea uterus, placenta	transient placental dysmorphogenesis	hearing impairment, erythrokeratoderma variabilis	hCx31
mCx31.1	skin	n.s.	n.s.	hCx31.1
mCx32	liver, Schwann cells, oligodendrocytes	decreased glycogen degradation, increased liver carcinogenesis	CMTX, (one of the hereditary peripheral neuropathies)	hCx32
mCx33	testis	n.s.		
mCx36	neurons retina	visual deficits	n.s.	hCx36
mCx37	endothelium, ovaries	female sterility, intensive bleeding	n.s.	hCx37
mCx39	n.s.	n.s.	n.s.	hCx40.1
mCx40	heart, endothelium	atrial arrhythmia	n.s.	hCx40
mCx43	many cell types and tissues	heart malformation and ventricular arrhythmia	visceroatrial heteroataxia?	hCx43
mCx45	heart, endothelia, neurons	lethal on ED 10.5	n.s.	hCx45
mCx46	lens	zonular nuclear cataract	congenital cataract	hCx46
mCx47	brain, spinal cord	n.s.	n.s.	hCx47
mCx50	lens	microphthalmia, zonular pulverulant and congenital cataract	zonular pulverulant cataract	hCx50
	n.s.	n.s.	n.s.	hCx59
mCx57	ovaries	n.s.	n.s.	hCx62

n.s. not studied. ED, embryonic days.

Table 1.3
Tissue expressing various mouse connexins and the phenotypes in connexin-deficient (knock-out) mice. Inherited human diseases that are associated with various connexin mutations are also shown. Table taken from Evans and Martin, 2002.

1.5.1 Cx43 mutations linked to oculodentodigital dysplasia (ODDD)

Relatively few loss of function mutations of Cx43 have been described in the heart. However in ODDD, 28 Cx43 mutations have been identified (Paznekas et al., 2003). ODDD is a pleiotropic development disorder that causes craniofacial abnormalities, lens and corneal defects, abnormalities of the hair, nails and teeth, syndactyly and occasionally heart and neurological problems (Loddenkemper et al., 2002). Although rare, most patients live long lives in relatively good health. A mouse model of ODDD has been developed and genetic analysis has revealed that a G60S mutation (Flenniken et al., 2005) in the first extracellular loop is very similar to a P59H mutation recently discovered in humans (Vasconcellos et al., 2005), thus showing the importance of this model as a tool for studying ODDD and Cx43 mutations in humans (Laird 2006).

1.5.2 Genetic abnormalities in Cx26 associated with non-syndromal deafness

Over 30 mutations of Cx26 have been identified, of which approximately half account for inherited non-syndromal deafness. This has led to the first practical genetic marker of inherited hearing loss (Steel & Kros 2001). The most common mutation in Cx26 causing deafness is 35delG, which results in protein translation terminating prematurely at amino acid 13 (Estivill et al., 1998; Kelsell et al., 1997). A different mutation that produces similar effects is the 167delT mutation resulting in truncation of the protein product at amino acid 56 (Zelante et al., 1997). These two mutations produce immature Cx26 that cannot form functional channels. However, other mutations cause defective Cx26 trafficking, such as the Trp77Arg and Met34Thr mutations, which fail to oligomerise correctly into hexameric complexes and thus no functional channels can form (Martin et al., 1999). For example, a Trp44Cys

mutation results in Cx26 that trafficked to the plasma membrane and oligomerised into hexameric channels, but was unable to form functional gap junctions transferring Lucifer yellow (Martin et al., 1999), indicating that poorly functioning or inactive gap junctions are produced by this mutation. Studies in Xenopus oocytes expression systems revealed that some mutations of Cx26 are unable to form electrically active channels (White et al., 1998).

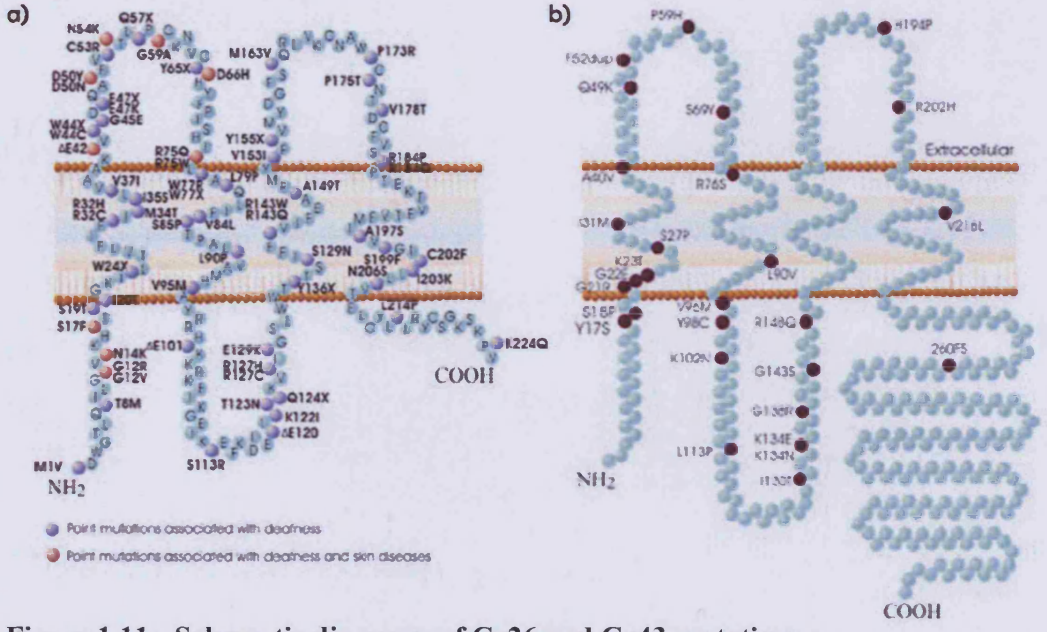

Figure 1.11: Schematic diagrams of Cx26 and Cx43 mutations
Cx26 mutations causing deafness and skin diseases are illustrated (a) with mutations associated with deafness shown in purple and mutations associated with both deafness and skin diseases shown in orange. Cx43 mutations causing ODDD are shown (b) with the locations of 28 mutations shown in red, all linked to ODDD. Reproduced from Laird 2006.

1.5.3 Cx32 mutations cause Charcot-Marie-Tooth X-linked disease (CMT-X)

Charcot-Marie-Tooth X-linked disease, a peripheral neuropathy, is a progressive atrophy of distal muscles and reduced axonal conduction by Schwann cells (Bergoffen et al., 1993), with patients revealing over 200 mutations in Cx32 (Nelis et al., 1999). The Cx32 mutations are quite varied but evenly distributed throughout the DNA,

affecting most connexin domains (Nelis et al., 1999). Truncation or a single amino acid substitution in Cx32 leads to dysfunctional channels (Abrams et al., 2001). The channel pore size can be reduced by the Ser26Leu mutation and channel opening probability is reduced by a Met34Thr mutation (Oh et al., 1997). Further Cx32 mutations modify intracellular trafficking and assembly thereby impairing Cx32 gap junctions to function normally (Martin et al., 2000). Also, Cx32 knockout mice developed decreased nerve conduction with age and demonstrated similar morphology to CMT-X in humans (Willecke et al., 1999).

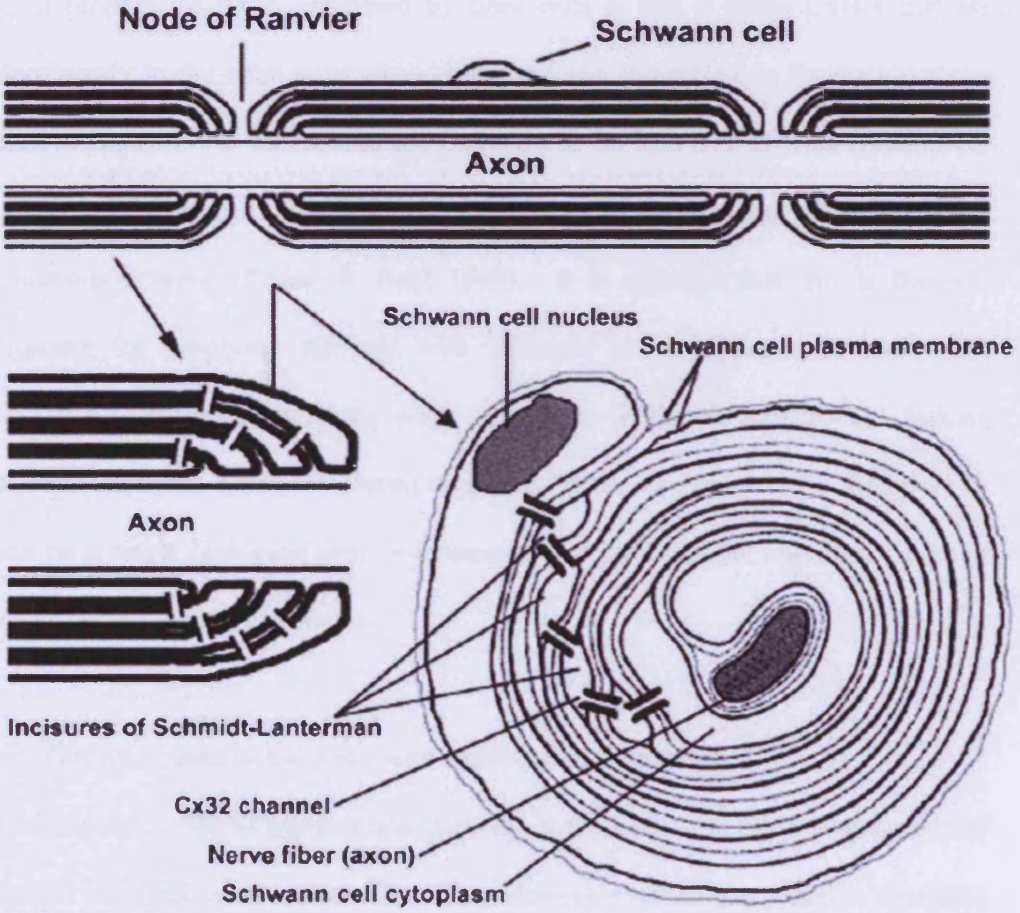

Figure 1.12: Myelin structure and location of connexin32 gap junction channels. The structure of peripheral myelin is shown at the *top*. The cytoplasm of a Schwann cell wraps several times around a nerve fibre (axon) forming the myelin sheath; Cx32 containing gap junction channels are formed between adjacent plasma membranes of the enwrapping layers that originate from the same Schwann cell connect the incisures of Schmidt-Lanterman. Reproduced from Saez et al, 2003.

1.5.4 Cataract

In the lens, Cx46 and Cx50 mutations are linked to cataract abnormalities (Pal et al., 2000). The eye lens is an avascular organ consisting of an epithelial layer covering the anterior surface of the organ and a large mass of fibre cells which form the bulk of the organ (Saez et al., 2003). In the lens, the anterior epithelial monolayer interfaces with the aqueous humour and contains high densities of ion channels and transporters. The epithelial monolayer where Cx43 is expressed controls cellular homeostasis for the entire lens via a network of intercellular channels (Goodenough et al., 1980). An unusual property of Cx46 expressed by fibre cells is that it forms CxHcs that are predominantly in the open state when expressed and assembled in Xenopus oocytes (Pfahnl & Dahl 1999). The role of the Cx46Hcs in the lens is to provide conduits for the passage of nutrients to the inner avascular parts of the lens that are remote from the aqueous humour (Pfahnl & Dahl 1999). It is apparent that this is the sole mechanism for supplying the lens with nutrients and therefore it is likely that malfunction of these channels may result in cataract (Pfahnl & Dahl 1999). Indeed, mice with abnormal Cx46 developed cataracts (White & Paul 1999). Reliance by organs on a single biological system is unusual and indicates the importance here of channels constructed of connexins.

1.6 Gap junctions in the heart and cardiovascular system

The principal function of gap junction channels in the heart is to allow propagation of the action potential from cell to cell. The distribution of the gap junction channels, mainly confined to intercalated disks at the cell poles with only small proportion located at the lateral borders of the cell ensure normal propagation of the activation wave front. The cardiac action potential is propagated along the fibre by activating a

sodium current, which is mainly dependent on sodium channel availability. At the cell pole, the action potential is transferred via gap junction channels to the next cell. Gap junctions located along the lateral border of the cell are likely to be responsible for a small transverse component of action potential propagation, causing propagation velocity (V) along the fibre axis to be transmitted much faster in the myocardium than transversely through it (anisotropy) (reviewed by (Bernstein & Morley 2006). An additional function of cardiac gap junctions is to metabolically couple myocardial cells, allowing the passage of small molecules between cells and transmission of chemical signals that can determine the fate of the cells, which may enable slow calcium wave spreading, transfer of ''death'' signals (Kanno et al., 2003) or of ''survival'' signals (Yasui et al., 2000).

1.6.1 Connexin distribution and physiology within the heart

Gap junction channels have an established role within the healthy heart since they provide the cell to cell pathways for the coordinated spread of current flow and the synchronous contraction of cardiomyocytes. The major connexin of the heart, Cx43, is found in abundance in ventricular and atrial cardiac myocytes of all mammalian species (Severs 2000). Cx40 and/or Cx45 may also be expressed in cardiac myocyte subtypes and specific regions of the heart (Gourdie et al., 1993; Vozzi et al., 1999). Co-expression of two or all three connexins occurs, subject to cardiac myocyte type and location. The various types of cardiac myocyte found in different regions of the heart are characterized by distinctive connexin expression profiles as well as differences in overall size and distribution (Severs et al., 2001).

The cardiac myocytes of functional ventricles are elongated, branching cells that are extensively interconnected by clusters of Cx43 gap junctions organized in intercalated disks (Figure 1.4.1). Present in the intercalated disks are two further types of anchoring junction, the *fascia adherens* and the desmosome. Respectively, these structures are responsible for the cell-cell linkage of the contractile filaments and cytoskeletal intermediate filaments (Gourdie et al., 1991). These anchoring junctions function in combination with gap junctions to integrate the electro-mechanical function of cardiac myocytes. In ventricular myocardium, gap junctions occupy laterally-facing segments of membrane (Figure 1.4.1), with large gap junctions enclosing the disk periphery (Gourdie et al., 1991).

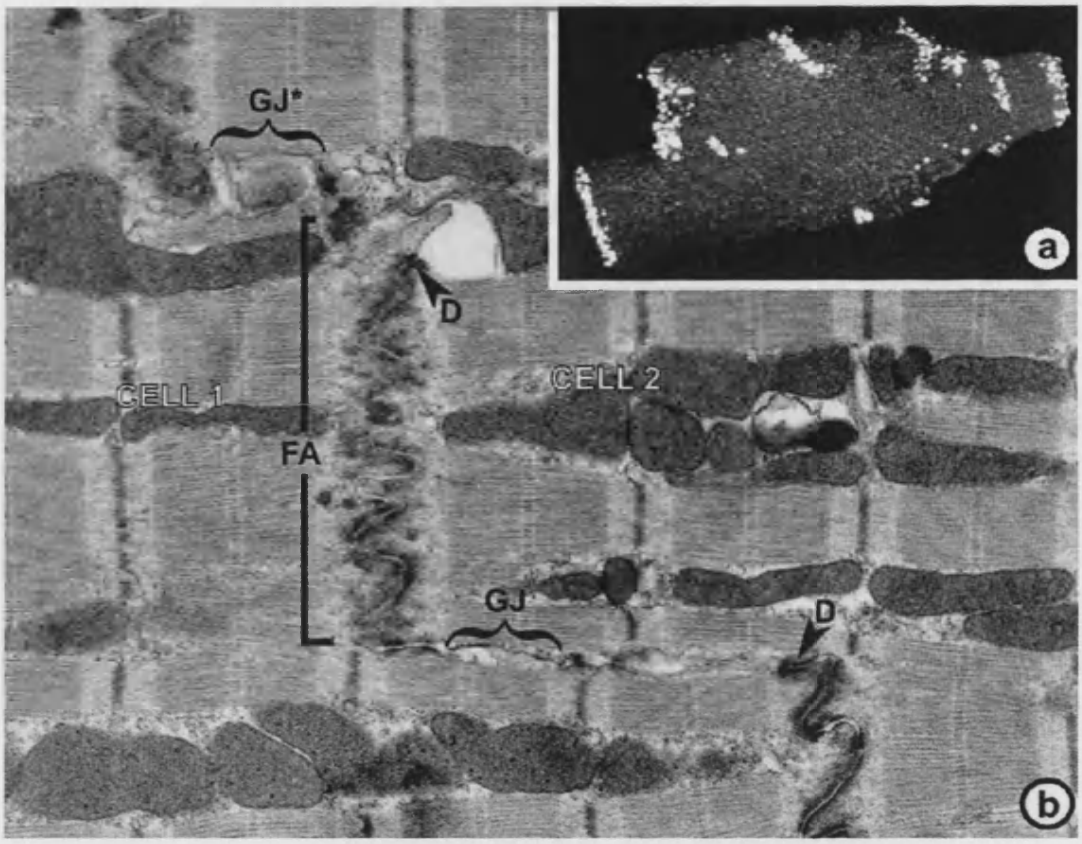

Figure 1.13: The intercalated disk of the cardiac myocyte
(a) illustrates localization of Cx43 in a dissociated ventricular myocyte, viewed by Cx43 immuno-staining using confocal microscopy. The intercalated disks are indicated by the bright staining of Cx43 gap junctions (x 650).
(b) shows the appearance of the intercalated disk between two cardiomyocytes in a thin-section electron micrograph. *Fasciae adherentes* junctions (FA) occupy the vertical segments of membrane, with the lateral segments of membrane dominated by gap junctions (GJ) and desmosomes (D) both regions. (GJ* indicates a gap junction that has been tangentially sectioned) (x 16,000). From (Severs 2001).

Atrial cardiac myocytes are slender cells compared with their ventricular counterparts. Intercalated disks are readily identified in atrial myocytes, but gap junctions are also located along the lateral borders. Ventricular cardiac myocytes usually lack Cx40, but this connexin is abundant in atrial myocytes, and is arranged with Cx43 in the same junctional plaques (Severs et al., 2001). In both ventricular and atrial working myocardium, Cx45 is present in very low quantities, in both ventricular and atrial

myocardium, with slightly higher levels identified in the atria (Coppen et al., 1998; Vozzi et al., 1999).

The impulse generation and conduction system are comprised of further subtypes of cardiac myocyte with distinctive morphologies (Severs 2001). The myocytes of the sino-atrial and atrioventricular nodes are typically small, with randomly orientated and poorly developed contractile elements, and dispersed gap junctions containing Cx45 (Coppen et al., 1999; Honjo et al., 2002), which forms low conductance channels *in vitro* (Moreno et al., 1995). The features of these gap junction are consistent with poor intercellular coupling which, in the sinoatrial node, may contribute to the ability to control atrial tissue without being prone to hyperpolarisation and, in the atrioventricular node, to the slowing of conduction which ensures sequential contraction of atria and ventricles (Severs 2001).

Cardiac myocytes of the His-Purkinje conduction system express Cx40 and Cx45 (Coppen et al., 1998; Gourdie et al., 1993). The bundle branches and Purkinje fibre system have large and abundant gap junctions containing high levels of Cx40 (Bastide et al., 1993; Gros et al., 1994), a connexin associated with high conductance channels (Bukauskas et al., 1995). This allows the system to distribute the impulse rapidly throughout the working ventricular myocardium. Cx45 shows overlapping expression with Cx40 in the bundle branches and Purkinje fibers but is also distributed throughout the entire conduction system (Coppen et al., 1999). In Cx40 knockout mice, there is reduced velocity through the conduction system and right bundle branch block (Tamaddon et al., 2000; van Rijen et al., 2001). Continued conduction with

these abnormal characteristics is attributed to the presence of connexin45 (Coppen et al., 1999).

1.6.2 Gap junctions in blood vessels

In the vasculature the main connexins are Cx37, Cx40 and Cx43 where they provide intercellular coupling between endothelial cells, between smooth muscle cells and myoendothelial cell to cell coupling. In general, most of the cell types that line the walls of blood vessels express gap junctions in varying patterns of distributions and are responsible for facilitating interactions between these cells (Nishii et al., 2001; Severs et al., 2001), in particular the spread of vasomotor signals (Segal & Duling 1989). All types of vessel wall cells have been shown to express Cx43, but Cx40 has been demonstrated as the main gap junction protein in adult endothelium (van Kempen & Jongsma 1999), although there are differences between different species. However Cx40 does exhibit heterogeneous expression along the vasculature (Hwan & Beyer 2000). Cx37 expression appears to be limited to endothelial cells (Reed et al., 1993), with exception to the ovary and certain lung cell types. The disparity in Cx37 and Cx43 distribution could indicate involvement in more dynamic processes than Cx40, but their expression patterns along vessel walls are poorly understood. Cx37 and Cx40 expression was observed to be uniformly distributed, but Cx43 was distributed to sites of turbulent flow in rat aortic endothelium (Gabriels & Paul 1998). In arterial smooth muscle cells, Cx43 is the major connexin but low amounts of Cx40 and Cx45 are also present (Hill et al., 2002; Ko et al., 2001; Little et al., 1995). Connexin expression patterns in endothelial and smooth muscle cells can be modulated by pathological conditions, such as early human coronary atherosclerosis

or arterial wall injury (Blackburn et al., 1995; Haefliger & Meda 2000; Kwak et al., 2002).

1.7 Pathophysiological roles of gap junctions in the heart

In diseased ventricular myocardium, gap junctions usually undergo two main changes; reduced expression of the main connexin, Cx43, and alterations to the distribution of gap junctions.

1.7.1 Reduced Cx43 expression in diseased ventricles

The most consistently observed alteration in ventricular connexin expression involves down-regulation of Cx43, seen in a number of cardiomyopathies (Dupont et al., 2001; Kaprielian et al., 1998; Kostin et al., 2003; Lin et al., 2005). Northern and Western blot analysis have demonstrated a considerable decrease in Cx43 transcription and protein expression in the left ventricles of transplant patients with end-stage congestive heart failure (Dupont et al., 2001). This reduction of connexin expression is observed regardless of the underlying cause of heart failure (Kostin et al., 2003). The reduced expression of ventricular Cx43 was shown to develop long before terminal heart failure (Peters et al., 1993). Consistent with this finding, a transgenic mouse model of juvenile dilated cardiomyopathy has demonstrated reduced Cx43 expression levels and conduction defects at 4 weeks postpartum, with contractile dysfunction and heart failure occurring at 12 weeks (Hall et al., 2000). A transient reduction of Cx43 expression can also occur after very brief episodes of ischaemia and reperfusion (ischaemic preconditioning) (Daleau et al., 2001).

The studies discussed so far have dealt with total Cx43 levels as indicators for potential signalling between cells, but do not provide relative information regarding the functionality of the channels. Computer modelling studies have shown that a 40% decrease in gap junctions would not significantly impact on conduction velocity (Jongsma & Wilders 2000). On this basis, a decrease in Cx43 expression in the diseased ventricle is unlikely to be of major functional relevance. However, the diversity of structural and functional alterations in the diseased heart and the complex relationship between passive and active membrane properties (Rudy & Shaw 1997; Shaw & Rudy 1997), added to the assumptions inherent in computer modelling, make continuing *in vivo* experimentation vital for gaining further insight.

Observations in foetal Cx43 knockout mice indicated that conduction velocity is slowed in these mice (Vaidya et al., 2001) but postnatal studies have been limited by the perinatal death of the mice (Reaume et al., 1995). In another transgenic mouse model, with restricted cardiac knockout of Cx43, a decrease of approximately 86–95% protein expression was observed causing sudden death due to spontaneous ventricular arrhythmia (Gutstein et al., 2001). However, in transgenic mice expressing half the normal level of Cx43 (Cx43+/-), acute ischemia induced in isolated perfused hearts resulted in a marked increase in incidence, frequency and duration of ventricular tachycardias (Lerner et al., 2000) despite possibly only a modest reduction in conduction velocities (Guerrero et al., 1997). There is often substantial variation in the degree of reduction of Cx43 expression, both between and within failing human hearts, with some areas of diseased hearts reducing to > 90% of control amounts of Cx43 protein expression (Dupont et al., 2001). A further mouse study of spatial heterogeneity of cardiac Cx43 expression demonstrated both abnormal conduction

and contractile dysfunction (Gutstein et al., 2001), a result fitting earlier predictions made in human studies (Dupont et al., 2001; Kaprielian et al., 1998). This suggests the possibility that spatial differences in Cx43 reduction is a major factor predisposing the heart to arrhythmia.

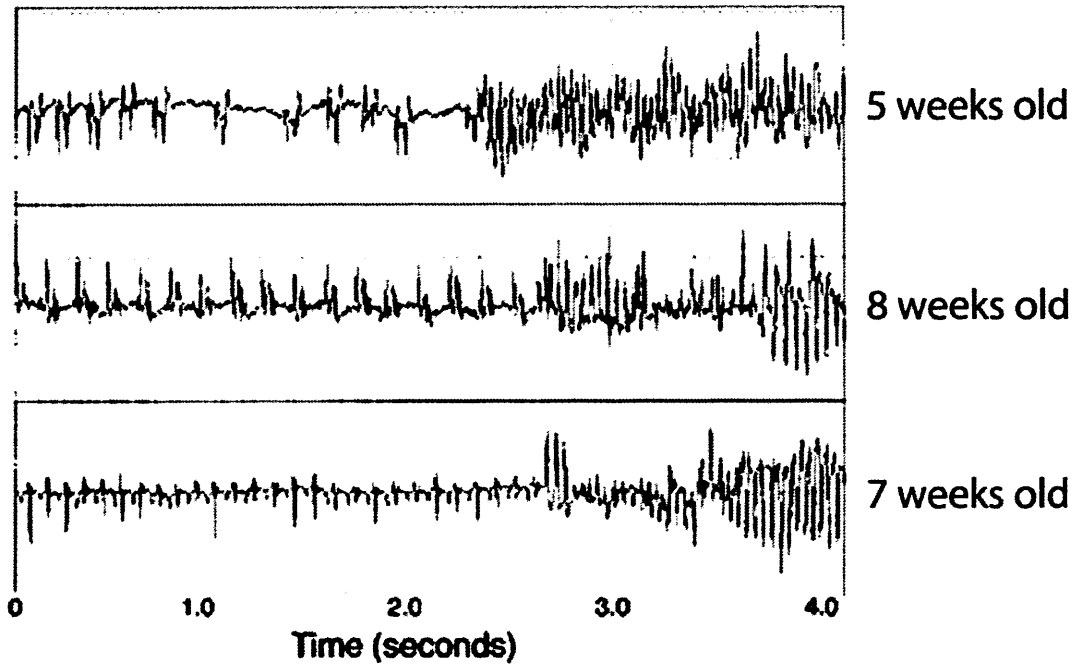

Figure 1.14: Electrocardiograms from Cx43 knockout mice.
The recordings show initially that sinus rhythm is normal, followed by ventricular tachycardia. The arrhythmias quickly degenerated into ventricular fibrillation. Reproduced from Gutstein et al., 2001.

1.7.2 Changes in gap junction distribution in diseased ventricles

In addition to the disturbances in gap junction expression, alteration to the normal ordered distribution of Cx43 gap junctions was first described in the myocardial zone bordering infarct scar tissue in the ventricles of patients with end-stage ischaemic heart disease (Smith et al., 1991). Immuno-detection of Cx43 in myocytes of the infarct border zone demonstrated a scattered and disordered distribution, with Cx43 present on the lateral surfaces of the cells rather than in the polar, intercalated disk arrays characteristic of normal myocardium (Green & Severs 1993). Using a canine

infarct model, 3–10 weeks postinfarction in the ventricle, remodelling featured reduction in the size and the number of gap junctions in the intercalated disk, and fewer lateral (side-to-side) connections between myocytes (with relative preservation of end-to-end contacts), disturbances that could increase transverse axial resistance (Luke & Saffitz 1991).

In studies using a rat model of hypertrophy of the right and left ventricle, it was observed that Cx43 was distributed over the entire cell surface (Emdad et al., 2001; Uzzaman et al., 2000) and hypertrophy induced in the right ventricle caused reduced longitudinal conduction velocity (Uzzaman et al., 2000). This trait is not usually evident in ventricular hypertrophy that is associated with coronary heart disease in patients undergoing by-pass surgery. However, disorganised localisation of Cx43 was observed in the explanted ventricles of heart transplant patients (Kostin et al., 2003). Hypertrophic cardiomyopathy in humans is characterised by extensive and chaotic arrangements of ventricular gap junctions and consequently is the most frequent cause of sudden cardiac death due to arrhythmia in young adults (Sepp et al., 1996).

'Hibernating myocardium' is a condition in which coronary artery disease patients have a region of myocardium with impaired contractility that retains the ability to recover contractile function after coronary artery by-pass surgery (Heusch 1998). Cx43 gap junctions found at the edge of the intercalated disk were smaller in size and overall Cx43 detected in the intercalated disk was decreased when compared with normally perfused region of the same heart (Kaprielian et al., 1998). These observations suggest a possible link between Cx43 gap junction alterations and impaired ventricular contraction in human heart disease, a link that has been

confirmed in a transgenic mouse model of heart-specific Cx43 conditional knockout (Danik et al., 2004).

1.7.3 Ischaemia and Cx43 knockout (+/-) mice

Mice with homozygous knockout of Cx43 (-/-) die shortly after birth (Guerrero et al., 1997). In contrast, mice with heterozygous knockout of Cx43 (+/-) have a normal life expectancy and development, but only have 50% of Cx43 expression and no up-regulation of other connexins (Reaume et al., 1995). On exposure to ischemia, these mice develop ventricular arrhythmia more frequently and earlier in the ischaemic insult than wild-type mice (Lerner et al., 2000); therefore, a Cx43 deficiency would appear to be a disadvantage during ischemia. However, several investigators have correlated smaller areas of myocardial infarction with reduced numbers of Cx43 gap junction and inhibition gap-junctional communication (Garcia-Dorado et al., 1997; Kanno et al., 2003). This may be due to the prevention of hypercontractures caused by elevated Ca^{2+} that is transmitted through gap junctions and inhibition of this by heptanol stops the spread of necrosis from cell to cell (Ruiz-Meana et al., 1999). During ischaemia, gap junction communication persisted resulting in the lasting cardiac muscle rigor, despite acidosis and increased intracellular Ca^{2+}, which would normally attenuate gap junction communication (Ruiz-Meana et al., 2001). It has also been observed that Cx43 deficient mice do not benefit from the effects of ischaemic preconditioning (Schwanke et al., 2002). The authors concluded that Cx43 is involved in ischaemic preconditioning and postulated that PKCε-Cx43 complexes are essential for ischaemic preconditioning to occur. However, 50% of the functioning gap junctions and hemichannels remain, so the absence of any ischaemic preconditioning at all is surprising and there is no evidence showing that PKCε-Cx43

complexes are either present in the wild-type mice or absent in the Cx43 deficient mice.

1.7.4 Gap junction remodelling in atrial fibrillation

Atrial fibrillation is a phenomenon in which waves of electrical activity propagate in many directions, causing disorganized depolarization and ineffective atrial contraction (Zipes 1997). The condition is associated with progressive remodelling of electrical, contractile and structural elements, including altered cell size and mitochondrial shape (Allessie et al., 2002). Once atrial fibrillation is established it tends to endure due to the remodelling changes (Wijffels et al., 1995). Studies monitoring changes in Cx40 expression in human atrial samples from chronic atrial fibrillation patients have provided inconsistent reports, with some observing a decrease in expression (Kostin et al., 2002; Nao et al., 2003) and others an increase (Polontchouk et al., 2001). Cx40 also appeared to be redistributed towards the edges of the myocytes (Kostin et al., 2002; Polontchouk et al., 2001). In addition, other associated junction proteins such as desmoplakin and N-cadherin showed similar changes in distribution to those of Cx40 (Kostin et al., 2002). This could indicate a spatial association between gap junctions and other adhesive junctions during remodelling at the cell surface, a feature that has also been observed in the ageing heart (Angst et al., 1997; Peters et al., 1994).

In a goat model of persistent atrial fibrillation there were noticeable differences in Cx40 distribution (van der Velden et al., 1998) and reduction in the Cx40/Cx43 ratio (van der Velden et al., 2000). However, there was no apparent redistribution of Cx40 to the myocyte borders, as seen in the human studies. These differences observed are

probably due to differences between species, age or manner of induction of atrial fibrillation.

In a considerable number of patients, it appears that atrial fibrillation is initiated in the proximal portions of the thoracic veins, which have an area of myocardium continuous with that of the atria (Haissaguerre et al., 1998; Jalife 2003). In a study of this myocardial area in canine superior vena cava, gap junctions were principally located at intercalated disks, with Cx43, Cx40 and Cx45 co-localized (Yeh et al., 2001). Areas of unusual expression patterns have been identified in which Cx43 gap junctions are spread across a cluster of myocytes which are in turn surrounded by myocytes expressing small Cx40 gap junctions (Yeh et al., 2001). This variation in gap junction distribution and structural heterogeneity structure could potentially form an area more liable to cell coupling difficulties and thus the development of arrhythmias.

1.8 The neonatal cardiac myocyte cellular model

Within this thesis, neonatal cardiac myocytes have been used to analyse cellular aspects of processes within the heart. Neonatal cardiac myocytes retain many cardio-specific properties such as the ability to synchronously contract. In a study by Poindexter et al. (2001) neonatal cardiac myocytes were compared to adult cardiac myocytes. It was found that when cultured, both neonatal and adult cardiac myocytes rely heavily on the IP3 pathway in the control of intracellular calcium concentrations and the control of their contractile function. Freshly isolated adult myocytes use sarcoplasmic reticulum calcium stores for the initiation of contractile function. In addition, the method of isolation for adult myocytes is more complex than for neonatal

cells and does not hold any significant advantage as a cellular model (Poindexter et al., 2001). With this in mind and a method for isolating neonatal cardiac already in place, it was decided that rat neonatal cardiac myocytes were sufficient for my studies contained within this thesis.

Another model that is often used to study aspects of heart physiology and pathology is the Langendorff system (Beardslee et al., 1998) and involves perfusion of the isolated mammalian heart by carrying fluid under pressure into the sectioned aorta, and thus into the coronary system. This model can look at the heart as a whole organ as well as limited aspects at a cellular level. However, these models can never completely predict the events in the human heart due to the differences between species and the physiology of the cells, but in combination with the cellular model described in this thesis they provide a detailed insight into processes in cardiac system during health and disease.

1.8.1 Cardiac ischaemia model

Cardiac ischemia occurs when blood flow to the myocardium is obstructed by a partial or complete blockage of a coronary artery. A sudden, severe blockage may lead to myocardial infarction. It is usually a result of a coronary thrombosis owing to rupture of an atherosclerotic plaque, resulting from a previous history of coronary heart disease. Cardiac ischemia is often associated with serious arrhythmia, which can cause sudden death.

In this thesis, it is planned to develop a cellular model of cardiac ischaemia using rat neonatal cardiac myocytes. Ischaemia is a complex metabolic insult consisting of two

main components; hypoxia (no oxygen) and substrate depletion (no energy (glucose)). The synchronously beating myocytes will be placed in a specially designed hypoxic chamber (Ruskinn Invivo$_2$ 400 Hypoxic workstation with Ruskinn gas mixer) and cultured in a low-glucose cell culture medium. The ischaemic model system is explained in more detail in chapter 2.

1.8.2 Thesis aims

The aims of this thesis were:

a) Develop a model of simulated ischemia in a beating cardiac myocyte cell culture system and to study relationships between Cx43 phosphorylation and myocyte beating

b) To investigate the effects and therapeutic potential of antiarrhythmic peptides on Cx43 behaviour during ischaemic and normoxic conditions.

c) To determine whether simulated ischaemia can activate connexin hemichannels and thereby examine any substances released across them, especially ATP, and their susceptibility to reagents that influence Cx function.

d) To explore the development and use of Cx-fluorescent probes in a cardiac myocyte model system.

Chapter 2

General materials and methods

2.1 General materials

2.1.1 Animals

Neonatal Wistar rats were used in the preparation of primary cultures of neonatal cardiac ventricular myocytes. Rats were obtained from breeding stocks from the animal house facility, UWCM and were housed in the same facility.

2.1.2 General laboratory reagents and chemicals

All reagents and chemicals were AnalaR grade and were obtained from Sigma (UK) or Fisons (UK) unless otherwise stated. All reagents and equipment for protein and DNA gel electrophoresis were from Biorad (UK) unless stated.

2.1.3 Composition of general buffers and solutions

- PBS: NaCl (137mM), Na_2HPO_4 (10mM), KCl (2.7mM); pH 7.4.
- Tris-HCl: Molar stocks of Tris-HCl at pH 7.4, 8.0 and 8.5 were prepared and stored at room temperature.

2.1.4 Myocyte culture solutions

- CBFHH: NaCl (137mM), KCl (5mM), $MgSO_4$ (0.8mM), KH_2PO_4 (0.4mM), Na_2HPO_4 (0.3mM), HEPES (18mM), Glucose (5mM), pH 7.4
- Trypsin stock solution: 1:250 trypsin (1g) dissolved in 10ml CBFHH at 4°C
- DNase stock solution: Deoxyribonuclease II from bovine spleen (30000 units, sigma) dissolved in 16ml 0.15M NaCl

- Trypsin working solution: Trypsin stock solution (1.5ml), DNase stock solution (0.7ml), P/S (100 $mgml^{-1}$) (0.5ml), volume adjusted to 50ml with CBFHH at 4°C
- DNase working solution: DNase stock solution (0.7ml), P/S (100 $mgml^{-1}$) (0.5ml), FCS (1ml), volume adjusted to 50ml with CBFHH at 4°C
- Cardiac myocyte cDMEM: Dulbecco's modified essential medium (DMEM), foetal calf serum (FCS) (5% (v/v)), penicillin/streptomycin (P/S) (100 $mgml^{-1}$)

2.1.5 Protein biochemistry reagents

- ATP-assay neutralisation buffer: HEPES (50mM), $MgSO_4$ (4mM), pH 7.4; in PBS
- Cell permeabilisation buffer: Triton X-100 (0.1% v/v), lysine (0.1M); in PBS.
- Blocking solution: TBS-T containing Marvel fat-free milk (5% (w/v))
- Lysis buffer: SDS (1% w/v), DTT 1mM, $NaVO_4$ 300mM, PMSF 100mM, protease inhibitor cocktail, PBS
- Nitrocellulose stripping buffer: 100mM β-mercaptoethanol, SDS (2% (w/v)), Tris-HCl (62.5mM), pH 6.7.

- Protease inhibitor cocktail (100x): Leupeptin (5mg), chymostatin (5mg), antipain (5mg), aprotonin (5mg), pepstatin A (0.5mg); volume adjusted to 10ml with dH_2O.
- SDS-PAGE running buffer (10x): Glycine (0.5M), Tris (250mM), SDS (1%(w/v));
- Separating gel buffer (SDS-PAGE): Tris (1.5M), SDS (0.4% (w/v)); pH 8.8.
- Stacking gel buffer (SDS-PAGE): Tris (0.5M), SDS (0.4% (w/v)); pH 6.8.
- SDS-PAGE sample buffer (4x): Stacking gel buffer (25% (v/v)), glycerol (40% (w/v)), β-mercaptoethanol (10% (v/v)), SDS (4% (w/v)), bromophenol blue; volume adjusted to 10ml with dH_2O.
- TBS-T (10X): NaCl (1.5M), Tris (0.2M), Tween-20 (1% (v/v)); pH 7.5.
- Transfer buffer: Na_2CO_3 (20mM).
- Molecular weight markers: Prestained SDS-PAGE standards (Precision plus protein standards, range 10-250kD; Kaleidoscope prestained standards, range 7-221kD, both Biorad, UK)

2.1.6 Molecular biology reagents and buffers :

- Agarose gel loading Buffer: TAE buffer (1X), glycerol (50% (v/v)), orange G; pH 8.0.

- LB-Agar: Bacto-tryptone (2% (w/v)), yeast extract (0.5% (w/v)), NaCl (10mM), Agar (1% (w/v))
- LB medium: Bacto-tryptone (2% (w/v)), yeast extract (0.5% (w/v)), NaCl (10mM)
- SOC medium: Bacto-tryptone (2% (w/v)), yeast extract (0.5% (w/v)), NaCl (10mM), KCl (2.5mM), $MgCl_2$ (10mM), $MgSO_4$ (10mM), glucose (20mM); pH 7.0
- TAE (50X Stock): EDTA (50mM), Tris (20mM), acetic acid (1mM).
- TE: Tris (10mM), EDTA (1mM); pH 8.0. Sterile filtered.
- Restriction enzymes: All restriction enzymes and appropriate buffers were obtained from Promega, UK unless stated otherwise.

Enzyme	**Restriction site recognised**	**Assay temperature**
***Eco* RI**	5'-G|AATTC-3'	37°C
***Xba* I**	5'-T|CTAGA-3'	37°C
***Not* I**	5'-GC|GGCCGC-3'	37°C

- Molecular weight markers: 1kB DNA ladder was obtained from Invitrogen, UK.
- **Bacterial cell culture**

All growth media were obtained from Sigma (UK), antibiotics from Promega (UK) and sterile plastic cultureware from Bibby Sterilin (UK). All glassware was washed in detergent free water and autoclaved (135°C, 90mins) before use. Growth media (LB, L-agar) were autoclaved under the same conditions prior to the addition of antibiotics (Promega UK). All bottles and containers were 'flamed' upon opening. Surfaces were swabbed with 70% (v/v) ethanol before and after use.

2.1.7 Cell culture reagents

All reagents and media and were obtained Gibco Life Technologies (UK) unless stated otherwise. Cell culture plasticware was obtained by Greiner bio-one (Germany). Media were free from mycoplasma contamination and were sterile filtered prior to use by passage through a 0.2μm filter. Sterile syringes and needles were obtained from WHRI Store (UWCM). All cell culture hoods were wiped with 70% (v/v) ethanol before and after use and fumigated regularly with vaporised formaldehyde.

2.1.8 Computer software and data analysis

Numerical data were stored in spread sheets (Excel, Microsoft) and were plotted in graphical form either using GraphPad Prism (GraphPad software inc., USA). All data are expressed as means ± standard deviation (SD) or as means ± standard error (SE). **SD** = $\sqrt{(n\sum x^2 - (\sum x)^2) / n(n-1)}$ and **SE** = SD/ $\sqrt{(n-1)}$ where n = number of variables and x = mean.

2.1.9 Health and safety

All reagents were handled and stored as recommended by manufacturer's safety sheets. All experiments were carried out in accordance with COSHH regulations and local college regulations. All genetic manipulation was registered and carried out following GMAG (genetically modified application guidelines). All mammalian and bacterial culture medium was disinfected with chloros (2% (v/v)); Philip Harris, UK and plastic culture wares were sterilised by autoclaving (135°C, 90mins) prior to disposal.

2.2 General methods

2.2.1 Preparation of primary cultures of neonatal rat cardiac myocytes

i) Preparatory work

On the day prior to the cell preparation, calcium and bicarbonate-free Hanks with Hepes buffer (CBFHH) was prepared and sterilised by filtration. In addition, trypsin solution was prepared and stored at 4°C overnight. Instruments for the cell preparation were sterilised by autoclave. The instruments consisted of large and small forceps, large scissors, small curved sprung scissors and a tissue culture sieve.

ii) Preparation of neonatal rat hearts

Approximately 50 – 60 Wistar rats aged 1 – 5 days were killed by cervical dislocation according to Schedule 1 of the Animals (Scientific Procedures) Act 1986 followed by removal of the head. The skin was sprayed with 70% ethanol, and the thorax opened on the left and right sides of the sternum by two separate incisions. The heart was removed and placed immediately in ice-cold CBFHH in a 100mm sterile tissue culture dish. During the procedure the instruments were sprayed frequently with 70% ethanol to maintain a high level of sterility. The animal carcases were then disposed of according to local regulations.

In a tissue culture hood, a second 100mm dish of cold CBFHH was prepared. Using small forceps, the hearts were removed one at a time from the first 100mm dish, extra-cardiac tissue (aorta, pulmonary artery and pericardium) removed using small curved scissors and the hearts cut in half and placed in the second 100mm dish of CBFHH. Hearts were washed repeatedly in CBFHH to remove red cells and any remaining fragments of non-cardiac tissue, using a 10ml wide-tip pipette. A small

volume of CBFHH was added to the heart fragments. Then, using small sprung scissors, heart fragments were minced into tiny pieces of no more than 0.3mm diameter. The minced hearts were suspended in cold CBFHH and transferred to a 50ml Falcon tube, marked "cells", using a 10ml wide-tip pipette. Once the minced hearts sedimented to the bottom of the tube, the supernatant was removed and discarded. The minced hearts were then washed further until the supernatant was clear of red cell contamination.

iii) Dissociation of tissue into cardiac myocytes

After removal of CBFHH, 10ml trypsin solution was added to the minced hearts in the "cells" tube. The "cells" tube was then placed on a rotary shaker set at a medium rate and left for 20mins. DNase solution (7ml) was then added to the "cells" tube, and, using a 10ml wide-tip pipette, the minced hearts were triturated to break up the DNA and release the dissociated cells. This trituration step usually required about 5mins. Following trituration, the minced heart fragments were allowed to settle and the supernatant was collected in a Falcon tube, marked "collection", containing 2ml of foetal calf serum (FCS). A further 10ml trypsin solution was added and the "cells" tube was placed on the rotary shaker for 5mins. A further 7ml of the DNase solution was added and the trituration step repeated. The minced heart fragments were again allowed to settle and the supernatant was transferred to the "collection" tube. This process was repeated for approximately 3-5hrs, which allowed most of the myocytes to be dissociated and left white fibrous tissue in the "cells" tube. A total of 4 collection tubes were usually necessary. Once each collection tube was full it was stored on ice until the next stage of the procedure.

iv) Centrifugation stage

The four collection tubes were centrifuged at 1200rpm for 6mins to loosely pellet the cells. The supernatants from the collection tubes were transferred to four 50ml Falcon tubes labelled "respin" and recentrifuged at 1200rpm for 6mins. The four pellets in the collection tubes were resuspended in DMEM supplemented with 5% FCS and 1% P/S (cDMEM) (2ml per pellet) and combined in a 50ml Falcon tube labelled "pooled cells". The supernatants from the "respin" tubes were discarded. The four pellets in the "respin" tubes were resuspended in cDMEM and added to the "pooled cells" tube. Stock DNase (400µl) was added to the "pooled cells" tube and the cell suspension was triturated using a wide-tip pipette. The "pooled cells" tube was centrifuged at 1200rpm for 6mins. The supernatant was discarded and the pellet was resuspended in 32ml cDMEM

v) Pre-plating stage

Four 100mm diameter dishes were used for pre-plating to remove fibroblasts. A sterile tissue culture sieve was prepared by passing 3ml cDMEM through it into the first dish. The cell suspension (8ml) was then added to each dish through the sieve. Finally, 3ml cDMEM was passed through the sieve into the final plate to wash off any cells trapped in the sieve. The four dishes were then incubated at 37°C, 80% humidity and 5% CO_2 for 1hr.

vi) Harvesting of cardiac myocytes

The medium from the 4 pre-plating dishes was harvested into a new 50ml Falcon tube, labelled "myocytes". The plates were then washed with cDMEM 3 – 4 times

and the medium transferred to the "myocytes" tube. The volume of the "myocytes" tube was adjusting to 50ml with cDMEM.

vii) Cell counting and plating

The cell suspension (10µl) from the "myocytes" tube was applied to a haemocytometer and cells were counted using the standard method. Cells were plated out in 60mm dishes at 5 x 10^6 cells per dish in a volume of 4ml per dish in cDMEM, supplemented with bromodeoxyuridine (BrDu) (0.1mM), added to suppress cell division in non-myocyte cells such as fibroblasts. Cells were then incubated at 37°C, 80% humidity and 5% CO_2. Typically each cell preparation yielded between 160-180 million cells, generating 40-50 60mm dishes if plated at the stated density. The resultant cultures of cardiac myocytes (>95%) (Clarke et al., 2006; Webster et al., 1999) contracted synchronously at >100 beats min^{-1} (bpm).

2.2.2 Maintenance of rat neonatal cardiac myocytes

On the day after the preparation, care was taken not to disturb the cells. Thereafter, the medium was changed every day with cDMEM with BrDu (0.1mM). The cardiac myocytes usually began to synchronously beat on day two after the cell preparation. Thereafter, the beating rate was monitored daily on a light microscope (Nikon). On day four after cell preparation, the type of medium was changed to serum-free medium. This consisted of DMEM with P/S (100µgml^{-1}), BrDu (0.1mM), insulin (20µgml^{-1}) and vitamin B12 (1.5µM). All experiments were performed on days 5,6 or 7 after cell preparation.

2.3 Ischaemia and hypoxia

2.3.1 The hypoxic workstation

Cells were made hypoxic within a specially designed chamber (Ruskinn Invivo$_2$ 400 Hypoxic Workstation with Ruskinn gas mixer), essentially a tissue culture incubator that was hermetically sealed, enabling precise control of the internal atmosphere. Humidity was maintained at 80% and the temperature at 37°C. Within the chamber an oxygen electrode measured the internal oxygen level and automatically flushed the chamber with nitrogen if the oxygen level increased, thus maintaining the internal gas composition at 0.5% oxygen, 5% CO_2 and the balance of the gas being nitrogen. The pressure in the chamber was maintained slightly above ambient so that any minor leak would cause egress of hypoxic gasses rather than ingress of atmospheric oxygen, further safeguarding the hypoxic environment.

Cells, instruments and solutions were placed in the chamber using a gas-tight air-lock. Items were placed inside the air-lock and the external door closed. Nitrogen was then pumped into the lock to remove any oxygen. The internal door could then be opened. Manipulation of cells inside the chamber was achieved using gas-tight sleeves. Rubber cuffs made a seal around the upper arms, air was removed by a vacuum pump and nitrogen was pumped in. The vacuum/flush cycle (operated by foot pedals) was repeated three times to ensure no oxygen remained in the sleeves. Small circular doors then allowed entry into the chamber.

Figure 2.1: In Vivo400 hypoxia cabinet
Manufacture's image of the In Vivo 400 cabinet (Ruskinn, UK). The main ports are open with the gas-tight sleeves removed. Within the chamber 60mm cell culture dishes are visible. On the right of the cabinet is the air-lock door which allows cells and equipment to enter the chamber without introducing oxygen. Reproduced from Ruskinn brochure, UK.

2.3.2 Monitoring myocytes beating rates

Myocyte beating rates were monitored during ischaemic and hypoxic experiments using a Nikon light microscope with camera linked up to a video monitor and computer. During ischaemia or hypoxia, myocyte beating rates were recorded by viewing and counting the cells by eye. Occasionally, to monitor these results taken manually the cells were video captured using the computer and software used to work out the beating rate of the cells. The results from the video capture showed that beating rates taken manually were very accurate, with differences only being on average <2 bpm.

2.3.3 Harvesting of cells during hypoxia

Since brief periods of reoxygenation may activate kinase pathways within the cells, great attention was paid to ensure that cells in the chamber remained ischaemic or hypoxic. Small volumes of ice-cold PBS and appropriate lysis buffer were made hypoxic by placing them in the air-lock on ice at least 30mins prior to harvesting. This allowed any oxygen dissolved in the PBS or lysis buffer to diffuse out of the liquid prior to its coming into contact with any cells. Once deoxygenated, the hypoxic PBS and lysis buffer were positioned in the chamber. Cells were washed twice with the deoxygenated PBS and excess removed completely. Cells were then scraped within the chamber in a suitable volume of hypoxic lysis buffer. The cell lysate was then collected in an Eppendorf tube that was kept on ice and immediately snap frozen on dry-ice once removed from the chamber. Cell lysate were then stored at -80°C for later analysis.

2.3.4 Anoxic experiments

i) Ischaemic experiments

In order to simulate ischaemic conditions, cells were placed in serum-free low glucose medium prior to hypoxic incubation. The medium consisted of glucose-free DMEM with P/S ($100\mu gml^{-1}$), BrDu (0.1mM), insulin ($20\mu gml^{-1}$), vitamin B12 ($1.5\mu M$) and glucose ($0.2mgml^{-1}$). The time spent in ischaemia began as soon as the cells entered the hypoxic chamber and varied between experiments from 1-10hrs. The ischaemic cells were then harvested within the hypoxic chamber as described above. Control cells were also placed in the low glucose medium for the duration of the experiment.

ii) Hypoxic experiments

Hypoxia treated cells were placed in serum-free cDMEM (described in section 2.2.2) prior to hypoxic incubation. The time spent in hypoxia began as soon as the cells entered the hypoxic chamber and varied between experiments from 1-10hrs. The hypoxic cells were then harvested within the hypoxic chamber as described above.

2.3.5 Reoxygenated cells

Ischaemic or hypoxic treated cells were removed from the chamber and placed in fresh serum-free cDMEM. These cells were then incubated at 37°C, 80% humidity and 5% CO_2 for 1hr following ischaemic/hypoxic incubation. Cells were then washed twice with ice-cold PBS and then scraped in a suitable volume of the appropriate lysis buffer. The cell lysate was then snap frozen in dry-ice and then stored at -80°C for later analysis.

2.4 Characterisation of connexin proteins in cardiac myocytes

2.4.1 Extraction of protein from myocytes

The lysis buffer was prepared on ice by adding protease inhibitor cocktail and PMSF, both at a dilution factor of 1:100. The cell culture medium was removed and the cells were washed twice in PBS. All liquid was completely removed and 200µl of lysis buffer was added. The cells were then scraped using a cell-scraper (Greiner, UK), then the lysate was transferred to an Eppendorf, snap frozen then stored at -80°C for later Western analysis. Before further analysis, the cell lysates were thawed and sonicated individually with 2 bursts of 10secs, using a sonicator probe to break down any residual DNA and to disperse the aggregated membranes.

2.4.2 Measurement of protein concentration using a colourmetric assay

The Biorad DC protein assay (Biorad, UK) was used as a colourmetric assay for the estimation of protein concentrations in the range of 100-500μgml^{-1}. The assay, based on the Lowry assay (Lowry et al., 1951), measures the reaction of proteins with alkaline copper tartarate and Folin reagent. Briefly, 5μl of protein sample was mixed with 25μl of reagent A (contains NaOH (1-5% (w/v), sodium tartatrate (<1% (w/v)) and copper sulphate (<0.1% (w/v) in a well of a microtitre plate. Following this, 200μl of reagent B (which is dilute Folin's reagent) was added and gently agitated to mix the reagents. Colour was allowed to develop for 15mins and absorbance read in a plate reader (Denley, UK) at 695nm (A_{695}). Protein concentration was calculated from the linear regression graph generated using the A_{695} of known concentration solutions of BSA (10-1500 μg/ml) prepared in the same buffer used in the extraction of protein.

2.4.3 Protein separation by SDS-polyacrylamide gel electrophoresis (PAGE)

Protein samples were separated mainly on the basis of size using discontinuous polyacrylamide gel electrophoresis and denaturing conditions as described by Laemmli (1970). Protein samples (100μg) extracted from treated cells were mixed by vortexing with a volume of SDS-PAGE (4X) sample buffer and agitated for 30mins at room temperature prior to loading the gel for electrophoresis. Discontinuous SDS-PAGE involved protein concentrating (stacking phase) and separating components. The separating gel mixture was mixed by swirling and was immediately transferred into a gel casting system (Biorad, UK). The gel was overlaid with dH_2O and allowed to set for 1hr at room temperature. After this time, the gel surface was washed with dH_2O and dried. The stacking gel was applied on top of the separating gel phase and an appropriate sample-well comb was inserted.

Reagents	Separating gel (10% (v/v)) (ml)	Stacking gel (5.0% (v/v)) (ml)
Stock acrylamide (40% (w/v)	7.2	0.9
Buffer	7.6 (separating)	1.8 (stacking)
Ammonium persulphate (10% (w/v))	0.448	0.060
TEMED	0.02	0.006
dH_2O	14.72	3.1
Final volume	30.0	5.9

The stacking gel was allowed to set for 30mins, the comb removed and sample wells were rinsed with dH_2O. Protein samples were loaded on to the gel and were separated by electrophoresis in SDS-PAGE running buffer at 40mA until the samples had run out from the sample wells. The current was then adjusted to 15mA and run overnight at room temperature until the dye front (bromophenol blue) diffused into the running buffer. Apparent size of proteins was deduced by reference to known molecular weight standards (Precision plus protein standards, range 10-250kD; and Kaleidoscope prestained standards, range 7-221kD, both Biorad, UK) separated under the same conditions.

2.4.4 Detection of connexin proteins by Western blotting

i) Transfer of proteins to nitrocellulose membranes

Proteins from acrylamide gels were transferred to a nitrocellulose membrane (Hybond-ECL, Amersham-Pharmacia Biotech, UK) for immuno-labelling analysis. The separating phase of the gel was overlaid with nitrocellulose membrane pre-wetted in transfer buffer and sandwiched between filter paper. The gel : membrane filter was

loaded into the transfer apparatus (Biorad, UK) with the membrane placed between the gel and the positive electrode. The proteins were transferred onto the membrane by electrophoresis in transfer buffer for 3hrs at room temperature and at 300V. Protein transfer was determined by staining the membrane (protein-side up) with Ponceau S solution (Ponceau S 0.1% (w/v)), acetic acid (5% (v/v); Sigma, UK).

ii) Immuno-labelling of protein on nitrocellulose membranes

Ponceau S stain on the nitrocellulose membrane was removed by washing the membrane several times in dH_2O and then with TBS-T for 1hr, changing the solution regularly. To prevent non-specific antibody binding, the membrane was blocked, by incubation in blocking solution at room temperature for 1hr. Membranes were then incubated with antibodies specific to the proteins, (normally at a dilution of 1:2000 in blocking solution as determined by previous titration of antibody against antigen) at 4°C for 12-15hrs. Primary antibodies used were Zymed rabbit anti Cx43 (Cambridge UK) (specific for phosphorylated and non-phosphorylated forms of Cx43) and Zymed mouse monoclonal anti Cx43 (specific for the non-phosphorylated form of Cx43). After this time, the membranes were thoroughly washed (~1hr) in TBS-T changing the solution frequently. Membranes were blocked at room temperature for a further 1hr in blocking solution as above. Membranes were then incubated in secondary antibody (goat anti rabbit or goat anti mouse conjugated to horse-radish peroxidase) (Biorad, UK) used at a dilution of usually 1:2000 in TBS-T at room temperature for 1hr. Membranes were extensively washed in TBS-T, changing the solution often and finally with PBS.

iii) Detection of immuno-labelled protein

Detection of immuno-labelled protein was carried out using enhanced chemiluminescence (ECL) (Super-Signal; Pierce, UK). A stable peroxide solution was mixed with an equal volume of luminol containing buffer and the membrane was overlaid with sufficient solution (5ml) to allow complete coverage for 1min. ECL solution was removed, the membrane placed on a thin transparent sheet and then covered with saran wrap. Air bubbles were removed using a roller. The membrane was transferred to a photographic cassette and exposed to X-ray film (Hyper Film, Amersham-Pharmacia Biotech, UK) for periods ranging from 15secs-2mins depending on the intensity of the chemiluminescence signal. The film was developed and dried at 50°C for 15mins.

iv) Densitometric analysis of protein blots

Developed films were scanned at 400-750nm using a densitometer (300dpi, GS-700, Biorad, UK). Bands corresponding to proteins were highlighted using Colour Scan software (Biorad, UK) and were compared by density analysis. All measurements were calibrated against an area of the blots containing no protein.

2.5 ATP measurements

ATP was measured using a luciferase-luciferin based bioluminescence assay (Sigma, USA). Briefly, ATP is consumed and light is emitted when firefly luciferase catalyzes the oxidation of D-luciferin:

$$\text{ATP} + \text{Luciferin} \underset{Mg^{2+}}{\overset{\text{Firefly Luciferase}}{\rightleftharpoons}} \text{Adenyl-luciferin} + PP_i$$

$$\text{Adenyl-luciferin} + O_2 \longrightarrow \text{Oxyluciferin} + \text{AMP} + CO_2 + \text{light}$$

The first reaction is reversible and the equilibrium lies far to the right, but the second reaction is essentially irreversible. When ATP is the limiting reagent, the light emitted is proportional to the ATP present. All ATP measurements were expressed as a percentage of the control.

i) Extracellular ATP measurements

Cell culture medium (250µl) was removed from the cell monolayer by sterile pipette tips at specific time points, then snap frozen and stored at -80°C. Extracellular samples were then centrifuged at 250g for 4mins at 4°C and analysed for ATP content using the ATP assay outlined below.

ii) Intracellular ATP measurements

Intracellular ATP measurements were made as previously described (Turner et al., 2004). Cells were washed twice with ice-cold PBS then 500µl 5% trichloroacetic acid (TCA) was added and the cells were scraped. The lysate and the pink coloured precipitate were collected in an Eppendorf tube, which was snap frozen and stored at -80°C for later analysis of ATP content. Intracellular samples were then thawed on ice, and then centrifuged at 12000rpm for 10mins at 4°C.

2.5.1 ATP Assay

ATP standards were made up to known concentrations in the range 0.5-10µM for intracellular samples or 1-100nM for extracellular samples, from a stock of 0.1M ATP stored at -80°C. For intracellular samples, luminometer cuvettes were with 200µL of ATP-assay neutralisation buffer in each and left at room temperature for 30mins. The ATP assay mix (Sigma, FL-AAM) was then prepared, at a dilution of 1:25 for

intracellular samples or 1:10 for extracellular samples, in ATP-Assay Mix Dilution buffer, and stored on ice. For extracellular samples, 50µl of ATP-assay mix working dilution was added to a luminometer cuvette followed by 50µl of sample, briefly mixed, and then measured for luminescence (Turner Designs 20/20 luminometer) three times for 10secs with the mean being recorded. For intracellular samples, 50µl of ATP-assay mix working dilution was added to the ATP-assay neutralisation buffer in the cuvette and 30 seconds allowed to elapse to ensure mixing. 5µl of standards or sample was added to the cuvette, briefly mixed, and then measured for luminescence three times for 10secs with the average being recorded.

2.5.2 ATP sample protein analysis

The protein concentration was calculated as a control for number of cells on each plate. The excess supernatant was removed and the TCA was neutralised with 500µL of 1M NaOH. The samples were left at room temperature and agitated for 30mins to allow the protein to dissolve. Protein concentration was then calculated using a Biorad DC protein assay kit as described in section 2.4.1. Intracellular ATP values were then normalised for protein concentration and expressed as ATP per unit of protein.

2.6 Immunofluorescence

2.6.1 Preparation of cells for immunostaining

Cardiac myocytes were prepared on two well glass coverchambers (Nunc) at a density of $1x10^6$ per well, or on 16mm diameter circular glass coverslips at a density of $5x10^5$ per coverslip. Following exposure to the experimental conditions cells were washed twice in ice-cold PBS and were fixed in 3.7% paraformaldehyde in PBS for 10mins or

-20°C methanol for 5mins. They were then washed twice with PBS and stored at 4°C in PBS.

2.6.2 Immunohistochemistry

Cells were permeabilised with PBS containing 0.1% Triton for 30 minutes and blocked with PBS containing 1% BSA for 30mins. Then 200µl of primary antibody to the samples incubated for 2hrs at 37°C in the dark. The primary antibody was then removed and samples were washed several times with ice-cold PBS. The secondary antibody was then added and incubated in a dark environment for 45mins at 37°C. The secondary antibody was then removed and the samples then washed thoroughly with PBS for 1hr, changing the solution regularly.

The samples in coverchambers were then stored in PBS at 4°C in the dark until analysis. The samples on coverslips were mounted on glass slides using FluorSave™ Reagent (Calbiochem, Germany) and stored in the dark at 4°C until analysis.

2.6.3 Antibodies

The main primary antibodies used for immunostaining Cx43 were the polyclonal antibody against Cx43 (raised in rabbit) (Zymed, Cambridge UK), or the monoclonal antibody against non-phosphorylated Cx43 ((Chemicon, Chandlers Ford, UK) or (Zymed, Cambridge, UK)). All were used at a dilution of 1:250 in PBS. The secondary antibodies used were a selection of either goat anti rabbit or goat anti mouse antibodies that were conjugated to either Alexa-488 or Alexa-546 fluorescent dyes.

2.7 Microinjection into cells

Microinjection into cells was used to assess direct cell-cell communication and to transfect cardiac myocytes with cDNA. Intracytoplasmic microinjection of dye or cDNA was achieved using an Eppendorf Femtojet 5247 device.

2.7.1 Monitoring direct cell-cell communication

Direct cell-cell communication was studied by monitoring the transfer of small fluorescent dyes between the cells in the monolayer. The dyes used were Lucifer yellow (charge -2, MW 457Da), Alexa-488 (charge –1, MW 570Da) or Alexa-594 (charge -1 MW 758Da). All dyes were from Molecular Probes (Leiden, The Netherlands). To ensure success, experiments were repeated in triplicate with >30 cells injected per experiment. Five minutes after injection cells were fixed in 4%w/v paraformaldehyde for 5mins and washed in PBS. The percentage of injections resulting in dye transfer to different numbers of neighbouring cells was assessed on an Zeiss Axiovert 200 fluorescence microscope using appropriate filter sets (Zeiss, UK) (Martin et al., 2004).

2.8 General molecular biology methods

2.8.1 DNA amplification by polymerase chain reaction (PCR)

PCR is an *in vitro* method of nucleic acid amplification involving repeated thermal cycles that cause DNA denaturation, primer annealing and DNA extension (Saiki et al., 1988). Briefly, substrate DNA is denatured at high temperature to give single stranded templates, followed by the annealing of oligonucleotide primers to specific, nucleotide sequences defined regions of the template at a lower temperature (T_{opt}). The primers are then extended enzymatically by a thermal stable DNA polymerase,

such as Taq polymerase. The resulting product is an additional double stranded DNA copy of the original template. The amplification process is exponential; therefore large quantities of DNA (μg) are generated from very small amount of template (ng). Bio-x-act Taq DNA polymerase (Bioline, UK) was used for all PCRs unless stated. Bio-x-act uses a complex of temperature-stable DNA polymerases possess 3'-5' exonuclease (proof-reading) activity. The optimum temperature of dNTP (Pharmacia, UK) incorporation using Bio-x-act is 68°C.

Optimal conditions for the DNA polymerase used in the reactions were achieved using buffers provided by the manufacturers. Reactions were set up in the thin walled tubes on ice with all reagents added to the dH_2O and mixed by brief vortexing. Negative controls were setup in all experiments which contained no DNA templates. The protocols for the reaction mixture and cycling conditions are shown below:

Reagents	**Per Reaction (μl)**
$MgCl_2$ (50nM)	2.2
10x Buffer	5
dNTPs (25mM)	0.5
Forward Primer	1
Reverse Primer	1
DNA Taq polymerase	0.5
DNA Template	X*
Ultrapure H_2O	38.8-X
Final volume	50

*Amount of DNA Template varied (3-60ng/μl)

Sample reactions were subjected to the following cycling conditions

- Hot start 94°C, 2mins
- 94°C, 2mins; 55°C, 1min; 68°C, 2 mins; (10 cycles)
- 94°C, 2mins; 55°C, 1min; 68°C, 2 mins + 20secs extension/cycle; (25 cycles)
- 68°C, 10mins

Following completion of cycling, reactions were kept at 4°C until analysis. All amplifications were carried out using a PCR Sprint Thermal Cycler (Thermo Electron, USA)

2.8.2 Analysis of DNA products by agarose gel electrophoresis

Double stranded DNA fragments were separated according to size and concentration by agarose gel electrophoresis. Agarose gels (1% (w/v)) were made by adding ultra-pure agarose (Biorad, UK) to TAE (1x) and heated for several minutes in a microwave (800W, Sanyo, UK) until completely dissolved. The gel solution was cooled and 1µl ethidium bromide added. The gel was then poured and a comb inserted into a gel tray (Mini Sub-DNA cell, Biorad, UK). DNA samples (5µl) were mixed with an equal volume of DNA loading buffer and loaded into the gel. DNA molecular size markers (5µl; Invitrogen, UK) were also loaded. Electrophoresis was carried out at 90V until the dye front migrated approximately two-thirds through the gel (orange G co-migrates with DNA ~200bp). The gel was visualised and photographed using a UV transilluminator lamp (302nm) integrated into a ChemiDoc™ (Biorad, UK) apparatus. Known amounts of DNA were run on an agarose gel and used as a comparison in order to estimate amounts of DNA produced by PCR.

2.8.3 DNA purification and modification

i) Purification of PCR products

PCR products were purified using the Qiagen PCR purification system (Qiagen, UK). Briefly, the PCR sample was mixed with 5 volumes of buffer containing 50mM KCl, 10mM Tris, 1.5mM $MgCl_2$, Triton X-100 (0.1% (v/v)); pH 8.8, vortexed and applied to a spin column membrane (column retains fragments 100bp-10kb). The column was centrifuged at 12,000g for 30secs. The flow through was discarded and washed twice in buffer PE (Qiagen, UK) containing 80% ethanol (0.75ml) and recentrifuged. To elute the DNA dH_20 (30µl) was added to the column and incubated for 1min at room temperature then centrifuged at 12,000g for a further minute.

ii) DNA extraction and purification of from agarose gels

PCR products analysed on agarose gels were then extracted and purified using the Qiagen gel extraction system (Qiagen, UK). Briefly, the desired DNA fragments were excised from the agarose gel with a clean scalpel, weighed, and incubated with 3 gel volumes of buffer QG (Qiagen, UK) at 50°C for 10-15mins. Once completely dissolved, one gel volume of isopropanol was added, vortexed and the solution applied to a spin column. The column was centrifuged at 12,000g for 30secs and the flow through discarded. Column washing and elution of DNA was as described above.

iii) Klenow modification

PCR products used for cloning or *in vitro* expression were modified using the Klenow fragment, a proteolytic cleavage fragment of DNA polymerase I (Klenow & Henningsen 1970) (Promega, UK) to fill in incomplete DNA chains and to remove

excess 3'A residues. Purified PCR fragments were incubated with Klenow fragment (1μl; 5U/μl), dNTPs (1μl; 20mM) and appropriate buffer at 25°C for 30mins.

2.8.4 Subcloning of PCR products

i) Ligation of PCR products

PCR products were ligated into plasmid vectors by a number of similar methods including TA cloning and TOPO cloning as described in chapter 6.2. Once ligated into the vector, plasmids were amplified in the competent bacteria DH5α.

ii) Transformation and culture of competent bacteria

Transformation of competent bacteria with plasmid DNA is a procedure that enables rapid and large scale replication of the plasmid DNA, which can be used for subsequent use and analysis. Plasmid DNA was introduced into competent DH5α E. coli (Invitrogen, UK) (50μl) by adding 10ng plasmid DNA to the cells and mixing by pipetting. Cells were incubated on ice for 30mins and then subjected to 'heat-shock' at 37°C for 20secs, and then returned to the ice for a further 2mins. Following the incubation on ice, 700μl of pre-warmed SOC medium (Invitrogen, UK) without antibiotics was added to the cells and incubated at 37°C in an orbital incubator (~150rpm) for 60mins. After this time, transformed E. coli (200μl) were plated out on duplicate LB-agar plates containing the necessary antibiotics: 50μg/ml ampicillin for pGEM-T, 50μg/ml carbenicillin and kanamycin for pCR3. The remaining cells were concentrated and plated out as necessary. The LB-agar plates were inverted and incubated at 37°C for 15–24hrs and stored at 4°C.

iii) Harvesting recombinant plasmids

Bacterial colonies should contain only transformed cells as antibiotic resistance is conferred by the recombinant plasmid. However, it is important to determine whether the cells contain plasmid only or plasmid plus insert DNA and whether the insert, if present, is in the correct orientation for expression.

Cells were harvested for DNA analysis using a QIAprep miniprep kit (Qiagen, UK), which uses the principle of alkaline lysis of bacterial cells followed by adsorption of DNA onto silica membranes in the presence of high salt. Colonies of cells were picked from L-agar plates using a sterile pipette tip and added to 3ml of pre-warmed LB containing the appropriate antibiotics into microfuge tubes. The cells were then propagated on an orbital shaker at 37°C for 12-15hrs. The cells were centrifuged at 6000rpm, the supernatant removed and then resuspended in buffer P1 (50 mM Tris-Cl, pH 8.0; 10 mM EDTA; 100μg/ml RNase A). A lysis buffer (200 mM NaOH, 1% SDS (w/v)) was then added and the tubes carefully inverted several times. The lysates were neutalised by adding a buffer containing 3M potassium acetate, pH 5.5 and mixed by inverting the tubes immediately, and a white precipitate formed. The precipitates were then centrifuged at 6000rpm for 10mins forming a compact white pellet. The resulting supernatants were applied to a QIAprep spin column and centrifuged for 1min to ensure that the DNA binds to the silica membrane in the column. The columns containing the bound DNA is then centrifuged twice in the presence of a wash buffer (1.0 M NaCl; 50 mM MOPS, pH 7.0; 15% isopropanol (v/v)). The columns were re-centrifuged to ensure any residual buffer was eliminated, and then the DNA was eluted in dh2O by centrifuging the column.

iv) Analysis of recombinant plasmids

The resultant plasmid DNA samples were digested with appropriate restriction endonucleases to analyse whether they contained the inserted DNA fragment and determine its orientation. The endonucleases were selected as their recognition sites were close to 5' or 3' termini of the DNA insert and in the MCS of the plasmid, resulting in a recognised diagnostic pattern when visualised on an agarose gel. A typical example of a restriction digest setup is shown below and was carried out at the respective recommended temperature and length of time (usually 37°C and 2-3hrs).

Plasmid DNA	1μg
Restriction enzyme (5U/μl)	1μl
10X Buffer*	1μl
H_20	to 10μl

*Buffer appropriate to restriction enzyme used.

v) Preparation of large quantities of DNA

If large quantities of DNA were required, the bacterial culture (1.5ml) transformed with recombinant plasmid was transferred into LB medium (250ml) containing the appropriate antibiotic and incubated at 37°C in an orbital shaker for 15hrs at 150rpm. The plasmid DNA was isolated and purified according to the Qiagen maxi-prep protocols check. Briefly, bacterial culture (250ml) was transferred to a 300ml centrifuge tube (Sorvall instruments, UK) and cells were pelleted by centrifugation at 6,000g for 30mins at 4°C. Pellets were resuspended, lysed and proteins precipitated by using resuspension buffer, lysis solution and neutralisation buffer (10ml each, Qiagen, UK), as described in the previous section. Samples were centrifuged at 30,000g for 30mins at 4°C. Supernatants were filtered through gauze onto a Qiagen

ion-exchange column (Tip 500) pre-equilibrated with equilibration buffer (10ml) (containing NaCl (750mM), MOPS (50mM), ethanol (15% (v/v)), Triton X-100 (0.15% (v/v)); pH 7.0). A wash buffer (NaCl (1M), MOPS (50mM), isopropanol (15% (v/v)) pH 7.0; 2 x 30ml) was passed twice through the columns and DNA was eluted with 15ml elution buffer (NaCl (1.25M), Tris-Cl (50mM), isopropanol (15% (v/v)); pH 8.5). DNA was precipitated from solutions using isopropanol (75% (v/v), 10.5ml) and centrifuged at 11000rpm for 30mins at 4°C After the supernatant was removed ethanol (70% (v/v), 15ml) was added and the DNA was centrifuged at 11000rpm for 15mins at 4°C. The supernatant was removed and dried before being resuspended in 300µl dH_2O. The concentrations and purity of the DNA were determined, and stock solutions (1mg/ml) were stored at –20°C.

2.8.5 DNA Sequencing

i) Sequencing reactions

Automated sequencing was carried out using the BigDye® Terminator v3.1 cycle sequencing kit (Applied Biosystems, USA) on an ABI Prism 377 sequencer (Applied Biosystems, USA). The standard protocol is shown below:

Terminator ready reaction mix*	4.0µl
DNA Template	250-500ng
Primer (3.2pmole/µl)	3.2pmol (1µl)
dH_2O	to 10µl

*Terminator ready mix includes fluorescently labelled dye terminators dNTPs (dCTP, Rox (Red); dTTP, Tamra (Yellow); dATP, R6G (Green); dGTP, R110 (Blue)), Tris-HCl, pH 9.0, $MgCl_2$, thermal stable pyrophosphate and AmpliTaq DNA polymerase, FS.

Samples were subjected to cycling conditions as follows using a PCR Sprint Thermal Cycler (Thermo Electron, USA).

- Hot start 96°C
- 96°C, 10secs; 50°C, 5secs; 60°C, 4mins; (25cycles)

Samples were incubated on held at 4°C until ready to use.

ii) Sample preparation

Following cycle sequencing, the DNA extension products were precipitated. Tubes were briefly centrifuged and isopropanol (75% (v/v), 80µl) was added, vortexed, and incubated at room temperature for 20mins. The precipitated DNA was then centrifuged at 14,000g for 45mins at 4°C and the DNA pellet was washed with 75% (v/v) isopropanol by centrifugation at 14,000g for 10mins and air dried for 10mins. Sequencing results were obtained by Core Molecular Biology Facility, Heath Hospital, Cardiff.

Chapter 3

Effects of simulated ischaemia, reoxygenation and connexin mimetic peptides on rat neonatal cardiac myocytes

3.1 Introduction

Coronary or ischaemic heart disease (CHD) is the leading cause of death in the Western world (30% of male, 23% of female deaths). In CHD, the blood supply to the myocardium is insufficient for its needs and leads to ischaemia. Ischaemia is a complex metabolic insult comprising hypoxia, substrate depletion, acidosis and a build up of toxic metabolites. Cardiac ischaemia is frequently accompanied by lethal arrhythmias, likely caused by electrical conduction abnormalities possibly resulting from changes in the extent of phosphorylation of Cx43 that may, in turn be linked to reduced electrical coupling of myocytes via gap junctions (Saffitz 2000). Cx43 dephosphorylation is associated with electrical uncoupling of cardiac myocytes during global ischaemia induced with the Langendorff model (Beardslee et al., 2000). However, the cessation of mechanical function (beating) occurs much earlier than the dephosphorylation of Cx43 (Beardslee et al., 2000).

Cardiac ischaemia causes a number of possible clinical presentations. Acute myocardial infarction occurs when an epicardial coronary artery is occluded, usually by thrombosis within a diseased vessel (Fuster et al., 1992). Subsequently, an area of myocardium is deprived of blood flow and causes a short-lived period of angina pectoris. Patients usually develop ventricular arrhythmia (ventricular fibrillation or ventricular tachycardia). As ischemia continues, the affected area of myocardium stops contracting, but is susceptible to a second period of ventricular arrhythmia. Ventricular damage can be minimised if sufficient blood flow is restored quickly (Simes et al., 1995). Thus, the therapeutic approach to myocardial infarction is to re-open the artery and restore blood

flow (reperfusion). This is usually achieved with thrombolytic drugs (such as warfarin or heparin) or percutaneous transluminal coronary angioplasty (PTCA) usually in combination with implantation of an intra-coronary stent (Braunwald et al., 2000; Keeley et al., 2003). However, reperfusion can cause "reperfusion arrhythmia" and oxidative stress in the myocytes (Yellon & Baxter 1999).

In studies using rabbit hearts, ischemia was shown to induce two phases of ventricular arrhythmia, the first of which occurred between 5-7mins after arrest of perfusion and was associated with membrane depolarization and mild acidification (Cascio et al., 2005). A second phase of ventricular arrhythmia occurs later between 20-30mins after stopping perfusion and was associated with a rapid increase of tissue impedance, thought to be due to conductance properties of the gap junctions accounting for cell-to-cell coupling. An important property that is modulated by ischemia is intercellular resistance and is determined primarily by gap junctional conductance. During ischemia, conduction slowing accounts for changes of cellular excitability and during the first 10 minutes of ischemia, 70% of the decrease of conduction velocity is owing to the change in active membrane properties (i.e. gap junctions and membrane channels) (Cascio et al., 2005).

3.1.1 Ischaemia and Cx43 Phosphorylation

Cx43 phosphorylation occurs primarily on multiple serine residues located on the carboxyl tail and is mediated by several known and unknown protein kinases, for example, PKC and MAP kinase (Chapter 1, Figure 1.9). The carboxyl tail of Cx43

contains 21 serine residues and the amino tail contains two. Phosphorylation of Cx43 by PKC has been shown to have variable effects on gap junction channel conductance. In rat neonatal cardiac myocytes, activation of PKC is variously reported to cause an increase in conductance (Kwak et al., 1995), a decrease in conductance (Munster & Weingart 1993) or no change in conductance (Spray & Burt 1990). Clearly, phosphorylation of gap junction proteins is a complex process and its functional role remains controversial.

Global ischemia in a rat Langendorff model results in dephosphorylation of Cx43 in the intact heart (Beardslee et al., 2000). The reversibility of this dephosphorylation event upon reperfusion has not been definitively demonstrated with data being inconsistent. Beardslee et al. (2000) reported a degree of rephosphorylation in some hearts, with others showing continued dephosphorylation. It has been observed that infarct size was reduced upon application of the gap junction blocker heptanol at the time of reperfusion (Garcia-Dorado et al., 1997), which suggests that gap junctions may have a cardiotoxic effect during or after reperfusion, i.e. communication across gap junctions exacerbates damage following infarction. Therefore, it is important to determine the regulatory processes involving Cx43 during ischaemia/reperfusion, in order to explore any therapeutic potential for gap junction modifying drugs.

3.1.2 Intrinsic responses in the myocardium

Following the onset of ischaemia, intrinsic responses protect the cell. ATP and pH levels fall causing the cell to change to glycolytic metabolism. The increase in intracellular Ca^{2+} is initially buffered by uptake into mitochondria, but phospholipids and free-fatty acid levels also rise as mitochondrial respiration stops. As membrane integrity fails, damage to the cell becomes irreversible (Williams & Benjamin 2000). Reperfusion puts the cell under significant stress, and as blood flow is restored reactive oxygen species activate apoptotic signalling cascades (Hernandez et al., 2000). Apoptosis can also be induced by mitochondrial damage (Bialik et al., 1999) and hypercontractive necrosis can occur due to Ca^{2+} overload of the mitochondria (Wang & Ashraf 1999).

Hypoxia inducible factor 1 (HIF-1) is a transcriptional activator that functions as the main regulator of oxygen homeostasis (Semenza 2001). HIF-1 is a heterodimer composed of HIF-1α and HIF-1β subunits. During normoxia, the HIF-1α subunit is ubiquitinated and subjected to rapid proteasomal degradation whereas in hypoxia the amount of HIF-1α that is ubiquitinated is dramatically reduced, causing the protein to accumulate (Kallio et al., 1999; Sutter et al., 2000). The two subunits of HIF-1 then form the active heterodimer and can now activate a number of oxygen responsive genes.

Hypoxia/ischaemia has dramatically stimulatory effects on vascularization of the coronary vasculature in foetal and juvenile animals. However, in aged animals, angiogenesis is impaired due to inhibition of vascular endothelial growth factor (VEGF)

production by HIF-1 activity (Rivard et al., 2000). During hypoxia it was also shown that HIF-1 was essential for the regulation of iNOS gene expression in cardiac myocytes (Jung et al., 2000).

Previous models of hypoxia have used metabolic poisons such as potassium cyanide and iodoacetic acid (Li & Nagy 2000), which have additional effects to the induction of hypoxia especially the chemical inhibition of essential metabolic processes that ultimately kill the cell. In our approach described in this chapter, we have devised an ischaemia model that simulates more accurately the events that occur in infarction. Primary rat neonatal cardiac myocytes were utilised and ischaemia was simulated by combining hypoxia, induced precisely using a hypoxic chamber, with substrate depletion, achieved by using a low glucose cell culture medium.

3.1.3 Chapter aims

The investigations in this chapter were to study the effects of hypoxia and simulated ischaemia on Cx43 phosphorylation status and cell beating rates in our cardiac ischaemia cellular model system of rat neonatal cardiac myocytes. The effects of two connexin mimetic peptides on the cardiac myocytes were examined.

3.2 Methods

3.2.1 Materials

Calf intestinal phosphatase was from Promega (Southampton, UK) and Alexa-488 was obtained from Molecular Probes (Leiden, The Netherlands). GAP 26 and GAP 27 were synthesised by Fmoc (9-fluorenylmethyl carbamate) - polyamide solid-phase chemistry and assessed for purity by MALDI-TOF mass spectrometry and reversed phase HPLC (Sigma-Genosys, Cambridge, UK). All other reagents were obtained from Sigma (Poole, U.K).

3.2.2 Cell culture

Rat neonatal cardiac myocytes were prepared and plated as described in chapter 2 (Clarke et al., 2006; Turner et al., 2004). Cells were maintained cDMEM with BrDu (0.1mM) for the first 3 days and thereafter in serum-free medium as described in 2.2.2.

3.2.3 Hypoxia and ischaemia

Cardiac myocytes were made hypoxic in a gas tight humidified 37°C anaerobic chamber, with an internal environment of 0.5% oxygen and 5% carbon dioxide, as described in chapter 2. Cardiac myocytes were manipulated inside the hypoxic chamber to maintain a hypoxic environment at all times, as described in 2.3. Cell beating rate was monitored using a Nikon light microscope located within the hypoxic chamber. Control cells were incubated in a tissue culture incubator (Heraeus® HERAcell® 150) at 37°C and an environment of 21% oxygen and 5% carbon dioxide. For ischaemic treatment, cells were placed in low glucose ($0.2gL^{-1}$) serum free medium for the duration of the experiment

and for hypoxic and control treatments, cells remained in the serum-free medium ($3gL^{-1}$ glucose), as described in 2.3.4.

3.2.4 Dye transfer across gap junctions

Rat neonatal cardiac myocytes were seeded at a density of $4x10^6$ cells/60mm dish. Direct cell-cell communication was assessed before and after treatment of the cells with the connexin mimetic peptides GAP26 and GAP 27, by studying transfer of Alexa-488 (charge –1, MW 570Da) following intracytoplasmic microinjection of dye using an Eppendorf Femtojet 5247 device. Experiments were repeated in triplicate with >30 cells injected per experiment. Five minutes after injection cells were fixed in 4%w/v paraformaldehyde for 5mins and washed in PBS prior to the percentage of injections resulting in dye transfer to different numbers of neighbouring cells being assessed on an Zeiss Axiovert 200 fluorescence microscope using appropriate filter sets (Zeiss, UK) (Martin et al., 2004).

3.2.5 Western blot analysis

Rat neonatal cardiac myocytes on 60mm dishes ($4x10^6$), were treated and then harvested as described 2.4.1. Equal amounts of protein (100μg rat neonatal cardiac myocyte lysates; 50μg HeLa cell lysates) were analysed by SDS-PAGE (10% w/v) (described in 2.4.3) and transferred to nitrocellulose membrane for immuno-detection of Cx43 as described in 2.4.4. Membranes were probed with a polyclonal antibody to Cx43 (Zymed, USA) (1:4000 dilution) that recognises multiple phosphorylated/nonphosphorylated isoforms of Cx43 and a secondary goat anti rabbit horseradish peroxidase antibody

(1:2000 dilution). To standardise protein expression, blots were also probed with a monoclonal antibody to α-tubulin (1:10000 dilution) and a secondary goat anti mouse horseradish peroxidase antibody (1:2000 dilution). Blots were developed by enhanced chemiluminescene (ECL) and quantified using a Biorad GS-700 densitometer as described in 2.4.4.

3.2.6 Connexin 43 phosphorylation assays

Protein extracts (30μg) were digested with 60 units of calf intestinal phosphatase for 1hr at 37°C and analysed by SDS-PAGE and Western blotting as described above. In some experiments cells were treated with 100ng/ml TPA, a protein kinase C activator, for 30mins prior to harvesting the cells to serve as a positive control when analysing serine 368 phosphorylation of Cx43.

3.2.7 Statistical analysis

Cell beating rate data was analysed by unpaired t-test and ANOVA (analysis of variance) followed by Dunnett's multiple comparison test, with $P<0.05$ being considered significant.

3.3 Results

3.3.1 Immunoblot analysis of Cx43

Immunoblot analysis of rat neonatal cardiac myocytes showed that Cx43 separated into two phosphorylated forms (P1 and P2 bands) that migrated at 43 – 45 kDa and a minor band at 41 kDa, which represents the non-phosphorylated form. Occasionally, an additional phosphorylated band (P3) migrated at 46 – 48 kDa. These observations are shown in Figure 3.1a. Removal of the phosphorylated bands occurred after alkaline phosphatase treatment, confirming that the 41kDa band was the non-phosphorylated form of Cx43 (Figure 3.1b). These results concur with previous reports regarding the phosphorylation state of Cx43 in cardiac myocytes (Beardslee et al., 2000).

3.3.2 The effects of simulated ischaemia on cardiac myocyte beating and Cx43 phosphorylation

Cultured rat neonatal cardiac myocytes maintained in serum-free low glucose (0.2g/L) medium contracted synchronously at an average rate of 160bpm. Incubation of cardiac myocytes in hypoxia (0.5% O_2), in combination with the substrate-depleted cell culture medium (see above) caused cessation of beating within 3-4hrs, as shown in Figure 3.2. The beating rate then gradually decreased during the first 2hrs of ischaemic incubation, and it was also observed that cessation of beating after this time was mainly due to a gradual loss of amplitude (Figure 3.2).

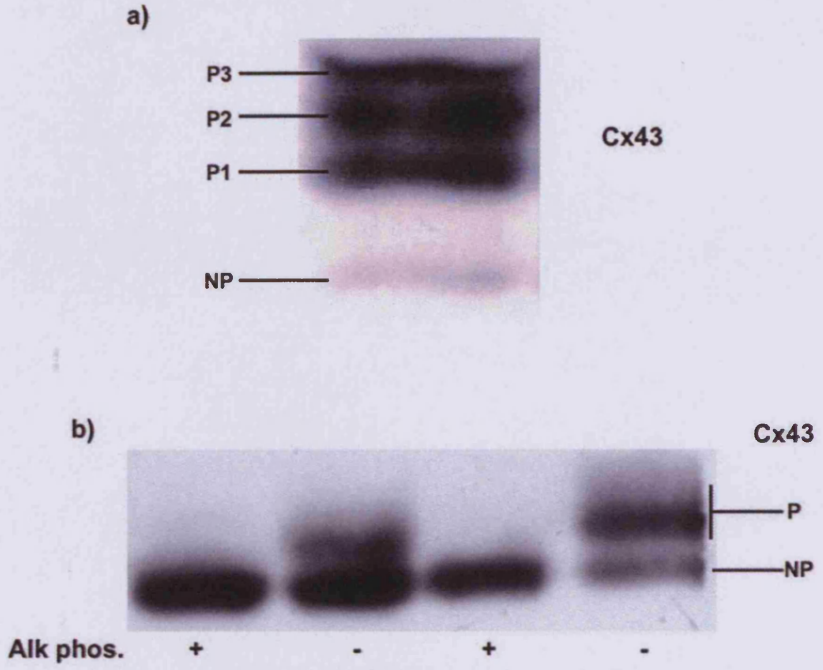

Figure 3.1: Analysis of Cx43 in rat neonatal cardiac myocytes
Confluent monolayers of rat neonatal cardiac myocytes were harvested for protein analysis and the cell lysates analyzed by standard SDS-PAGE and Western blotting with an antibody targeted to Cx43. a) shows typical state of Cx43 in the cardiac myocyte in normoxia, and b) after alkaline phosphatase (alk phos.) treatment of cardiac myocyte cell lysates illustrating the elimination of the phosphorylated isoforms of Cx43.

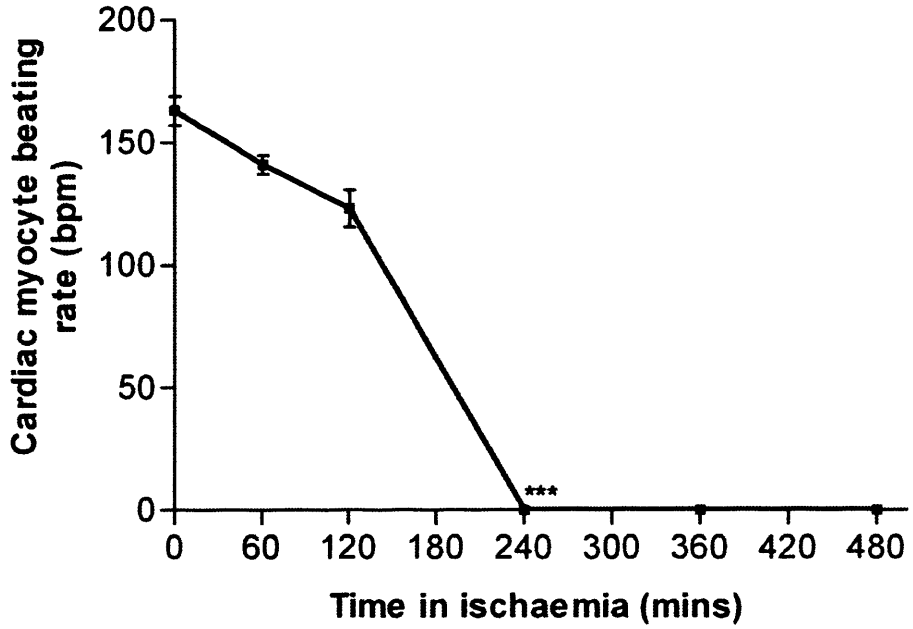

Figure 3.2: The effect of ischaemia on the beating rates of rat neonatal cardiac myocytes

Confluent monolayers of rat neonatal cardiac myocytes were exposed to ischaemia and cell beating rates were recorded. Cells were viewed under a light microscope within the hypoxic chamber. Data analysed by unpaired t-test. *** $P<0.001$ (n=4).

During ischaemia, the phosphorylated component of Cx43 was maintained up to 4hrs (Figure 3.3), but after 5hrs of ischaemia, the phosphorylated component of Cx43 decreased from 51.4% to 23.3% of total Cx43. The phosphorylation state of Cx43 then remained stable for further periods of 6 and 7hrs of ischaemic insult. However, Cx43 expression levels were decreased by approximately half after 7hrs of ischaemia (Figure 3.4).

In some experiments involving ischaemic incubations, Cx43 phosphorylation was not always completely abolished. However, the levels of phosphorylated Cx43 always decreased from control levels with expression levels remaining fairly constant. Variations in the quality of the cardiac myocytes from each preparation and insufficient length of hypoxic incubations may account for these variations.

3.3.3 The effects of simulated ischaemia and reoxygenation on cardiac myocyte beating and Cx43 phosphorylation

Incubation of cardiac myocytes in ischaemic conditions caused cessation of synchronous beating after 3-4hrs. After 5-7hrs of ischaemia, the cells were reoxygenated and resumed their synchronous beating, with cells recovering to 76.1% and 59.5% of the starting beating rate, for reoxygenation after 6hrs and 8hrs respectively (Figure 3.5a).

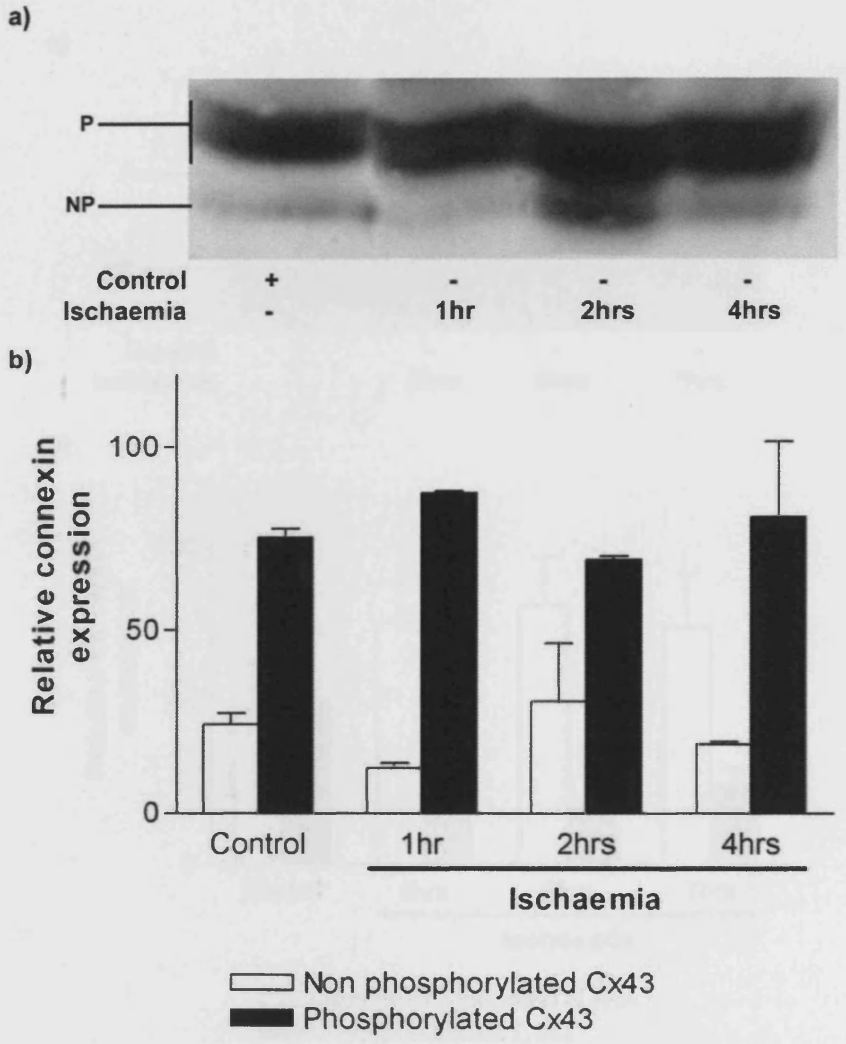

Figure 3.3: The effect of ischaemia on the phosphorylation status of Cx43
a) A typical (representative) Western blot of confluent monolayers of rat neonatal cardiac myocytes were subjected to ischaemia for 1-4hrs and the cell lysates analyzed by standard SDS-PAGE and Western blotting with an antibody targeted to Cx43. (b) Rat neonatal cardiac myocytes were treated as mentioned above. The graph shows the combined densitometric analysis of 2 Western blots.

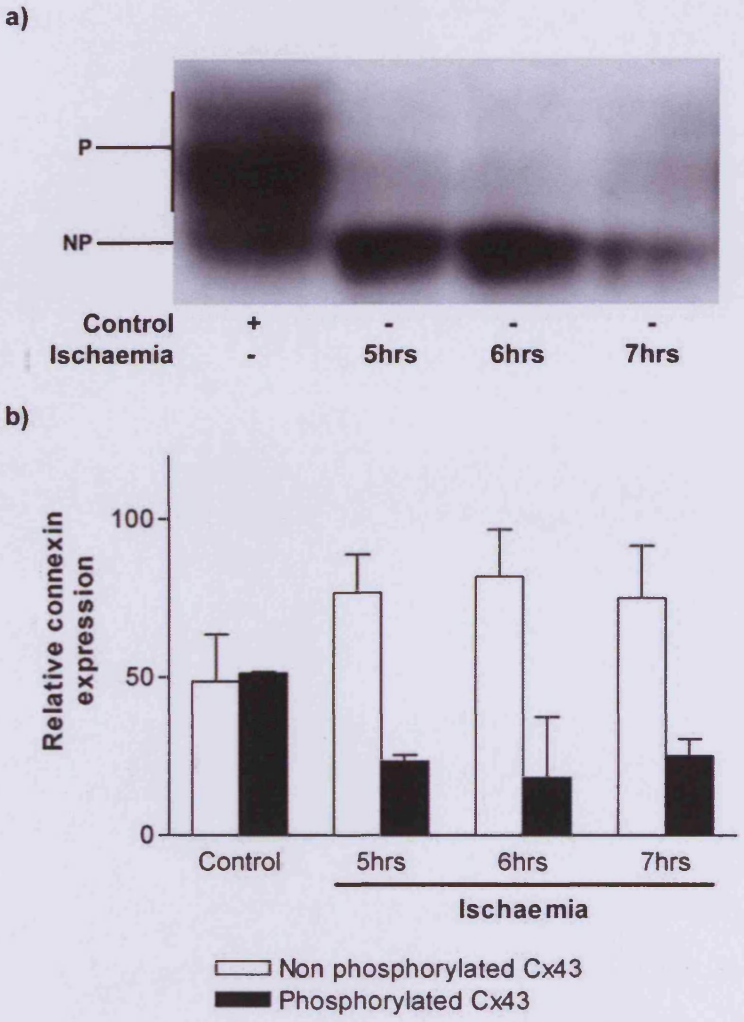

Figure 3.4: The effect of prolonged ischaemia on the phosphorylation status of Cx43

a) Confluent monolayers of rat neonatal cardiac myocytes were subjected to ischaemia for 5-7hrs and the cell lysates analyzed by standard SDS-PAGE and Western blotting with an antibody targeted to Cx43. (b) Rat neonatal cardiac myocytes were treated as mentioned above. The graph shows the combined densitometric analysis of 2 Western blots.

As shown in Figure 3.4, ischaemic incubation for greater than 5hrs abolished the phosphorylated component of Cx43. Reoxygenation of ischaemic cardiac myocytes after 5hrs of insult resulted in the recovery to control levels of the phosphorylated component of Cx43 (Figure 3.6). Cx43 rephosphorylation also occurred after more prolonged periods of ischaemia of 6 and 7hrs (Figure 3.6).

Reoxygenation of ischaemic cardiac myocytes resulted in a recovery of Cx43 phosphorylation and beating function. To assess the dynamics of the recovery, cardiac myocytes were subjected to ischaemic insult for 6hrs and then reoxygenated. Upon reoxygenation, cells began to beat after 10mins of reoxygenation, with synchronous beating restored after 20mins (Figure 3.5b). This suggests that gap-junctional communication is restored rapidly.

Ischaemic incubation (6hrs) of cardiac myocytes resulted in a reduction in Cx43 phosphorylation levels (Figure 3.7). Reoxygenation of ischaemic myocytes for 2 minutes had little effect on Cx43 phosphorylation, but after 5mins reoxygenation Cx43 phosphorylation had recovered to approximately control levels and was maintained thereafter (Figure 3.7). Importantly, recovery of phosphorylation occurred before the recovery of synchronous beating.

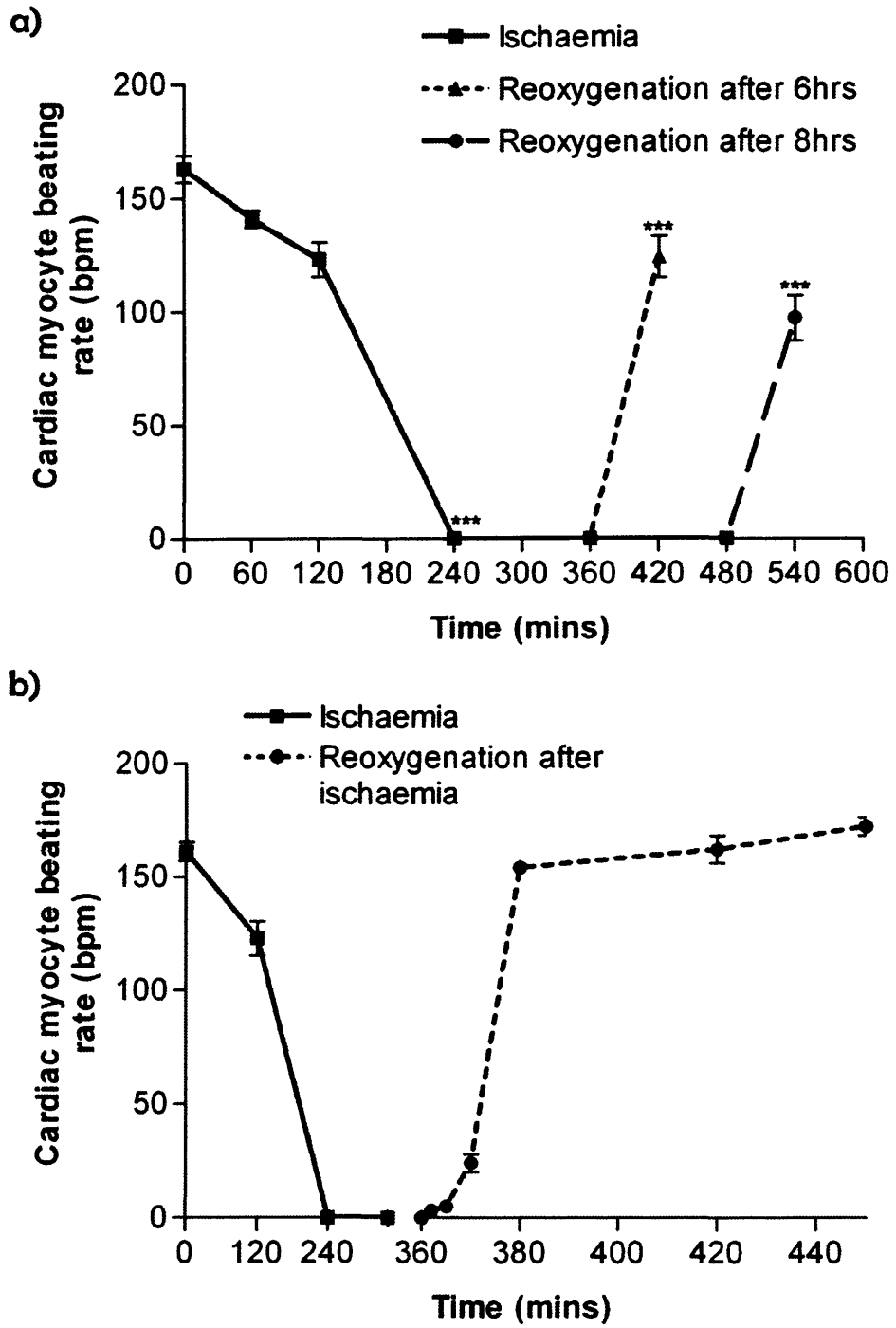

Figure 3.5: The effect of ischaemia/reoxygenation on the beating rates of rat neonatal cardiac myocytes

Confluent monolayers of rat neonatal cardiac myocytes were exposed to ischaemia for either 6hrs or 8hrs and then reoxygenated a) cell beating rates were recorded after 30mins or b) cell beating rate was recorded at specific time points. Cells were viewed under a light microscope within the hypoxic chamber. Data analysed using one-way ANOVA followed by Dunnett's Multiple Comparison Test. *** $P<0.001$ (n=4).

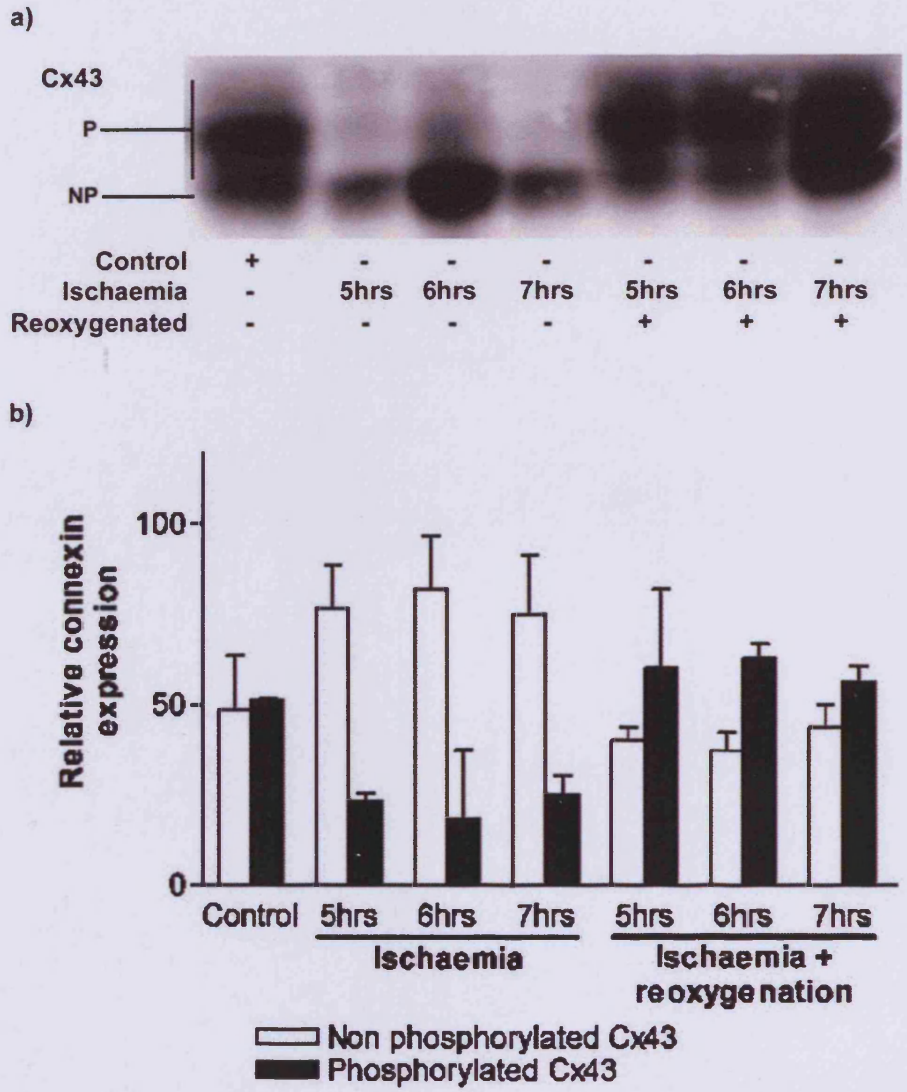

Figure 3.6: The effect of ischaemia/reoxygenation on the phosphorylation status of Cx43

a) Confluent monolayers rat neonatal cardiac myocytes were subjected to normoxia, ischaemic insult for 5hrs, 6hrs or 7hrs, or reoxygenation after 5hrs, 6hrs or 7hrs of ischaemic insult. Cell lysates analyzed by standard SDS-PAGE and Western blotting with an antibody targeted to Cx43 and α-tubulin. Lane 1 - Control; Lane 2 - 5hrs ischaemia; Lane 3 - 6hrs ischaemia; Lane 4 - 7hrs ischaemia; Lane 5 - 5hrs ischaemia followed by 1hr reoxygenation; Lane 6 - 6hrs ischaemia followed by 1hr reoxygenation; Lane 7 - 7hrs ischaemia followed by 1hr reoxygenation. (b) Rat neonatal cardiac myocytes were treated as mentioned above. The graph shows the combined densitometric analysis of 2 Western blots.

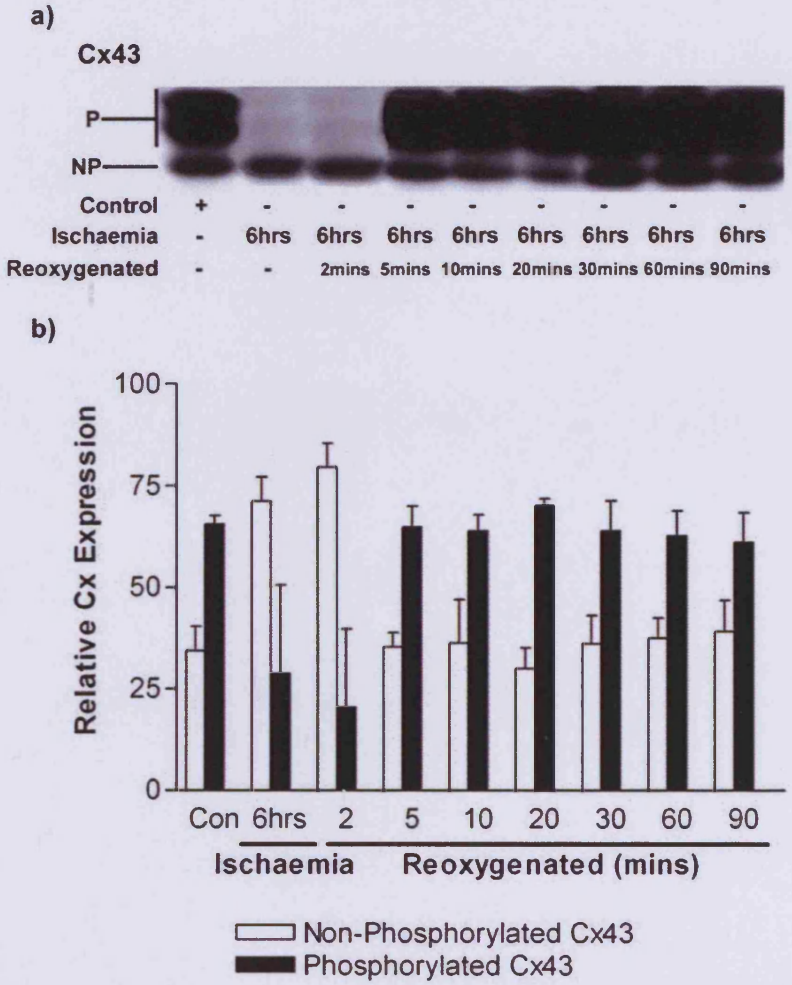

Figure 3.7: The effect of reoxygenation on the phosphorylation status of Cx43 in ischaemic rat neonatal cardiac myocytes

a) Confluent monolayers rat neonatal cardiac myocytes were treated with 6hrs of ischaemic insult, then subjected to reoxygenation and harvested for protein analysis at specific time points. Cell lysates analyzed by standard SDS-PAGE and Western blotting with an antibody targeted to Cx43. Lane 1 - Control; Lane 2 - 6hrs ischaemia; Lane 3 - 6hrs ischaemia + 2 minutes reoxygenation; Lane 4 - 6hrs ischaemia + 5 minutes reoxygenation; Lane 5 - 6hrs ischaemia + 10 minutes reoxygenation; Lane 6 - 6hrs ischaemia + 20 minutes reoxygenation; Lane 7 - 6hrs ischaemia + 30 minutes reoxygenation; Lane 8 - 6hrs ischaemia + 60 minutes reoxygenation; Lane 9 - 6hrs ischaemia + 90 minutes reoxygenation. (b) Rat neonatal cardiac myocytes were treated as mentioned above. The graph shows the combined densitometric analysis of 2 Western blots.

3.3.4 Effects of connexin mimetic peptides on gap-junctional communication in rat neonatal cardiac myocytes

To demonstrate that intercellular transfer of dye occurred across gap junctions, cardiac myocytes were treated with the connexin mimetic peptides GAP 26 (300μM) and GAP 27 (300μM) 30mins prior to microinjection (Figure 3.8). Dye transfer was dramatically reduced by both peptides with GAP 26 causing 10% and 35% of cells to transfer dye to no cells or 1-4 cells respectively (Figure 3.9a). GAP 27 reduced dye transfer, with 25% and 55% of cells transferring dye to no cell or 1-4 cells respectively (Figure 3.9b). Previous reports showed GAP 27 decreased dye transfer but to a lesser extent (Chaytor et al., 1999), likely due to the use of COS-7 cells which do not communicate as efficiently by gap junctions as cardiac myocytes. Both peptides reversibly reduced dye transfer and after washout, transfer was restored with 55% and 75% of cells transferring dye to >11 cells after GAP 26 and GAP 27 treatment respectively (Figure 3.8iv,vi and 3.9). In combination with a reduction in intercellular communication the connexin mimetic peptides caused a reduction in cardiac myocyte beating rate (Figure 3.10). The beating rate decreased by approximately 45% after treatment with GAP 26 for 1hr. After 2hrs of treatment the beating rate was further reduced to approximately 25% of the control rate (Figure 3.10a). Importantly, the synchronicity of the cardiac myocyte beating was not affected by the connexin mimetic peptides.

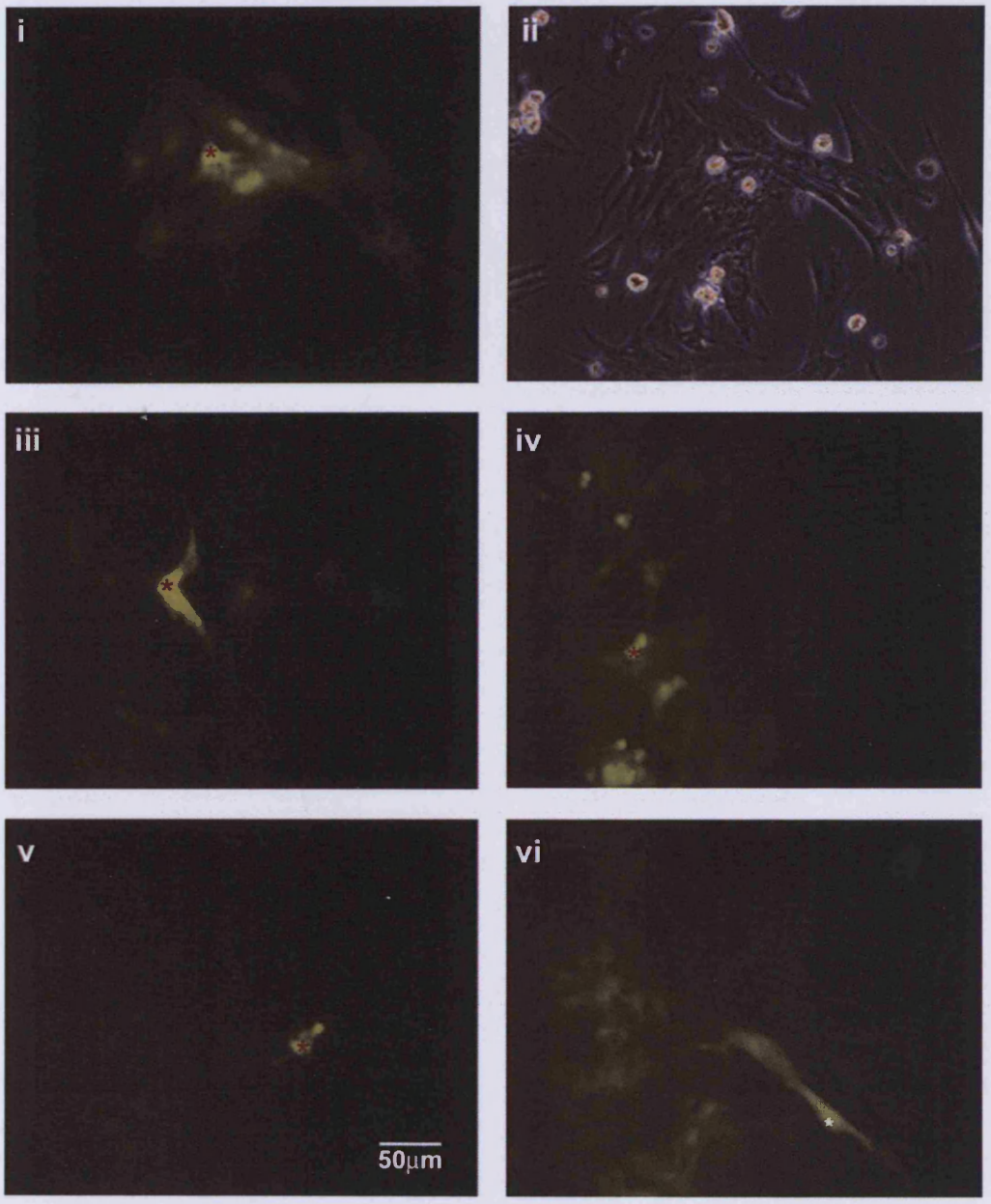

Figure 3.8: The effect of the connexin mimetic peptides GAP 26 and GAP 27 on Alexa-488 transfer in rat neonatal cardiac myocytes

Confluent monolayers of rat neonatal cardiac myocytes were viewed under a fluorescent microscope immediately after microinjection of Alexa-488. (i) Control cells; (ii) Control cells phase view; (iii) Following 30mins treatment with 300μM GAP 26; (iv) Following washout after 30mins treatment with 300μM GAP 26; (v) Following 30mins treatment with 300μM GAP 27; (vi) Following washout after 30 minutes treatment with 300μM GAP 27. *Injected cell. Bar = 50μm.

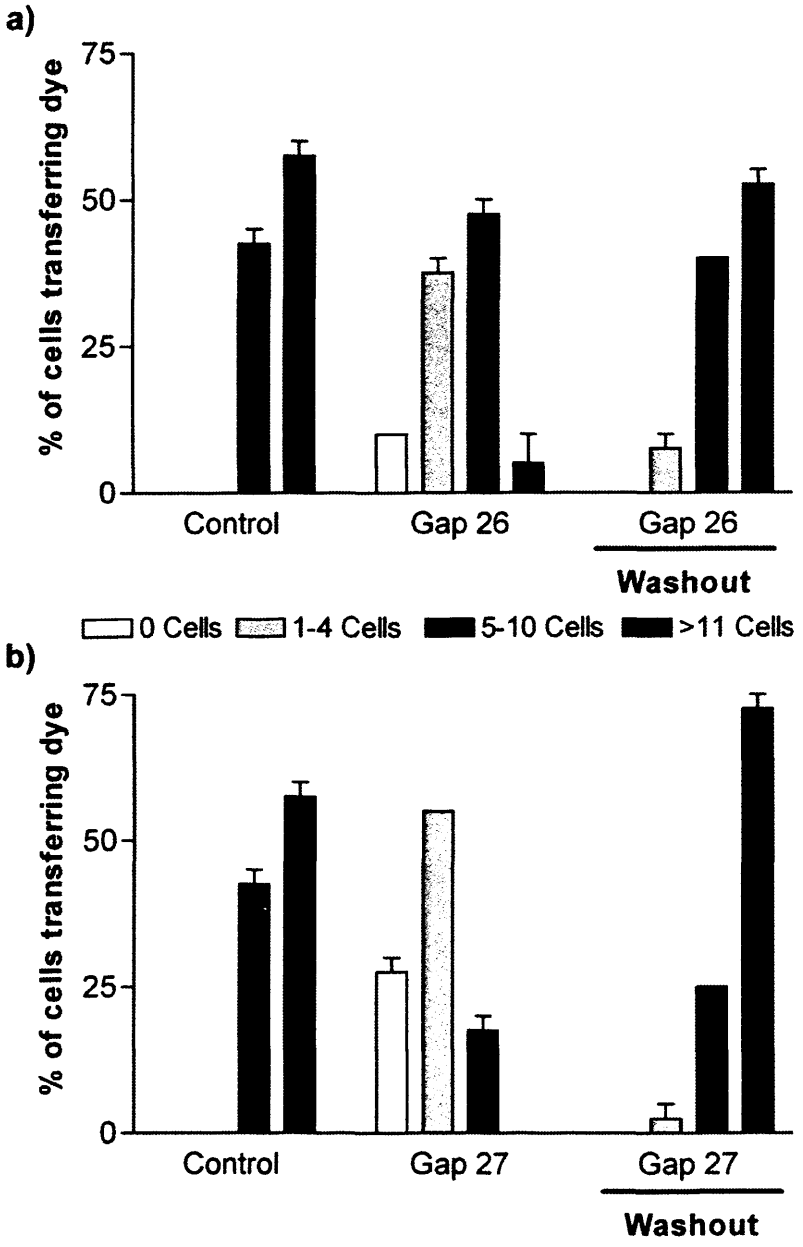

Figure 3.9: The effect of the connexin mimetic peptides GAP 26 and GAP 27 on Alexa-488 transfer in rat neonatal cardiac myocytes

a) Confluent monolayers of rat neonatal cardiac myocytes were viewed under a fluorescent microscope immediately after microinjection of Alexa-488 under control conditions or following 30mins treatment with 300μM GAP 26 and following washout after 30mins treatment with 300μM GAP 26. b) Confluent monolayers of rat neonatal cardiac myocytes were viewed under a fluorescent microscope immediately after microinjection of Alexa-488 under control conditions or following 30mins treatment with 300μM GAP 27 and following washout after 30mins treatment with 300μM GAP 27. The extent of dye spread was monitored. Approximately 30 cells were injected per set of experiments.

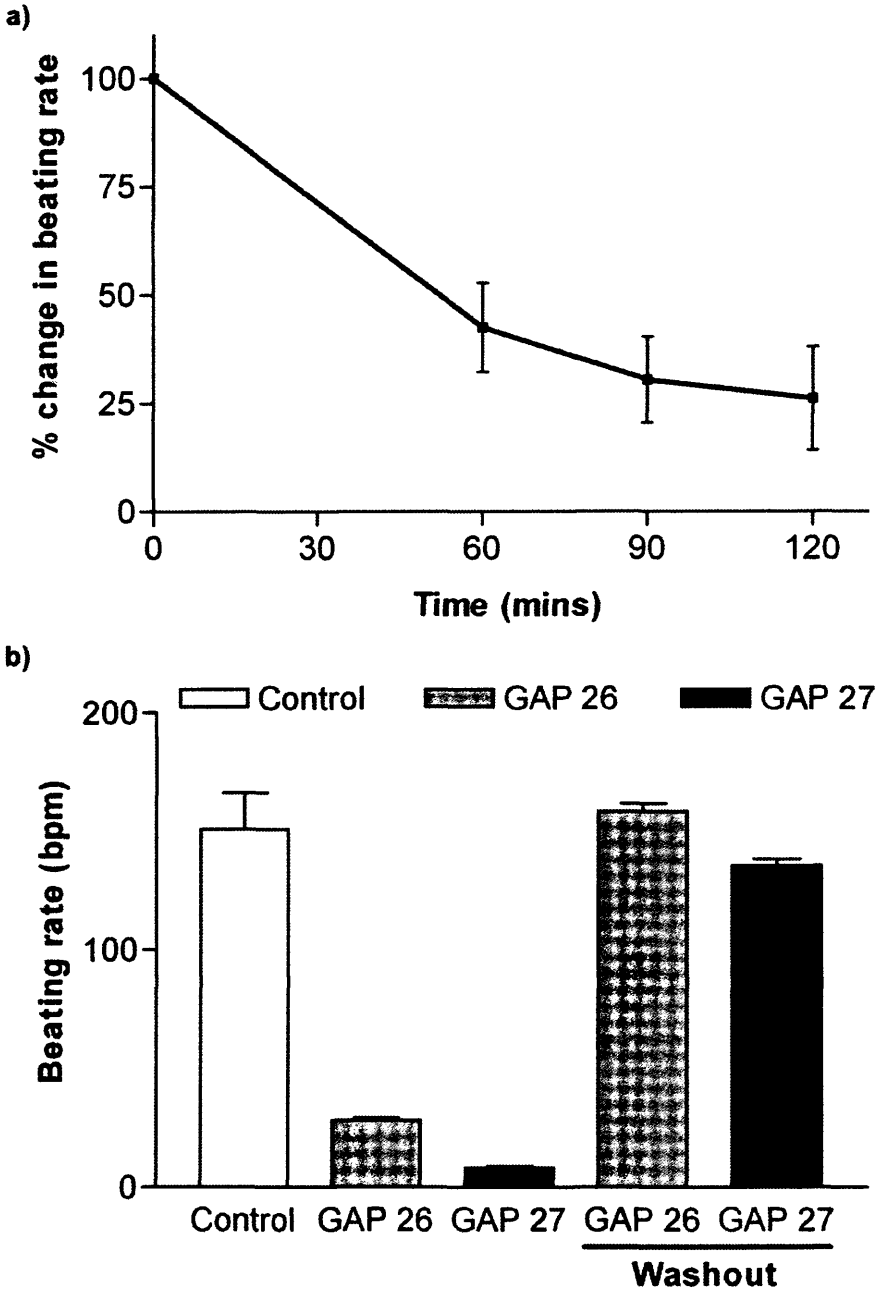

Figure 3.10: The effect of the connexin mimetic peptides GAP 26 and GAP 27 on the synchronous beating rate of rat neonatal cardiac myocytes

a) Confluent monolayers of rat neonatal cardiac myocytes were treated with 300μM GAP 26 and viewed under a light microscope to record cell beating rates at specific time points. b) Confluent monolayers of rat neonatal cardiac myocytes were viewed under a light microscope and cell beating rates were recorded under control conditions or following treatment with 300μM GAP 26 or GAP 27 and following washout after 30mins treatment with 300μM GAP 26 or GAP 27.

3.4 Discussion

A neonatal cardiomyocyte model was developed to study the effects of ischaemic insult on the heart at the cellular level. Gap junctions, constructed primarily of Cx43, are widely regarded as an essential component in maintaining the synchrony of beating between cardiomyocytes in the heart (Saffitz & Yamada 1998; Severs 2000). Onset of ischaemia often results in heart arrhythmias, presumably due to the uncoupling of gap junction mediated communication. Our ischaemic model system uses a hypoxic chamber and nutrient-free media. An advantage of using a specially designed chamber to induce hypoxia is that the cellular responses are a consequence of a hypoxic environment whereas in chemical hypoxia, the chemicals presumably reduce oxidative metabolism and damage cells, making the relevance of the results questionable.

The present studies indicate that this model is robust and reliable. The cells beat synchronously and protein analysis of Cx43 extracted from cardiac myocytes consistently produced two phosphorylated components, that were abolished by alkaline phosphatase treatment, and a third non-phosphorylated component. In healthy, synchronously beating cardiomyocytes, Cx43 is mainly in the phosphorylated state.

Ischaemia caused cessation of beating after 2-3 hours and this was followed by dephosphorylation of Cx43 after 4-5 hours. In comparison, whole organ Langendorf ischaemia (no perfusion) studies report that gap junction uncoupling occurs after 22 minutes and Cx43 dephosphorylation after 15-30 minutes (Beardslee et al., 2000). This is a more rapid response to ischaemia, probably due to the differences in behaviour in

whole heart organ studies where there are more cell types involved, for example fibroblasts. The time taken for synchronous beating to cease (2-3 hours) corresponds with the half-life of Cx43 but there was no difference detected in total Cx43. This indicates that newly synthesised Cx43 loses the ability to form functional gap junctions or may not reach the plasma membrane. Gap junction uncoupling caused cardiac myocytes to cease beating. Under control conditions, when Cx43 is phosphorylated, cardiac myocytes beat rapidly and synchronously. Ischaemia-induced cessation of beating is followed by dephosphorylation of Cx43. However, following reoxygenation, my studies showed that synchronous beating only recovered after Cx43 phosphorylation was restored, suggesting a possible association between synchronous beating and Cx43 phosphorylation. This recovery phenomenon occurred within minutes, suggesting that newly synthesised Cx43 is not involved and pre-existing dephosphorylated Cx43 is rephosphorylated. Immunofluorescent studies before and after ischaemic insult showed that gap junctions probably constructed of Cx43 were internalised during hypoxia (Turner et al., 2001). The recovery of Cx43 phosphorylation could be due to attachment of already synthesised connexins and CxHcs to gap junction plaques or less likely reinsertion of internalised Cx43 into the plasma membrane and not newly synthesised Cx43. This is supported by studies using the protein synthesis inhibitor cycloheximide that showed that the recovery of Cx43 phosphorylation was very robust and not affected by inhibition of protein synthesis (Turner et al., 2004). Further, immunofluorescent studies would have helped to confirm this possibility. The identity of the protein kinase responsible for the robust recovery of Cx43 phosphorylation after ischaemia and reoxygenation is unknown (Turner et al., 2004). Indeed, it is likely that many protein

kinases are involved as Cx43 recovers both phosphorylation components (P1 and P2), likely to be at different phosphorylation sites on the carboxyl tail. The involvement of the MAP kinases, PKA and PKG has been shown to be limited as the inhibitors of these protein kinases had no effect on the recovery of phosphorylation after hypoxia and reoxygenation (Turner et al., unpublished results). However, Cx43 phosphorylation failed to recover after reoxygenation of hypoxic treated cells in the presence of a non-isoform specific PKC inhibitor has indicated that PKC could be involved (Turner et al., unpublished results).

In summary, the present results illustrated that ischaemia induced the cessation of synchronous beating in neonatal cardiac myocytes and was followed later by complete dephosphorylation of Cx43. In addition, upon reoxygenation restoration of synchronous contraction in cardiac myocytes occurred once Cx43 phosphorylation was restored. These step-wise sequences indicate that Cx43 phosphorylation state and synchronous contraction of neonatal rat myocytes are closely related.

Chapter 4

The effects of an antiarrhythmic peptide rotigaptide (ZP123) on communication across gap junctions and connexin properties

4.1 Introduction

Direct communication across gap junctions facilitates the functional coordination of cell networks (Loewenstein 1981). Modifying the extent of cell to cell signalling across gap junction channels is likely to disrupt the synchronisation of individual activities of constituent cells in tissues and organs. Remodelling of gap junctions and changes in intercellular communication believed to occur across these channels are associated with a number of pathophysiological conditions including ischaemia, cardiac arrhythmia as well as endothelial and epithelial wound healing events (Saez et al., 2003; Severs et al., 2004). Connexins are increasingly identified as therapeutic targets functioning in cellular co-ordination (Dhein 2004).

4.1.1 Rotigaptide (ZP123)

In the heart, gap junctions located primarily at the intercalated discs couple myocytes electrically and mechanically ensuring intercellular propagation of action potentials that trigger Ca^{2+} transients, communication processes that underpin synchronous contraction at the cellular and organ level (Kleber & Rudy 2004). During acute myocardial infarction the blood supply to areas of the heart is interrupted and gap junctions close (Beardslee et al., 2000), stopping the electrical communication between the myocytes, a process often leading to fatal arrhythmia. To address cardiac arrhythmia, hexa-peptides such as AAP10 derived from bovine atria and its stable analogue ZP123 have been developed to modify gap-junctional channel properties and intercellular communication (Dhein et al., 2003; Muller et al., 1997). ZP123 was developed by the Danish pharmaceutical company Zealand Pharma (Glostrup, Denmark) and has since been renamed rotigaptide. Rotigaptide is believed to be the first specific gap junction modifying product to be developed for a specific indication, being designed to

normalize cardiac arrhythmias. Rotigaptide promoted electrical coupling between ventricular myocytes without changing membrane conductance (Xing et al., 2003). The peptide attenuated gap junction closure during acidosis, preserved intercellular coupling and improved synchronisation of beating of clusters of heart cells (Eloff et al., 2003; Haugan et al., 2005; Kjolbye et al., 2003; Xing et al., 2003). Most importantly, rotigaptide reduced the inducibility of re-entry ventricular tachycardia during acute ischaemia in dogs (Xing et al., 2003). These properties suggest that rotigaptide could be a prototype of a new class of antiarrhythmic drug. Indeed, rotigaptide successfully underwent three phase I clinical trials during 2005. These were safety and tolerability trials involving healthy volunteers and drug interaction trials with digoxin. Rotigaptide has now entered Phase II with the primary objective being to determine whether rotigaptide administration decreases the occurrence of ventricular arrhythmia in patients with chronic heart failure and acute myocardial infarction.

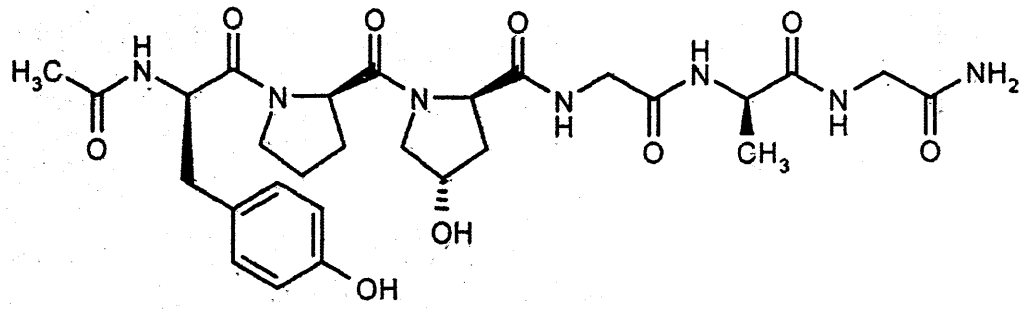

Rotigaptide

Figure 4.1: The chemical structure of the hexa-peptide rotigaptide. Rotigaptide is an antiarrhythmic peptide currently in phase II clinical trials.

4.1.2 Permeability of connexin channels

Channels constructed from each connexin subtype have slightly different permeability properties. For example, Cx43 channels are generally accepted to have broad range permeability to most molecules less than 1kDa in size. By contrast, Cx26 channels are more selective and are permeable to small dyes such as Lucifer yellow (MW 457D) and

Alexa 488 (MW 570D) but impermeable to larger marker dyes such as Alexa594 (MW 780D) (Nicholson et al., 2000). Differences in the permeabilities of Cx26, Cx32 and Cx43 channels to secondary messengers that include cAMP, adenosine and IP3 have also been reported (Goldberg et al., 2002; Harris 2001; Niessen et al., 2000).

Cells in most tissues often express different combinations of connexins. Connexin 43 is the most widely expressed connexin in mammals and is the dominant connexin expressed in heart. It is also highly expressed in skin but Cx26 and up to ten other connexins are also differentially expressed in the dermal cell layers (Di et al., 2001; Willecke et al., 2002). Cx32 is found in several tissues including the nervous system and liver (Willecke et al., 2002). The distinctive permeability properties observed with different connexins are believed to reflect specific physiological requirements of different tissues. The dynamic role that connexin channels play in various physiological and pathophysiological conditions makes agents that target gap-junctional communication potentially useful therapeutic tools.

4.1.3 HL-1 cells

There have been many attempts to create a cardiac muscle cell line that proliferates in culture, with limited success so far (Claycomb et al., 1998). HL-1 cells are an immortalized cardiac muscle cell line derived from the AT-1 mouse atrial cardiac myocyte cells with a tumour lineage (Claycomb et al., 1998; Delcarpio et al., 1991). HL-1 cells can be passaged indefinitely in culture, yet they maintain an ability to contract. They retain differentiated cardiac morphological, biochemical and electrophysiological properties (Claycomb et al., 1998). However, while Hl-1 cells have the ability to beat, the cells are inconsistent with respect to this function.

Nevertheless, they remain a useful tool for cardiac specific studies, but they are still not a completely successful replacement for primary ventricular cardiac myocytes.

4.1.4 Chapter Aims

The investigations described in this chapter are concerned with the effects of rotigaptide on the cell communication properties and protein expression profiles of Cx43 in three cell model systems: rat neonatal cardiac myocytes, HL-1 cells (Claycomb et al., 1998) and HeLa cells transfected and selected to express different connexins. The effect of rotigaptide on the permeability of Cx32 and Cx26 gap junctions in HeLa cell model systems allowed the connexin specificity of rotigaptide action to be examined.

4.2 Methods

4.2.1 Materials

G418-sulphate and Calf Intestinal Phosphatase were purchased from Promega (Southampton UK). Lucifer yellow, Alexa-488, Alexa-594 and goat anti-rabbit and mouse Alexa-488 and Alexa-594 secondary antibodies were obtained from Molecular Probes (Leiden, The Netherlands). The Cx43 monoclonal and P368 antibodies were obtained from Chemicon (Chandlers Ford, UK). Rotigaptide was supplied by Zealand Pharma (Glostrop, Denmark) and dissolved in water to give a 50μM stock and 18αGA was dissolved in DMSO to give a 25mM stock. GAP 26 was obtained from Sigma-Genosys (Cambridge, UK). All other reagents were obtained from Sigma (Poole, U.K).

4.2.2 Cell culture

Rat neonatal cardiac myocytes were prepared and plated as described in chapter 2 (Clarke et al., 2006; Turner et al., 2004). HL-1 cardiomyocytes were maintained in Claycomb medium, supplemented with 10% foetal calf serum, P/S (100μg/ml), epinephrine (0.1mM) and L-glutamine (2mM) as previously described (Claycomb et al., 1998). HeLa cells selected to express Cx43-GFP, Cx32-GFP or Cx26-GFP were prepared as described (Paemeleire et al., 2000) and maintained in DMEM, supplemented with 10% foetal calf serum, P/S (100μg/ml), amphotericin (100μg/ml), L-glutamine (2mM) and geneticin sulphate (G-418-sulphate 4mg/ml). HeLa cells expressing wild type Cx26 or Cx43 were maintained in cDMEM supplemented with 0.5μg/ml puromycin (Elfgang et al., 1995).

4.2.3 Dye transfer across gap junctions

Rat neonatal cardiac myocytes and HeLa cells were seeded at a density of $4x10^6$ cells/60mm dish and $1x10^6$ cells/60mm dish respectively. Cx-GFP protein expression in

HeLa cells was enhanced by addition of 5mM sodium butyrate to the medium 18hrs prior to the experiments (George et al., 1998). Direct cell-cell communication was assessed before and after treatment of the cells with rotigaptide by studying transfer of Lucifer yellow (charge -2, MW 457Da), Alexa-488 (charge –1, MW 570Da) or Alexa-594 (charge -1 MW 758Da) following intracytoplasmic microinjection of dye using an Eppendorf Femtojet 5247 device. Experiments were carried out in triplicate with >30 cells injected per experiment. Five minutes after injection cells were fixed in 4%w/v paraformaldehyde for 5mins and washed in PBS prior to the percentage of injections resulting in dye transfer to different numbers of neighbouring cells being assessed on an Zeiss Axiovert 200 fluorescence microscope using appropriate filter sets (Zeiss, UK) (Martin et al., 2004).

4.2.4 Hypoxia and ischaemia

Cardiac myocytes were made hypoxic in a gas-tight humidified 37°C anaerobic chamber, with an internal environment of 0.5% oxygen and 5% carbon dioxide, as described in chapter 2. Cardiac myocytes were manipulated inside the hypoxic chamber to maintain a hypoxic environment at all times, as described in 2.3. Cell beating rate was monitored using a Nikon light microscope within the hypoxic chamber. Control cells were incubated in a tissue culture incubator (Heraeus® HERAcell® 150) at 37°C and an environment of 21% oxygen and 5% carbon dioxide. For ischaemic treatment, cells were placed in a low glucose ($0.2gL^{-1}$) serum free medium for the duration of the experiment and for hypoxic and control treatments, cells remained in the serum-free medium ($3gL^{-1}$), as described in 2.3.4.

4.2.5 Cell Cytometric analysis

HeLa cells expressing Cx43-GFP were plated onto 6 well dishes ($1x10^5$ cells) and were exposed to 50nM or 250nM rotigaptide for periods of 1 or 5hrs. Cells were harvested by trypsinisation, washed in PBS and resuspended to a final concentration of $1x10^6$/ml. Cells ($1x10^5$) were added to 500µl of FACS sheath fluid (Becton Dickson) and subject to fluorescent activated cell sorting (FACS) analysis after excitation at 488nm. Data was exported to a Microsoft Excel spreadsheet and analysed. Experiments were carried out 3 times and data presented as mean ± sem.

4.2.6 Protein localisation and image analysis

HeLa cells expressing wild type Cx43 ($3x10^5$ cells) were seeded onto $16mm^2$ coverslips and allowed to settle as monolayers. Following treatment with rotigaptide at concentrations of 50nM, 100nM and 250nM for 5hrs respectively cells were fixed and processed for immunocytochemical staining (described 2.6.2) with a monoclonal antibody targeted to the carboxyl tail of Cx43 (1:250 dilution). The secondary antibody was goat anti-mouse conjugated to Alexa-488 (Martin et al., 2004). Slides were viewed under an Axiovert 200 microscope linked up to a Zeiss confocal laser scanning system. Images were acquired under identical conditions and magnification. In parallel experiments, HeLa cells expressing Cx43-GFP ($5x10^5$ cells) were seeded onto $24mm^2$ cover-chambers (LabTek) and cells were viewed before and after treatment of the cells with rotigaptide as described above.

4.2.7 Western blot analysis

Cells grown on 60mm dishes ($4x10^6$ rat neonatal cardiac myocytes; $1x10^6$ HeLa cells) were treated for periods of 1 to 5hrs with 50nM, 100nM or 250nM rotigaptide, or 25µM

18α-glycyrrhetinic acid (18αGA) prior to harvesting as described 2.4.1. Equal amounts of protein (100μg rat neonatal cardiac myocyte lysates; 50μg HeLa cell lysates) were analysed by SDS-PAGE (10% w/v) (described 2.4.3) and transferred to nitrocellulose membrane for immuno-detection of Cx43 as described in 2.4.4. Membranes were probed with a polyclonal antibody to Cx43 (Zymed, USA; 1:4000 dilution) that recognises multiple phosphorylated/nonphosphorylated isoforms of Cx43 and a secondary goat anti rabbit horseradish peroxidase antibody (1:2000 dilution). In some experiments, blots were also probed with a polyclonal antibody that recognises site-specific phosphorylation of serine 368 on the carboxyl tail of Cx43 (1:1000 dilution). To standardise protein expression, blots were also probed with a monoclonal antibody to α-tubulin (1:10000 dilution) and a secondary goat anti mouse horseradish peroxidase antibody (1:2000 dilution). Blots were developed by enhanced chemiluminescene (ECL) and quantified using a Biorad GS-700 densitometer as described in chapter 2 (Martin et al., 2004).

4.2.8 Connexin 43 phosphorylation assays

Protein extracts (30μg) were digested with 60 Units of calf intestinal phosphatase for 1hr at 37°C and analysed by SDS-PAGE and Western blotting as described above. In some experiments cells were treated with 100ng/ml TPA, a protein kinase C activator, for 30mins prior to harvesting the cells to serve as a positive control when analysing serine 368 phosphorylation of Cx43.

4.2.9 Statistical analysis

Data were evaluated by ANOVA followed by Dunnett's multiple comparison test, with $P<0.05$ being considered significant.

4.3 Results

4.3.1 Rotigaptide increases gap-junctional communication in rat neonatal cardiac myocytes.

Rat neonatal cardiac myocytes were efficiently coupled with 20.9% of cells transferring dye to ≥11 neighbouring cells. Rotigaptide treatment at 50nM, 100nM or 250nM for 1 hour had no significant effect on dye transfer (Figure 4.3a). Exposure of the cells to 50nM rotigaptide for 5hrs increased dye spread approximately 4 fold, with 75.6 ± 9.7% of cells transferring dye to ≥ 11 cells (Figure 4.2 and 4.3b). Treatment of the cells for 5hrs with 100nM and 250nM rotigaptide also significantly increased intercellular coupling (Figure 4.2 and 4.3b). There was no further modification of dye spread at these increased doses, suggesting that 50nM is the optimal concentration at which rotigaptide operates in this system and that any further enhancement is not readily distinguished by monitoring spread of dye.

To demonstrate that intercellular transfer of dye occurred across gap junctions, cells were treated with 18αGA for 1hr prior to microinjection and following exposure to rotigaptide for 5hrs (Figure 4.2). Dye transfer was totally blocked under both conditions (Table 4.1). These results suggest that rotigaptide does not offset the effects of 18αGA, a known gap junction uncoupler (Davidson & Baumgarten 1988). Despite the increase in intercellular coupling elicited by rotigaptide, the peptide had no significant effect on beating rates and their synchronicity in cardiac myocytes, which was maintained at approximately 150bpm during each of the drug treatments (Figure 4.4).

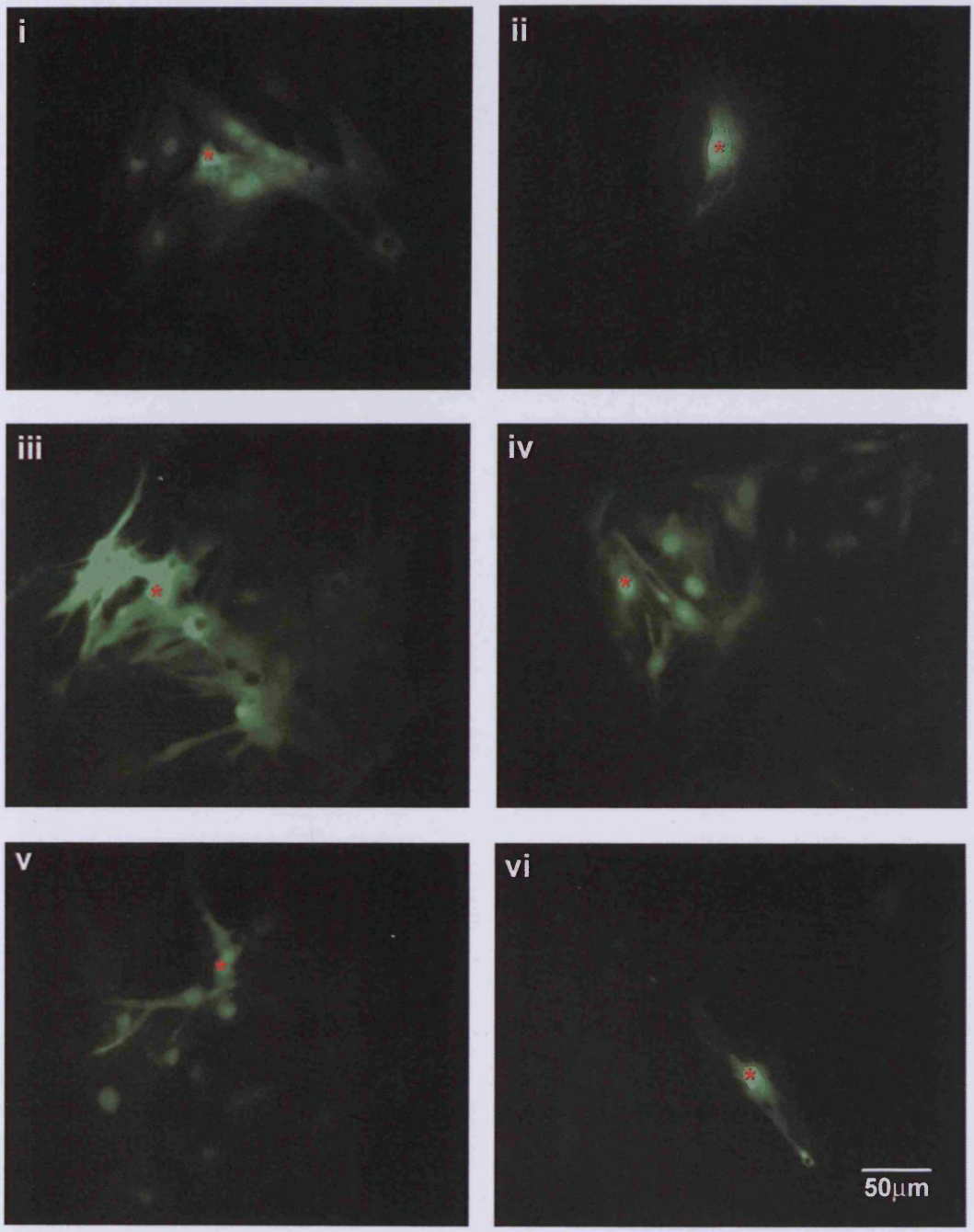

Figure 4.2: The effect of rotigaptide (ZP123) and 18αGA on Alexa-488 transfer in rat neonatal cardiac myocytes

Confluent monolayers of rat neonatal cardiac myocytes were viewed under a fluorescent microscope immediately after microinjection of Alexa-488. (i) Control cells; (ii) Control cells following 1hr pre-treatment with 25mM 18aGA; (iii) Following 5hrs treatment with 50nM rotigaptide; (iv) Following 5hrs treatment with 100nM rotigaptide; (v) Following 5hrs treatment with 250nM rotigaptide; (vi) 5hrs treatment with 50nM rotigaptide followed by 1hr 25mM 18αGA. * Injected cell. Bar = 50μm.

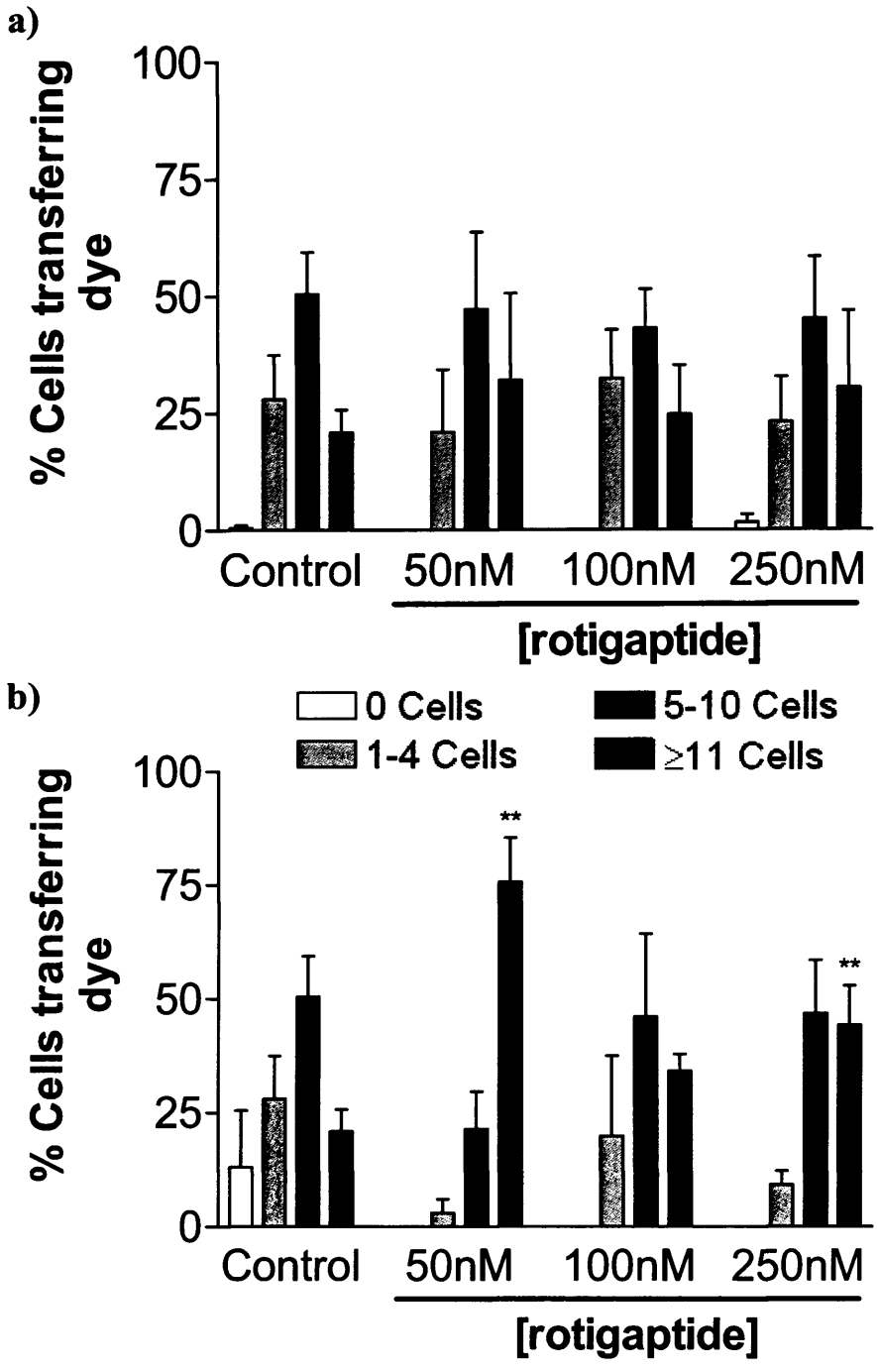

Figure 4.3: The effect of rotigaptide (ZP123) on Alexa-488 transfer in rat neonatal cardiac myocytes

Confluent monolayers of rat neonatal cardiac myocytes were microinjected with Alexa-488 under control conditions or following treatment with 50nM, 100nM or 250nM ZP123 a) for 1hr and b) 5hrs. The extent of dye spread was monitored. Approximately 30 cells were injected per set of experiments, which were repeated in triplicate. **P<0.01.

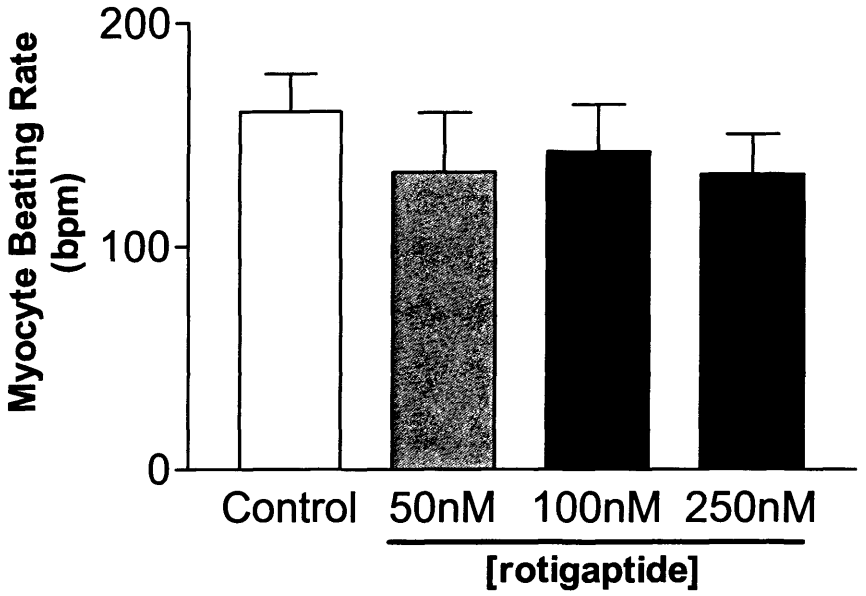

Figure 4.4: The effect of rotigaptide (ZP123) on the beating rate of rat neonatal cardiac myocytes

Confluent monolayers of rat neonatal cardiac myocytes were viewed under a light microscope and cell beating rates were recorded under control conditions or following treatment with 50nM, 100nM or 250nM ZP123 for 5hrs (n=12).

4.3.2 Rotigaptide increases gap-junctional communication in HL-1 cells.

HL-1 cells displayed a lower degree of dye coupling than cardiac myocytes with 61.7 ± 9.3% of cells transferring dye to 5-10 neighbouring cells and 1.7% of cells transferring dye to ≥11 cells. Treatment of HL-1 cells with rotigaptide at 50nM, 100nM or 250nM for 5hrs significantly increased transfer of dye to ≥11 cells to 38.3 ± 4%, 32.5 ± 4.9% and 57.5 ± 8.1% respectively (Table 4.1, Figure 4.5).

4.3.3 The connexin specificity of rotigaptide action.

Untransfected HeLa cells are communication incompetent and do not transfer dyes to neighbouring cells (Elfgang et al., 1995; George et al., 1998). Therefore, HeLa cells were made communication competent by transfection and selection of variants expressing Cx43-GFP, Cx32-GFP or Cx26-GFP, or wild type Cx43 or Cx26. Following induction of Cx43-GFP expression with sodium butyrate, 37.9 ± 8.2% of the transfected cells transferred dye to ≥5 neighbours confirming previous results (Martin et al., 2001) (Figure 4.6). Time course experiments, pursued to analyse the effects of rotigaptide (50nM) on the efficiency of gap-junctional coupling, showed that 2-3hrs incubation with the peptide was without significant effect on the intercellular spread of Lucifer yellow (Figure 4.6a). However, as with HL-1 cells, after 5-6hrs incubation with rotigaptide, increased dye transfer was observed with 69.1 ± 7.1% of cells transferring dye to ≥5 cells, although overnight incubation did not result in further dye spread. Dye transfer was significantly reduced following pre-incubation of the cells with 18αGA for 1hr prior to microinjection of dye under control conditions and following 5hrs rotigaptide (50nM) treatment; a similar result was obtained with cardiac myocytes (Figure 4.2).

The effect of rotigaptide on dye transfer properties of different cells and connexins					
Cell and Cx subtype expressed	**Treatment**	**Dose**	**Time**	**Dye**	**% coupling ± sem**
[1]Rat neonatal cardiac myocytes expressing Cx43 (transferring to 11 or more cells)	Control	-	0 hr	Alexa-488	20.90 ± 4.82
	Rotigaptide	50nM	1hr	Alexa-488	31.93 ± 18.64
	Rotigaptide	100nM	1hr	Alexa-488	24.68 ± 10.46
	Rotigaptide	250nM	1hr	Alexa-488	30.33 ± 16.33
	Rotigaptide	50nM	5hrs	Alexa-488	75.60 ± 9.79 **
	Rotigaptide	100nM	5hrs	Alexa-488	34.09 ± 3.70
	Rotigaptide	250nM	5hrs	Alexa-488	44.10 ± 8.70 **
	18αGA	50μM	30mins	Alexa-488	0**
[1]HL-1 cardiomyocytes expressing Cx43 (transferring to 11 or more cells)	Control	-	0 hr	Alexa-488	1.667 ± 1.667
	Rotigaptide	50nM	5hrs	Alexa-488	38.33 ± 4.01 **
	Rotigaptide	100nM	5hrs	Alexa-488	32.50 ± 4.96 *
	Rotigaptide	250nM	5hrs	Alexa-488	57.50 ± 8.14 **
	18αGA	50μM	30mins	Alexa-488	0**
HeLa cells expressing wild type Cx26 (transferring to 11 or more cells)	Control	-	0hr	Alexa 488	15.5 ± 3.9
	Rotigaptide	50nM	5hrs	Alexa 488	18.9 ± 3.2
[2]HeLa cells expressing Cx43-GFP (transferring to 5 or more cells)	Control	-	0 hr	LY	37.91 ± 8.2
	Rotigaptide	50nM	2-3hrs	LY	35.6 ± 5.97
	Rotigaptide	50nM	5-6hrs	LY	69.1 ± 7.12 **
	Rotigaptide	50nM	o/n	LY	56.7 ± 6.84 *
	Control	-	0 hr	Alexa-594	9.06 ± 1.24
	Rotigaptide	50nM	5-6hrs	Alexa-594	54.8 ± 9.16*
[3]HeLa cells expressing Cx32-GFP (transferring to 3 or more cells)	Control	-	0 hr	LY	37.73 ± 3.38
	Rotigaptide	50nM	5-6hrs	LY	42.12 ± 4.57
	Rotigaptide	100nM	5-6hrs	LY	27.13 ± 2.62
	Rotigaptide	250nM	5-6hrs	LY	46.27 ± 6.12
[3]HeLa cells expressing Cx26-GFP (transferring to 3 or more cells)	Control	-	0 hr	LY	45.20 ± 6.13
	Rotigaptide	50nM	5-6hrs	LY	29.31 ± 5.28
	Rotigaptide	100nM	5-6hrs	LY	27.75 ± 0.25
	Rotigaptide	250nM	5-6hrs	LY	28.50 ± 7.90

Table 4.1: Confluent monolayers of rat neonatal cardiac myocytes, HL-1 cardiomyocytes and HeLa cells expressing Cx43-GFP, Cx32-GFP or Cx26-GFP were microinjected with Alexa-488, Lucifer yellow or Alexa-594 following treatment with Rotigaptide at various concentrations and times as indicated in the table. The extent of dye transfer was recorded and the data here represented as % of cells transferring dye to ≥11 neighbouring cells for [1]rat neonatal cardiac myocytes and HL-1 cardiomyocytes, to ≥5 neighbouring cells for [2]HeLa cells expressing Cx43-GFP and to ≥3 neighbouring cells for [3]HeLa cells expressing Cx32-GFP and Cx26-GFP. * $P<0.05$, ** $P<0.01$ compared with non treated cells.

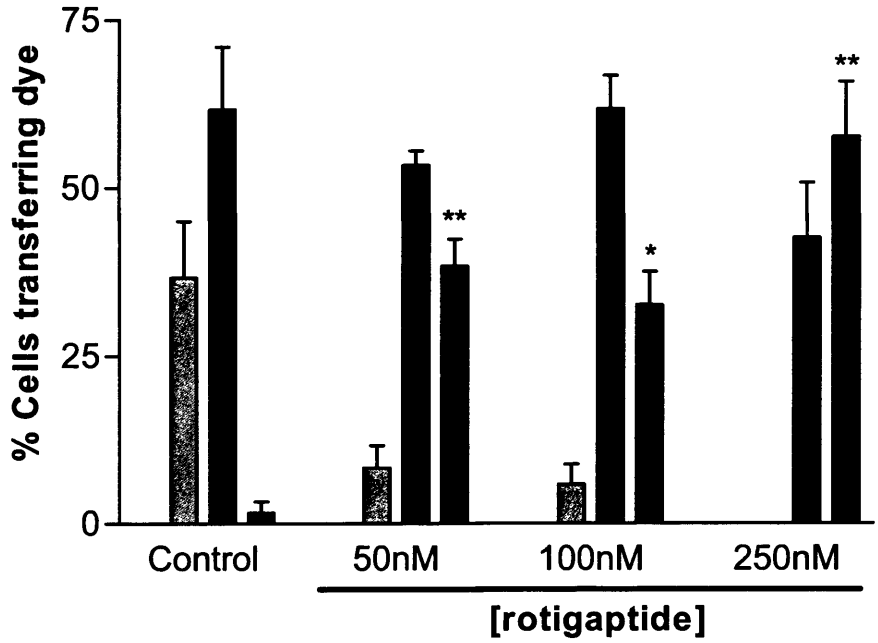

Figure 4.5: The effect of rotigaptide (ZP123) on Alexa-488 transfer in HL-1 cardiomyocytes

Confluent monolayers of HL-1 cardiomyocytes were microinjected with Alexa-488 under control conditions or following treatment with 50nM, 100nM or 250nM ZP123 for 5hrs. The extent of dye spread was monitored. Approximately 30 cells were injected per set of experiments, which were repeated in triplicate. **P<0.01.

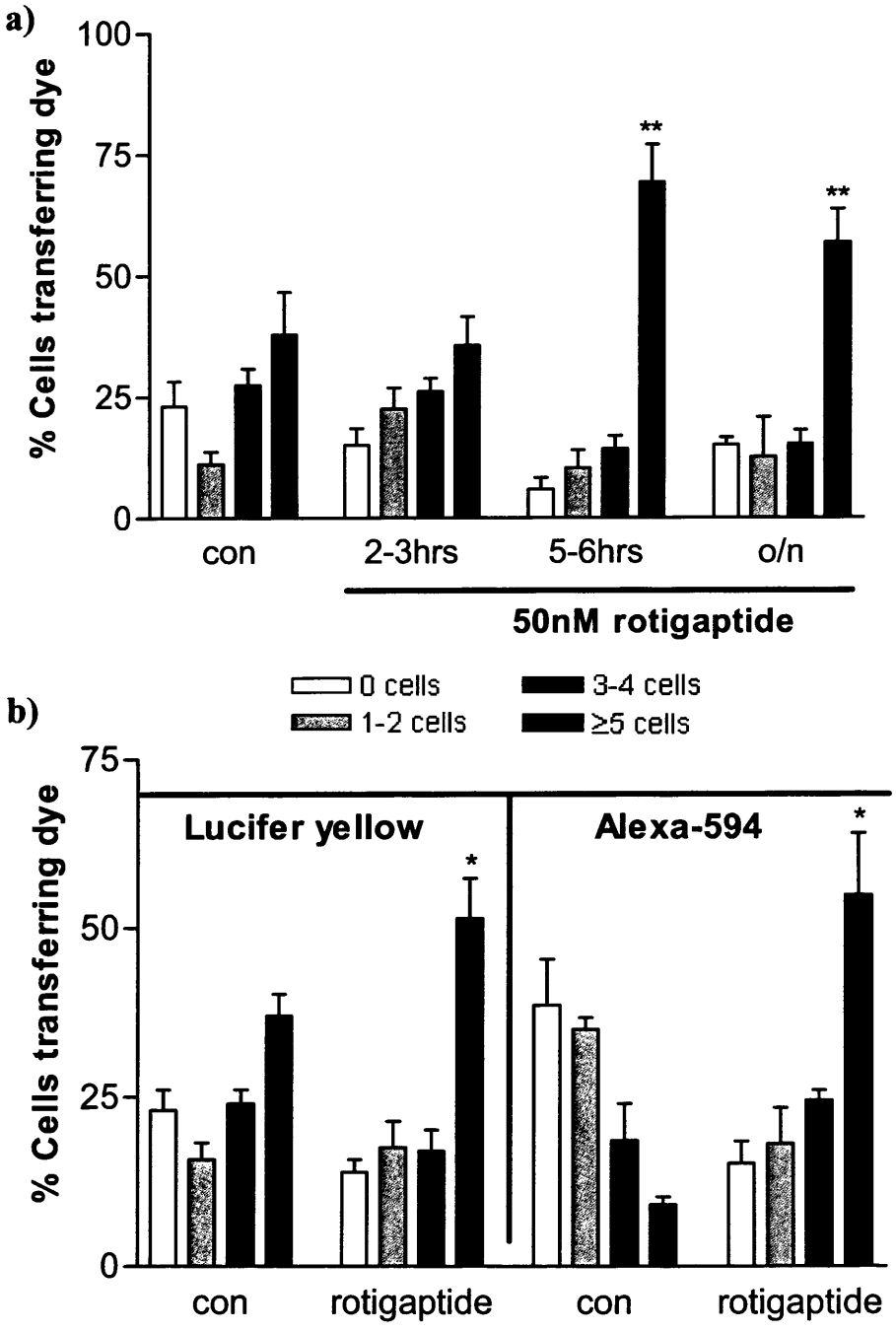

Figure 4.6: The effect of rotigaptide (ZP123) on dye transfer in HeLa cells expressing Cx43-GFP

Confluent monolayers of HeLa cells expressing Cx43-GFP were microinjected with: a) Lucifer yellow under control conditions or following treatment with 50nM ZP123 for 2-3hrs, 5-6hrs or overnight or b) Lucifer yellow or Alexa-594 under control conditions or following treatment with 50nM ZP123 for 5hrs. In all experiments the extent of dye spread was monitored and approximately 30 cells were injected per set of experiments, which were repeated in triplicate. *P<0.05, **P<0.001 in a. In b *P<0.05 between control cells and ZP123 treated cells was determined by student t test, for Lucifer yellow and Alexa-594 transfer respectively.

To investigate the effect of rotigaptide on the intercellular spread of various dyes, the spread of Lucifer yellow and Alexa-594 was compared in HeLa cells expressing Cx43-GFP. Lucifer yellow was found to diffuse more efficiently through Cx43-GFP gap junctions than Alexa-594, with 37.9% of cells transferring Lucifer yellow whereas only 9% of cells transferred Alexa-594 to ≥5 neighbouring cells respectively. Transfer of both dyes increased significantly after 5hrs treatment with rotigaptide (50nM) (Figure 4.6b). In general, Cx43-GFP channels transferred Lucifer yellow to a greater number of cells than Alexa-594.

HeLa cells expressing Cx32-GFP and Cx26-GFP exhibited lower dye coupling efficiency than Cx43-GFP transfected HeLa cells, with 37.3 ± 3.4% of Cx32-GFP expressing cells transferring Lucifer yellow to ≥3 neighbouring cells (Figure 4.7a). Incubation with 50nM rotigaptide for 5hrs had no significant effect on the extent of Lucifer yellow transfer. Furthermore, incubation of these cells for 5hrs with 100nM or 250nM rotigaptide caused no significant change in dye transfer. Similar results were obtained with Cx26-GFP expressing cells (Figure 4.7b). Rotigaptide caused no significant difference in the extent of transfer of Alexa 488 (charge -1, MW 570) between Cx26 expressing HeLa cells that under control conditions were extensively coupled with 15.5 ± 3.9% transferred the dye to ≥11 cells. Following five hours of preincubation with 50nM rotigaptide, 18.9 ± 3.2% of cells transferred dye ($P<0.5\%$).

4.3.4 The effects of rotigaptide on cardiac myocytes during ischaemia

Cardiac myocytes were exposed to ischaemia resulting in the cessation of synchronous beating after approximately 3hrs of the insult. Upon reoxygenation, after 6hrs of ischaemia, the synchronous contraction of cardiac myocytes was restored as shown in

Figure 4.8a. The dynamics of these events mimicked those seen in control (non-rotigaptide treated) cardiac myocytes. Therefore, it appears that rotigaptide has no apparent effects on cardiac myocyte beating rates under ischaemic or reoxygenated conditions.

Cardiac myocytes treated with rotigaptide (50nM) were subjected to prolonged ischaemia, leading to complete dephosphorylation of Cx43 after 6hrs of ischaemia (Figure 4.9). Similar results were seen with non-rotigaptide treated cardiac myocytes when exposed to ischaemia (chapter 3, figure 3.6). Reoxygenation of rotigaptide treated cells after 5 and 6hrs of ischaemia resulted in recovery of phosphorylated Cx43. After 7hrs of ischaemic incubation, Cx43 phosphorylation recovered only slightly and synchronous beating was not resumed, following reoxygenation, as shown in Figure 4.9.

Since 50nM rotigaptide had no significant effects on beating rate or Cx43 phosphorylation, a dose response experiment was performed, the results being displayed in Figures 4.8b and 4.10. The doses of rotigaptide used were 100nM, 500nM and 1μM. At all doses, rotigaptide had no significant effect on cardiac myocyte beating rates, when compared with non-rotigaptide treated cells, as shown in Figure 4.8b. The 100nM rotigaptide treated cells had reduced beating rates at the start and after reoxygenation. However, observations revealed that these cells were beating irregularly, i.e. not synchronously. Treatment of control cells with rotigaptide at the two higher concentrations resulted approximately in a 3-fold increase in total Cx43 expression (Figure 4.10). Rotigaptide treatment had no effect on Cx43 phosphorylation during ischaemia and reoxygenation. Any changes in Cx43 expression and phosphorylation

during ischaemia/reoxygenation were shown to be insignificant and could not be reproduced consistently.

4.3.5 Effects of rotigaptide on connexin43 expression profiles in rat neonatal cardiac myocytes.

Immunoblot analysis of rat neonatal cardiac myocytes confirmed that Cx43 migrated electrophoretically as two phosphorylated forms (P1 and P2 bands; 43 - 45kD), with a minor band at 41 kDa as shown in chapter 3 (Figure 3.1). Cx43 in rat neonatal cardiac myocytes also showed a 41kDa band that was likely to be a non-phosphorylated form of Cx43 (Chapter 3, Figure 3.1), consistent with previous reports (Beardslee et al., 2000).

Rat neonatal cardiac myocytes treated with 50nM, 100nM and 250nM rotigaptide for 1 or 5hrs showed little change in Cx43 phosphorylation status using an antibody that recognises multiple phosphorylated isoforms of Cx43 (Beardslee et al., 2000) (Figure 4.11a). Densitometric analysis of the gels confirmed that there was no significant difference between the phosphorylation status of Cx43 under control conditions or rotigaptide treatment detected by this antibody (Figure 4.11b).

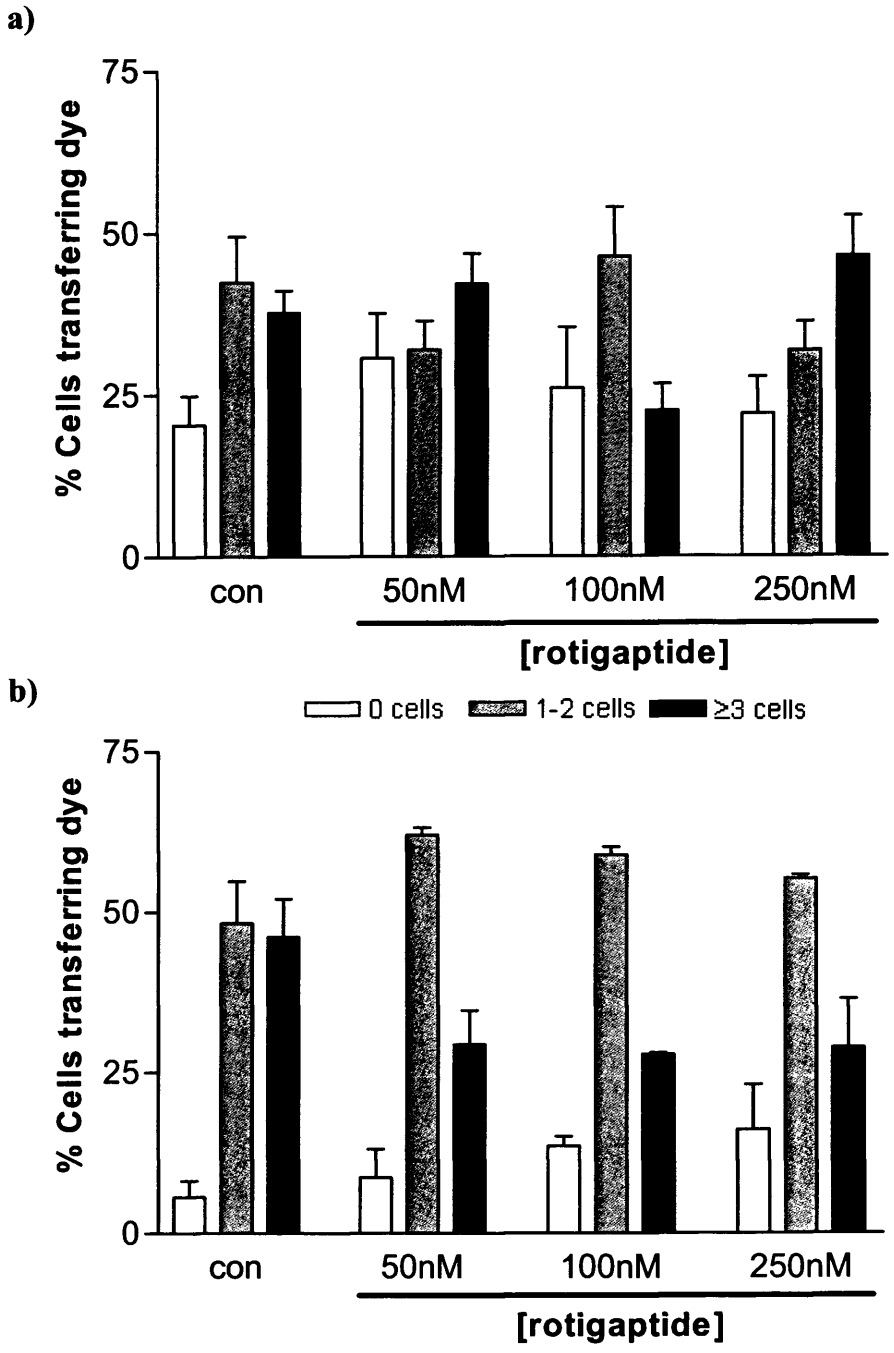

Figure 4.7: The effect of rotigaptide (ZP123) on dye transfer in HeLa cells expressing Cx32-GFP and Cx26-GFP

a) Confluent monolayers of HeLa cells expressing Cx32-GFP were microinjected with Lucifer yellow under control conditions or following treatment with 50nM, 100nM or 250nM rotigaptide for 5hrs. b) Confluent monolayers of HeLa cells expressing Cx26-GFP were microinjected with Lucifer yellow under control conditions or following treatment with 50nM, 100nM or 250nM rotigaptide for 5hrs. In all experiments the extent of dye spread was monitored and approximately 30 cells were injected per set of experiments, which were repeated in triplicate.

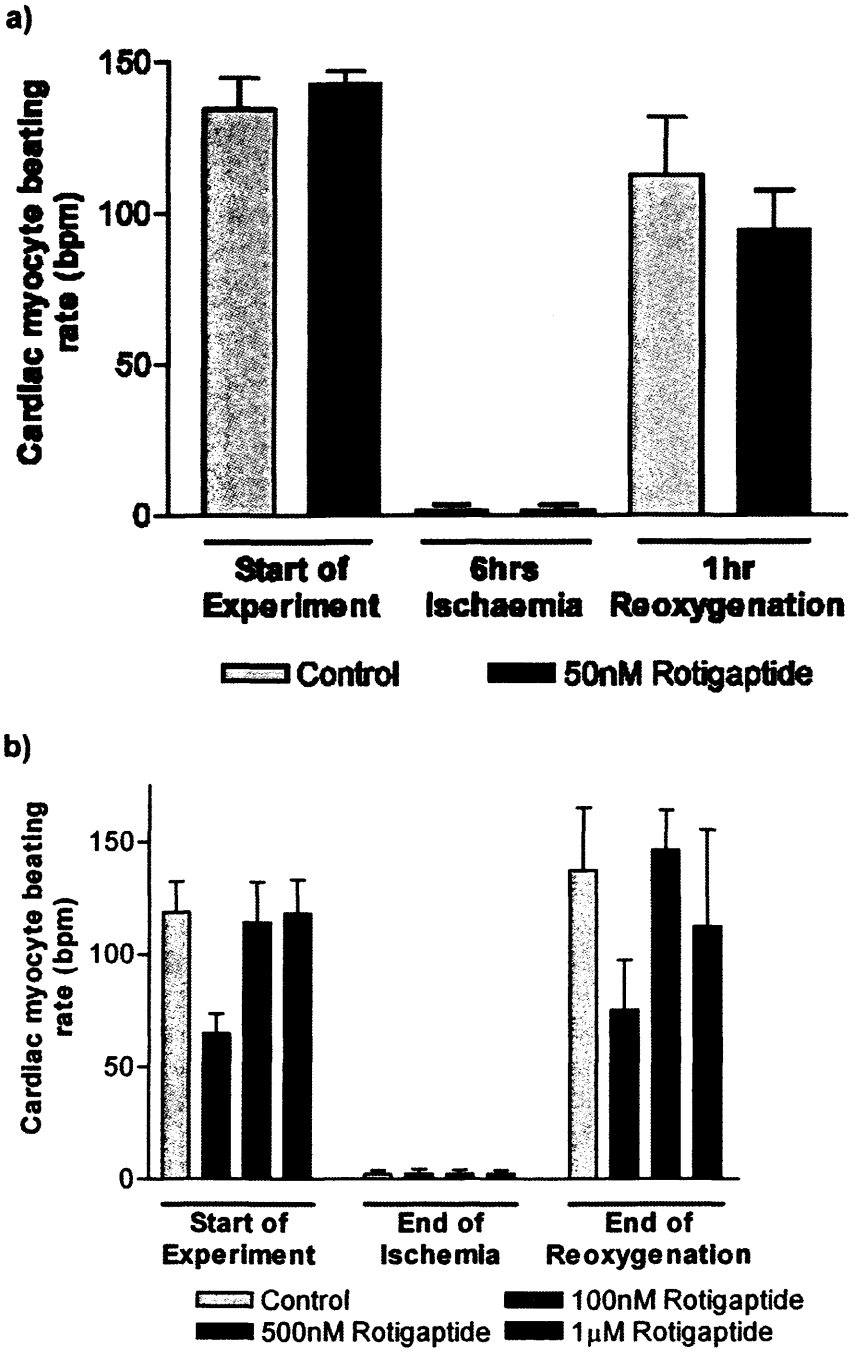

Figure 4.8: The effect of rotigaptide (ZP123) on the beating rate of rat neonatal cardiac myocytes during ischaemia/reoxygenation

Confluent monolayers of rat neonatal cardiac myocytes were viewed under a light microscope and cell beating rates were recorded a) after 50nM rotigaptide treatment in normoxia, during ischaemia or following treatment reoxygenation after 6hr ischaemic insult, or b) after treatment with 100nM, 500nM or 1μM rotigaptide in normoxia, during ischaemia or following treatment reoxygenation after 6hrs ischaemic insult (n=3).

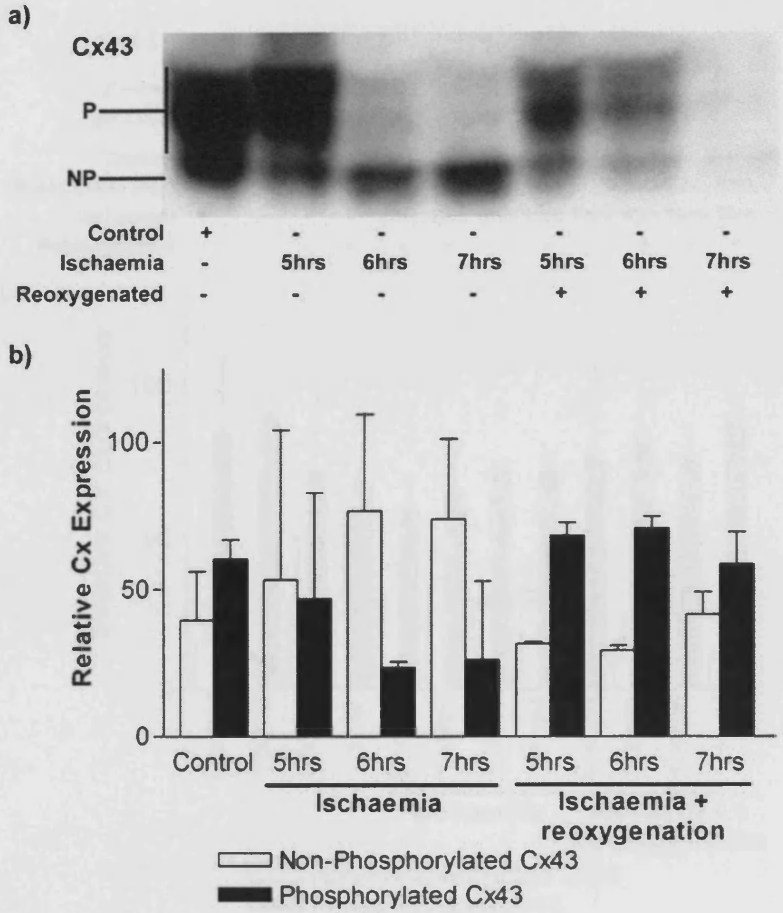

Figure 4.9: The effect of rotigaptide (ZP123) on the phosphorylation status of Cx43 during ischaemia/reoxygenation

a) Confluent monolayers rat neonatal cardiac myocytes were treated with 50nM rotigaptide. Cells were then subjected to normoxia, ischaemic insult for 5hrs, 6hrs or 7hrs, or reoxygenation after 5hrs, 6hrs or 7hrs of ischaemic insult. Cell lysates analyzed by standard SDS-PAGE and Western blotting with an antibody targeted to Cx43 and α-tubulin. Lane 1 - Control; Lane 2 - 50nM rotigaptide + 5hrs ischaemia; Lane 3 - 50nM rotigaptide + 6hrs ischaemia; Lane 4 - 50nM rotigaptide + 7hrs ischaemia; Lane 5 - 50nM rotigaptide + 5hrs ischaemia followed by 1hr reoxygenation; Lane 6 - 50nM rotigaptide + 6hrs ischaemia followed by 1hr reoxygenation; Lane 7 - 50nM rotigaptide + 7hrs ischaemia followed by 1hr reoxygenation. (b) Rat neonatal cardiac myocytes were treated as mentioned above. The graph shows the combined densitometric analysis of 2 separate Western blots. P = Phosphorylated Cx43; NP = non-phosphorylated Cx43.

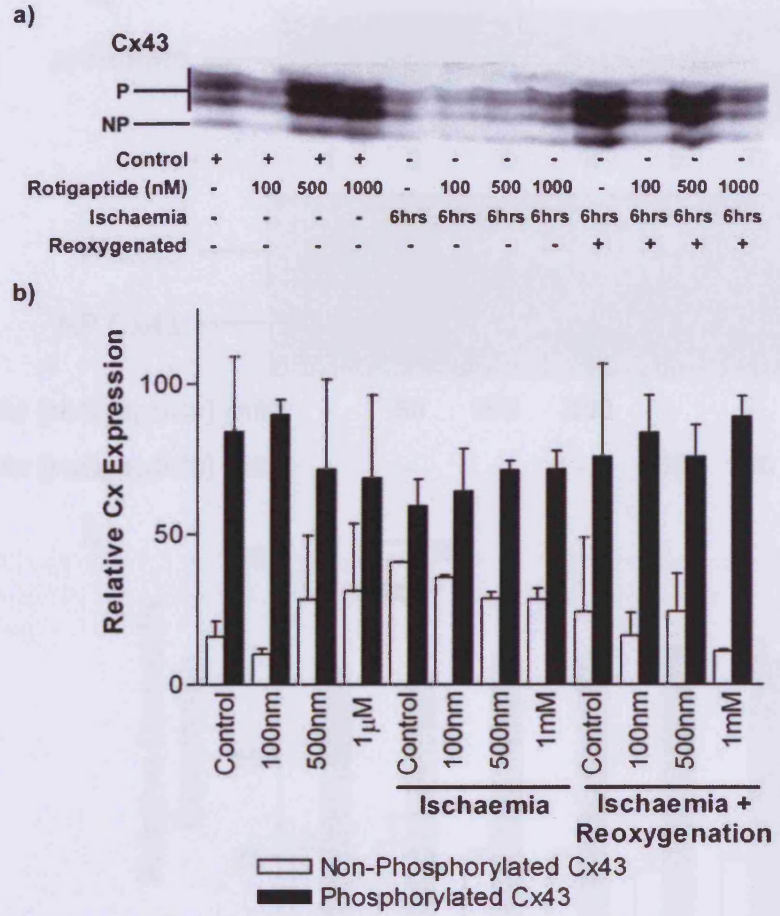

Figure 4.10: The effect of rotigaptide (ZP123) on the phosphorylation status of Cx43 during ischaemia/reoxygenation

a) Confluent monolayers rat neonatal cardiac myocytes were treated with 100nM, 500nM or 1000μM rotigaptide or had no drug treatment (Control). Cells were then subjected to normoxia, ischaemic insult for 6hrs, or reoxygenation after 6hrs of ischaemic insult. Cell lysates analyzed by standard SDS-PAGE and Western blotting with an antibody targeted to Cx43 and α-tubulin. Lane 1 – Control normoxia; Lane 2 - 100nM rotigaptide; Lane 3 - 500nM rotigaptide; Lane 4 - 1μM rotigaptide; Lane 5 – Control 6hrs ischaemia; Lane 6 - 100nM rotigaptide + 6hrs ischaemia; Lane 7 - 500nM rotigaptide + 6hrs ischaemia; Lane 8 - 1μM rotigaptide + 6hrs ischaemia; Lane9 – Control 6hrs ischaemia followed by 1hr reoxygenation; Lane 10 - 100nM rotigaptide + 6hrs ischaemia followed by 1hr reoxygenation; Lane 11 - 500nM rotigaptide + 6hrs ischaemia followed by 1hr reoxygenation; Lane 12 - 1μM rotigaptide + 6hrs ischaemia followed by 1hr reoxygenation. (b) Rat neonatal cardiac myocytes were treated as mentioned above. The graph shows the combined densitometric analysis of 2 separate Western blots. P = Phosphorylated Cx43; NP = non-phosphorylated Cx43.

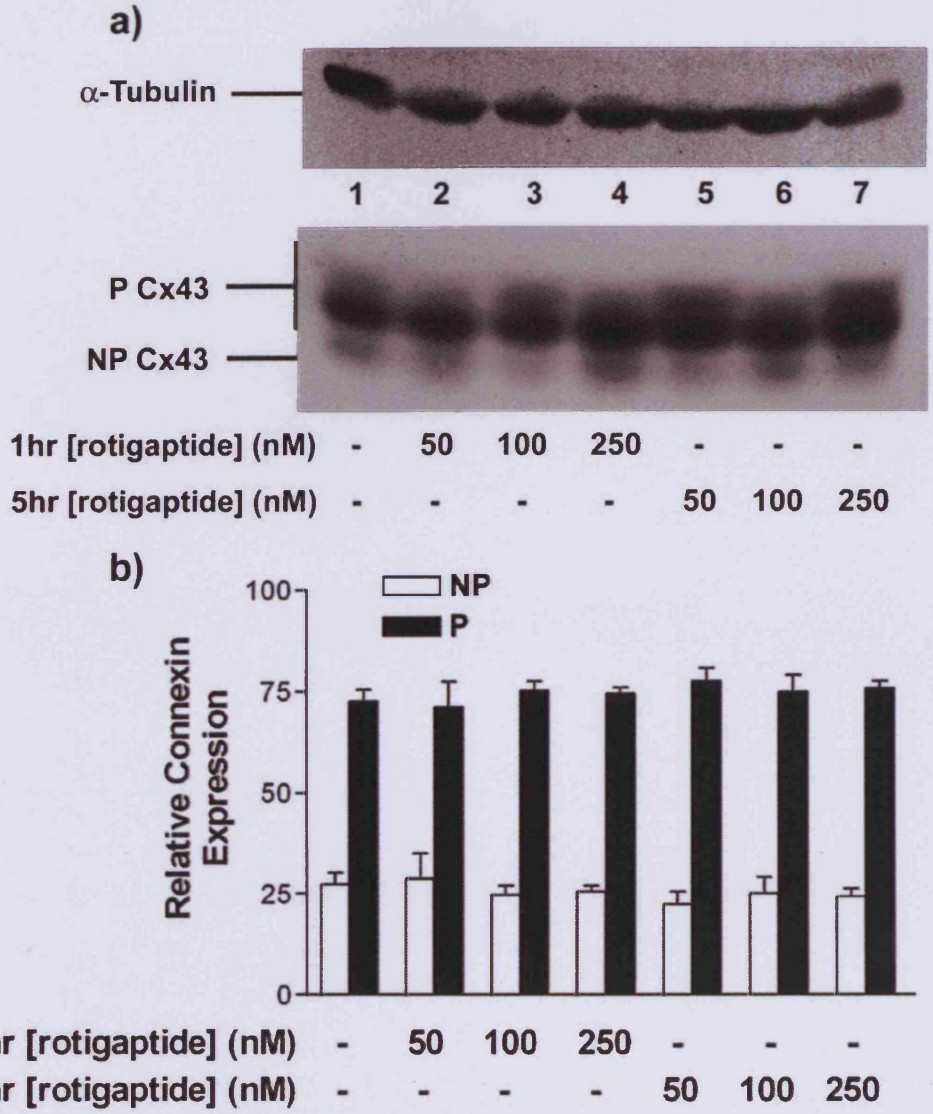

Figure 4.11: The effect of rotigaptide (ZP123) on the phosphorylation status of Cx43

a) Confluent monolayers rat neonatal cardiac myocytes were treated with 50, 100 or 250nM rotigaptide for 1 or 5hrs and cell lysates analyzed by standard SDS-PAGE and Western blotting with an antibody targeted to Cx43 and α-tubulin. Lane 1 - Control; Lane 2 - 50nM rotigaptide for 1hr; Lane 3 - 100nM rotigaptide for 1hr; Lane 4 - 250nM rotigaptide for 1hr; Lane 5 - 50nM rotigaptide for 5hrs; Lane 6 - 100nM rotigaptide for 5hrs; Lane 7 - 250nM rotigaptide for 5hrs. (b) Rat neonatal cardiac myocytes were treated with 50, 100 or 250nM rotigaptide for 1 or 5hrs. The graph shows the combined densitometric analysis of 4 separate Western blots. P = Phosphorylated Cx43; NP = non-phosphorylated Cx43.

4.3.6 Effects of rotigaptide on connexin43-GFP distribution and expression levels

The inherent autofluorescent properties of Cx43-GFP permitted analysis of the effect of rotigaptide on Cx43-GFP expression in live cells by FACS analysis. The results showed that exposure of cells to rotigaptide did not change the overall level of Cx43-GFP fluorescence (Figure 4.13). Further studies using confocal microscopy determined that treatment of the cells with 50nM rotigaptide also had little effect on the cellular distribution of Cx43-GFP, with the protein located predominantly at areas of cell-to-cell contact probably corresponding to gap junction plaques (Figure 4.12e and f). Immunofluorescent analysis of HeLa cells expressing wild type Cx43 before and following treatment with 50nM, 100nM or 250nM rotigaptide illustrated that the peptide did not change the distribution of Cx43 within the cell with similar patterns of Cx43 gap junction plaques seen at areas of cell-to-cell contact under each treatment group (Figure 4.12a-d).

4.3.7 Effects of rotigaptide on connexin43 expression profiles in transfected HeLa cells.

Under control conditions, Cx43-GFP migrated at ~70kDa and band intensity increased following 18-24hrs treatment with sodium butyrate i.e. at times when dye transfer studies were performed (Figure 4.14a). A further band, at ~81kD was confirmed as a phosphorylated isoform of Cx43-GFP in these cells (Figure 4.14a) since the chimera was dephosphorylated by alkaline phosphatase treatment. Parallel data from HeLa cells expressing wild type Cx43 gave similar results.

The effect of rotigaptide on the phosphorylation status and expression of Cx43-GFP in HeLa cells was studied. After treatment with rotigaptide (50nM) for 1-5hrs in the

presence or absence of 18αGA (25μM), the phosphorylation status of Cx43-GFP, after 5hrs treatment of the cells with rotigaptide (50nM) remained unaltered (Figure 4.14c and d). However, preincubation of cells with the gap junction inhibitor 18αGA reduced the phosphorylation of Cx43-GFP; phosphorylation of Cx43 was similarly reduced following incubation with 18αGA in the rotigaptide treated cells (Figure 4.14b).

Rotigaptide is reported to stimulate protein kinase C (Dhein et al., 2003) and it is possible that the antibodies used in the current work failed to detect significant changes in phosphorylation at specific sites. We therefore investigated the effects of rotigaptide on Cx43 expression using an antibody specifically recognising the Ser368 phosphorylation site that is reported to be phosphorylated by protein kinase C (Lampe et al., 2000). Treatment of cells with TPA, a potent activator of protein kinase C (Lampe et al., 2000), confirmed that phosphorylation of Cx43 and Cx43-GFP at position ser368 occurred (Figure 4.15b and c). HeLa cells expressing wild type Cx43 under control conditions, following TPA treatment and 5hrs treatment with 50nM rotigaptide were also probed with another antibody that detects multiple Cx43 isoforms (Rivedal et al., 1996). In both cases, there was no indication of alteration in the amount of Cx43 expressed following rotigaptide treatment, but it was noted that substantial phosphorylation occurs following TPA treatment (Figure 4.15a and b).

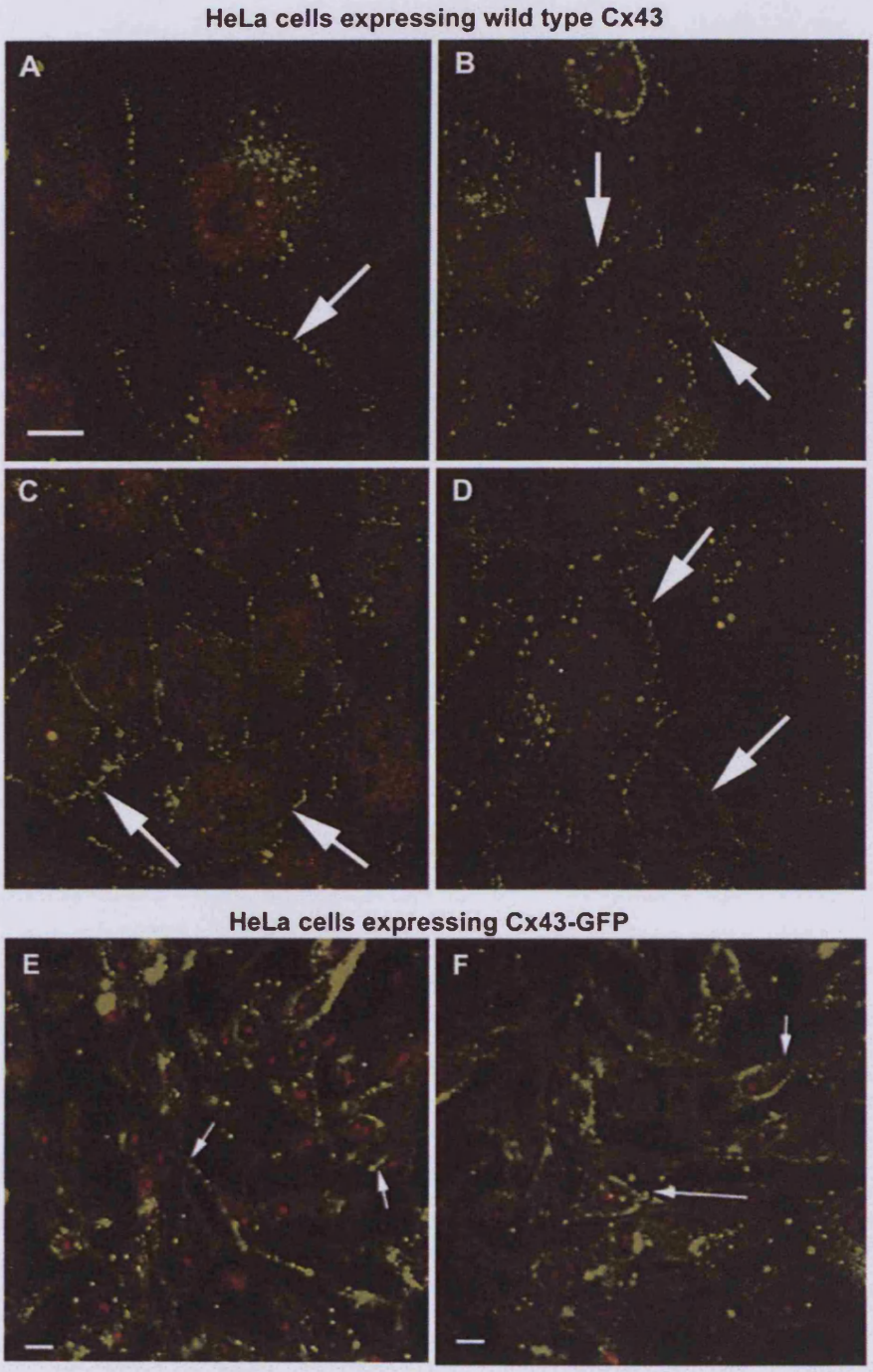

Figure 4.12: The effect of rotigaptide (ZP123) on Cx43 spatial localisation
Confluent monolayers of HeLa cells expressing wild type Cx43 were fixed and stained with a monoclonal antibody targeted to Cx43 following (a) Control conditions, (b) preincubation with 50nM rotigaptide for 5hrs, (c) preincubation with 100nM rotigaptide for 5hrs, (d) preincubation with 250nM rotigaptide for 5hrs.
Confluent monolayers of HeLa cells expressing Cx43-GFP and its intracellular distribution was assessed e) under control conditions and f) following 50nm rotigaptide treatment. It also appears that when GFP is tagged to Cx43 there is also greater accumulation of Cx43-GFP in the cytoplasm. Nuclei were stained with propidium iodide. The white arrows point to Cx43 gap junction plaques. Bar = 20μm (a-d) or 10μm (e-f).

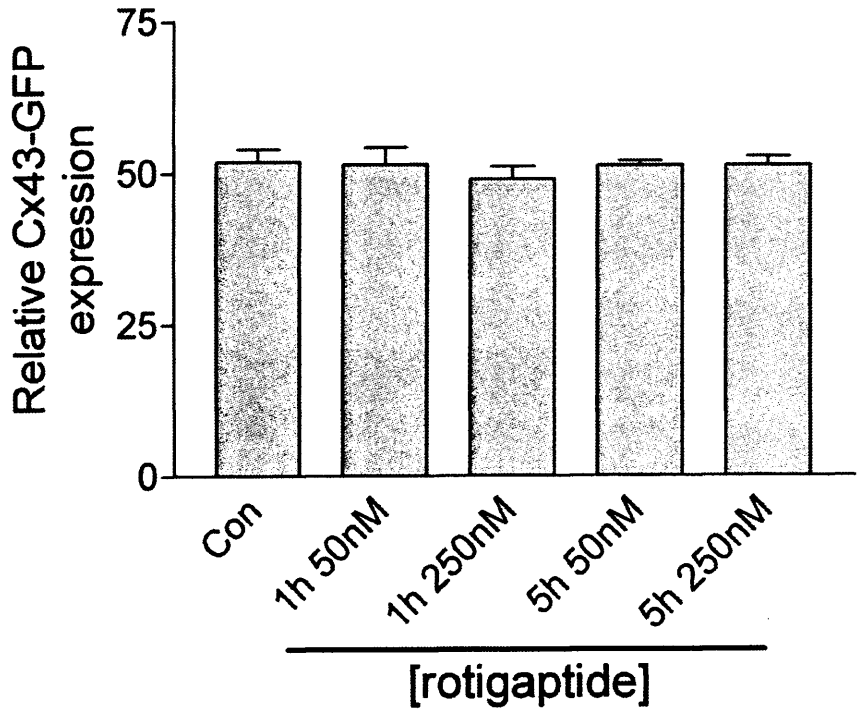

Figure 4.13: The effect of rotigaptide (ZP123) on Cx43-GFP expression.
Cx43-GFP expressing HeLa cells were subject to FACS analysis and the % of cells expressing Cx43-GFP recorded following treatment for 1 and 5hrs with 50 and 250nM ZP123 respectively (n=3).

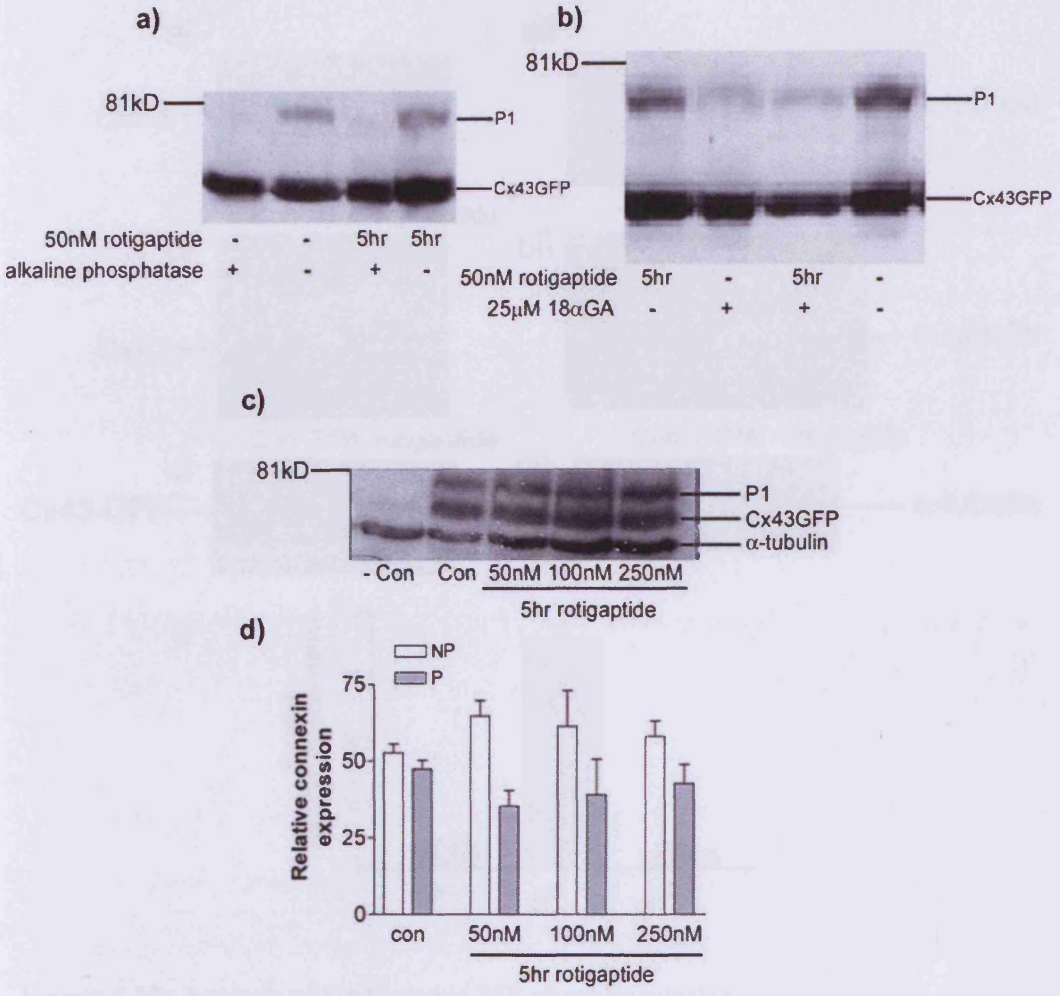

Figure 4.14: The effect of rotigaptide and 18aGA on Cx43-GFP expression
a) Confluent monolayers of HeLa cells expressing Cx43-GFP were lysed under control conditions or following treatment with 50nM rotigaptide for 5hrs. Cell lysates were digested with alkaline phosphatase for 1hr at 37°C followed by SDS-PAGE and Western blotting with antibodies to Cx43. b) Cx43-GFP HeLa cells were treated with 50nM rotigaptide and or 25μM 18αGA. c) Cx43-GFP HeLa cells were treated with 50, 100 or 250nM rotigaptide for 5hrs. d) The graph shows the combined densitometric analysis of three separate Western blots following treatment of Cx43-GFP HeLa cells with 50, 100 or 250nM rotigaptide for 5hrs. P1 = Phosphorylated Cx43; NP = non-phosphorylated Cx43.

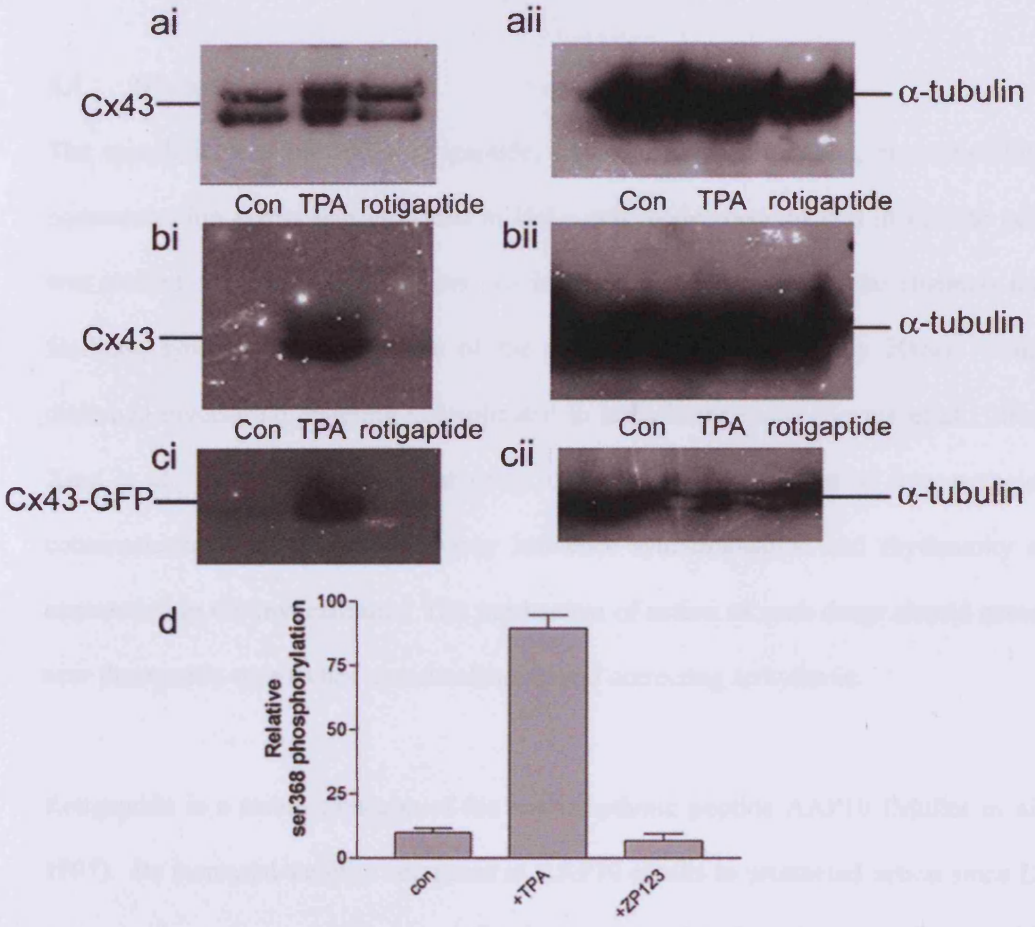

Figure 4.15: Analysis of Cx43 serine 368 phosphorylation
a) (i) HeLa cells expressing wild type Cx43 were probed with an antibody specifically targeted to the carboxyl tail of Cx43 under control conditions, treated with 100ng/ml TPA for 30mins or with 50nM rotigaptide for 5hrs prior to harvesting and Western blot analysis. (ii) α-tubulin staining. b) (i) Cx43 expressing HeLa cells were probed with an antibody specifically targeted to serine 368 on the carboxyl tail of Cx43 under control conditions, treated with 100ng/ml TPA for 30mins or with 50nM rotigaptide for 5hrs prior to harvesting and Western blot analysis. (ii) α-tubulin staining. c) (i) HeLa cells expressing Cx43-GFP were probed with an antibody specifically targeted to serine 368 on the carboxyl tail of Cx43 under control conditions, treated with 100ng/ml TPA for 30mins or with 50nM rotigaptide for 5hrs prior to harvesting and Western blot analysis. (ii) α-tubulin staining. (d) Densitometric analysis of ser 368 phosphorylation in Cx43-GFP expressing HeLa cells. All blots were performed in triplicate.

4.4 Discussion

The specificity and effects of rotigaptide, an antiarrhythmic peptide, on intercellular communication across gap junctions in HeLa cell model systems and in cardiac cells was studied. In heart, gap junctions provide low resistance intercellular channels that facilitate synchronous contraction of the myocytes (Kleber & Rudy 2004). Since disturbed myocardial coupling is implicated in arrhythmogenesis (Severs et al., 2004; Xing et al., 2003) it is likely that drugs that modulate the extent of inter-myocyte communication via gap junctions may influence synchronisation and rhythmicity of contraction in the myocardium. The mechanism of action of such drugs should reveal new therapeutic approaches to understanding and correcting arrhythmia.

Rotigaptide is a stable analogue of the antiarrhythmic peptide AAP10 (Muller et al., 1997). Its increased stability compared to AAP10 results in protracted action since D-amino acids are less prone to degradation by proteases than L-amino acids. Rotigaptide has an *in vitro* half-life in human plasma of 14 days compared to 3-4 minutes for AAP10 (Kjolbye et al., 2003). Previous studies have shown that AAP10 enhanced conductance in adult cardiac myocytes and in HeLa cells expressing Cx43 (Dhein et al., 2001). Rotigaptide prevented re-entrant ventricular tachycardia during myocardial ischaemia in dogs (Xing et al., 2003). Although some effects of rotigaptide on cardiac electrophysiology and Cx43 mediated communication have been studied (Dhein et al., 2003; Eloff et al., 2003) its influence on other functional properties of gap junctions were unknown.

The present results show that rotigaptide increased gap-junctional intercellular communication in cells expressing Cx43 as monitored by the direct intercellular transfer

of fluorescent dyes. This increased communication was demonstrated in HeLa cells expressing wild type Cx43 and Cx43-GFP, but was not observed in HeLa cells expressing wild type Cx26, Cx26-GFP or Cx32-GFP. Although some connexins used in the present work were fused to GFP at its carboxyl terminus, HeLa cells expressing Cx43-GFP, Cx32-GFP and Cx26-GFP were shown previously to be electrically and dye coupled and to propagate intercellular Ca^{2+} waves to each other via gap junctions (Paemeleire et al., 2000) or CxHcs (Bukauskas et al., 2000; Contreras et al., 2002). Fluorescent and non-fluorescent wild type Cx43 expressing channels show similar functional characteristics in a variety of cell types, although subtle differences in channel gating have been reported (Bukauskas et al., 2000; 2002; Paemeleire et al., 2000). The present studies show that rotigaptide acts on both wild type and chimeric Cx43 but not on Cx32 and Cx26 chimeric channels. Increased intercellular dye coupling was also observed in beating neonatal cardiac myocytes and a cell line derived from cardiac atria that possesses cardio-specific properties (Claycomb et al., 1998). Cx43 is the dominant gap junction protein in both cell types but all express low amounts of Cx40 (unpublished data from our laboratory). The enhancing effect on Cx43 dye coupling via gap junctions occurred after 5 hours exposure to rotigaptide. In contrast, the accelerated transmission of electrical signals following rotigaptide treatment was observed within 15 minutes using isolated guinea pig ventricular myocytes and rat atrial strip preparations (Haugan et al., 2005; Xing et al., 2003). These differences in the speed of action suggest that rotigaptide may act rapidly on electrical coupling across gap junctions followed later by an increase in the spread of larger molecules/ions across the junctions. Despite the enhanced propagation of dye now reported and the increase in electrical coupling (Eloff et al., 2003; Haugan et al., 2005), rotigaptide had no effect on the overall synchronisation and contraction rate of the cardiac myocytes and the

spatial localisation of Cx43 in cells was unaltered, in our cardiomyocytes model. Furthermore, even after exposure of cells to rotigaptide for 5 hours, the overall expression level of Cx43 the HeLa cell model or in neonatal cardiac myocytes was unchanged.

The present study has also shown that rotigaptide does not affect ischaemic cardiac myocytes. After cells were exposed to prolonged ischaemia (5-7hrs), rotigaptide had no apparent effect on the dynamics of the response of cells to this insult (Chapter 3). Indeed the beating rate and Cx43 phosphorylation remained similar to that in cells not treated with rotigaptide. It is unsurprising, but encouraging, that rotigaptide has little effect on cells that are beating normally and in synchrony and that its effects may be limited to cells that beat asynchronously.

Exposure of cells for 30 minutes to AAP10 and rotigaptide has been associated with enhanced PKC activity in HeLa cells expressing Cx43 (Weng et al., 2002) suggesting that rotigaptide influenced phosphorylation of Cx43 via a protein kinase C dependent mechanism associated with enhanced electrical communication and these studies implicated a 200kDa plasma membrane protein (Weng et al., 2002). Phosphorylation of Cx43 may be linked to the control of gap junction mediated communication during connexin biogenesis and degradation (Laird 2005) and in the response of cardiac myocytes to normoxia and hypoxia (Lampe & Lau 2004; Turner et al., 2004). Activation of PKC results in phosphorylation of several serine sites including Ser368 and Ser 262 located near the carboxyl terminal tail of Cx43 (Lampe & Lau 2004). However, no detectable changes in the phosphorylation status or expression levels of Cx43 were observed following rotigaptide treatment by Western blot analysis,

examined using a range of antibodies that detect multiple Cx43 phosphorylated isoforms or a specific protein kinase C phosphorylation site (Serine 368) (Lampe et al., 2000). Control experiments using the phorbol ester TPA, a potent inducer of protein kinase C (Lampe et al., 2000), showed that Cx43-GFP is subject to protein kinase C dependent phosphorylation at serine 368 further demonstrating that the attached GFP reporter protein does not modify normal Cx43 function. To determine ultimately whether rotigaptide modulates the phosphorylation status of Cx43 may require other techniques such as mass spectrometry to detect whether specific phosphorylation modifications occur after treatment with the peptide (Axelsen et al., 2006). It was also noteworthy that the Cx26-GFP and Cx32-GFP expressing HeLa cells were unaffected by rotigaptide and that these modified connexins were either not phosphorylated or were subject to minor phosphorylation (Lampe & Lau 2004).

Intercellular communication across gap junctions in cells expressing various connexins, including homotypic Cx43, 32 and 26 have been extensively studied electrophysiologically (Harris 2001) and by dye coupling (Cao et al., 1998; Elfgang et al., 1995). These studies have shown that connexin channels show differential permeabilities to a range of dyes, including those currently studied. The present data indicate that rotigaptide selectively influences homotypic gap junctions constructed of Cx43, but was without effect on gap junctions constructed of Cx26 and 32. However, it is noteworthy that any relationship between gap junction permeability and gap junction conductance is yet to be elucidated.

The highly specific effect of rotigaptide on gap junction intercellular communication is further supported by radioligand binding assays in which rotigaptide displayed only

weak binding affinity to 80 different receptors and ion channels including K^+ ATP channels and dopamine (Haugan et al., 2005). Further analysis of the selective action of rotigaptide on connexins, to supplement electrophysiological studies in cardiac tissue (Eloff et al., 2003) are expected to elucidate the biochemical mechanisms that result in the action of rotigaptide occurring at Cx43 gap junctions but not on junctions constructed of Cx26 and Cx32.

The emergence of rotigaptide as an enhancer of intercellular communication across gap junctions constructed of Cx43 supports the view that it shows promise for further development as a therapeutic tool for modulating acute cardiac arrhythmias.

Chapter 5

Simulated ischaemia induces ATP release from Connexin hemichannels in rat neonatal cardiac myocytes

5.1 Introduction

Cardiac tissue and its constituent myocytes exposed to hypoxia undergo a number of changes, including remodelling involving changes in Cx43 expression and in electrical conduction velocity. A well established metabolic response to hypoxia by cardiac myocytes involves an increased release of ATP (Forrester & Williams 1977). It is possible that this response to hypoxia and ischaemia could be a fundamental property of cardiac myocytes and possibly other cells in various tissues but to a different extent. In the heart, ATP release may have an effect on coronary circulation and also induce changes in cardiac arrhythmia.

5.1.1 ATP is released across connexin hemichannels (CxHcs)

Cells release ATP by various mechanisms, including the emptying of secretory vesicles hitting the plasma membrane, by ABC transporter proteins (Lazarowski et al., 2003) and a large ATP dependent plasma membrane anion channel (Dutta et al., 2004). More recently, CxHcs have emerged as a further release pathway for purines including ATP, implicating a role in paracrine intercellular signalling (Braet et al., 2003; Stout et al., 2002). As discussed in chapter 1, CxHcs are high conductance un-apposed hexameric channels located in the plasma membrane (Martin & Evans 2004; Saez et al., 2003). CxHcs are normally maintained in a closed configuration, but have been shown to open under stress allowing release from the cell of ATP, NAD^+, glutamate and prostaglandins (Bennett et al., 2003; Bruzzone et al., 2001; Cherian et al., 2005; Ebihara 2003; Goodenough & Paul 2003). CxHcs have been detected in isolated primary cardiac myocytes and a range of cell cultures (Evans et al., 2006; Kondo et al., 2000). They can be opened by metabolic inhibition and low extracellular Ca^{2+} levels in various cell types (Contreras et al., 2002; Kondo et al.,

2000), hypo-osmotic challenges (John et al., 2003) and high intracellular Ca^{2+} levels induced by the photoliberation of IP_3 (Leybaert et al., 2003).

5.1.2 Purinergic signalling in the cardiovascular system

Extracellular ATP binds to cell surface P_2Y and P_2X receptor classes; the former are seven trans-membrane domain G-protein linked receptors and the latter are transmitter-gated cation channels (Burnstock 2006; North 2002). ATP binds to P_2Y receptors in vascular endothelium and smooth muscle, regulating vascular tone (Burnstock 1999). Binding and activation of the P_2Y receptor by ATP leads to Ca^{2+} activation of eNOS and the production of nitric oxide, a potent endothelium-derived vasodilator (Burnstock 1999). In addition, adenosine, a breakdown product of ATP, acts on P1 receptors resulting in vasodilation (Burnstock 2002). Adenosine has also been shown to have several cardiovascular protective effects, including the promotion of endothelial cell proliferation (Burnstock 2006).

5.1.3 Chapter Aims

Investigations described in this chapter were carried out to determine the dynamics of cardiac myocyte Cx43Hc opening during a physiological model of ischaemia involving profound hypoxia with glucose depletion. Relationships between CxHc opening during ischaemia and extracellular and intracellular ATP levels were studied and the question addressed as to whether ATP levels can be maintained within physiological limits by inhibition/blockage of open CxHcs. The temporal relationship between Cx43 dephosphorylation and hemichannel opening during ischaemia was also examined. The studies can lead to a better appreciation of the therapeutic value

of peptides that inhibit or enhance gap junction communication, especially in the context of their potential future use as myocardial protective agents following ischaemia.

5.1 Methods

5.2.1 Materials

AAP10 was supplied by Zealand Pharma (Glostrop, Denmark) and dissolved in water to give a 50μM stock and 18αGA (Sigma, UK) was dissolved in DMSO to give a 25mM stock. GAP 26 and GAP 26 scrambled peptide were dissolved in dH_20 and was synthesized by Sigma-Genosys (Cambridge, UK). All other reagents were obtained from Sigma (Poole, U.K).

5.2.2 Cell culture

Rat neonatal cardiac myocytes were prepared and plated as described in chapter 2 (Clarke et al., 2006; Turner et al., 2004). Cells were maintained cDMEM with BrDu (0.1mM) for the first 3 days and thereafter in serum-free medium as described in section 2.2.2.

5.2.3 Hypoxia and Ischaemia treatments

Cardiac myocytes were rendered hypoxic in a hermetically sealed environmental chamber ($InVivo_2$ Hypoxic workstation 400 with Ruskinn gas mixer) with a humidified atmosphere at 37°C containing 0.5% O_2, 5% CO_2 and nitrogen to balance as previously described (Turner et al., 2004). Hypoxic cells were maintained in serum-free DMEM supplemented as shown above and containing $3gL^{-1}$ glucose. To simulate ischaemia, cardiac myocytes were maintained in supplemented serum-free DMEM containing $0.2gL^{-1}$ glucose and placed within the hypoxic chamber with 0.5% O_2. Control cells were maintained in ambient (21%) O_2 and 5% CO_2 conditions at 37°C in a standard tissue culture incubator (Heraeus® HERAcell® 150).

5.2.4 Drug treatments

Cells were treated with the following drugs and peptides: 50μM 18α-glycyrrhetinic acid; 300μM GAP 26, a connexin mimetic peptide specific to Cx43 that has a sequence of VCYDKSFPISHVR; 50nM AAP10, an anti-arrhythmic peptide that has a sequence of Gly-Ala-Gly-Hyp-Pro-Tyr; 300μM GAP 26 scrambled peptide, a non-functional version of GAP 26 with a sequence of CVDISKYRHSVFP. Cells were exposed to the agents for the duration of the experiments.

5.2.5 ATP measurements

ATP was measured using a luciferase-luciferin based luminescence assay (Sigma, USA) as described in section 2.5. For extracellular ATP measurements, cell culture medium was removed at specific time points, centrifuged at 250g for 4mins and supernatants analysed for ATP content, as described in 2.5. Intracellular ATP measurements were made as described in section 2.5.2.

5.2.6 Lactate dehydrogenase measurements

Lactate dehydrogenase (LDH) content of media used to incubate cells was measured using a colourmetric assay (Sigma, USA). NAD reduced to NADH resulted in the stoichiometric conversion of a tetrozolium dye, measured colourimetrically. Cell culture medium was removed at specific time points, centrifuged at 250g for 4mins and analysed for LDH content (Decker & Lohmann-Matthes 1988).

5.2.7 Western blot analysis

Rat neonatal cardiac myocytes grown on 60mm dishes ($4x10^6$) were subjected to ischaemia for periods of 1 to 7hrs, or hypoxia for 5 or 10hrs prior to harvesting as

described in 2.4.1. Equal amounts (100μg) of protein were analysed by SDS-PAGE (10% w/v) (described section 2.4.3) and transferred to nitrocellulose membrane for 3hrs at 300mA. The resulting blots were probed with a polyclonal antibody to Cx43 (Zymed, USA; 1:4000 dilution) that recognises multiple phosphorylated or nonphosphorylated isoforms of Cx43 and a secondary goat anti rabbit horseradish peroxidase antibody (1:2000 dilution). Blots were developed by enhanced chemiluminescene (ECL) and quantified using a Biorad GS-700 densitometer (Martin et al., 2004).

5.3 Results

5.3.1 Ischaemia causes a transient release of extracellular ATP

Extracellular and intracellular ATP levels were stable for 120mins in normoxic conditions before cells were subjected to ischaemia or hypoxia (Figure 5.1). After the first 60mins of ischaemia, neonatal cardiac myocytes still maintained their ATP content with no perceptible change observed in extracellular and intracellular ATP levels. However, after approximately 80mins of ischaemia, ATP release increased substantially (166% ± 16.9 of pre-ischaemic values) (Figure 5.1a), and then returned to ATP levels similar to those prior to this peak of release. These 'basal' ATP levels were again maintained for a further 240mins of ischaemia until they steadily decreased over the following 300mins of ischaemia. Relatively little released ATP was detected between 360-600mins.

Intracellular ATP levels measured concurrently also remained approximately constant but then decreased steadily after 120mins of ischaemia over the subsequent 8hrs to 29.0% ± 3.9 of initial levels (Figure 5.1b). However, this ATP loss was largely reversed after transfer to a normoxic environment following 6 and 8hrs of ischaemia with intracellular ATP levels recovering to 78.5% ± 13.2 and 75.2% ± 13.3 respectively. When the myocytes were reoxygenated following 10hrs of ischaemia, a much smaller recovery of intracellular ATP levels was observed (Figure 5.1b).

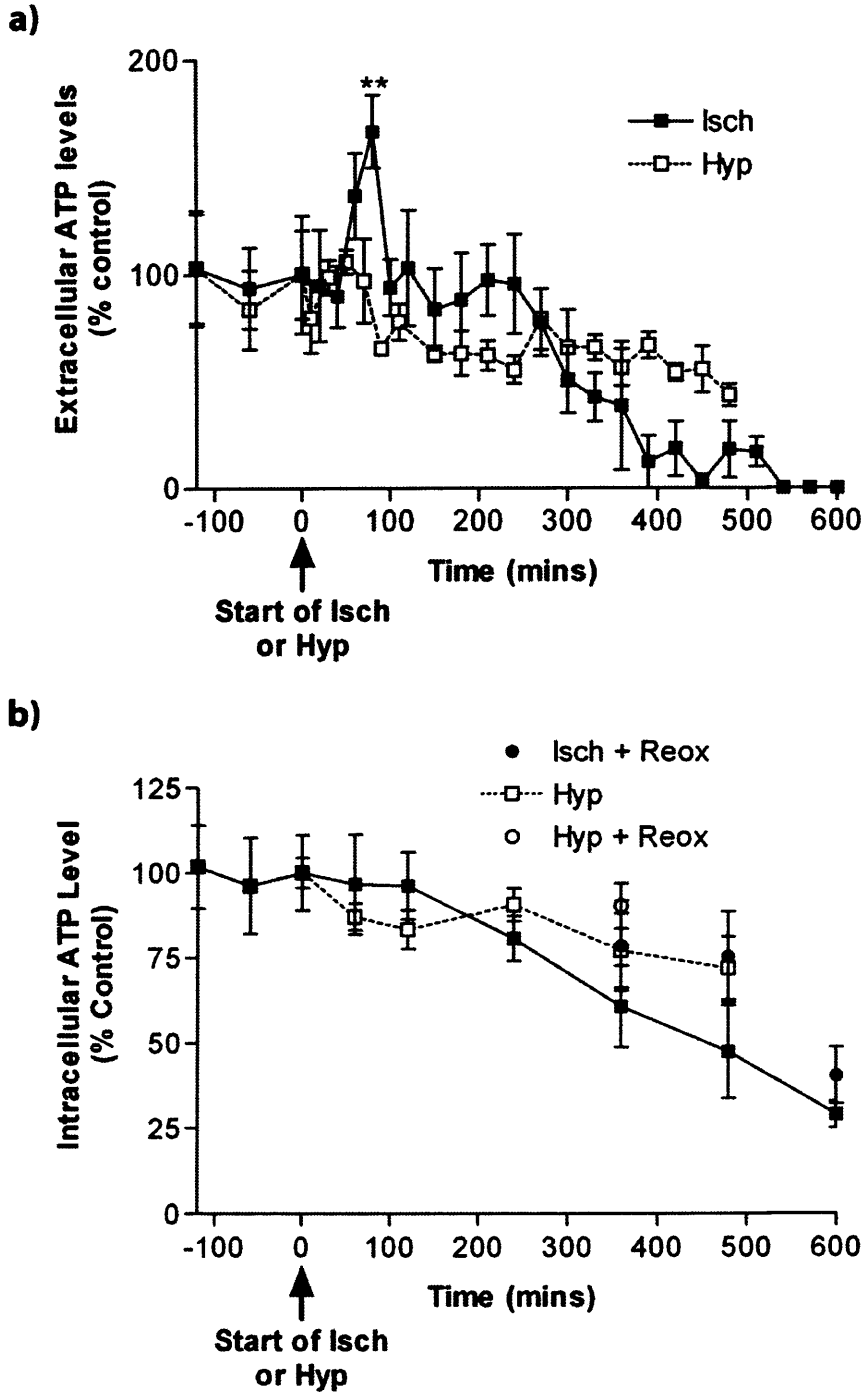

Figure 5.1: The effect of ischaemia and hypoxia on extra- and intra-cellular ATP levels in rat neonatal cardiac myocytes.

Confluent monolayers of rat neonatal cardiac myocytes were made either ischaemic (Isch) or hypoxic (Hyp) as described in the methods. (a) Extracellular medium was sampled at determined time points during treatment and then analysed for ATP content; **P<0.01 unpaired T-test. (b) Cells were harvested in 5% TCA at determined time points during treatment and then analysed for intracellular ATP content; ischaemia (n=7); hypoxia (n=4).

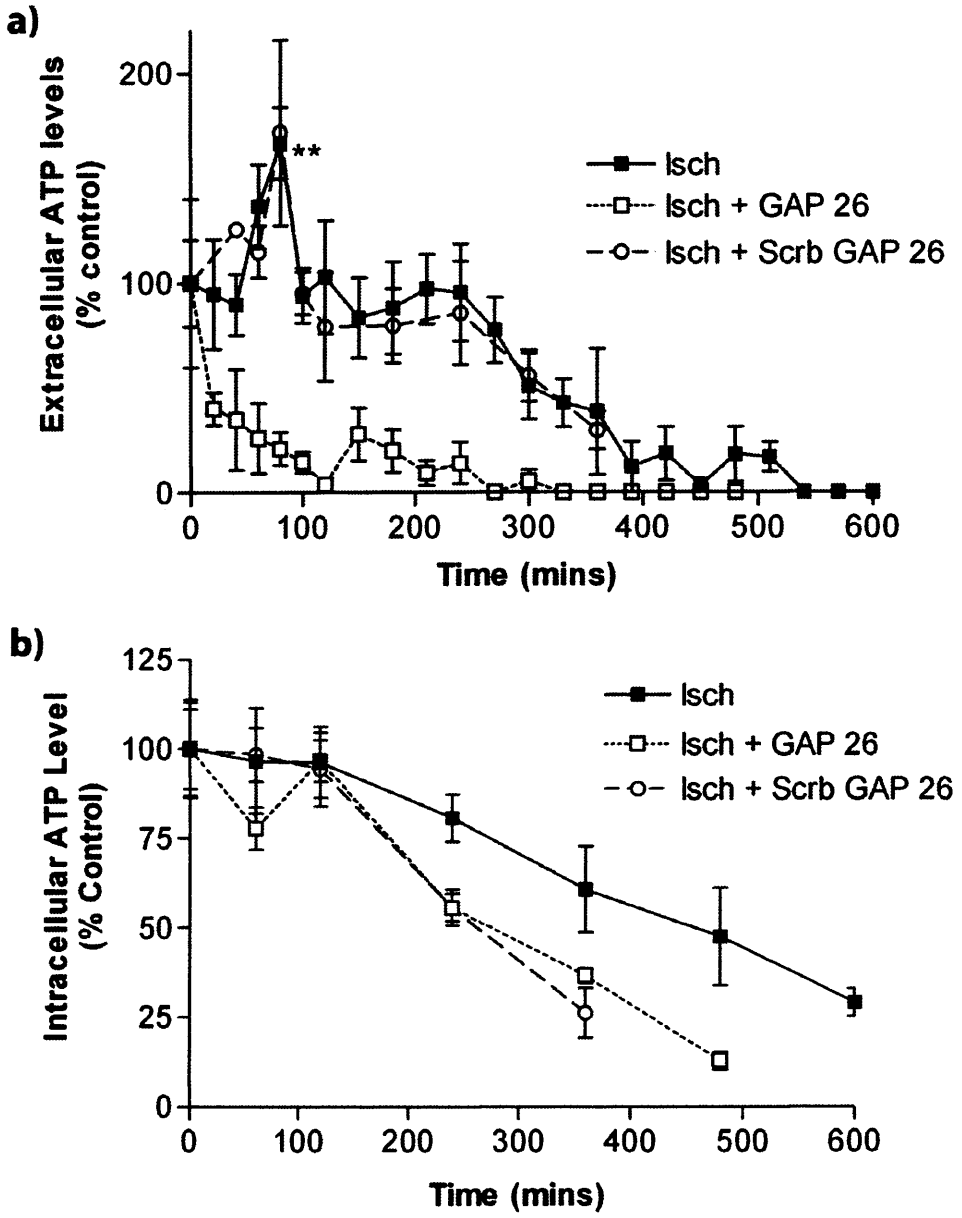

Figure 5.2: The effect of the gap junction inhibitor GAP 26 on extra- and intra-cellular ATP levels in rat neonatal cardiac myocytes during ischaemia. Confluent monolayers of rat neonatal cardiac myocytes were made ischaemic (Isch) as described in the methods and treated with 300μM GAP 26 or 300μM Scrambled (Scrb) GAP 26 at the beginning of the timecourse. (a) Extracellular medium was sampled at determined time points during treatment and then analysed for ATP content. (b) Cells were harvested in 5% TCA at determined time points during treatment and then analysed for intracellular ATP content. Ischaemia (n=7) **P<0.01 unpaired T-test; Ischaemia + GAP 26 (n=4); Ischaemia + Scramble GAP 26 (n=4).

5.3.2 Gap junction channel inhibitors block the transient release of ATP

Exposure of ischaemic myocytes to GAP26, a specific gap junction inhibitor, markedly reduced the transient peak of ATP release that occurred after 80mins (Figure 5.2a); a scrambled GAP26 peptide used as a control was without effect. Furthermore, extracellular ATP levels in myocytes exposed to GAP26 were generally much lower than control levels throughout ischaemia (e.g. 21.0% ± 7.9 after 80mins).

A further gap junction inhibitor, 18αGA, produced a similar response by attenuating the transient ATP release that was observed consistently at 80mins of ischaemia (Figure 5.3a).

Intracellular ATP levels in ischaemic myocytes exposed to GAP26 and 18αGA decreased after the first 60mins of ischaemia but then recovered, and after this time the level of intracellular ATP was similar to that observed in ischaemia. However, ATP loss by the cells then increased after 8hrs (12.9% ± 2.4 GAP26; 23.8% ± 2.9 18αGA) (Figure 5.2b & 5.3b). The scrambled GAP26 peptide caused a greater decrease in intracellular ATP levels after 6 or 8hrs (Figure 5.2b), compared to cardiac myocytes treated with ischaemia.

5.3.3 The effect of AAP10 on extra- and intracellular ATP during ischaemia

Treatment of myocytes with AAP10 during ischaemia resulted in a 2-3 fold increase in ATP release (313% ± 48.4), and this peak observed at 80mins was followed by a less pronounced second peak of ATP release at 180mins (229% ± 55.3) (Figure 5.4a). At later time periods, ATP returned to control levels and continued to decrease steadily, eventually reaching zero after 6hrs of ischaemia. Ischaemic cardiac

myocytes treated with AAP10 showed a steady decrease in intracellular ATP levels, with slight fluctuations. In comparison, in the absence of the peptide myocytes subjected to ischaemia showed a lesser decrease in intracellular ATP levels after 6 or 8hrs (Figure 5.4b).

5.3.4 Cardiac myocytes remain intact during hypoxia and short periods of ischaemia

LDH release from cardiac myocytes remained around basal levels up to 180mins of ischaemic treatment but at later times, they increased gradually over 360mins. Thereafter, LDH increased sharply especially after 8hrs of ischaemia (Figure 5.5a). Lower LDH levels were recorded in hypoxia, and the marked increase seen in ischaemia at later times was not observed (Figure 5.5b). The addition of GAP 26 and 18αGA had no significant effect on LDH release from cardiac myocytes during ischaemia and hypoxia.

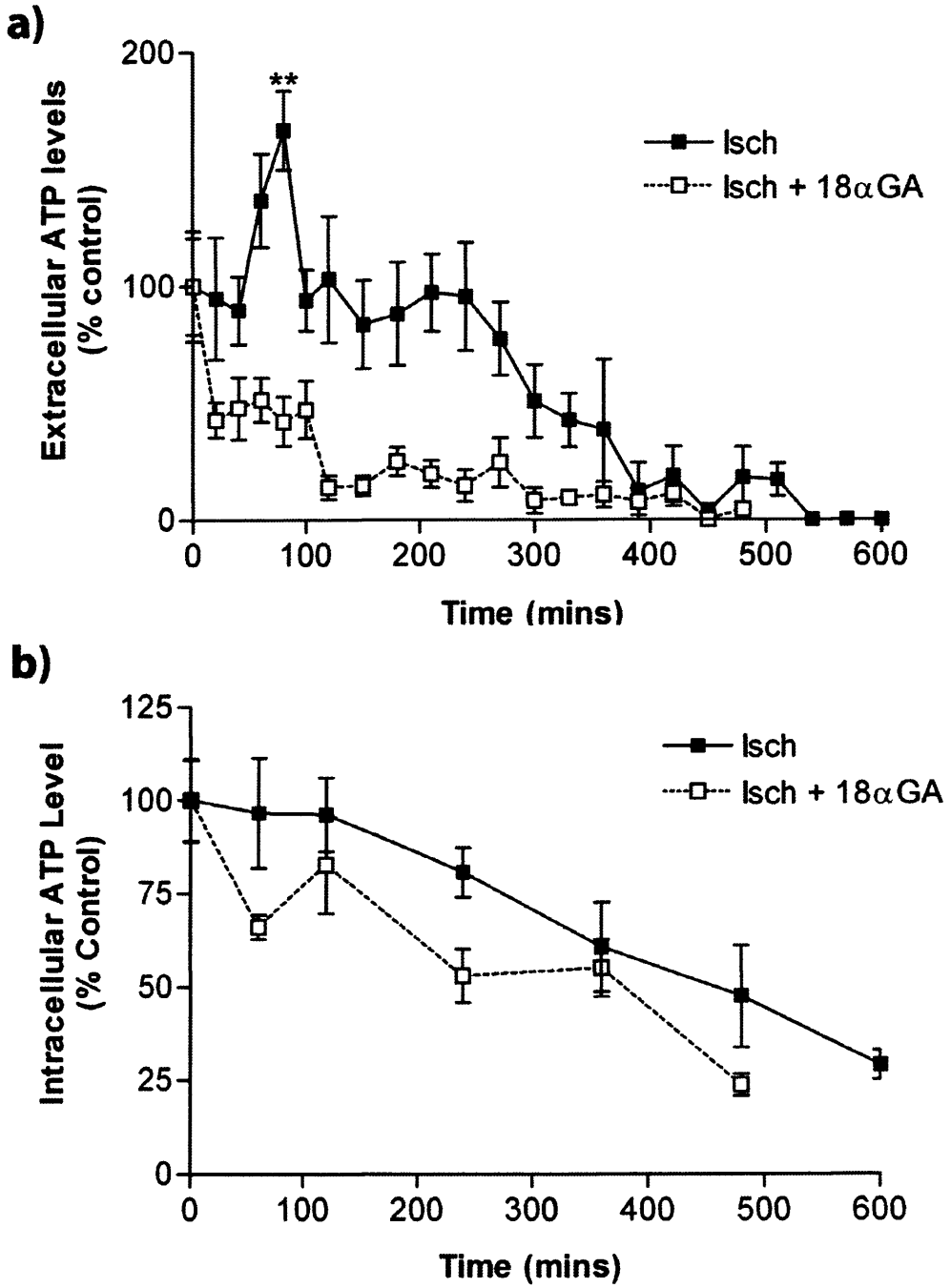

Figure 5.3: The effect of the gap junction inhibitor 18αGA on extra- and intra-cellular ATP levels in rat neonatal cardiac myocytes during ischaemia.
Confluent monolayers of rat neonatal cardiac myocytes were made ischaemic (Isch) as described in the methods and treated with 50μM 18αGA at the beginning of the timecourse. (a) Extracellular medium was sampled at determined time points during treatment and then analysed for ATP content. (b) Cells were harvested in 5% TCA at determined time points during treatment and then analysed for intracellular ATP content. Ischaemia (n=7) **P<0.01 unpaired T-test; Ischaemia + 18αGA (n=6).

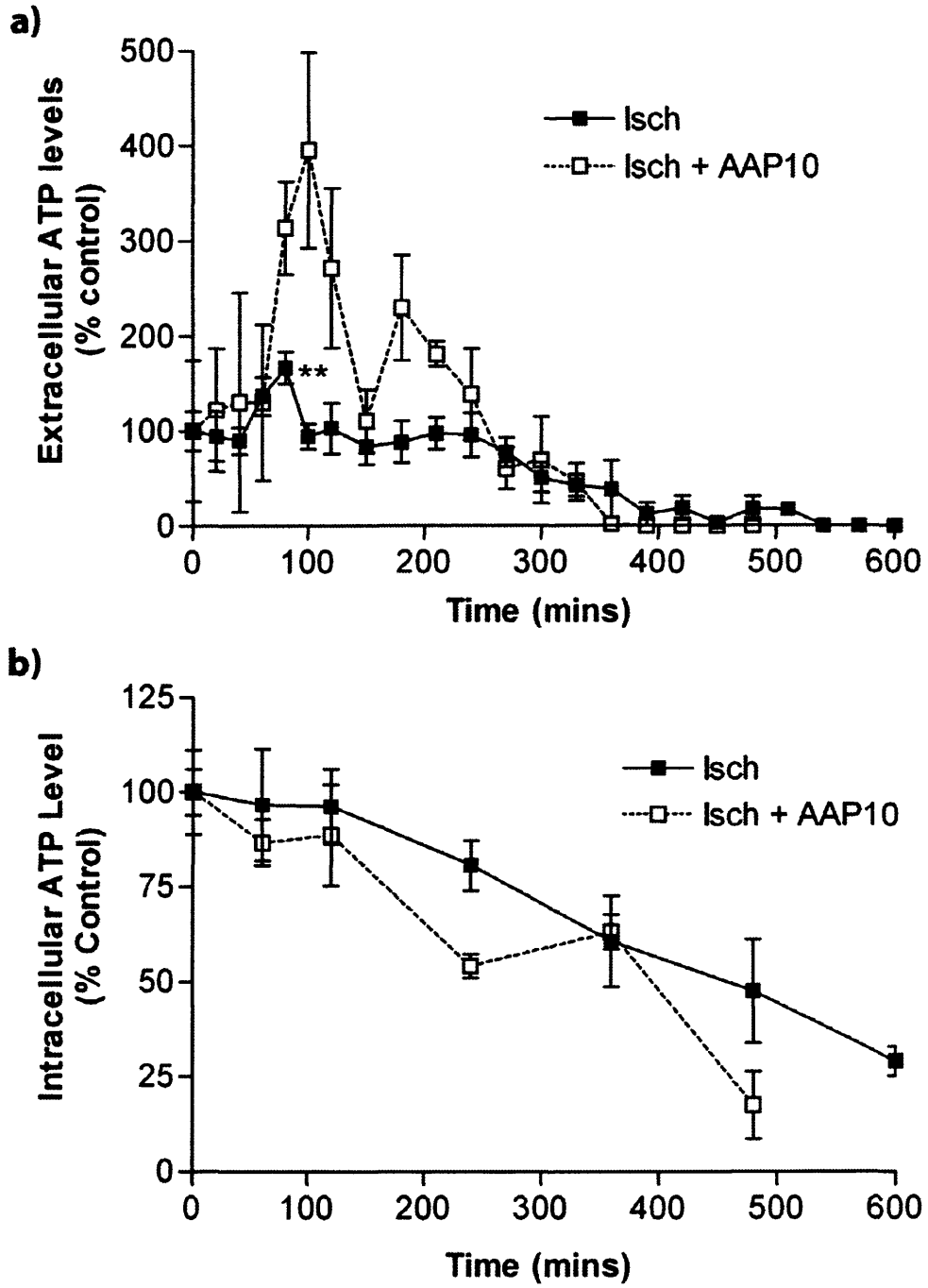

Figure 5.4: The effect of the anti-arrhythmic peptide AAP10 on extra- and intra-cellular ATP levels in rat neonatal cardiac myocytes during ischaemia. Confluent monolayers of rat neonatal cardiac myocytes were made ischaemic (Isch) as described in the methods and treated with 50nM AAP10. (a) Extracellular medium was sampled at determined time points during treatment and then analysed for ATP content. (b) Cells were harvested in 5% TCA at determined time points during treatment and then analysed for intracellular ATP content. Ischaemia (n=7) **P<0.01 unpaired T-test; Ischaemia + AAP10 (n=4).

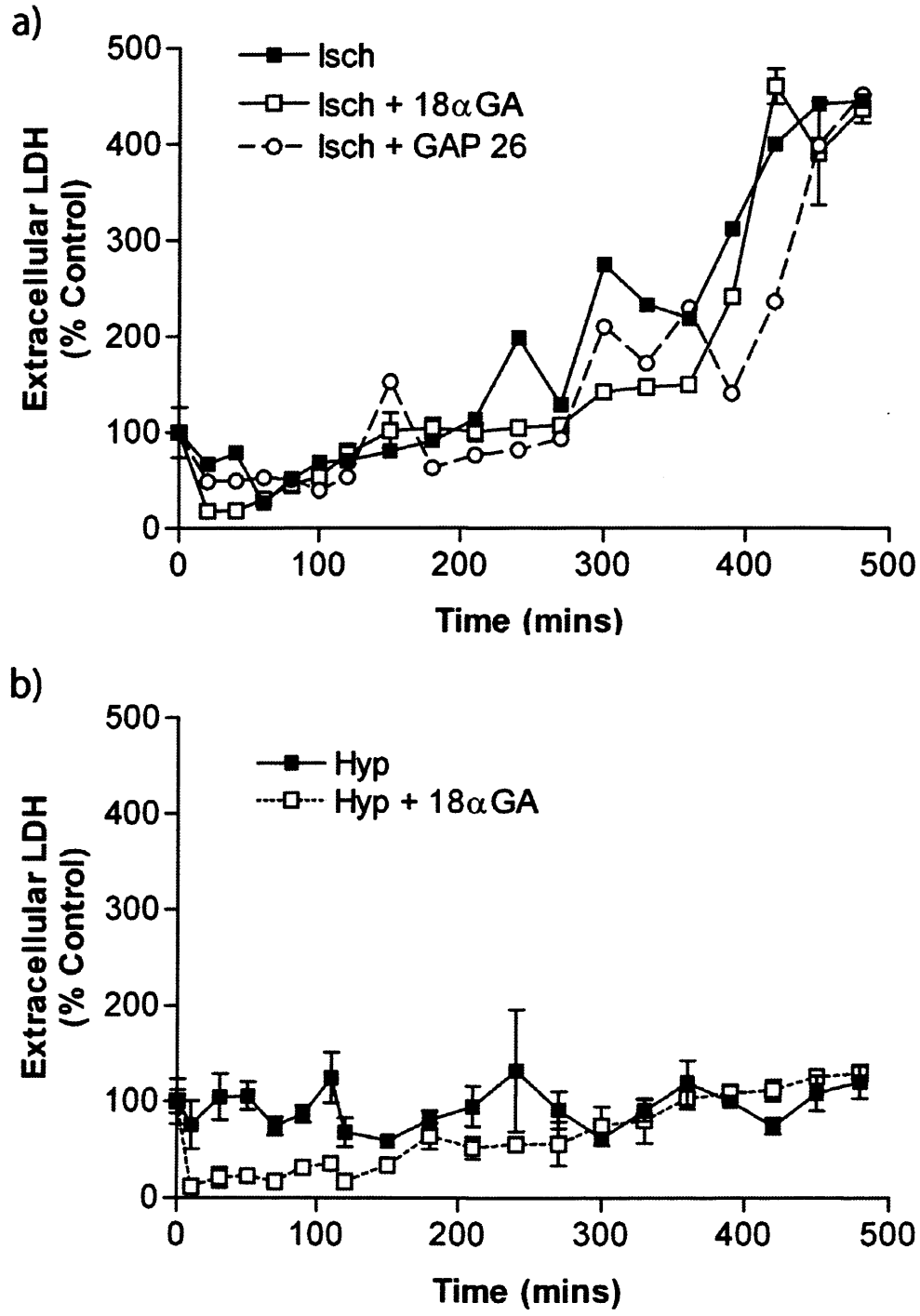

Figure 5.5: The effect of ischaemia and hypoxia on lactic dehydrogenase (LDH) leakage from cardiac myocytes.

(a) Extracellular medium from confluent monolayers of ischaemic (Isch) rat neonatal cardiac myocytes were treated with prolonged ischaemia alone, 18αGA or GAP 26 and then assessed for LDH content. (b) Extracellular medium from confluent monolayers of hypoxic (Hyp) rat neonatal cardiac myocytes were treated with prolonged hypoxia alone or 18αGA and then assessed for LDH content. (For all treatments n=4)

5.3.5 Ischaemia causes dephosphorylation of Cx43 and cessation of synchronous contraction in cardiac myocytes

Exposure of beating cardiac myocytes to ischaemia resulted in the phosphorylated component of Cx43 being maintained for up to 4hrs of insult, thus encompassing the period when the characteristic peaks of ATP release observed (Chapter 3, Figure 3.3). However, after 5 and 10hrs of ischaemia, the phosphorylated component of Cx43 had decreased from 69.2% to 30.6% and 18% of initial total Cx43 values respectively (Figure 5.6). Rat neonatal cardiac myocytes contracted synchronously at 150-210 beats per minute, but exposure to ischaemia caused the cell beating rate to steadily decrease until after 240mins when beating stopped (Figure 5.7).

5.3.6 Effects of hypoxia on ATP levels, Cx43 expression and myocyte contraction

In contrast to the effects of ischaemia, hypoxia had little effect on extracellular ATP levels, which remained approximately constant in cardiac myocytes (Figure 5.1a). In hypoxic myocytes exposed to 50μM 18αGA, ATP levels fluctuated slightly but showed little overall change until about 240mins when they decreased steadily (Figure 5.8a), possibly due to the cytotoxic effects of prolonged exposure to 18αGA. Intracellular ATP levels in hypoxic myocytes decreased to approximately 15% less than the basal level and were maintained for the duration of the 8hrs treatment (Figure 5.1b), with 50μM 18αGA also having little effect (Figure 5.8b). Exposure to prolonged (8hrs) hypoxic insult had little effect the synchronous beating rate that remained approximately constant (Figure 5.7). Also, 10hrs hypoxia resulted in little change Cx43 phosphorylation status (Figure 5.9).

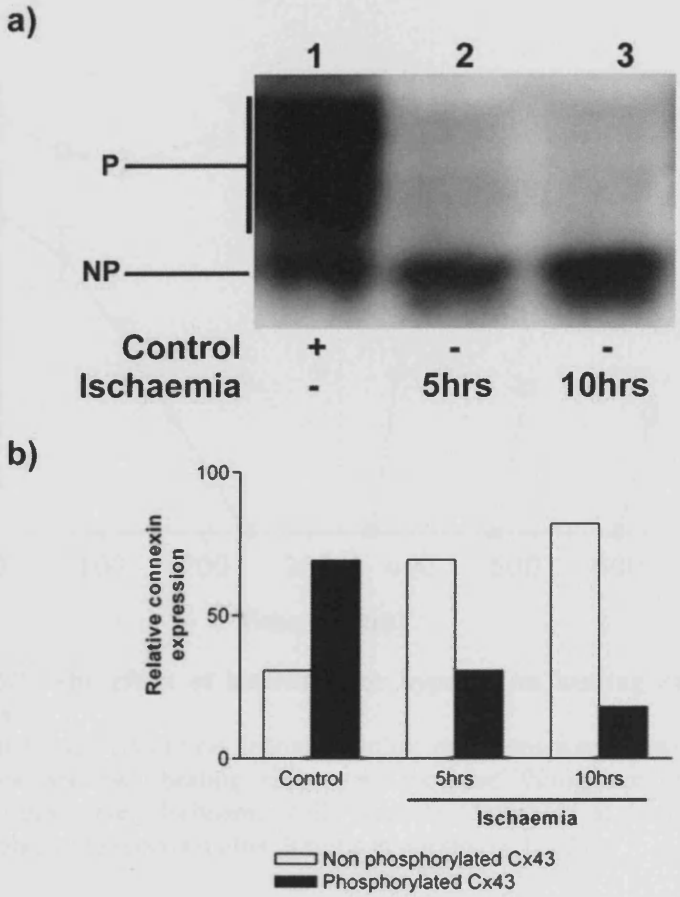

Figure 5.6: The effect of ischaemia on the phosphorylation status of Cx43
a) Confluent monolayers of rat neonatal cardiac myocytes were subjected to ischaemia for 5 and 10hrs and the cell lysates analyzed by standard SDS-PAGE and Western blotting with an antibody targeted to Cx43, Lane 1 - Control; Lane 2 - 5hrs ischaemia; Lane 3 - 10hrs ischaemia. (b) Rat neonatal cardiac myocytes were treated as mentioned above. The graph shows the densitometric analysis of the Western blot.

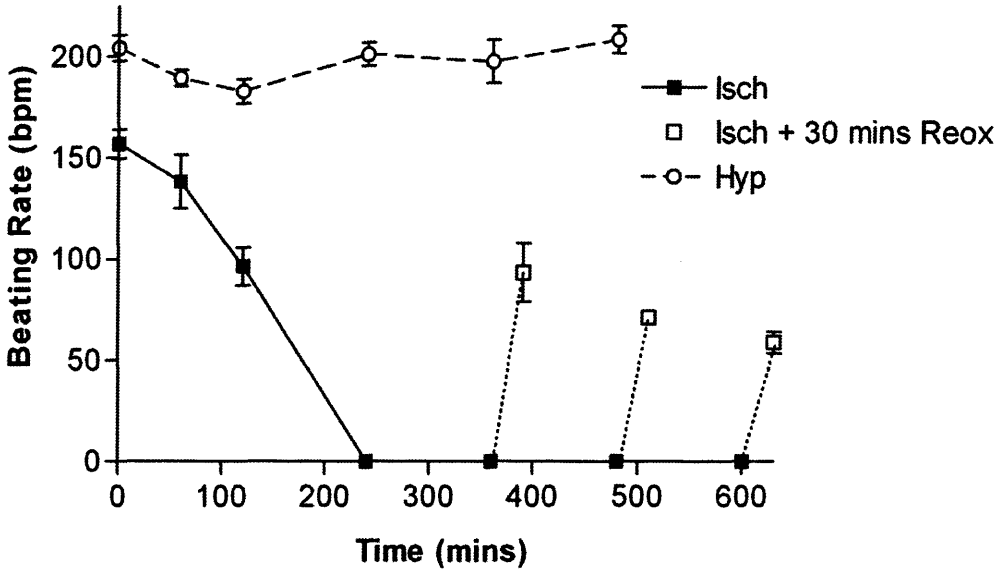

Figure 5.7: The effect of ischaemia or hypoxia on beating rates of cardiac myocytes.

Confluent monolayers of rat neonatal cardiac myocytes were viewed under a light microscope and cell beating rates were recorded throughout an ischaemic or hypoxic timecourse. Ischaemic cells were reoxygenated at 6, 8 and 10hrs and beating rates were recorded after 30mins in normoxia. (n=3)

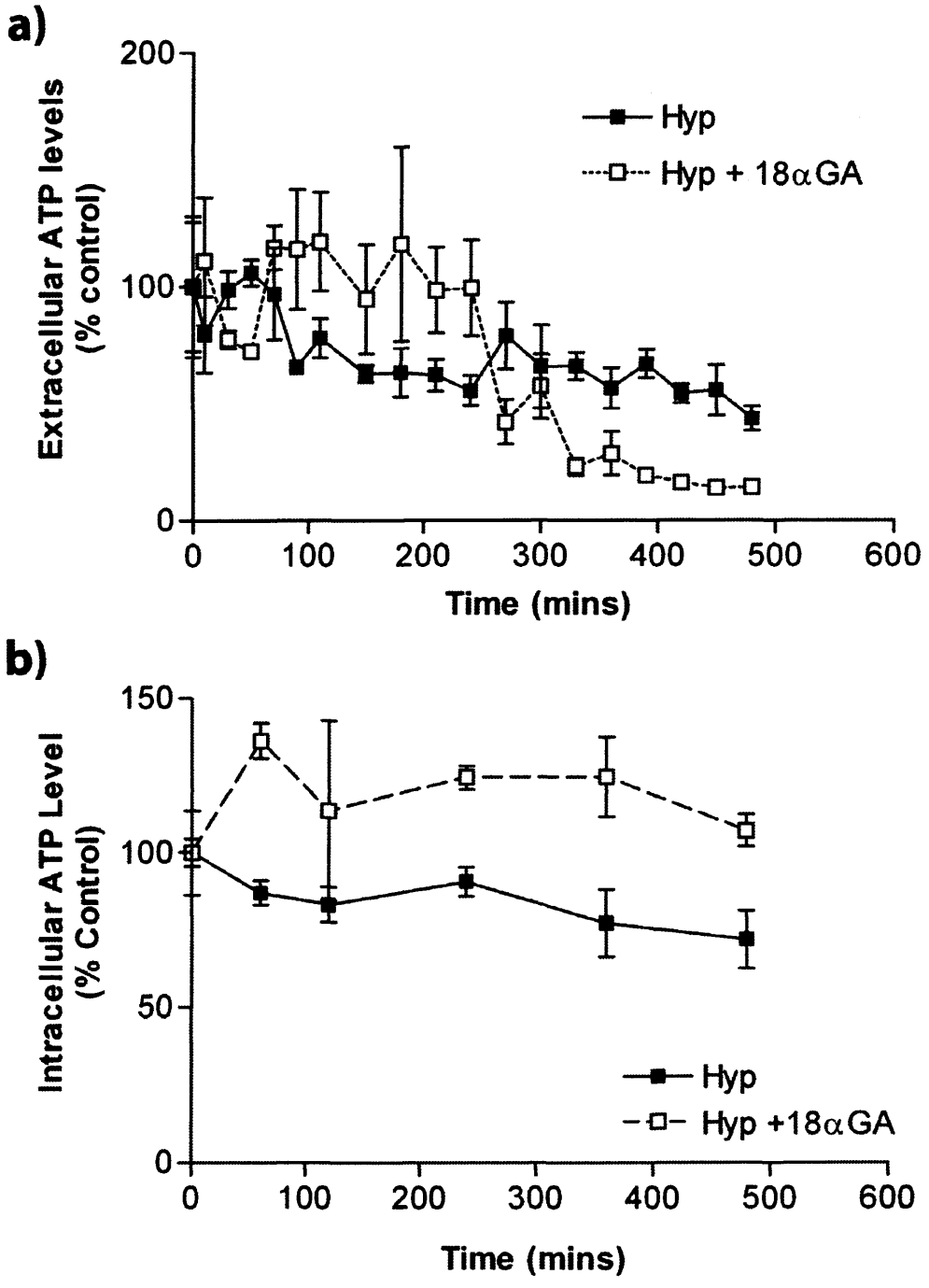

Figure 5.8: The effect of 18αGA on extracellular ATP levels in rat neonatal cardiac myocytes during hypoxia.

Confluent monolayers of rat neonatal cardiac myocytes were made hypoxic (Hyp) as described in the methods. The cells were then treated with 50μM 18αGA at the beginning of the timecourse. (a) Extracellular medium was sampled at determined time points during treatment and then analysed for ATP content. (b) Cells were harvested in 5% TCA at determined time points during treatment and then analysed for ATP content. Hypoxia (n=4); Hypoxia + 18αGA (n=4).

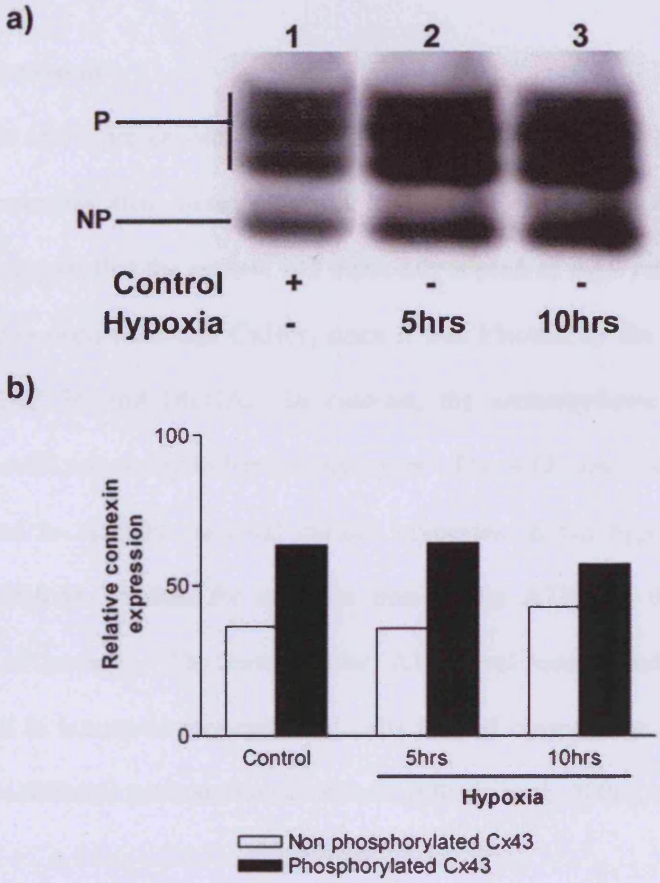

Figure 5.9: The effect of hypoxia on the phosphorylation status of Cx43
a) Confluent monolayers of rat neonatal cardiac myocytes were subjected to hypoxia for 5 and 10hrs and the cell lysates analyzed by standard SDS-PAGE and Western blotting (equal amounts of protein were run) with an antibody targeted to Cx43, Lane 1 - Control; Lane 2 - 5hrs hypoxia; Lane 3 - 6hrs hypoxia. (b) Rat neonatal cardiac myocytes were treated as mentioned above. The overall expression appears, by eye, to be greater in hypoxia than in normoxia. The graph shows the densitometric analysis of the Western blot.

5.4 Discussion

The results of the present study show that there is low level ATP release by cultured cardiac myocytes that increases under conditions of ischaemic stress. The data strongly suggests that the general and especially a peak of ATP release at 80 minutes of ischaemia occurs through CxHcs, since it was blocked by the connexin mimetic peptide GAP 26 and 18αGA. In contrast, the antiarrhythmic peptide, AAP10, enhanced ATP release by ischaemic myocytes. The ATP concentration measured in media used to incubate neonatal cardiac myocytes in the hypoxic chamber was 4.78 ± 0.764nM. Values for myocyte intracellular ATP was 9.09 ± 1.298mmol ATP/mg of protein. The extracellular ATP level corresponds closely to that determined in human airway epithelial cells located close to the plasma membrane and using a different method of measurement (Okada et al., 2006).

CxHcs were previously regarded as evanescent precursors of gap junctions, structures that are essentially two hemichannels in opposition and providing a direct communication channel between cells (Evans et al., 2006; Martin & Evans 2004). However, CxHcs are emerging as plasma membrane channels with unitary conductances that vary according to Cx subtype (Saez et al., 2005). CxHcs have been the subject of intense research, with many mechanisms of channel opening being highlighted. The most common strategies for studying the gating of CxHcs involve the manipulation of extracellular ion concentrations, especially low extracellular Ca^{2+} (Contreras et al., 2003; Quist et al., 2000), in addition to low concentrations of other extracellular ions such as Mg^{2+} (Contreras et al., 2003), Cl^- (Kondo et al., 2000) and Na^+ (John et al., 1999). Depolarisation is another method utilised along with sheer stress (Cherian et al., 2005), point mechanical stimulation (Gomes et al., 2005;

Romanello et al., 2003), negative pressure (Bao et al., 2004) and osmolarity changes (John et al., 2003; Quist et al., 2000).

The present studies allow ischaemic stress to be added to the list of those changes, especially environmental, that open CxHcs. Another study (Thompson et al., 2006) has also shown that ischaemia opens hemichannels in neuronal cells and although the protein nature of the neuronal channels was not investigated, it was proposed that they were pannexins and not connexins. The precise mechanisms involved in CxHc opening under these conditions are unknown but it is highly likely that changes in phosphorylation could be involved (De Vuyst et al., 2006). CxHcs have been shown to be inhibited by activation of kinases such as PKC and v-Src (Bao et al., 2004; Lampe & Lau 2004), and therefore dephosphorylation could result in increased channel opening under these conditions.

In the present study, ischaemia caused ATP (molecular mass 501Da) but not LDH (molecular mass 140kDa) to be released from cardiac myocytes. Extracellular LDH increased during ischaemia, as expected, but the increase appeared to be due to a steady leakage followed by a vast release as ischaemia continued. This indicates that the plasma membrane remains intact and only allows a small leakage until approximately 6-7 hours of ischaemia when the plasma membrane's permeability is seriously compromised. ATP release during ischaemia was low until a peak appeared at around 80 minutes. This suggests that cells have a mechanism to regulate the loss of ATP via CxHcs. The results indicate that there is a basal release of ATP from cardiac myocytes during normoxia and ischaemia and this is prevented by GAP26 and

18αGA, indicating that much of the ATP release from cells is most likely to be through CxHcs.

ATP released from cells through CxHcs adds further information to how cardiac cells respond to conditions of low oxygen. ATP and its breakdown products are known to influence movement of blood through the vasculature by causing blood vessel relaxation via purinergic receptors. ATP released from cells dilates blood vessels and thus facilitates increased oxygen delivery to the heart. ATP is converted via ecto-apyrase (CD39) to AMP, which is then further processed to adenosine by ecto - 5'-nucleotidase (CD73), and both metabolites are well characterised modulators of cardiac function (Eltzschig et al., 2006). Adenosine is also a biochemical mediator of bradyarrhythmias associated with hypoxia and ischaemia (Belardinelli 1987). Indeed, in addition to adenosine, ATP and other adenosine nucleotides have been known for a long time to cause atrioventricular block (Drury & Szent-Gyorgyi 1929). More recently, adenosine was shown to induce cardiac arrhythmia and especially ventricular automaticity (Hernandez & Ribeiro 1996).

In the present studies, hypoxia was tolerated better than ischaemia by cardiac myocytes; cells continued to beat in hypoxic conditions whereas in ischaemia they stopped synchronous beating after 4hrs (Chapter 3). This is perhaps unsurprising, since ischaemia puts cells under greater stress than hypoxia, due to the lack of metabolic substrates and the disruption of glycolysis. In ischaemia, there was continued loss of ATP, which could not be sustained (Turner et al., 2004) and this ultimately lead to cell death as reflected by LDH measurements. Ischaemic preconditioning involves the phosphorylation of Cx43 and implicates the involvement

of Cx43Hcs at non-junctional areas in cardiac myocytes (Schulz & Heusch 2004). Similar molecular mechanisms involving CxHcs are likely to operate in stroke/hypoxia models (de Pina-Benabou et al., 2005; Kirchhoff et al., 2001). Overall, these studies suggest that open CxHcs are major participants/contributors in cell death. The data shows that the connexin mimetic peptides could be useful therapeutic tools for cardio- and neuro-protection in ischaemic injury. Interestingly, traditional connexin inhibitors (halothane/octanol), that are far less specific than the Cx mimetics used in the present studies, have been shown to reduce Cx43-linked brain injury in animal models (de Pina-Benabou et al., 2005).

The data showed that ischaemia but not hypoxia was accompanied by dephosphorylation of Cx43. The roles of Cx43 phosphorylation in the functioning of gap junctions and CxHcs continue to be debated (Lampe & Lau 2004; Moreno 2005; van Veen et al., 2006), with the kinases phosphorylating specific connexins slowly being revealed (Ek-Vitorin et al., 2006; Somekawa et al., 2005) and the relevant phospho-serines subject to modification in ischaemia identified (Axelsen et al., 2006). Many investigations have shown that ATP metabolism is disrupted in hypoxic/ischaemic hearts. For example, Beardslee et al. (2000) showed that dephosphorylation of Cx43 occurred within 30-40 minutes of induction of ischaemia in perfused hearts. Using isolated cardiac myocytes, dephosphorylation occurred within 8 hours and was rapidly and robustly reversed within 30 minutes (Turner et al., 2004). Using cultured neonatal rat ventricular myocytes, Zeevi-Levin et al., (2005) showed that total Cx43, including phosphorylated and unphosphorylated forms, increased initially before Cx43 dephosphorylation occurred at later times of hypoxia. The present results are broadly in agreement with the above, and variations, especially

in the timings of dephosphorylation, can be ascribed to the efficiency and induction of sustained low oxygen tensions.

Connexin mimetic peptides are 11/12mers that corresponded to extracellular loop sequences of connexin 32 (Warner et al., 1995). These peptides were modified later to mimic extracellular loop sequences in Cx43 and were shown to block the gap junctions connecting vascular smooth muscle cells and endothelial cells (Chaytor et al., 1997; 1998). The broad action of connexin mimetic peptides is demonstrated by the blockage of gap junction communication in cells of the immune system (Oviedo-Orta & Evans 2004) as well as in brain endothelial cells (Braet et al., 2003). Connexin mimetic peptides have been shown to reduce ATP release in a range of cells subjected to various types of stress (Boudreault & Grygorczyk 2004; Braet et al., 2003; Gomes et al., 2005; Pearson et al., 2005)

The studies obtained with two different short peptides indicate that CxHcs are prospective therapeutic targets in addressing cardioprotection in hypoxic/ischaemic stress (Murphy 2004; Salameh & Dhein 2005). Indeed, plasma membrane channels constructed of connexins as well as their orthologues, the pannexins, are emerging as key components in the response of cells to hypoxia/ischaemia in physiologically susceptible tissues (Thompson et al., 2006) and their roles in regulating cell death especially in nervous tissue (Contreras et al., 2004). With regard to the molecular mechanism of action, the connexin mimetic peptides are proposed to bind to CxHcs located in unopposed plasma membrane regions thereby limiting the movements of ions and metabolites across these channels (Evans et al., 2006). In ischaemia, it is possible that CxHcs open and allow increased Ca^{2+} entry leading to Ca^{2+} overload,

adenine nucleotide depletion and oxidative stress ultimately involving mitochondrial dysfunction (Halestrap et al., 2004). The present results show that ATP depletion and release that is blocked by the connexin mimetic peptide, and increased by AAP10, becomes evident after 80-90 minutes, possibly caused by the opening of mitochondrial transition pores. The mechanism of action of AAP10 as well as its analogue rotigaptide is less clear. Nevertheless, the observation that the peak of ATP release evident in ischaemic neonatal cardiomyocytes at 80 minutes is blocked by connexin mimetic peptides likely to interact with CxHcs and increased by AAP10 at the same time following initiation of ischaemia suggests that both peptides act, with opposite outcomes, on CxHc permeability.

Chapter 6

Approaches to studying trafficking and assembly of gap junctions in cardiac myocytes

6.1 Introduction

Reporter proteins tagged to connexin proteins have been used extensively to study gap junction biogenesis, and this approach has featured the use of connexins tagged at the carboxyl terminus with reporter proteins such as aequorin and green fluorescent protein (GFP) (George et al., 1998; Jordan et al., 1999; Martin et al., 2001). After transfection into cells of the relevant cDNA and expression of the chimeric connexins, they are assembled into functionally active gap junctions, allowing intercellular Ca^{2+} wave propagation and transfer of small fluorescent dyes, with similar gating parameters to their wild type equivalents (Bukauskas et al., 2000; 2002; Paemeleire et al., 2000). When used in conjunction with high-resolution time-lapse microscopy the chimeric fluorescent connexins allow imaging of the dynamics of gap junction channel assembly in live cells (Laird 2006; Martin et al., 2001). However, GFP and its variants are 25-27kD proteins and are often of similar bulk to the protein of interest. They are usually fused to the carboxyl tail of connexins which varies in length from about 18 (Cx26) to 275 (Cx57) amino acids. Attachment of GFP to the end of the C-terminus, but not to regions nearer to the membrane of the C-terminus of Cx32, resulted in the connexin being trafficked normally to the plasma membrane and forming functional gap junctions (Martin et al., 2000).

Cyan (CFP), red (DsRedFP) and yellow (YFP) variants of GFP have enabled analysis of co-expressed connexin proteins and protein-protein interactions using advanced imaging procedures such as FRET. Fluorescent protein tags are very versatile but due to their large size as described above there are some disadvantages despite the fact that most of

the fluorescently tagged connexins form functional gap junction channels. DsRedFP chimera of Cx43 is an example of a non-functional tag since it has difficulties in folding and becomes aggregated (Lauf et al., 2001; Martin et al., 2001).

6.1.1 The visual identification of Cx43 in cardiac myocytes

Connexins in the heart are usually detected as large punctate stains at the intercalated disc by immuno-labelling, utilising antibodies that specifically detect connexin proteins (or more specifically epitopes on the cytoplasmic side of the connexin) followed by labelling with a secondary antibody that is fluorescent (Kaba et al., 2001; Severs et al., 2001; 2004). Immunostaining of connexins is an effective technique for studying protein localisation in HeLa, Cos-7 as well as others cultured cells when used in combination with live cell imaging (Martin et al., 2001). However, the trafficking pathways of connexins during their assembly and delivery to the intercalated discs in the heart have not yet been elucidated. A major reason is that it is very difficult to express fluorescently labelled connexins in primary rat cardiac myocytes. Indeed, a recent literature search revealed that no investigator to my knowledge has successfully transfected primary neonatal cardiac myocytes with recombinant connexin genes.

6.1.2 FlAsH fluorescent labelling system

A novel labelling system, FlAsH (**Fl**uorescein **As**enical **H**airpin binder), was described by Griffin et al. (1998), that allows live cell imaging and 'pulse-chase' labelling of a continuously expressed protein such as Cx43. Cx43 was labelled with FlAsH (green) and later ReAsH (a red label) was added, thereby allowing older and newer copies of Cx43 to

be identified in a single image (i.e. pulse-labelling), as shown in Figure 6.1 (Evans & Martin 2002; Gaietta et al., 2002).

Using recombinant techniques, the carboxyl tail of Cx43 can be labelled with a small motif (6 – 20 residues) containing the sequence – Cys – Cys – Xaa – Xaa – Cys – Cys – (Gaietta et al., 2002), although the motif – Cys – Cys – Pro – Gly – Cys – Cys – was recommended due to higher affinity and more rapid binding (Adams et al., 2002). Cells containing the tagged Cx43 are then exposed to a membrane permeant nonfluorescent biarsenical derivative of fluorescein, FlAsH-EDT_2 (Panvera (now Invitrogen), USA). FlAsH binds with high affinity and specificity to the tetracysteine motif conferring strong green fluorescence (Figure 6.2b) (Griffin et al., 1998). The FlAsH molecule is a combination of fluorescein with trivalent arsenic substituents on the 4'- and 5'- positions (Figure 6.2a). The rigid spacing of the two arsenics in the FlAsH molecule enables it to bind with the thiol groups of the tetracysteine motif with high affinity and specificity. The simultaneous addition of EDT (1,2-ethanedithiol) minimises possible toxicity and non-specific binding to endogenous thiols caused by the trivalent arsenic atoms (Gaietta et al., 2002). The tetracysteine motif is clearly much smaller than a fluorescent protein tag such as GFP or aequorin and therefore is less likely to influence protein trafficking or functions. In addition, red and blue emitting analogues have also been developed known as ReAsH-EDT_2 and HoXAsH-EDT_2 respectively (Adams et al., 2002). It was proposed by the authors that use of these reagents will enhance the study of the dynamics of protein trafficking events, protein interactions and protein-protein interactions in living cells.

6.1.3 Chapter Aims

The investigations in this chapter aimed to express Cx43 in primary rat neonatal cardiac myocytes. Upon successful Cx43-GFP expression in cardiac myocytes, the biogenesis and trafficking characteristics in cardiac myocytes and how they are affected by ischaemia or hypoxia would then become open to analysis.

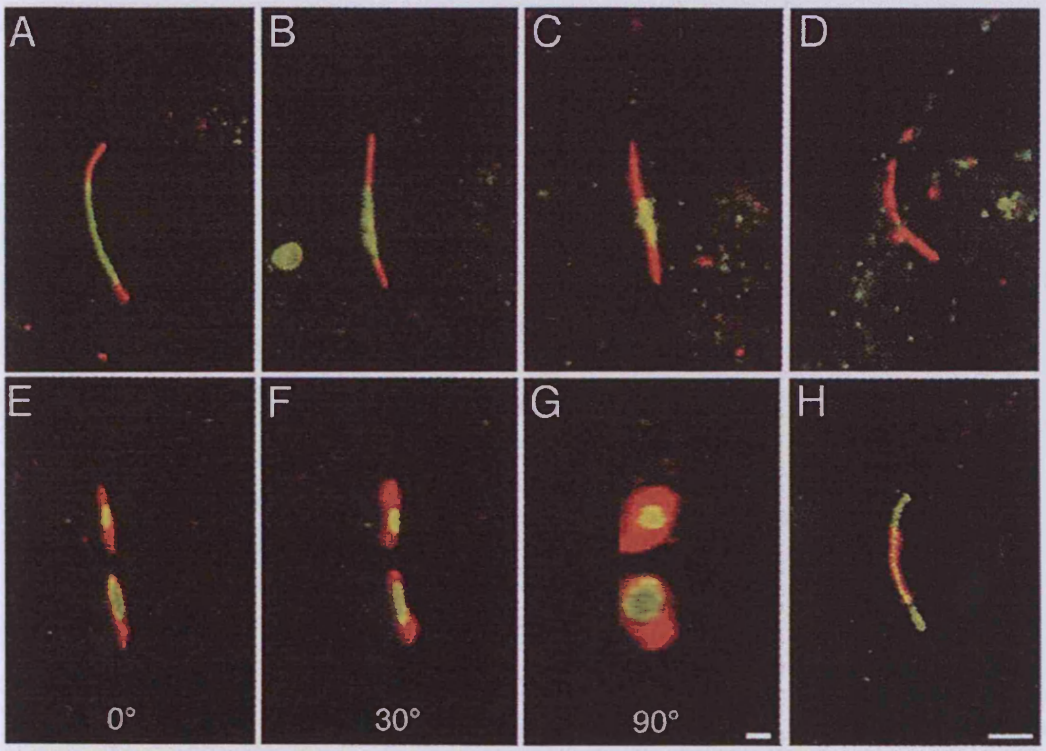

Figure 6.1: FlAsH and ReAsH labeling of Cx43-TC
Two temporally separated pools of Cx43-TC can be labelled with FlAsH and ReAsH to allow monitoring of gap junction plaque formation over time. Cx43-TC was stably expressed in HeLa cells and stained with FlAsH-EDT_2, then incubated over 4 (A,B) or 8 hours (C,D) at 37°C, and then further stained with ReAsH-EDT_2. This illustrates the gap junction plaque at varying states of renewal with FlAsH (green) labelling representing older and ReAsH (red) labelling representing newer gap junctions. A 3D volume projection of Cx43-TC with pulse-chase labelling rotated through different angles (E-G) illustrates that newly-synthesised connexins (red) is added to the periphery of the existing gap junction plaque (green). To illustrate there is no bias of binding between the two dyes the order of the pulse-chase labelling was reversed results in a reversal of the pattern of staining (H). Reproduced from Gaietta et al, 2002.

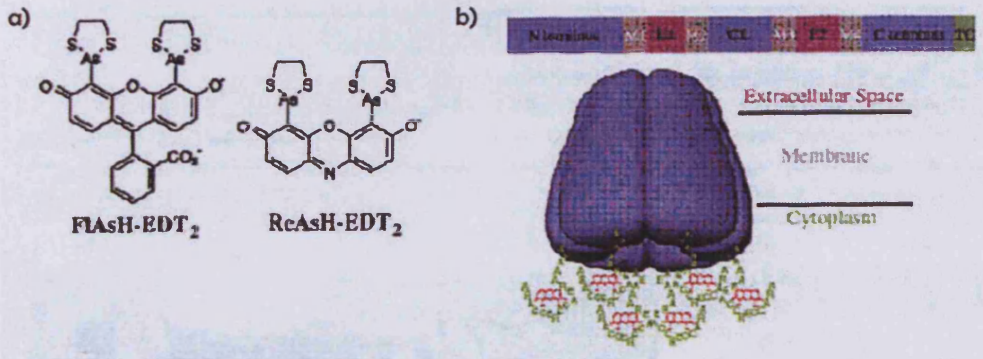

Figure 6.2: FlAsH-EDT2, ReAsH-EDT2 and Cx43-TC construct
a) Diagram showing the chemical structure of FlAsH-EDT2 and ReAsH-EDT2 ligands and b) Schematic diagram showing the position of the tetracysteine domain within the Cx43-TC construct and a connexon hexamer with 6 ReAsH ligands bound to the tetracysteine domains. Modified from Gaietta et al, 2002.

6.2 Methods and Results

6.2.1 Preparation of GFP labelled Cx43 in cardiac myocytes for trafficking studies

A Cx43-GFP chimera had already been developed in our laboratory. Enhanced-GFP (eGFP) was attached to the carboxyl terminus of the connexin, and used in HeLa and COS-7 cells (Martin et al., 2001; Paemeleire et al., 2000). Briefly, Cx43 cDNA was inserted into a vector containing the eGFP sequence (pEGFP-N1 vector, Clontech, USA, Figure 6.3b) by cutting with the appropriate restriction enzyme which ensured inframe fusion between the Cx43 and the amino terminus of eGFP. The pEGFP-N1 vector contains a CMV promoter so it can be expressed immediately in mammalian cells.

As primary cells such as neonatal cardiac myocytes are notoriously difficult to transfect and thereby express recombinant proteins different methods of transfection, including microinjection of cDNA and lipid-based transfection and an adenovirus expression system were carried out as described below.

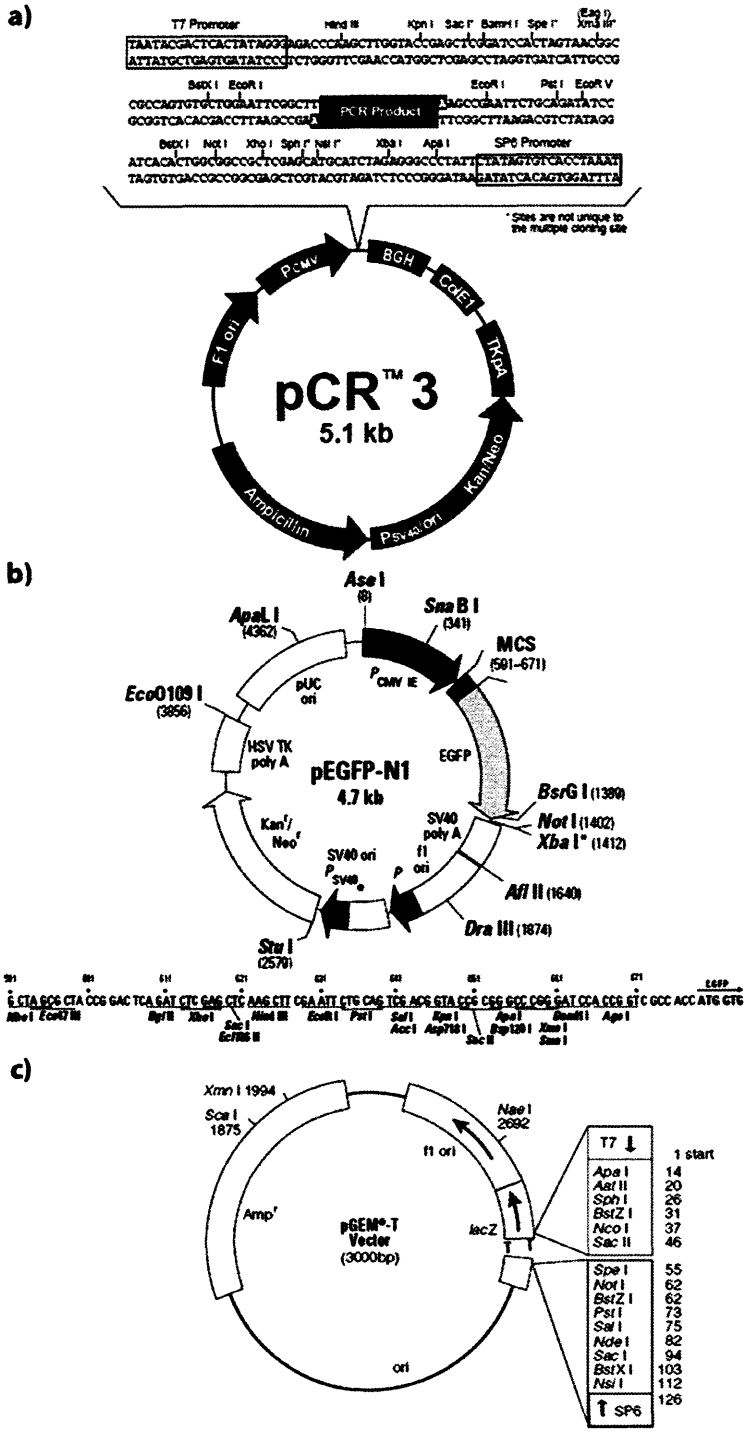

Figure 6.3: Plasmid vectors

The vector maps and multiple cloning sites (MCS) of a) the pCR3 vector that contains the wild-type Cx43 sequence insert, b) the pEGFP-N1 vector which contains the Cx43-GFP sequence insert, and c) the TA cloning vector pGEM-T.

6.2.1.1 Microinjection of cDNA

The Cx43-GFP in the pEGFP-N1 vector (500mg/ml in 3M Tris, 0.3M EDTA) was microinjected into confluent monolayers of beating rat neonatal cardiac myocytes or HeLa cells as described by George et al. (1998). Briefly, cDNA solution was injected into every cell nucleus within a marked area under low pressure (100hPa) and with an injection time of 0.2secs (Femtojet 5247, Eppendorf, USA). This resulted in Cx43-GFP being expressed by both cell types, although transfection efficiency was poor in cardiac myocytes, as illustrated in Figure 6.4. The location Cx43-GFP was mainly along the plasma membranes in both cell types. However, the transfection efficiency was low thus limiting analysis and therefore an alternative method was sought.

6.2.1.2 Lipid-based transfection of rat neonatal cardiac myocytes

The lipofectamine™2000 transfection reagent (Invitrogen, USA) was used on primary rat neonatal cardiac myocytes. Lipofectamine™2000 Transfection Reagent is a proprietary cationic lipid formulated to ensure maximum transfection efficiency in a number of cell types, including primary rat hepatocytes.

Transfection was carried out on confluent cardiac myocytes plated out in 24mm^2 glass cover-chambers (Labtek, USA). Cx43-GFP DNA-lipofectamine™ 2000 complexes were prepared by mixing 0.25μg of DNA (50μl in DMEM) with 2% (v/v) Lipofectamine™ 2000 (50μl in DMEM) and incubated for 30mins at room temperature to allow the DNA-Lipofectamine™ 2000 complexes to form. The DNA-Lipofectamine™ 2000 complexes (100μl) were then added to the cardiac myocytes and incubated at 37°C for 48hrs.

Transfection of primary rat neonatal cardiac myocytes with Lipofectamine™ 2000 resulted in Cx43-GFP expression observed 48hrs post transfection (Figure 6.5). However, the transfection efficiency was low, precluding useful analysis to be performed. To increase efficiency, various transfection parameters were altered, with the amount of DNA and Lipofectamine™ 2000 reagent being both increased and decreased, but to no effect.

6.2.1.3 Development of an adenoviral expression system

Since the transfection methods described above resulted in poor transfection efficiencies and low yields of expressed recombinant proteins, the utility of an adenovirus expression system was explored. To ensure neonatal cardiac myocytes were viable for adenovirus transfection, a GFP recombinant adenovirus was obtained (Lai group, WHRI, Cardiff). Rat neonatal cardiac myocytes were successfully transfected with GFP as shown in Figure 6.6. After this positive result the Adeno-X™ Expression System (BD biosciences (now Clontech), USA) was selected. The Adeno-X™ Expression System provides a method for constructing recombinant adenovirus, by using conventional in vitro ligation to incorporate a mammalian expression cassette into a replication-incompetent (ΔE1/ΔE3) human adenoviral type 5 (Ad5) genome (Mizuguchi & Kay 1998). The assembly and production of recombinant adenovirus involves three stages and the protocol is outlined in Figure 6.7.

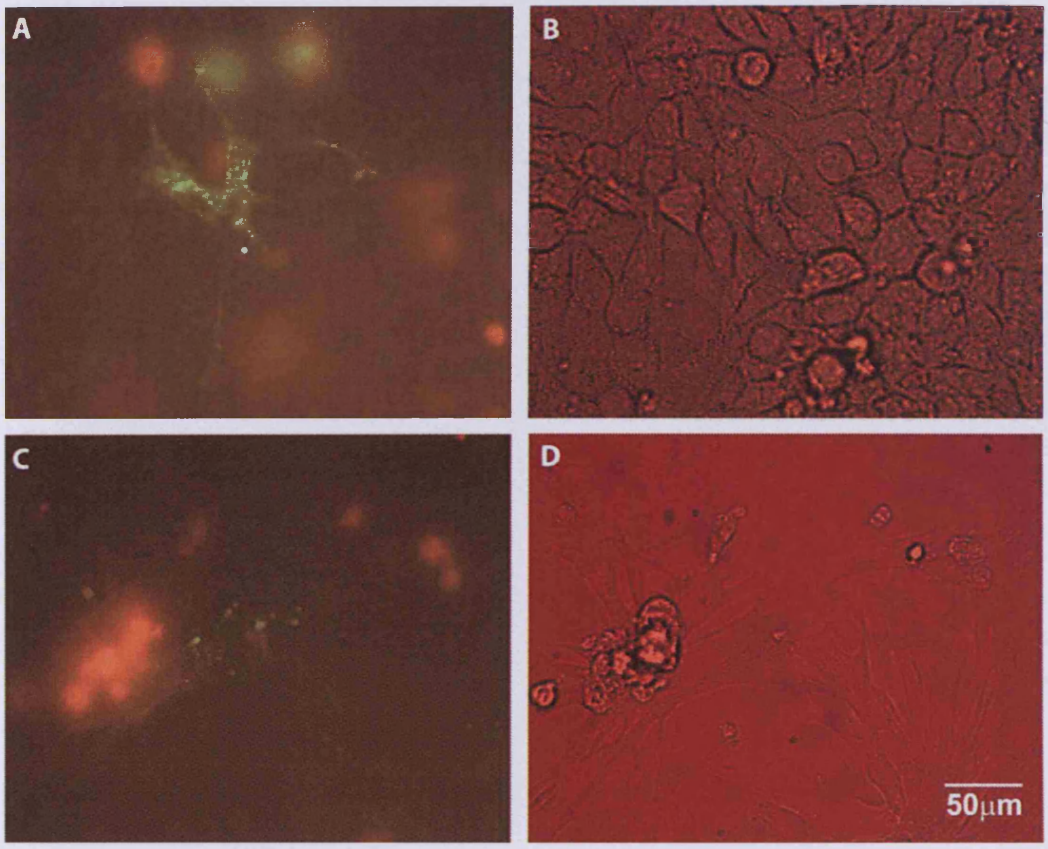

Figure 6.4: Rat neonatal cardiac myocytes and Hela cells transfected with Cx43-GFP by microinjection

Hela cells (A,B) and rat neonatal cardiac myocytes (C,D) were microinjected Cx43-GFP. The images were captured 48 hours after the cells were injected. B and D are the phase images of A and C respectively.

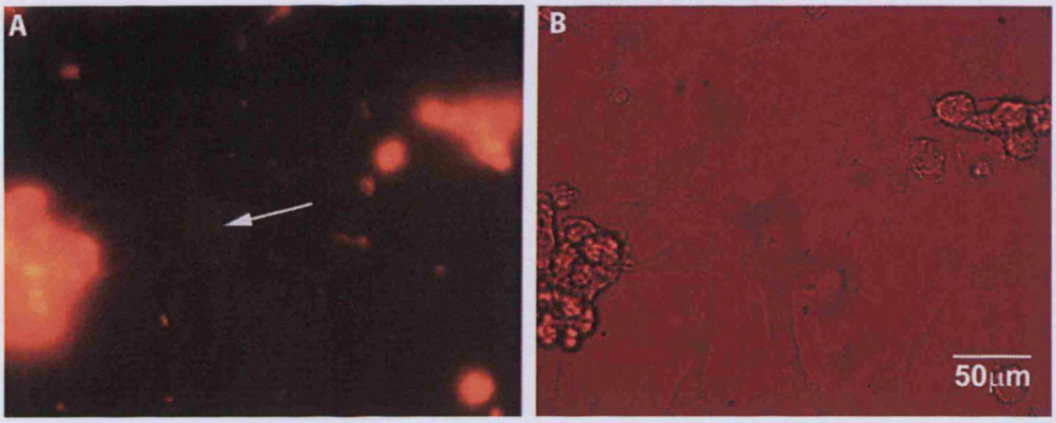

Figure 6.5: (A) Rat neonatal cardiac myocytes transfected with Cx43-GFP by lipofectamine 2000. Arrow points to the transfected myocyte. (B) is the phase image of (A). The autofluorescence shown is due to cell debris.

The mammalian expression cassette was constructed by cloning into a shuttle vector (pShuttle2) (Figure 6.8) and amplifying it in competent E. coli (described in 2.8.4). The second stage involved removal of the mammalian expression cassette containing the Cx43-GFP gene from the pShuttle2 vector using the specified restriction endonucleases (I-Ceu I, PI-Sce I). The excised cassette was then ligated into the Adeno-X viral DNA (the adenoviral genome). The final stage was to transfect human embryonic kidney (HEK) 293 cells with the recombinant Adeno-X vector where it is replicated and packaged into infectious adenovirus, and then harvested by lysing transfected cells. HEK 293 cells stably express the Ad5 E1 genes that are essential for replication and transcription of the adenovirus DNA.

In order to clone Cx43-GFP into the pShuttle2 vector new PCR primers were designed incorporating the appropriate restriction endonuclease sites, as shown below:

Forward Cx43 XbaI primer

5'-ACT-ATA-GGG-AGA-TCT-AGA-ATG-GGT-GAC-TGG-AGT-3'

Clamp | XbaI restriction enzyme site | First 15bp of Cx43

Reverse Cx43-GFP NotI primer

5'-AGT-TCC-CAG-GAT-TGC-GGC-TTA-CTT-GTA-CAG-CTC-3'

Clamp | NotI restriction enzyme site | Last 15bp of GFP

The PCR was successful and the DNA was purified (as described in 2.8.1-2.8.3). However, the PCR product could not be ligated successfully into the pShuttle2 plasmid vector. This was probably due to the failure of the restriction endonucleases (Xba I and

Not I) to cut the DNA correctly owing to a lack of DNA either side of the restriction enzyme site. To overcome this problem, it was decided to clone Cx43-GFP using "Topo cloning" (Invitrogen, USA), a method that eliminates the need for restriction digests and ligation reactions by allowing direct insertion of the PCR products into the pCR-XL-TOPO vector, thereby providing a renewable source of Cx43-GFP for cloning purposes. The vector has the ability for TA cloning (explained in section 6.2.3.2) and has topoisomerase covalently bound to the plasmid which facilitates the ligation of the PCR products as shown in Figure 6.9.

The PCR products containing the Cx43-GFP insert were successfully cloned into the pCR-XL-TOPO vector. However, this vector also contains Xba I and Not I sites in its MCS so new PCR primers without restriction endonuclease sites would be required and therefore the studies were discontinued.

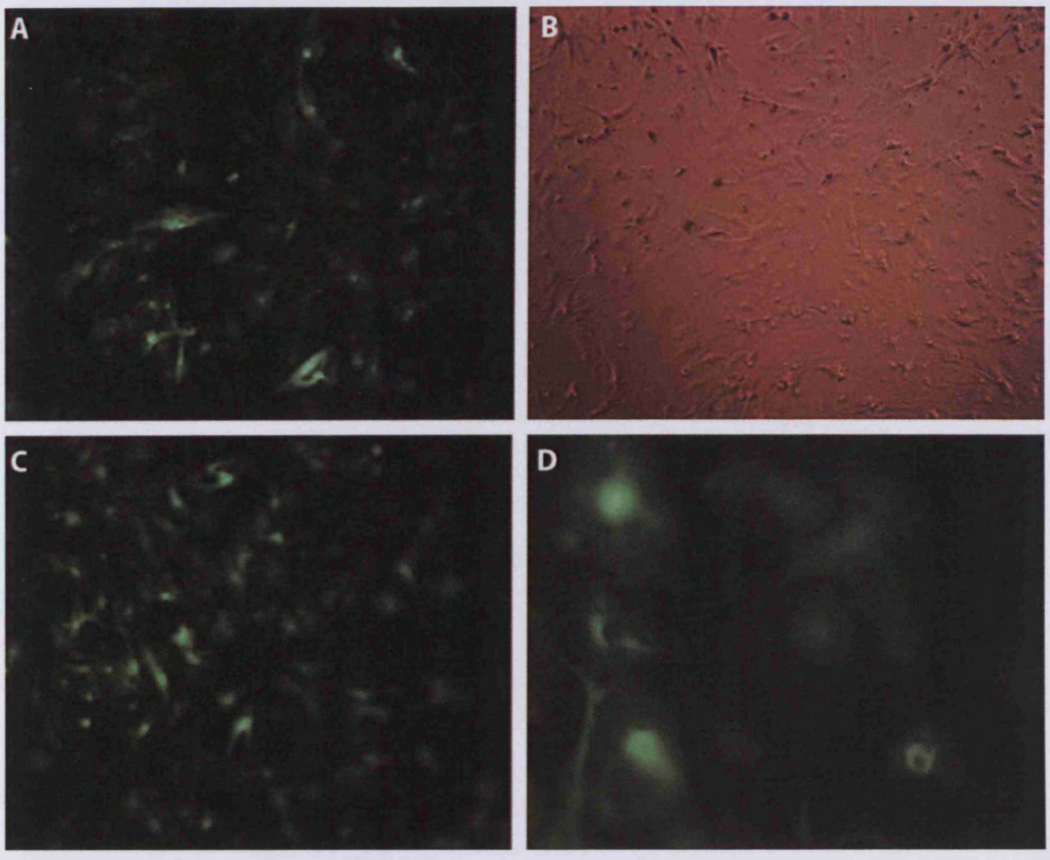

Figure 6.6: Expression of GFP in rat neonatal cardiac myocytes
GFP was expressed in rat neonatal cardiac myocytes using an adenovirus expression system. The virus was used at different moieties of 10 (A,B) and 100 (C,D). Images were x10 (A-C) and x40 (D) magnification.

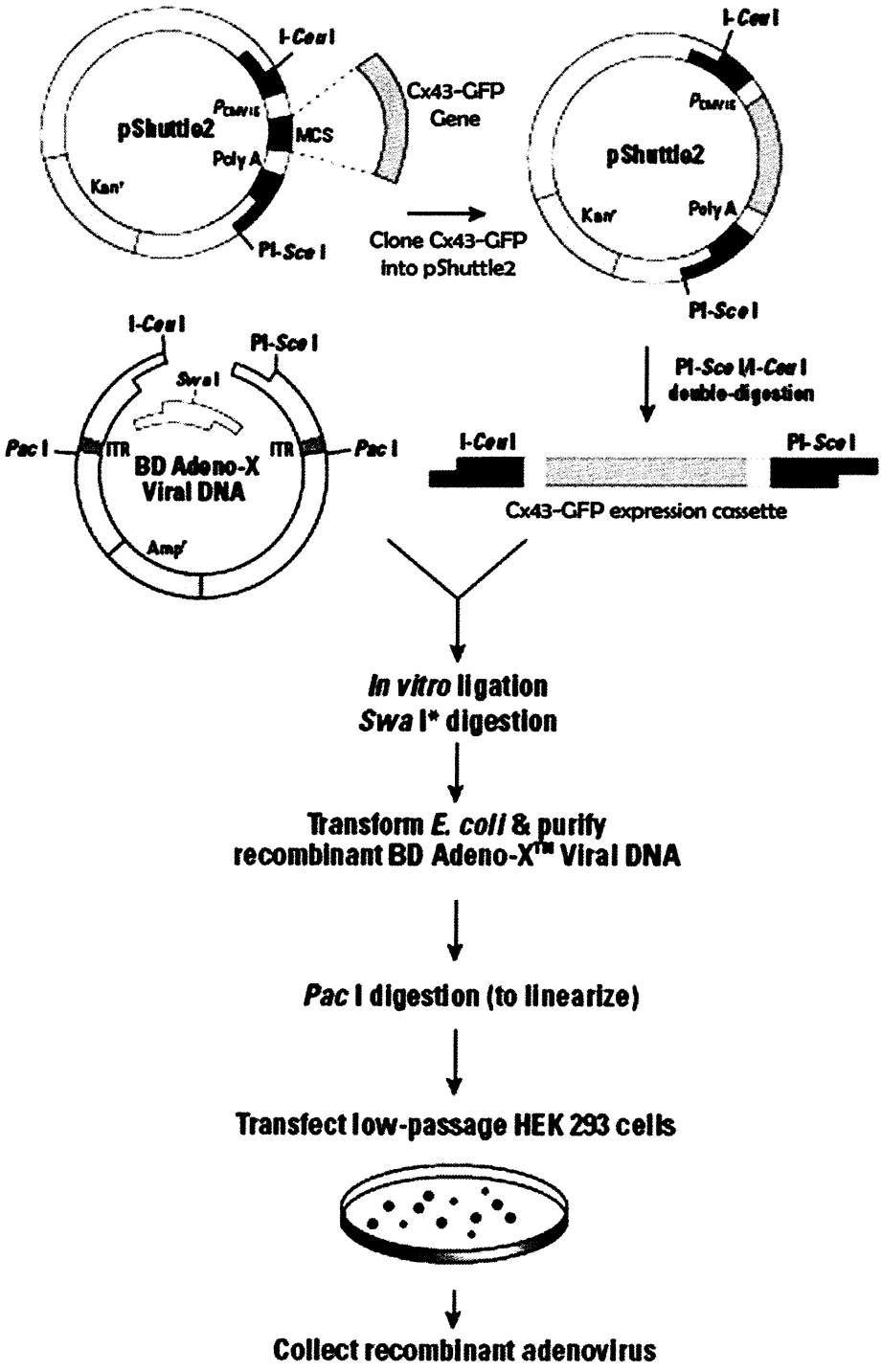

Figure 6.7:
Protocol for construction of a recombinant adenovirus with the Adeno-X™ Expression System. Modified from the BD Adeno-X™ Expression System 1 User Manual

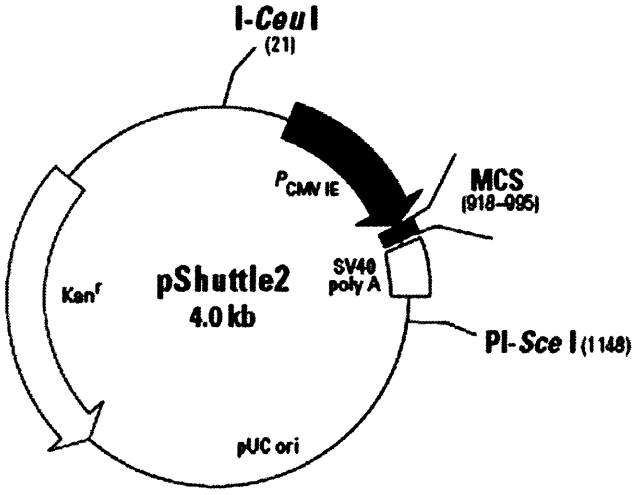

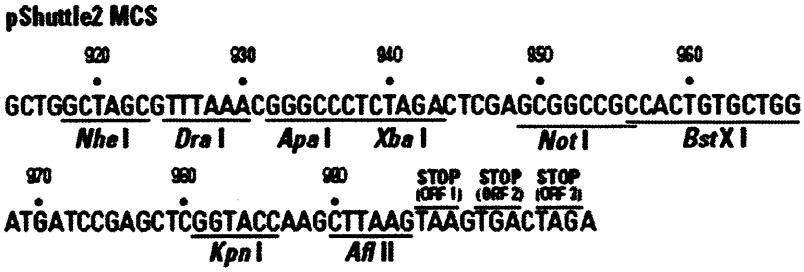

Figure 6.8: Plasmid vector map and multiple cloning site of pShuttle2.
pShuttle2 allows cloning of the Cx43-GFP gene into a mammalian expression cassette, which consists of the human cytomegalovirus immediate early promoter/enhancer (PCMV IE), a multiple cloning site (MCS), and the SV40 polyadenylation signal (SV40 poly A). The entire cassette is flanked by unique I-Ceu I and PI-Sce I restriction sites so that it can be excised and ligated to BD Adeno-X Viral DNA.

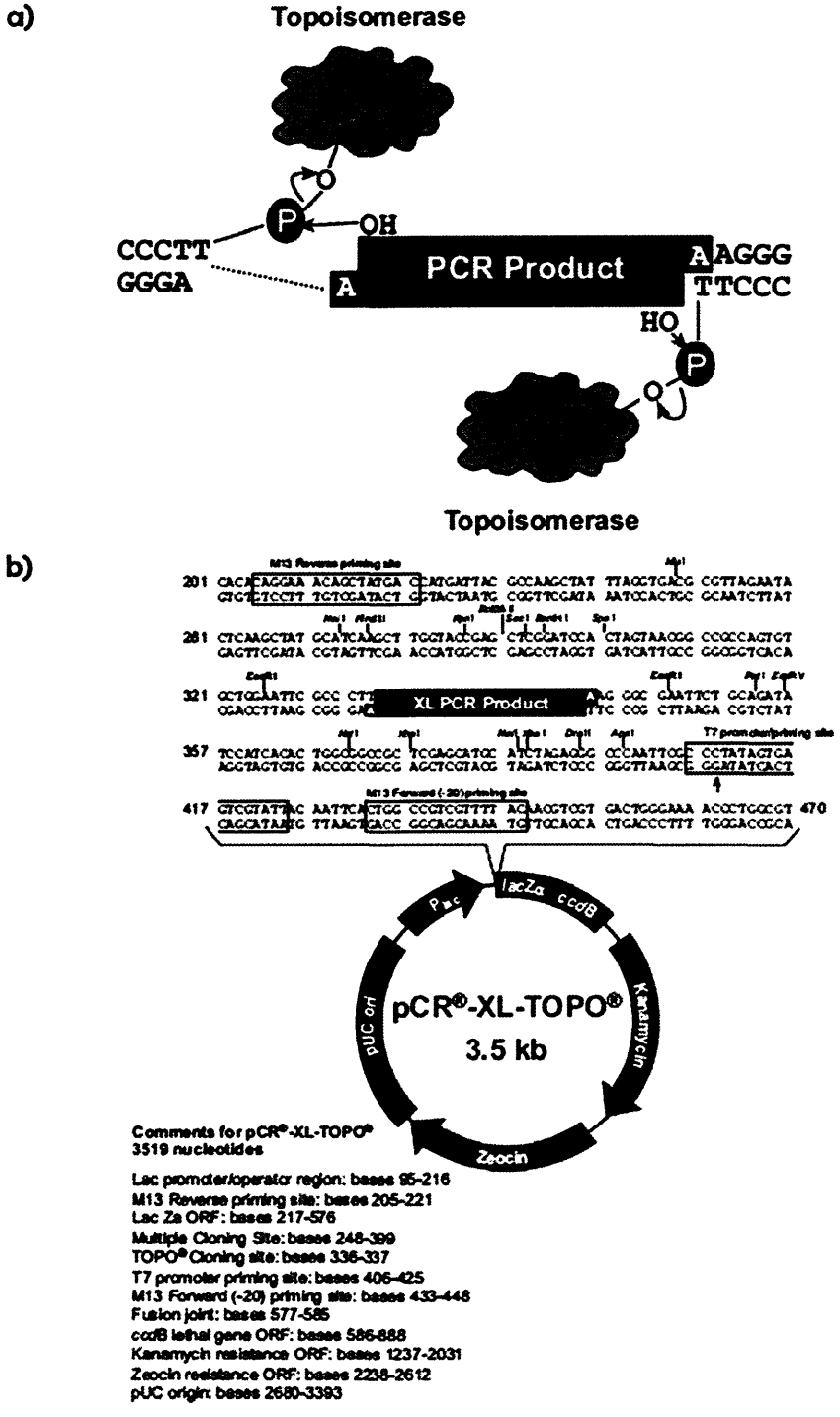

Figure 6.9: TOPO cloning
Topoisomerase facilitates the insertion of PCR products into the pCR-XL-TOPO vector as illustrated (a) and the plasmid vector map is shown in (b).

6.2.2 Immunostaining of rat neonatal cardiac myocytes

In earlier studies using HeLa cells expressing connexins 26, 32 and 43 it was observed that disrupting cytoskeletal elements altered connexin trafficking pathways (Martin et al., 2001). In primary rat neonatal myocytes, the integrity of microtubules and actin filaments was disturbed using nocodazole and cytochalasin D respectively for 5hrs. The microtubules were detected by an antibody specific for β-tubulin followed by a fluorescent secondary antibody (Alexa-488, green fluorescence) (Figure 6.10a). Treatment of cardiac myocytes with nocodazole (20 mg/ml) resulted in disruption of β-tubulin (Figure 6.10c,e). Actin filaments were stained directly with phalloidin (red fluorescence) before and after treatment with cytochalasin D (1 mg/ml) (Figure 6.10b,d,f). Cardiac myocytes were also treated with brefeldin A which disrupts the Golgi apparatus, but could not be analyzed as the anti-ERGIC-53/p58 antibody (Sigma, USA) needed to determine the location of ERGIC (Endoplasmic Reticulum Golgi Intermediate Compartment) components was unobtainable at the time of the study.

The localisation of Cx43 in primary rat neonatal cardiac myocytes was carried out with a Cx43 antibody that detects all Cx43 isoforms (Zymed, USA) and a fluorescent secondary antibody containing Alexa-546 (red fluorescence). Cx43 was located intracellularly and at the cell borders as shown in Figure 6.11.

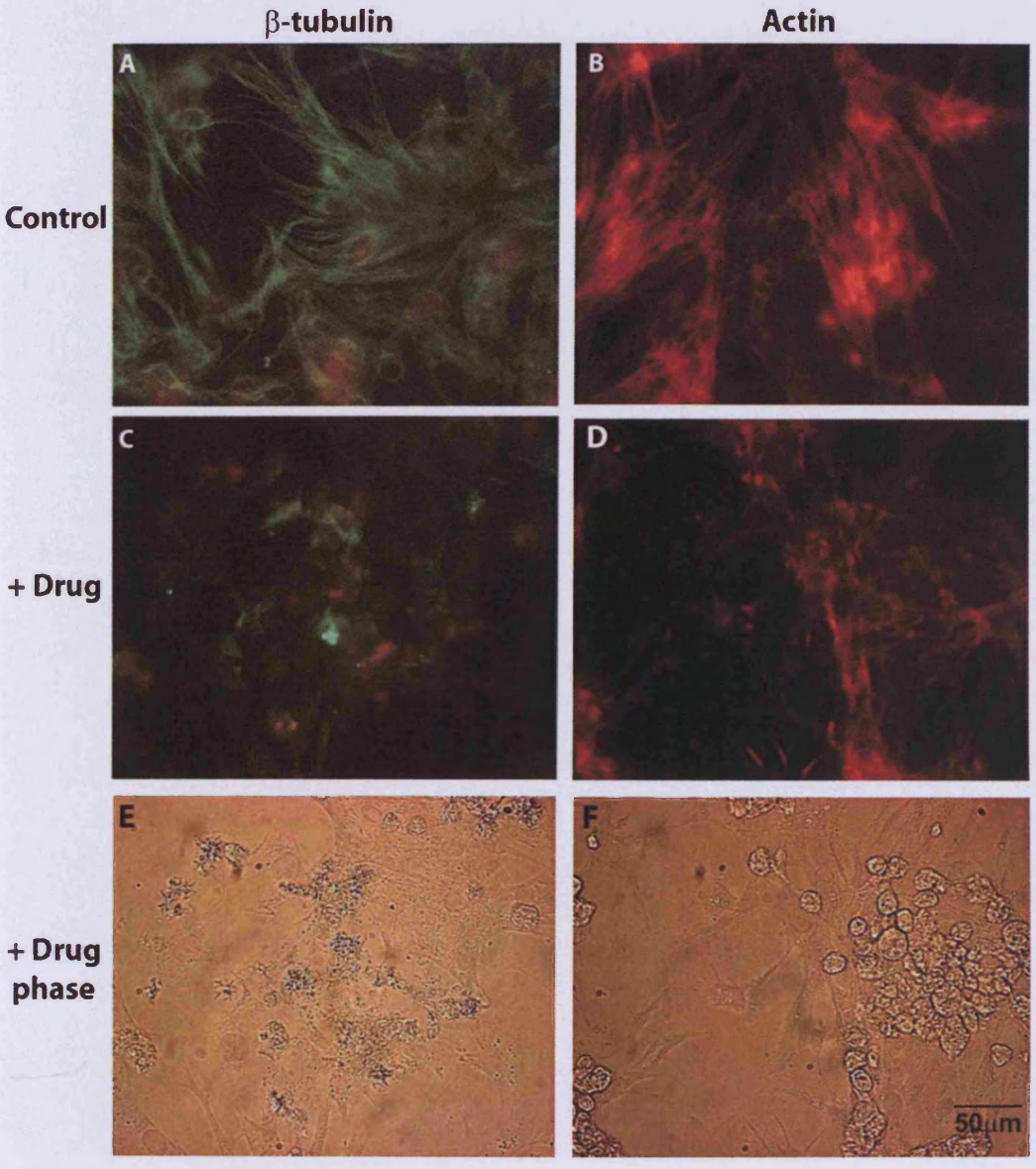

Figure 6.10: The effect of Nocodazole and Cytochalasin D on microtubules and actin filaments.

Confluent monolayers of rat neonatal cardiac myocytes were fixed and stained antibodies to b-tubulin under normal conditions (A) and following 5 hours treatment with 20 mg/ml nocodazole (C). The structural integrity of actin filaments was determined by staining with pholloidin before (B) and after 5 hours treatment with 1 mg/ml cytochalasin D (D). The phase images of (C) and (D) are shown in (E) and (F) respectively.

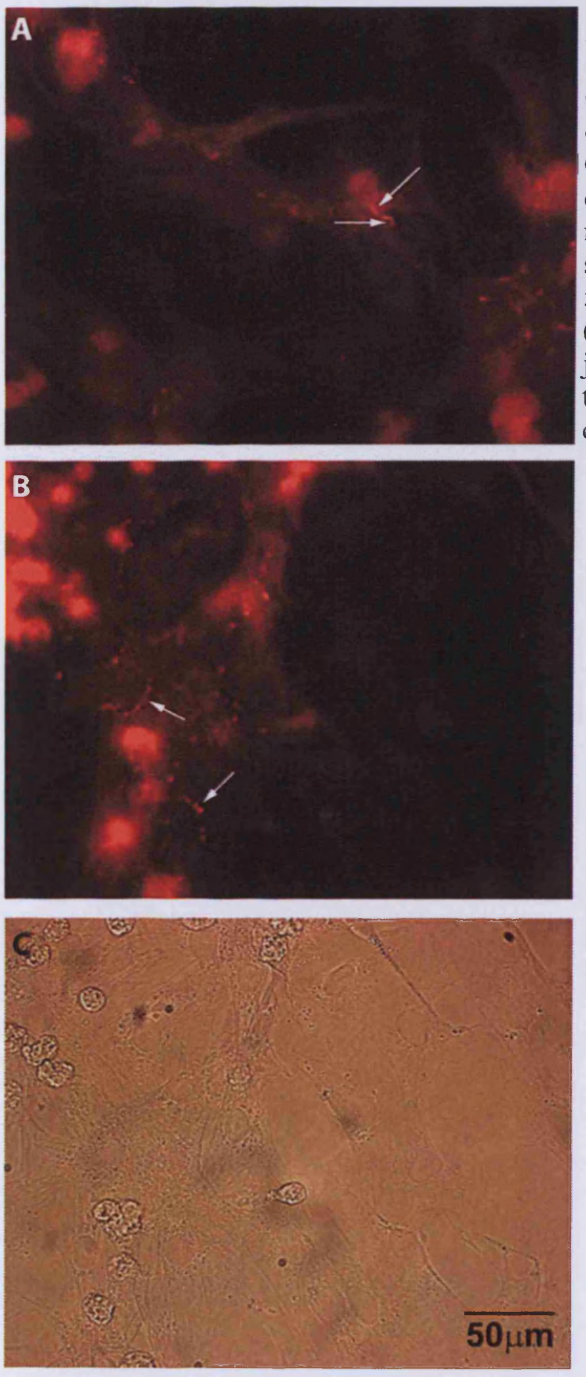

Figure 6.11: Cx43 immunostaining in rat neonatal cardiac myocytes. Confluent monolayers of rat neonatal cardiac myocytes were probed with a Cx43 antibody (Zymed, USA, which detects Cx43 (phosphorylated and non-phosphorylated)). A fluorescent secondary antibody containing Alexa 546 (red) was used to stain Cx43 (A,B). The arrows point to gap junction plaques and punctate staining typical of Cx43. (C) The phase image of (B) shows the cell boundaries.

6.2.3 Construction of Cx43-TC for FlAsH fluorescent labelling system

The FlAsH labelling system requires the addition of a small tetracysteine (TC) motif to the carboxyl terminus of Cx43 achieved by the processes outlined below.

6.2.3.1 Primer Design and PCR

The tetracysteine motif was tagged onto the carboxyl tail of Cx43 by PCR. The tetracysteine tag sequence was incorporated into custom designed primers (Invitrogen, USA). The designs of the Cx43-TC primers are shown below:

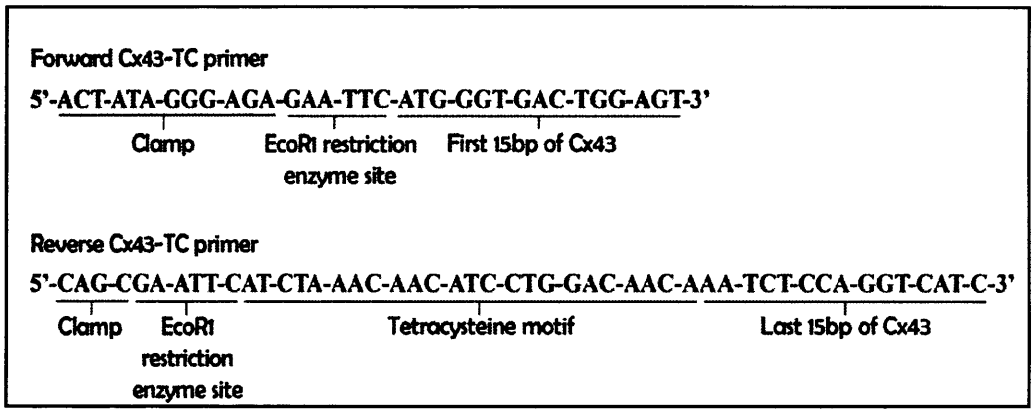

Both forward and reverse primers feature EcoR1 restriction enzyme sites. The forward primer is 33 base pairs (bp) long and features the sequence coding for the first 15bp of the Cx43, whereas the reverse primer is 49bp long and incorporates the sequence coding for the last 15bp of the Cx43. Wild type rat Cx43 cDNA in the PCR3 vector was available from our laboratory and was used as the DNA template for the PCR reaction. Bioexact Taq DNA polymerase was used and PCR reactions set up as described in 2.8.1. The Cx43 exon is 1145bp long, making the approximate length of Cx43-TC 1230bp.

PCR resulted in a band appearing at 1400bp on a DNA agarose gel as shown in Figure 6.12.

6.2.3.2 Subcloning of FlAsH PCR products

Bio-x-act Taq polymerase (Bioline,UK) leaves additional 3'A residues intact during PCR, thus generating ideal fragments for cloning into plasmid vectors that contain the corresponding 3'T overhang, such as pGEM-T (Promega, UK; Figure 6.3c). Purified PCR products and linearised vector (pGEM-T; 50ng) were ligated according to manufacturer's instruction with an insert:vector molar ratio of 3:1 proving to be the optimum condition. The amount of DNA insert used was calculated as shown below along with the ligation reaction setup:

$$\frac{\text{ng of vector} \times \text{kb size of insert}}{\text{kb size of vector}} \times \text{insert:vector molar ratio} = \text{ng of insert}$$

Ligation reaction setup

Vector DNA	50ng (1µl)
Insert DNA*	Xng
T4 DNA ligase (3U/µl)	1µl
2x rapid ligation buffer (Promega, UK)	5µl
dH_2O	to10µl

* Amount added to give insert:vector molar ratio of 3:1

Reactions were performed at 4°C (pGEM-T) for 15hrs. Ligation mixtures were stored at -20°C prior to use.

Following successful ligation of the Cx43-TC PCR product into the pGEM-T vector, the recombinant plasmid was transformed into DH5α competent bacteria and subjected to amplification and purification as described in section 2.8.3.

The purified DNA was then analysed by sequencing (section 2.8.5) to ensure correct insertion of the Cx43-TC DNA. However, only the first half of Cx43-TC was sequenced (Figure 6.13), causing these studies to be suspended.

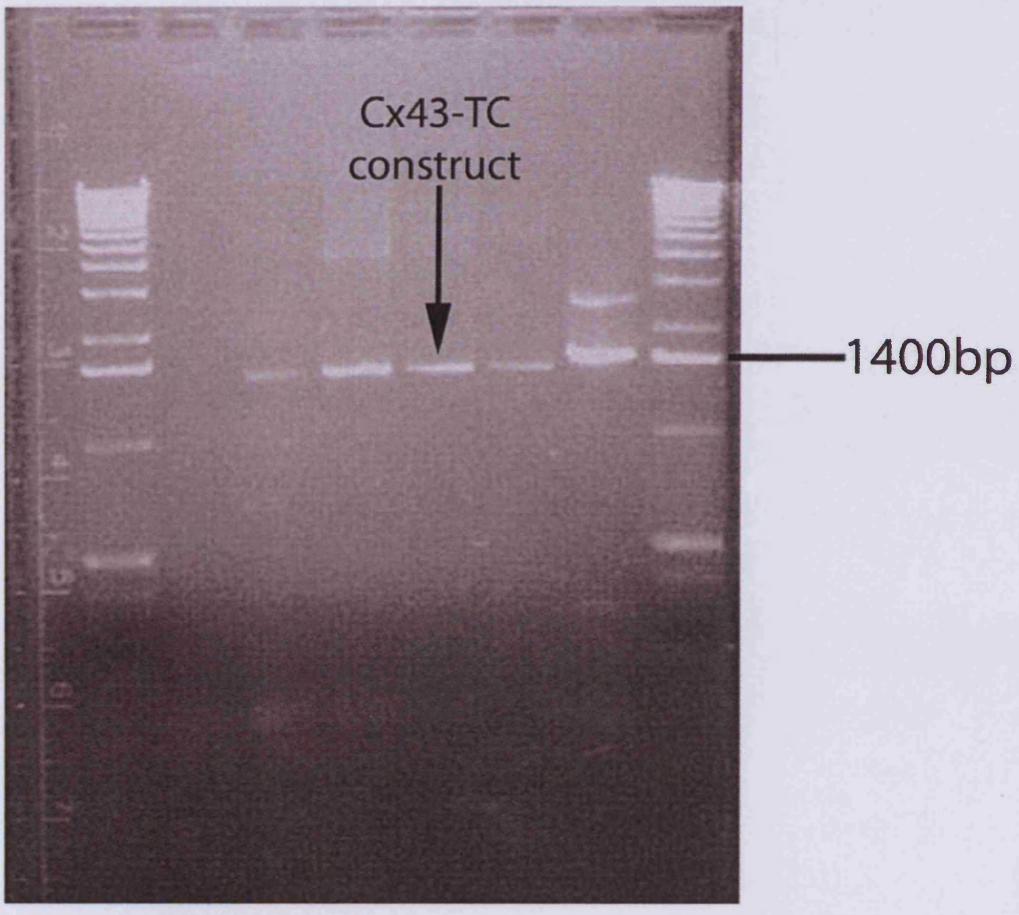

Figure 6.12:
DNA agarose gel showing PCR products for the Cx43-TC construct.

Figure 6.13: Sequencing printout showing the successful sequencing of the first half of the Cx43-TC construct using the T7 primer.

6.3 Discussion

The studies described in this chapter reveal attempts to use fluorescent reporter proteins tagged to Cx43 to monitor its location in live beating cardiac myocytes. Work in our laboratory has demonstrated two connexin trafficking pathways in HeLa cells (Martin et al., 2001). These earlier studies indicated that Cx43 and Cx32 are trafficked to the plasma membrane through the secretory pathway via the Golgi apparatus, although Cx26 was also trafficked to the plasma membrane via an alternative pathway that was highly sensitive to microtubule disruption (Diez et al., 1999; Martin et al., 2001). Other studies have shown that microtubules are necessary for enhanced assembly of Cx43 gap junctions (Johnson et al., 2002). We posed the question: in pathological situations, such as ischaemia, can Cx43 be trafficked to the plasma membrane by an alternative pathway or possibly by both pathways simultaneously, and designed experiments to test this possibility.

The studies described in this chapter although incomplete, have helped to lay a foundation for further work using Cx43 labelled with fluorescent reporter tags using primary rat neonatal cardiac myocytes to enable visualisation of the protein in live beating cells. The potential of the adenovirus expression system was demonstrated by the successful transfection of the cells with GFP. However, the expression of Cx43-GFP would have to be carefully controlled as connexin over-expression is likely to compromise cell function. Continuation of these studies would enable the trafficking characteristics of Cx43 to be assessed in primary neonatal cardiac myocytes under normal and hypoxic/ischaemic conditions.

The FlAsH labelling system at the time would be a useful addition to the tools used to assess the Cx43 turnover and behaviour in cardiac myocytes during hypoxia and ischaemia. Continued FlAsH studies could clone Cx43-TC in two stages, thereby utilising smaller oligonucleotide primers to ensure successful PCR and sequencing. As far as I am aware, no studies using the FlAsH system for labelling connexins outside the Tsien lab in San Diego, USA have appeared. This, together with my abortive attempts, indicate that although elegant results were obtained conceiving the way CxHcs are added to, and removed from the gap junction (Gaietta et al., 2002), the technology is still very complex and in experimental infancy. To my knowledge, there have been no further reports of its use outside the Tsien laboratory, suggesting that refinements will be necessary.

A further aspect emerging is the difficulty of transfecting primary neonatal cardiac myocytes using conventional methods that work on most other cells. The present studies have underlined the difficulties associated with the transfection of primary cardiac myocytes. However, the studies reveal the promise of alternative approaches using viral expression systems, illustrated in this instance by the adenovirus expression system.

Chapter 7

Final Discussion

The work presented in this thesis describes the properties of Cx43 in a cardiac environment. One of the major outcomes of this work was the development of a cellular model of ischaemic heart disease which was used to examine the properties of two classes of drugs; one that stimulated connexin based communication and one that inhibited it. The cells used were primary rat neonatal cardiac myocytes, which retain their cardio-specific properties and beat synchronously when cultured as a confluent monolayer. The model utilised a hypoxic chamber and substrate depleted cell culture medium to simulate ischaemia. It is extremely difficult to find a model that mimics exactly the effects occurring in the adult heart during ischaemic heat disease and myocardial infarction as these conditions can not be reproduced and recorded effectively by many systems. However, the results presented using this cellular model serve to strengthen our understanding of cardiac cellular responses during ischaemic and hypoxic stress and complement *in vivo* models which take into account the whole organ and other body system.

The present model provides a more physiological model of ischaemia and thus all effects observed are due to the ischaemia, unlike some traditional methods that use chemical inhibitors to induce ischaemia. These traditional "chemical" methods of inducing hypoxia and ischaemia have made use of iodoacetic acid (Contreras et al., 2002), potassium cyanide and deoxyglucose (Turner et al., 2004). These chemicals poison cells, and their lack of specificity is likely to mask the effects caused by hypoxia and ischaemia. In complementary studies, ischaemia has also been induced using whole heart preparation in the Langendorff (no perfusion) system (Beardslee et al., 2000). This

method is equally effective and provides information at the organ level of what happens during cardiac ischaemia. However, our model system, besides complementing heart perfusion systems, has proved to be an effective tool in studying specific aspects (such as the mechanisms of peptide drugs in cardiomyocytes) of Cx43 biology in detail at the cells level and within a cardiac context.

The results obtained using this approach showed that ischaemia caused the synchronous beating of cardiac myocytes to cease after 2-3 hours followed later at 5 hours by dephosphorylation of Cx43. Similar results were achieved using a whole heart Langendorf ischaemia (no perfusion) set up (Beardslee et al., 2000). In this study, the authors reported that gap junction uncoupling (and thereby arrest of beating) and Cx43 dephosphorylation occurred after approximately 30 minutes of ischaemia (Beardslee et al., 2000). My observations concur with these studies, but occur more slowly, most likely due to the differences in experimental conditions. Another possible reason is that adult heart cells is more dependant on mitochondrial oxidation for ATP generation than neonatal cells/hearts that rely more on glycolytic production of ATP.

The synchronous beating of cardiac myocytes and Cx43 phosphorylation state appears to be closely linked. My studies have revealed that synchronous contraction of reoxygenated ischaemic cardiac myocytes returns when Cx43 phosphorylation is restored. The mechanism underlying the uncoupling of cardiac myocytes during ischaemia could be the dephosphorylation of Cx43, but a causal link has not been demonstrated. This could be achieved by further studies using a Cx43 mutant lacking

one or more of the serine residues that are the main targets for phosphorylation, ideally expressed in a mammalian cardiac cell line, such as HL-1 cells, as primary neonatal cardiac myocytes are currently very difficult to transfect as outlined in chapter 6.

The work carried out also revealed that cardiac myocytes exposed to simulated ischaemia release a transient burst of ATP that was sensitive to two gap junction inhibitors. The results show that this burst of ATP release is likely to occur across Cx43 Hcs. As discussed previously, Cx43 Hcs remain in a closed configuration when they are un-apposed in the plasma membrane (i.e. they have not docked to form a gap junction). However, in a study using astrocytes treated with metabolic inhibitors (a non-physiological model of ischaemia), fluorescent dyes were shown to permeate the cell membrane and were sensitive to gap junction inhibitors and thus the authors concluded that the Cx43 hemichannels open during ischaemia (Contreras et al., 2002), as our present results also indicate. It was argued that opening of CxHcs in ischaemia would exacerbate the pathological situation by allowing ATP to leak out of the cell, lowering intra-cellular ATP levels to catastrophic levels. The present work has indicated that this is not the case, as a small amount of ATP is released in a controlled transient manner at a specific frame within the first two hours of ischaemia. Intracellular ATP levels remained constant during this time period, indicating that the small transient release of ATP did not greatly effect overall intracellular ATP concentration.

The release of ATP from cells is a central feature in purinergic signalling between cells with ATP, its breakdown products and especially adenosine possessing active signalling

capabilities via adenosine receptors and purinergic receptors. In further work, preliminary experiments were carried out to analyse ATP breakdown products present in the cell culture medium after ischaemia induced ATP release. However, the detection system was unable to provide the analysis required. The addition of ATPases and 5'-nucleotidase inhibitors could be introduced as well as newer more sensitive methods of ATP and adenosine nucleotide detection would be utilised.

It has also been suggested that if CxHc opening prevails under conditions of extreme stress it could provide cells with a method of isolating non-viable cells quickly from the healthy coupled cell population (Spray et al., 2006), a role that has been postulated for Cx43 in CNS and cardiac cell death (Contreras et al., 2004; John et al., 2003). In the present studies, ischaemic myocytes recovered by reoxygenation after approximately 8 hours of continuing ischaemia and the initial transient burst of ATP did not greatly effect the overall intracellular ATP concentrations. Intracellular ATP concentrations are much higher than extracellular (intracellular (low μM) to extracellular (low nM) for ATP concentrations).

The mechanism of CxHc opening during ischaemia is unknown. It is widely accepted that reduced extracellular Ca^{2+} opens hemichannels, and it has been suggested that reduced Ca^{2+} in the ischemic tissue would be capable of activating CxHcs. It is interesting to note that high intracellular Ca^{2+} (500nM) has also been shown to open Cx32Hcs (De Vuyst et al., 2006) and recently for Cx43Hcs (De Vuyst, Evans & Leybaert, unpublished work). It has also been proposed that alterations in Cx43

phosphorylation or nitrosylation are important initiating events (Bao et al., 2004; Contreras et al., 2002; Retamal et al., 2006). In contrast, the present studies showed Cx43 was still phosphorylated at the time of the ATP release, as detected by our methods, indicating the possibility that Cx43 phosphorylation might not be a crucial event in CxHc opening. However, the antiarrhythmic peptide AAP10 caused the pulsatile release of ATP to be exacerbated, which is proposed to operate via protein kinase C, suggesting that phosphorylation could be involved. A sensitive method of detecting small changes in Cx43 phosphorylation, such as mass spectrometry techniques (Axelsen et al. 2006), would add clarification to these questions.

In ischaemia the release of ATP and its breakdown products (ADP, AMP and adenosine) that possess vasodilatory properties into the cardiac vasculature can potentially increase blood supply to the myocardium and thus alleviate many of the symptoms of the ischaemia related to oxygen/metabolite deficiency. It would be worthwhile to investigate the levels of ATP metabolites and achieve better analysis of the nucleotide/nucleoside release during ischaemia, in order to elucidate the substances that are active as a consequence of ATP release from the cardiac myocytes. This could be accomplished using reverse phase high pressure liquid chromatography to measure adenosine and its nucleotides/nucleosides (Sala-Newby et al., 2000; Smolenski et al., 1990). Further studies would also record intracellular Ca^{2+} levels and the pH of the cell culture medium throughout the ischaemic timecourse as this may aid the understanding of Cx43Hc opening during ischaemia.

Connexin mimetic peptides were used in this thesis to inhibit connexin based communication. Both GAP 26 and GAP 27 were shown to reduce dye transfer between neonatal cardiac myocytes and shown to attenuate the beating rate of the cells. Dye transfer between cardiac myocytes was arrested after 30 minutes, but the peptides took longer to exert their maximal effects on the beating rate of the myocytes. GAP 26 was also used to inhibit ATP release from cardiac myocytes via Cx43Hcs during ischaemia. These results indicate that basal ATP release from cardiac myocytes was reduced by approximately half within the first 10-20 minutes of treatment. Connexin mimetic peptides have been hypothesised to act on CxHcs first and then followed later on gap junction channels (Evans et al., 2006) as illustrated in Figure 7.1.

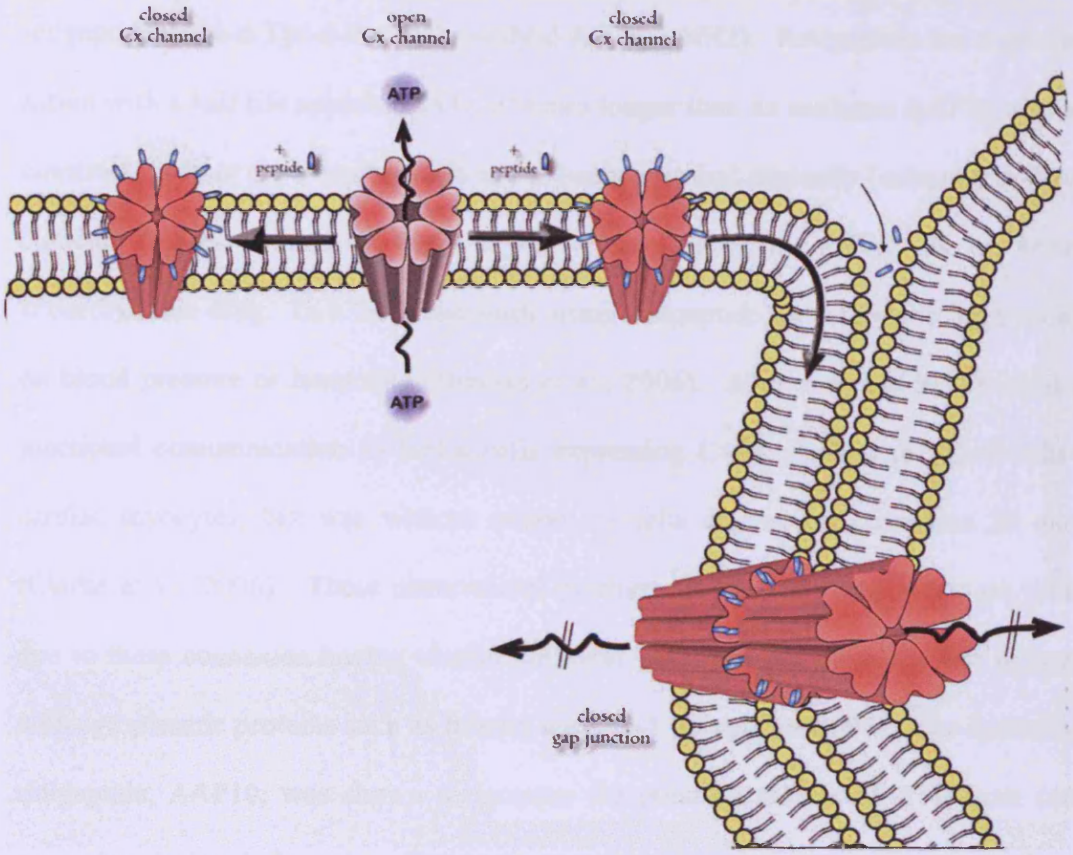

Figure 7.1: The proposed mechanism of action of connexin mimetic peptides Firstly the connexin mimetic peptides bind to CxHcs restricting channel release of ATP. Later, CxHcs become incorporated into gap junctions thereby inhibiting intercellular communication between cells or diffuse into the intercellular cleft between the cells and induce direct blockage of gap junctions. Reproduced from Evans et al., 2006.

Also in the present studies, we examined the effects of two antiarrhythmic peptides, AAP10 (in ischaemic studies) and rotigaptide (ZP123) (in cell communication studies). As discussed in chapter 1, AAP10 was developed as a synthetic derivative of the naturally occurring peptide AAP_{nat} which is present at relatively high levels in heart tissue. AAP10 in turn was chemically modified to generate an analogue, rotigaptide (ZP123). Rotigaptide has the same sequence as AAP10 but uses d-isoforms of the amino acids rather than the l-isoforms (AAP10 = H_2N-Gly-Ala-Gly-Hyp-Pro-Tyr-$CONH_2$;

rotigaptide = Ac-d-Tyr-d-Pro-d-Hyp-Gly-d-Ala-Gly-NH2). Rotigaptide has a protracted action with a half life approximately 10 times longer than its analogue AAP10, due to its construction from the d-amino acids and is being assessed clinically (currently in Phase II clinical studies, conducted by Wyeth Pharmaceuticals, USA) as a potential antiarrhythmic drug. In a the latest study using rotigaptide was shown to have no effect on blood pressure or heart rate (Hennan et al., 2006). Also, rotigaptide increased gap-junctional communication in HeLa cells expressing Cx43, as well as HL-1 cells and cardiac myocytes, but was without action on cells expressing connexins 26 and 32 (Clarke et al., 2006). These observations pointing to connexin specificity are possibly due to these connexins having shorter carboxyl tails, and are therefore less interactive with cytoplasmic proteins such as tubulin and ZO-1 (Giepmans 2004). The derivative of rotigaptide, AAP10, was shown to increase the pulsatile release of ATP from cardiac myocytes during ischaemia. Owing to commercial licensing agreements, rotigaptide could not be used officially for these studies but it is highly likely that similar data would be achieved. These studies with rotigaptide and AAP10 would now benefit from analysis of gap junction coupling in cells expressing other cardiac connexins, e.g. Cx40, Cx45 and Cx37.

Using a cardiac myocyte system, the sensitivity of the Western blotting utilised was too low to detect any changes in Cx43 phosphorylation (Clarke et al., 2006). A more recent study (Axelsen et al., 2006) using mass spectrometry, MALDI (matrix-assisted laser desorption/ionization) and LC-MS/MS (liquid chromatography tandem mass spectrometry), showed that the onset of the ischaemia induced dephosphorylation of

Cx43 and was delayed by rotigaptide (Axelsen et al., 2006). This thesis has highlighted the effects of antiarrhythmic peptides, such as rotigaptide (ZP123) on gap junctions and AAP10 on CxHcs, and shown them to be useful tools that enhance the activity of channels constructed from Cx43. Also, in additional unpublished studies carried out by us, rotigaptide had similar effects in ischaemic myocytes as AAP10. Therefore, their overall effects and mechanism of action are highly likely to be similar if not identical. The mechanism of action of both peptides has been associated with the phosphorylation of Cx43, specifically via the action of PKC_{α} (Dhein et al., 2003; Weng et al., 2002). Indeed, the therapeutic benefit produced by such peptides has already been recognised by the continuing clinical development of rotigaptide (ZP123).

The studies described examined the potential of several methods of transfection of primary cardiac myocytes with fluorescently labelled Cx43. Although these studies illustrated the difficulties surrounding the transfection of primary cells, they show that it can be achieved using an adenoviral expression system. The reasons for these difficulties in transfection in primary cardiac myocytes are presently unknown, but possible causes could be the extensive cytoskeletal system or limited exocytosis/endocytosis processes compared to other cultured cells and cells dissociated from organs. To my knowledge there has been little work to investigate the trafficking and assembly of gap junctions and CxHcs in cardiac cells although it is likely that the trafficking and assembly of connexin channels is similar in all cells. Thus, it would be of great benefit if these factors were studied further in a cardiac context using myocytes from young or old animals.

The relationship between gap junctions and cardiac arrhythmia make regulation of Cx43 an important field warranting further research. The evidence implicating Cx43 and gap junction channels in cardiac myocyte responses to ischaemia and reperfusion indicates that understanding the behaviour of channels composed of Cx43 is a vital requirement in cardiac biology. The use of the model described in this thesis will allow continued in depth evaluation of these processes.

Bibliography

Abrams, C. K., Freidin, M. M., Verselis, V. K., Bennett, M. V., & Bargiello, T. A. 2001, "Functional alterations in gap junction channels formed by mutant forms of connexin 32: evidence for loss of function as a pathogenic mechanism in the X-linked form of Charcot-Marie-Tooth disease", *Brain Res.*, vol. 900, no. 1, pp. 9-25.

Adams, M. D., Celniker, S. E., Holt, R. A., Evans, C. A., Gocayne, J. D. et al, 2000, "The genome sequence of Drosophila melanogaster", *Science*, vol. 287, no. 5461, pp. 2185-2195.

Adams, S. R., Campbell, R. E., Gross, L. A., Martin, B. R., Walkup, G. K., Yao, Y., Llopis, J., & Tsien, R. Y. 2002, "New biarsenical ligands and tetracysteine motifs for protein labeling in vitro and in vivo: synthesis and biological applications", *J.Am.Chem.Soc.*, vol. 124, no. 21, pp. 6063-6076.

Ahmad, S., Martin, P. E., & Evans, W. H. 2001, "Assembly of gap junction channels: mechanism, effects of calmodulin antagonists and identification of connexin oligomerization determinants", *Eur.J.Biochem.*, vol. 268, no. 16, pp. 4544-4552.

Allen, T., Iftinca, M., Cole, W. C., & Plane, F. 2002, "Smooth muscle membrane potential modulates endothelium-dependent relaxation of rat basilar artery via myo-endothelial gap junctions", *J.Physiol*, vol. 545, no. Pt 3, pp. 975-986.

Allessie, M., Ausma, J., & Schotten, U. 2002, "Electrical, contractile and structural remodeling during atrial fibrillation", *Cardiovasc.Res.*, vol. 54, no. 2, pp. 230-246.

Angst, B. D., Khan, L. U., Severs, N. J., Whitely, K., Rothery, S., Thompson, R. P., Magee, A. I., & Gourdie, R. G. 1997, "Dissociated spatial patterning of gap junctions and cell adhesion junctions during postnatal differentiation of ventricular myocardium", *Circ.Res.*, vol. 80, no. 1, pp. 88-94.

Aonuma, S., Kohama, Y., Makino, T., & Hattori, K. 1983, "[Studies on the heart (22). Inhibitory effect of an atrial peptide (AAP) on drug-induced arrhythmia]", *Yakugaku Zasshi*, vol. 103, no. 6, pp. 662-666.

Aonuma, S., Kohama, Y., Makino, T., & Fujisawa, Y. 1982, "Studies of heart. XXI. Amino acid sequence of antiarrhythmic peptide (AAP) isolated from atria", *J.Pharmacobiodyn.*, vol. 5, no. 1, pp. 40-48.

Aonuma, S., Kohama, Y., Akai, K., Komiyama, Y., Nakajima, S., Wakabayashi, M., & Makino, T. 1980, "Studies on heart. XIX. Isolation of an atrial peptide that improves the rhythmicity of cultured myocardial cell clusters", *Chem.Pharm.Bull.(Tokyo)*, vol. 28, no. 11, pp. 3332-3339.

Atkinson, M. M., Lampe, P. D., Lin, H. H., Kollander, R., Li, X. R., & Kiang, D. T. 1995, "Cyclic AMP modifies the cellular distribution of connexin43 and induces a persistent increase in the junctional permeability of mouse mammary tumor cells", *J.Cell Sci.*, vol. 108 (Pt 9), pp. 3079-3090.

Axelsen, L. N., Stahlhut, M., Mohammed, S., Larsen, B. D., Nielsen, M. S., Holstein-Rathlou, N. H., Andersen, S., Jensen, O. N., Hennan, J. K., & Kjolbye, A. L. 2006, "Identification of ischemia-regulated phosphorylation sites in connexin43: A possible target for the antiarrhythmic peptide analogue rotigaptide (ZP123)", *J.Mol.Cell Cardiol.*, vol. 40, no. 6, pp. 790-798.

Baker, T. S., Sosinsky, G. E., Caspar, D. L., Gall, C., & Goodenough, D. A. 1985, "Gap junction structures. VII. Analysis of connexon images obtained with cationic and anionic negative stains", *J.Mol.Biol.*, vol. 184, no. 1, pp. 81-98.

Bao, L., Sachs, F., & Dahl, G. 2004, "Connexins are mechanosensitive", *Am.J.Physiol Cell Physiol*, vol. 287, no. 5, p. C1389-C1395.

Bao, X., Reuss, L., & Altenberg, G. A. 2004, "Regulation of purified and reconstituted connexin 43 hemichannels by protein kinase C-mediated phosphorylation of Serine 368", *J.Biol.Chem.*, vol. 279, no. 19, pp. 20058-20066.

Baranova, A., Ivanov, D., Petrash, N., Pestova, A., Skoblov, M., Kelmanson, I., Shagin, D., Nazarenko, S., Geraymovych, E., Litvin, O., Tiunova, A., Born, T. L., Usman, N., Staroverov, D., Lukyanov, S., & Panchin, Y. 2004, "The mammalian pannexin family is homologous to the invertebrate innexin gap junction proteins", *Genomics*, vol. 83, no. 4, pp. 706-716.

Bastide, B., Neyses, L., Ganten, D., Paul, M., Willecke, K., & Traub, O. 1993, "Gap junction protein connexin40 is preferentially expressed in vascular endothelium and conductive bundles of rat myocardium and is increased under hypertensive conditions", *Circ.Res.*, vol. 73, no. 6, pp. 1138-1149.

Beardslee, M. A., Lerner, D. L., Tadros, P. N., Laing, J. G., Beyer, E. C., Yamada, K. A., Kleber, A. G., Schuessler, R. B., & Saffitz, J. E. 2000, "Dephosphorylation and intracellular redistribution of ventricular connexin43 during electrical uncoupling induced by ischemia", *Circ.Res.*, vol. 87, no. 8, pp. 656-662.

Beardslee, M. A., Laing, J. G., Beyer, E. C., & Saffitz, J. E. 1998, "Rapid turnover of connexin43 in the adult rat heart", *Circ.Res.*, vol. 83, no. 6, pp. 629-635.

Belardinelli, L. 1987, "Modulation of atrioventricular transmission by adenosine", *Prog.Clin.Biol.Res.*, vol. 230, pp. 109-118.

Benedetti, E. L. & Emmelot, P. 1965, "Electron microscopic observations on negatively stained plasma membranes isolated from rat liver", *J.Cell Biol.*, vol. 26, no. 1, pp. 299-305.

Bennett, M. V., Contreras, J. E., Bukauskas, F. F., & Saez, J. C. 2003, "New roles for astrocytes: gap junction hemichannels have something to communicate", *Trends Neurosci.*, vol. 26, no. 11, pp. 610-617.

Bergoffen, J., Scherer, S. S., Wang, S., Scott, M. O., Bone, L. J., Paul, D. L., Chen, K., Lensch, M. W., Chance, P. F., & Fischbeck, K. H. 1993, "Connexin mutations in X-linked Charcot-Marie-Tooth disease", *Science*, vol. 262, no. 5142, pp. 2039-2042.

Bernstein, S. A. & Morley, G. E. 2006, "Gap junctions and propagation of the cardiac action potential", *Adv.Cardiol.*, vol. 42, pp. 71-85.

Berthoud, V. M., Westphale, E. M., Grigoryeva, A., & Beyer, E. C. 2000, "PKC isoenzymes in the chicken lens and TPA-induced effects on intercellular communication", *Invest Ophthalmol.Vis.Sci.*, vol. 41, no. 3, pp. 850-858.

Berthoud, V. M., Ledbetter, M. L., Hertzberg, E. L., & Saez, J. C. 1992, "Connexin43 in MDCK cells: regulation by a tumor-promoting phorbol ester and Ca2+", *Eur.J.Cell Biol.*, vol. 57, no. 1, pp. 40-50.

Beyer, E. C., Paul, D. L., & Goodenough, D. A. 1987, "Connexin43: a protein from rat heart homologous to a gap junction protein from liver", *J.Cell Biol.*, vol. 105, no. 6 Pt 1, pp. 2621-2629.

Bialik, S., Cryns, V. L., Drincic, A., Miyata, S., Wollowick, A. L., Srinivasan, A., & Kitsis, R. N. 1999, "The mitochondrial apoptotic pathway is activated by serum and glucose deprivation in cardiac myocytes", *Circ.Res.*, vol. 85, no. 5, pp. 403-414.

Blackburn, J. P., Peters, N. S., Yeh, H. I., Rothery, S., Green, C. R., & Severs, N. J. 1995, "Upregulation of connexin43 gap junctions during early stages of human coronary atherosclerosis", *Arterioscler.Thromb.Vasc.Biol.*, vol. 15, no. 8, pp. 1219-1228.

Boitano, S., Dirksen, E. R., & Sanderson, M. J. 1992, "Intercellular propagation of calcium waves mediated by inositol trisphosphate", *Science*, vol. 258, no. 5080, pp. 292-295.

Boudreault, F. & Grygorczyk, R. 2004, "Cell swelling-induced ATP release is tightly dependent on intracellular calcium elevations", *J.Physiol*, vol. 561, no. Pt 2, pp. 499-513.

Bowling, N., Huang, X., Sandusky, G. E., Fouts, R. L., Mintze, K., Esterman, M., Allen, P. D., Maddi, R., McCall, E., & Vlahos, C. J. 2001, "Protein kinase C-alpha and -epsilon modulate connexin-43 phosphorylation in human heart", *J.Mol.Cell Cardiol.*, vol. 33, no. 4, pp. 789-798.

Braet, K., Aspeslagh, S., Vandamme, W., Willecke, K., Martin, P. E., Evans, W. H., & Leybaert, L. 2003, "Pharmacological sensitivity of ATP release triggered by photoliberation of inositol-1,4,5-trisphosphate and zero extracellular calcium in brain endothelial cells", *J.Cell Physiol*, vol. 197, no. 2, pp. 205-213.

Braet, K., Vandamme, W., Martin, P. E., Evans, W. H., & Leybaert, L. 2003, "Photoliberating inositol-1,4,5-trisphosphate triggers ATP release that is blocked by the connexin mimetic peptide gap 26", *Cell Calcium*, vol. 33, no. 1, pp. 37-48.

Braunwald, E., Antman, E. M., Beasley, J. W., Califf, R. M., Cheitlin, M. D., Hochman, J. S. et al, 2000, "ACC/AHA guidelines for the management of patients with unstable angina and non-ST-segment elevation myocardial infarction. A report of the American College of Cardiology/American Heart Association Task Force on Practice Guidelines (Committee on the Management of Patients With Unstable Angina)", *J.Am.Coll.Cardiol.*, vol. 36, no. 3, pp. 970-1062.

Brissette, J. L., Kumar, N. M., Gilula, N. B., & Dotto, G. P. 1991, "The tumor promoter 12-O-tetradecanoylphorbol-13-acetate and the ras oncogene modulate expression and phosphorylation of gap junction proteins", *Mol.Cell Biol.*, vol. 11, no. 10, pp. 5364-5371.

Bruzzone, R., Hormuzdi, S. G., Barbe, M. T., Herb, A., & Monyer, H. 2003, "Pannexins, a family of gap junction proteins expressed in brain", *Proc.Natl.Acad.Sci.U.S.A*, vol. 100, no. 23, pp. 13644-13649.

Bruzzone, S., Guida, L., Zocchi, E., Franco, L., & De Flora, A. 2001, "Connexin 43 hemi channels mediate Ca2+-regulated transmembrane NAD+ fluxes in intact cells", *FASEB J.*, vol. 15, no. 1, pp. 10-12.

Bukauskas, F. F., Kreuzberg, M. M., Rackauskas, M., Bukauskiene, A., Bennett, M. V., Verselis, V. K., & Willecke, K. 2006, "Properties of mouse connexin 30.2 and human connexin 31.9 hemichannels: implications for atrioventricular conduction in the heart", *Proc.Natl.Acad.Sci.U.S.A*, vol. 103, no. 25, pp. 9726-9731.

Bukauskas, F. F., Angele, A. B., Verselis, V. K., & Bennett, M. V. 2002, "Coupling asymmetry of heterotypic connexin 45/ connexin 43-EGFP gap junctions: properties of fast and slow gating mechanisms", *Proc.Natl.Acad.Sci.U.S.A*, vol. 99, no. 10, pp. 7113-7118.

Bukauskas, F. F., Jordan, K., Bukauskiene, A., Bennett, M. V., Lampe, P. D., Laird, D. W., & Verselis, V. K. 2000, "Clustering of connexin 43-enhanced green fluorescent protein gap junction channels and functional coupling in living cells", *Proc.Natl.Acad.Sci.U.S.A*, vol. 97, no. 6, pp. 2556-2561.

Bukauskas, F. F., Elfgang, C., Willecke, K., & Weingart, R. 1995, "Biophysical properties of gap junction channels formed by mouse connexin40 in induced pairs of transfected human HeLa cells", *Biophys.J.*, vol. 68, no. 6, pp. 2289-2298.

Burnstock, G. 2006, "Pathophysiology and therapeutic potential of purinergic signaling", *Pharmacol.Rev.*, vol. 58, no. 1, pp. 58-86.

Burnstock, G. 2006, "Purinergic signalling--an overview", *Novartis.Found.Symp.*, vol. 276, pp. 26-48.

Burnstock, G. 2002, "Potential therapeutic targets in the rapidly expanding field of purinergic signalling", *Clin.Med.*, vol. 2, no. 1, pp. 45-53.

Burnstock, G. 1999, "Release of vasoactive substances from endothelial cells by shear stress and purinergic mechanosensory transduction", *J Anat.*, vol. 194 (Pt 3), pp. 335-342.

Burt, J. M. & Spray, D. C. 1989, "Volatile anesthetics block intercellular communication between neonatal rat myocardial cells", *Circ.Res.*, vol. 65, no. 3, pp. 829-837.

C.elegans sequencing consortium 1998, "Genome sequence of the nematode C. elegans: a platform for investigating biology", *Science*, vol. 282, no. 5396, pp. 2012-2018.

Calero, G., Kanemitsu, M., Taffet, S. M., Lau, A. F., & Delmar, M. 1998, "A 17mer peptide interferes with acidification-induced uncoupling of connexin43", *Circ.Res.*, vol. 82, no. 9, pp. 929-935.

Cao, F., Eckert, R., Elfgang, C., Nitsche, J. M., Snyder, S. A., ulser, D. F., Willecke, K., & Nicholson, B. J. 1998, "A quantitative analysis of connexin-specific permeability differences of gap junctions expressed in HeLa transfectants and Xenopus oocytes", *J.Cell Sci.*, vol. 111 (Pt 1), pp. 31-43.

Cascio, M., Gogol, E., & Wallace, B. A. 1990, "The secondary structure of gap junctions. Influence of isolation methods and proteolysis", *J.Biol.Chem.*, vol. 265, no. 4, pp. 2358-2364.

Cascio, W. E., Yang, H., Muller-Borer, B. J., & Johnson, T. A. 2005, "Ischemia-induced arrhythmia: the role of connexins, gap junctions, and attendant changes in impulse propagation", *J.Electrocardiol.*, vol. 38, no. 4 Suppl, pp. 55-59.

Castro, C., Gomez-Hernandez, J. M., Silander, K., & Barrio, L. C. 1999, "Altered formation of hemichannels and gap junction channels caused by C-terminal connexin-32 mutations", *J.Neurosci.*, vol. 19, no. 10, pp. 3752-3760.

Chanson, M., White, M. M., & Garber, S. S. 1996, "cAMP promotes gap junctional coupling in T84 cells", *Am.J.Physiol*, vol. 271, no. 2 Pt 1, p. C533-C539.

Chaytor, A. T., Martin, P. E., Evans, W. H., Randall, M. D., & Griffith, T. M. 1999, "The endothelial component of cannabinoid-induced relaxation in rabbit mesenteric artery depends on gap junctional communication", *J.Physiol*, vol. 520 Pt 2, pp. 539-550.

Chaytor, A. T., Evans, W. H., & Griffith, T. M. 1998, "Central role of heterocellular gap junctional communication in endothelium-dependent relaxations of rabbit arteries", *J.Physiol*, vol. 508 (Pt 2), pp. 561-573.

Chaytor, A. T., Evans, W. H., & Griffith, T. M. 1997, "Peptides homologous to extracellular loop motifs of connexin 43 reversibly abolish rhythmic contractile activity in rabbit arteries", *J.Physiol*, vol. 503 (Pt 1), pp. 99-110.

Cheng, H. L. & Louis, C. F. 2001, "Functional effects of casein kinase I-catalyzed phosphorylation on lens cell-to-cell coupling", *J.Membr.Biol.*, vol. 181, no. 1, pp. 21-30.

Cherian, P. P., Siller-Jackson, A. J., Gu, S., Wang, X., Bonewald, L. F., Sprague, E., & Jiang, J. X. 2005, "Mechanical strain opens connexin 43 hemichannels in osteocytes: a novel mechanism for the release of prostaglandin", *Mol.Biol.Cell*, vol. 16, no. 7, pp. 3100-3106.

Clarke, T. C., Thomas, D., Petersen, J. S., Evans, W. H., & Martin, P. E. 2006, "The antiarrhythmic peptide rotigaptide (ZP123) increases gap junction intercellular communication in cardiac myocytes and HeLa cells expressing connexin 43", *Br.J.Pharmacol.*, vol. 147, no. 5, pp. 486-495.

Claycomb, W. C., Lanson, N. A., Jr., Stallworth, B. S., Egeland, D. B., Delcarpio, J. B., Bahinski, A., & Izzo, N. J., Jr. 1998, "HL-1 cells: a cardiac muscle cell line that contracts and retains phenotypic characteristics of the adult cardiomyocyte", *Proc.Natl.Acad.Sci.U.S.A*, vol. 95, no. 6, pp. 2979-2984.

Contreras, J. E., Sanchez, H. A., Veliz, L. P., Bukauskas, F. F., Bennett, M. V., & Saez, J. C. 2004, "Role of connexin-based gap junction channels and hemichannels in ischemia-induced cell death in nervous tissue", *Brain Res.Brain Res.Rev.*, vol. 47, no. 1-3, pp. 290-303.

Contreras, J. E., Saez, J. C., Bukauskas, F. F., & Bennett, M. V. 2003, "Gating and regulation of connexin 43 (Cx43) hemichannels", *Proc.Natl.Acad.Sci.U.S.A*, vol. 100, no. 20, pp. 11388-11393.

Contreras, J. E., Sanchez, H. A., Eugenin, E. A., Speidel, D., Theis, M., Willecke, K., Bukauskas, F. F., Bennett, M. V., & Saez, J. C. 2002, "Metabolic inhibition induces opening of unapposed connexin 43 gap junction hemichannels and reduces gap junctional communication in cortical astrocytes in culture", *Proc.Natl.Acad.Sci.U.S.A*, vol. 99, no. 1, pp. 495-500.

Cooper, C. D. & Lampe, P. D. 2002, "Casein kinase 1 regulates connexin-43 gap junction assembly", *J.Biol.Chem.*, vol. 277, no. 47, pp. 44962-44968.

Coppen, S. R., Kodama, I., Boyett, M. R., Dobrzynski, H., Takagishi, Y., Honjo, H., Yeh, H. I., & Severs, N. J. 1999, "Connexin45, a major connexin of the rabbit sinoatrial node, is co-expressed with connexin43 in a restricted zone at the nodal-crista terminalis border", *J.Histochem.Cytochem.*, vol. 47, no. 7, pp. 907-918.

Coppen, S. R., Severs, N. J., & Gourdie, R. G. 1999, "Connexin45 (alpha 6) expression delineates an extended conduction system in the embryonic and mature rodent heart", *Dev.Genet.*, vol. 24, no. 1-2, pp. 82-90.

Coppen, S. R., Dupont, E., Rothery, S., & Severs, N. J. 1998, "Connexin45 expression is preferentially associated with the ventricular conduction system in mouse and rat heart", *Circ.Res.*, vol. 82, no. 2, pp. 232-243.

Cotrina, M. L., Lin, J. H., ves-Rodrigues, A., Liu, S., Li, J., zmi-Ghadimi, H., Kang, J., Naus, C. C., & Nedergaard, M. 1998, "Connexins regulate calcium signaling by controlling ATP release", *Proc.Natl.Acad.Sci.U.S.A*, vol. 95, no. 26, pp. 15735-15740.

Cottrell, G. T., Wu, Y., & Burt, J. M. 2002, "Cx40 and Cx43 expression ratio influences heteromeric/ heterotypic gap junction channel properties", *Am.J.Physiol Cell Physiol*, vol. 282, no. 6, p. C1469-C1482.

Cottrell, G. T. & Burt, J. M. 2001, "Heterotypic gap junction channel formation between heteromeric and homomeric Cx40 and Cx43 connexons", *Am.J.Physiol Cell Physiol*, vol. 281, no. 5, p. C1559-C1567.

Cruciani, V., Husoy, T., & Mikalsen, S. O. 2001, "Pharmacological evidence for system-dependent involvement of protein kinase C isoenzymes in phorbol ester-suppressed gap junctional communication", *Exp.Cell Res.*, vol. 268, no. 2, pp. 150-161.

Dahl, G., Werner, R., Levine, E., & Rabadan-Diehl, C. 1992, "Mutational analysis of gap junction formation", *Biophys.J.*, vol. 62, no. 1, pp. 172-180.

Daleau, P., Boudriau, S., Michaud, M., Jolicoeur, C., & Kingma, J. G., Jr. 2001, "Preconditioning in the absence or presence of sustained ischemia modulates myocardial Cx43 protein levels and gap junction distribution", *Can.J.Physiol Pharmacol.*, vol. 79, no. 5, pp. 371-378.

Danik, S. B., Liu, F., Zhang, J., Suk, H. J., Morley, G. E., Fishman, G. I., & Gutstein, D. E. 2004, "Modulation of cardiac gap junction expression and arrhythmic susceptibility", *Circ.Res.*, vol. 95, no. 10, pp. 1035-1041.

Darrow, B. J., Laing, J. G., Lampe, P. D., Saffitz, J. E., & Beyer, E. C. 1995, "Expression of multiple connexins in cultured neonatal rat ventricular myocytes", *Circ.Res.*, vol. 76, no. 3, pp. 381-387.

Davidson, J. S. & Baumgarten, I. M. 1988, "Glycyrrhetinic acid derivatives: a novel class of inhibitors of gap-junctional intercellular communication. Structure-activity relationships", *J.Pharmacol.Exp.Ther.*, vol. 246, no. 3, pp. 1104-1107.

De Vuyst, E., Decrock, E., Cabooter, L., Dubyak, G. R., Naus, C. C., Evans, W. H., & Leybaert, L. 2006, "Intracellular calcium changes trigger connexin 32 hemichannel opening", *EMBO J.*, vol. 25, no. 1, pp. 34-44.

De Vuyst, V. E., Decrock, E., De, B. M., Yamasaki, H., Naus, C. C., Evans, W. H., & Leybaert, L. 2006, "Connexin Hemichannels and Gap Junction Channels Are Differentially Influenced by Lipopolysaccharide and bFGF", *Mol.Biol.Cell.*

De Mello, W. C. 1991, "Further studies on the influence of cAMP-dependent protein kinase on junctional conductance in isolated heart cell pairs", *J.Mol.Cell Cardiol.*, vol. 23, no. 3, pp. 371-379.

De Mello, W. C. 1976, "Influence of the sodium pump on intercellular communication in heart fibres: effect of intracellular injection of sodium ion on electrical coupling", *J.Physiol*, vol. 263, no. 2, pp. 171-197.

de Pina-Benabou, M. H., Szostak, V., Kyrozis, A., Rempe, D., Uziel, D., Urban-Maldonado, M., Benabou, S., Spray, D. C., Federoff, H. J., Stanton, P. K., & Rozental, R. 2005, "Blockade of gap junctions in vivo provides neuroprotection after perinatal global ischemia", *Stroke*, vol. 36, no. 10, pp. 2232-2237.

Decker, T. & Lohmann-Matthes, M. L. 1988, "A quick and simple method for the quantitation of lactate dehydrogenase release in measurements of cellular cytotoxicity and tumor necrosis factor (TNF) activity", *J.Immunol.Methods*, vol. 115, no. 1, pp. 61-69.

Delcarpio, J. B., Lanson, N. A., Jr., Field, L. J., & Claycomb, W. C. 1991, "Morphological characterization of cardiomyocytes isolated from a transplantable cardiac tumor derived from transgenic mouse atria (AT-1 cells)", *Circ.Res.*, vol. 69, no. 6, pp. 1591-1600.

Dhein, S. 2004, "Pharmacology of gap junctions in the cardiovascular system", *Cardiovasc.Res.*, vol. 62, no. 2, pp. 287-298.

Dhein, S., Larsen, B. D., Petersen, J. S., & Mohr, F. W. 2003, "Effects of the new antiarrhythmic peptide ZP123 on epicardial activation and repolarization pattern", *Cell Commun.Adhes.*, vol. 10, no. 4-6, pp. 371-378.

Dhein, S., Weng, S., Grover, R., Tudyka, T., Gottwald, M., Schaefer, T., & Polontchouk, L. 2001, "Protein kinase Calpha mediates the effect of antiarrhythmic peptide on gap junction conductance", *Cell Commun.Adhes.*, vol. 8, no. 4-6, pp. 257-264.

Dhein, S., Krusemann, K., & Schaefer, T. 1999, "Effects of the gap junction uncoupler palmitoleic acid on the activation and repolarization wavefronts in isolated rabbit hearts", *Br.J.Pharmacol.*, vol. 128, no. 7, pp. 1375-1384.

Di, W. L., Rugg, E. L., Leigh, I. M., & Kelsell, D. P. 2001, "Multiple epidermal connexins are expressed in different keratinocyte subpopulations including connexin 31", *J.Invest Dermatol.*, vol. 117, no. 4, pp. 958-964.

Diez, J. A., Ahmad, S., & Evans, W. H. 1999, "Assembly of heteromeric connexons in guinea-pig liver en route to the Golgi apparatus, plasma membrane and gap junctions", *Eur.J.Biochem.*, vol. 262, no. 1, pp. 142-148.

Diez, J. A., Elvira, M., & Villalobo, A. 1998, "The epidermal growth factor receptor tyrosine kinase phosphorylates connexin32", *Mol.Cell Biochem.*, vol. 187, no. 1-2, pp. 201-210.

Doble, B. W., Ping, P., & Kardami, E. 2000, "The epsilon subtype of protein kinase C is required for cardiomyocyte connexin-43 phosphorylation", *Circ.Res.*, vol. 86, no. 3, pp. 293-301.

Drury A.N. & Szent-Gyorgyi A. 1929, "The physiological activity of adenine compounds with especial reference to their action upon the mammalian heart", *J Physiol.*, vol. 68, no. 3, pp. 213-237.

Dupont, E., Matsushita, T., Kaba, R. A., Vozzi, C., Coppen, S. R., Khan, N., Kaprielian, R., Yacoub, M. H., & Severs, N. J. 2001, "Altered connexin expression in human congestive heart failure", *J.Mol.Cell Cardiol.*, vol. 33, no. 2, pp. 359-371.

Dutta, A. K., Sabirov, R. Z., Uramoto, H., & Okada, Y. 2004, "Role of ATP-conductive anion channel in ATP release from neonatal rat cardiomyocytes in ischaemic or hypoxic conditions", *J.Physiol*, vol. 559, no. Pt 3, pp. 799-812.

Ebihara, L. 2003, "New roles for connexons", *News Physiol Sci.*, vol. 18, pp. 100-103.

Ebihara, L., Liu, X., & Pal, J. D. 2003, "Effect of external magnesium and calcium on human connexin46 hemichannels", *Biophys.J.*, vol. 84, no. 1, pp. 277-286.

Ebihara, L., Xu, X., Oberti, C., Beyer, E. C., & Berthoud, V. M. 1999, "Co-expression of lens fiber connexins modifies hemi-gap-junctional channel behavior", *Biophys.J.*, vol. 76, no. 1 Pt 1, pp. 198-206.

Ebihara, L. & Steiner, E. 1993, "Properties of a nonjunctional current expressed from a rat connexin46 cDNA in Xenopus oocytes", *J.Gen.Physiol*, vol. 102, no. 1, pp. 59-74.

Ek-Vitorin, J. F., King, T. J., Heyman, N. S., Lampe, P. D., & Burt, J. M. 2006, "Selectivity of connexin 43 channels is regulated through protein kinase C-dependent phosphorylation", *Circ.Res.*, vol. 98, no. 12, pp. 1498-1505.

Ek-Vitorin, J. F., Calero, G., Morley, G. E., Coombs, W., Taffet, S. M., & Delmar, M. 1996, "PH regulation of connexin43: molecular analysis of the gating particle", *Biophys.J.*, vol. 71, no. 3, pp. 1273-1284.

Elfgang, C., Eckert, R., Lichtenberg-Frate, H., Butterweck, A., Traub, O., Klein, R. A., Hulser, D. F., & Willecke, K. 1995, "Specific permeability and selective formation of gap junction channels in connexin-transfected HeLa cells", *J.Cell Biol.*, vol. 129, no. 3, pp. 805-817.

Eloff, B. C., Gilat, E., Wan, X., & Rosenbaum, D. S. 2003, "Pharmacological modulation of cardiac gap junctions to enhance cardiac conduction: evidence supporting a novel target for antiarrhythmic therapy", *Circulation*, vol. 108, no. 25, pp. 3157-3163.

Eltzschig, H. K., Eckle, T., Mager, A., Kuper, N., Karcher, C., Weissmuller, T., Boengler, K., Schulz, R., Robson, S. C., & Colgan, S. P. 2006, "ATP Release From Activated Neutrophils Occurs via Connexin 43 and Modulates Adenosine-Dependent Endothelial Cell Function", *Circ.Res.*

Emdad, L., Uzzaman, M., Takagishi, Y., Honjo, H., Uchida, T., Severs, N. J., Kodama, I., & Murata, Y. 2001, "Gap junction remodeling in hypertrophied left ventricles of aortic-banded rats: prevention by angiotensin II type 1 receptor blockade", *J.Mol.Cell Cardiol.*, vol. 33, no. 2, pp. 219-231.

Estivill, X., Fortina, P., Surrey, S., Rabionet, R., Melchionda, S., D'Agruma, L., Mansfield, E., Rappaport, E., Govea, N., Mila, M., Zelante, L., & Gasparini, P. 1998, "Connexin-26 mutations in sporadic and inherited sensorineural deafness", *Lancet*, vol. 351, no. 9100, pp. 394-398.

Evans, W. H., De Vuyst, E., & Leybaert, L. 2006, "The gap junction cellular internet: connexin hemichannels enter the signalling limelight", *Biochem.J.*, vol. 397, no. 1, pp. 1-14.

Evans, W. H. & Martin, P. E. 2002, "Gap junctions: structure and function (Review)", *Mol.Membr.Biol.*, vol. 19, no. 2, pp. 121-136.

Evans, W. H. & Martin, P. E. 2002, "Lighting up gap junction channels in a flash", *Bioessays*, vol. 24, no. 10, pp. 876-880.

Evans, W. H. & Boitano, S. 2001, "Connexin mimetic peptides: specific inhibitors of gap-junctional intercellular communication", *Biochem.Soc.Trans.*, vol. 29, no. Pt 4, pp. 606-612.

Falk, M. M., Buehler, L. K., Kumar, N. M., & Gilula, N. B. 1997, "Cell-free synthesis and assembly of connexins into functional gap junction membrane channels", *EMBO J.*, vol. 16, no. 10, pp. 2703-2716.

Firek, L. & Weingart, R. 1995, "Modification of gap junction conductance by divalent cations and protons in neonatal rat heart cells", *J.Mol.Cell Cardiol.*, vol. 27, no. 8, pp. 1633-1643.

Fishman, G. I., Moreno, A. P., Spray, D. C., & Leinwand, L. A. 1991, "Functional analysis of human cardiac gap junction channel mutants", *Proc.Natl.Acad.Sci.U.S.A*, vol. 88, no. 9, pp. 3525-3529.

Fleishman, S. J., Sabag, A. D., Ophir, E., Avraham, K. B., & Ben-Tal, N. 2006, "The structural context of disease-causing mutations in gap junctions", *J.Biol.Chem.*, vol. 281, no. 39, pp. 28958-28963.

Flenniken, A. M., Osborne, L. R., Anderson, N., Ciliberti, N., Fleming, C., Gittens, J. E. et al, 2005, "A Gja1 missense mutation in a mouse model of oculodentodigital dysplasia", *Development*, vol. 132, no. 19, pp. 4375-4386.

Foote, C. I., Zhou, L., Zhu, X., & Nicholson, B. J. 1998, "The pattern of disulfide linkages in the extracellular loop regions of connexin 32 suggests a model for the docking interface of gap junctions", *J.Cell Biol.*, vol. 140, no. 5, pp. 1187-1197.

Forrester, T. & Williams, C. A. 1977, "Release of adenosine triphosphate from isolated adult heart cells in response to hypoxia", *J.Physiol*, vol. 268, no. 2, pp. 371-390.

Fuster, V., Badimon, L., Badimon, J. J., & Chesebro, J. H. 1992, "The pathogenesis of coronary artery disease and the acute coronary syndromes (1)", *N.Engl.J.Med.*, vol. 326, no. 4, pp. 242-250.

Gabriels, J. E. & Paul, D. L. 1998, "Connexin43 is highly localized to sites of disturbed flow in rat aortic endothelium but connexin37 and connexin40 are more uniformly distributed", *Circ.Res.*, vol. 83, no. 6, pp. 636-643.

Gaietta, G., Deerinck, T. J., Adams, S. R., Bouwer, J., Tour, O., Laird, D. W., Sosinsky, G. E., Tsien, R. Y., & Ellisman, M. H. 2002, "Multicolor and electron microscopic imaging of connexin trafficking", *Science*, vol. 296, no. 5567, pp. 503-507.

Garcia-Dorado, D., Inserte, J., Ruiz-Meana, M., Gonzalez, M. A., Solares, J., Julia, M., Barrabes, J. A., & Soler-Soler, J. 1997, "Gap junction uncoupler heptanol prevents cell-to-cell progression of hypercontracture and limits necrosis during myocardial reperfusion", *Circulation*, vol. 96, no. 10, pp. 3579-3586.

George, C. H., Kendall, J. M., & Evans, W. H. 1999, "Intracellular trafficking pathways in the assembly of connexins into gap junctions", *J.Biol.Chem.*, vol. 274, no. 13, pp. 8678-8685.

George, C. H., Kendall, J. M., Campbell, A. K., & Evans, W. H. 1998, "Connexin-aequorin chimerae report cytoplasmic calcium environments along trafficking pathways leading to gap junction biogenesis in living COS-7 cells", *J.Biol.Chem.*, vol. 273, no. 45, pp. 29822-29829.

George, C. H., Martin, P. E., & Evans, W. H. 1998, "Rapid determination of gap junction formation using HeLa cells microinjected with cDNAs encoding wild-type and chimeric connexins", *Biochem.Biophys.Res.Commun.*, vol. 247, no. 3, pp. 785-789.

Giaume, C. & Venance, L. 1998, "Intercellular calcium signaling and gap junctional communication in astrocytes", *Glia*, vol. 24, no. 1, pp. 50-64.

Giepmans, B. N. 2004, "Gap junctions and connexin-interacting proteins", *Cardiovasc.Res.*, vol. 62, no. 2, pp. 233-245.

Giepmans, B. N., Verlaan, I., Hengeveld, T., Janssen, H., Calafat, J., Falk, M. M., & Moolenaar, W. H. 2001, "Gap junction protein connexin-43 interacts directly with microtubules", *Curr.Biol.*, vol. 11, no. 17, pp. 1364-1368.

Goldberg, G. S., Moreno, A. P., & Lampe, P. D. 2002, "Gap junctions between cells expressing connexin 43 or 32 show inverse permselectivity to adenosine and ATP", *J.Biol.Chem.*, vol. 277, no. 39, pp. 36725-36730.

Gomes, P., Srinivas, S. P., Van, D. W., Vereecke, J., & Himpens, B. 2005, "ATP release through connexin hemichannels in corneal endothelial cells", *Invest Ophthalmol.Vis.Sci.*, vol. 46, no. 4, pp. 1208-1218.

Gomez-Hernandez, J. M., de, M. M., Larrosa, B., Gonzalez, D., & Barrio, L. C. 2003, "Molecular basis of calcium regulation in connexin-32 hemichannels", *Proc.Natl.Acad.Sci.U.S.A*, vol. 100, no. 26, pp. 16030-16035.

Goodenough, D. A. & Paul, D. L. 2003, "Beyond the gap: functions of unpaired connexon channels", *Nat.Rev.Mol.Cell Biol.*, vol. 4, no. 4, pp. 285-294.

Goodenough, D. A., Dick, J. S., & Lyons, J. E. 1980, "Lens metabolic cooperation: a study of mouse lens transport and permeability visualized with freeze-substitution autoradiography and electron microscopy", *J.Cell Biol.*, vol. 86, no. 2, pp. 576-589.

Goodenough, D. A. & Revel, J. P. 1970, "A fine structural analysis of intercellular junctions in the mouse liver", *J.Cell Biol.*, vol. 45, no. 2, pp. 272-290.

Gourdie, R. G., Severs, N. J., Green, C. R., Rothery, S., Germroth, P., & Thompson, R. P. 1993, "The spatial distribution and relative abundance of gap-junctional connexin40 and connexin43 correlate to functional properties of components of the cardiac atrioventricular conduction system", *J.Cell Sci.*, vol. 105 (Pt 4), pp. 985-991.

Gourdie, R. G., Green, C. R., & Severs, N. J. 1991, "Gap junction distribution in adult mammalian myocardium revealed by an anti-peptide antibody and laser scanning confocal microscopy", *J.Cell Sci.*, vol. 99 (Pt 1), pp. 41-55.

Green, C. R. & Severs, N. J. 1993, "Robert Feulgen Prize Lecture. Distribution and role of gap junctions in normal myocardium and human ischaemic heart disease", *Histochemistry*, vol. 99, no. 2, pp. 105-120.

Griffin, B. A., Adams, S. R., & Tsien, R. Y. 1998, "Specific covalent labeling of recombinant protein molecules inside live cells", *Science*, vol. 281, no. 5374, pp. 269-272.

Gros, D., Jarry-Guichard, T., Ten, V., I, de, M. A., van Kempen, M. J., Davoust, J., Briand, J. P., Moorman, A. F., & Jongsma, H. J. 1994, "Restricted distribution of connexin40, a gap junctional protein, in mammalian heart", *Circ.Res.*, vol. 74, no. 5, pp. 839-851.

Grover, R. & Dhein, S. 2001, "Structure-activity relationships of novel peptides related to the antiarrhythmic peptide AAP10 which reduce the dispersion of epicardial action potential duration", *Peptides*, vol. 22, no. 7, pp. 1011-1021.

Guerrero, P. A., Schuessler, R. B., Davis, L. M., Beyer, E. C., Johnson, C. M., Yamada, K. A., & Saffitz, J. E. 1997, "Slow ventricular conduction in mice heterozygous for a connexin43 null mutation", *J.Clin.Invest*, vol. 99, no. 8, pp. 1991-1998.

Gutstein, D. E., Morley, G. E., Tamaddon, H., Vaidya, D., Schneider, M. D., Chen, J., Chien, K. R., Stuhlmann, H., & Fishman, G. I. 2001, "Conduction slowing and sudden arrhythmic death in mice with cardiac-restricted inactivation of connexin43", *Circ.Res.*, vol. 88, no. 3, pp. 333-339.

Gutstein, D. E., Morley, G. E., Vaidya, D., Liu, F., Chen, F. L., Stuhlmann, H., & Fishman, G. I. 2001, "Heterogeneous expression of Gap junction channels in the heart leads to conduction defects and ventricular dysfunction", *Circulation*, vol. 104, no. 10, pp. 1194-1199.

Haefliger, J. A. & Meda, P. 2000, "Chronic hypertension alters the expression of Cx43 in cardiovascular muscle cells", *Braz.J.Med.Biol.Res.*, vol. 33, no. 4, pp. 431-438.

Haissaguerre, M., Jais, P., Shah, D. C., Takahashi, A., Hocini, M., Quiniou, G., Garrigue, S., Le, M. A., Le, M. P., & Clementy, J. 1998, "Spontaneous initiation of atrial fibrillation by ectopic beats originating in the pulmonary veins", *N.Engl.J.Med.*, vol. 339, no. 10, pp. 659-666.

Halestrap, A. P., Clarke, S. J., & Javadov, S. A. 2004, "Mitochondrial permeability transition pore opening during myocardial reperfusion--a target for cardioprotection", *Cardiovasc.Res.*, vol. 61, no. 3, pp. 372-385.

Hall, D. G., Morley, G. E., Vaidya, D., Ard, M., Kimball, T. R., Witt, S. A., & Colbert, M. C. 2000, "Early onset heart failure in transgenic mice with dilated cardiomyopathy", *Pediatr.Res.*, vol. 48, no. 1, pp. 36-42.

Harris, A. L. 2001, "Emerging issues of connexin channels: biophysics fills the gap", *Q.Rev.Biophys.*, vol. 34, no. 3, pp. 325-472.

Haugan, K., Olsen, K. B., Hartvig, L., Petersen, J. S., Holstein-Rathlou, N. H., Hennan, J. K., & Nielsen, M. S. 2005, "The antiarrhythmic peptide analog ZP123 prevents atrial conduction slowing during metabolic stress", *J.Cardiovasc.Electrophysiol.*, vol. 16, no. 5, pp. 537-545.

Hennan, J. K., Swillo, R. E., Morgan, G. A., Keith, J. C., Jr., Schaub, R. G., Smith, R. P., Feldman, H. S., Haugan, K., Kantrowitz, J., Wang, P. J., bu-Qare, A., Butera, J., Larsen, B. D., & Crandall, D. L. 2006, "Rotigaptide (ZP123) prevents spontaneous ventricular arrhythmias and reduces infarct size during myocardial ischemia/reperfusion injury in open-chest dogs", *J.Pharmacol.Exp.Ther.*, vol. 317, no. 1, pp. 236-243.

Hernandez, J. & Ribeiro, J. A. 1996, "Excitatory actions of adenosine on ventricular automaticity", *Trends Pharmacol.Sci.*, vol. 17, no. 4, pp. 141-144.

Hernandez, O. M., Discher, D. J., Bishopric, N. H., & Webster, K. A. 2000, "Rapid activation of neutral sphingomyelinase by hypoxia-reoxygenation of cardiac myocytes", *Circ.Res.*, vol. 86, no. 2, pp. 198-204.

Hertlein, B., Butterweck, A., Haubrich, S., Willecke, K., & Traub, O. 1998, "Phosphorylated carboxy terminal serine residues stabilize the mouse gap junction protein connexin45 against degradation", *J.Membr.Biol.*, vol. 162, no. 3, pp. 247-257.

Heusch, G. 1998, "Hibernating myocardium", *Physiol Rev.*, vol. 78, no. 4, pp. 1055-1085.

Hill, C. E., Rummery, N., Hickey, H., & Sandow, S. L. 2002, "Heterogeneity in the distribution of vascular gap junctions and connexins: implications for function", *Clin.Exp.Pharmacol.Physiol*, vol. 29, no. 7, pp. 620-625.

Hirschi, K. K., Minnich, B. N., Moore, L. K., & Burt, J. M. 1993, "Oleic acid differentially affects gap junction-mediated communication in heart and vascular smooth muscle cells", *Am.J.Physiol*, vol. 265, no. 6 Pt 1, p. C1517-C1526.

Hoh, J. H., John, S. A., & Revel, J. P. 1991, "Molecular cloning and characterization of a new member of the gap junction gene family, connexin-31", *J.Biol.Chem.*, vol. 266, no. 10, pp. 6524-6531.

Honjo, H., Boyett, M. R., Coppen, S. R., Takagishi, Y., Opthof, T., Severs, N. J., & Kodama, I. 2002, "Heterogeneous expression of connexins in rabbit sinoatrial node cells: correlation between connexin isotype and cell size", *Cardiovasc.Res.*, vol. 53, no. 1, pp. 89-96.

Hu, X. & Dahl, G. 1999, "Exchange of conductance and gating properties between gap junction hemichannels", *FEBS Lett.*, vol. 451, no. 2, pp. 113-117.

Hurtley, S. M. & Helenius, A. 1989, "Protein oligomerization in the endoplasmic reticulum", *Annu.Rev.Cell Biol.*, vol. 5, pp. 277-307.

Hwan, S. K. & Beyer, E. C. 2000, "Heterogeneous localization of connexin40 in the renal vasculature", *Microvasc.Res.*, vol. 59, no. 1, pp. 140-148.

Isakson, B. E., Evans, W. H., & Boitano, S. 2001, "Intercellular Ca2+ signaling in alveolar epithelial cells through gap junctions and by extracellular ATP", *Am.J.Physiol Lung Cell Mol.Physiol*, vol. 280, no. 2, p. L221-L228.

Jalife, J. 2003, "Rotors and spiral waves in atrial fibrillation", *J.Cardiovasc.Electrophysiol.*, vol. 14, no. 7, pp. 776-780.

John, S., Cesario, D., & Weiss, J. N. 2003, "Gap junctional hemichannels in the heart", *Acta Physiol Scand.*, vol. 179, no. 1, pp. 23-31.

John, S. A., Kondo, R., Wang, S. Y., Goldhaber, J. I., & Weiss, J. N. 1999, "Connexin-43 hemichannels opened by metabolic inhibition", *J.Biol.Chem.*, vol. 274, no. 1, pp. 236-240.

Johnson, R. G., Meyer, R. A., Li, X. R., Preus, D. M., Tan, L., Grunenwald, H., Paulson, A. F., Laird, D. W., & Sheridan, J. D. 2002, "Gap junctions assemble in the presence of cytoskeletal inhibitors, but enhanced assembly requires microtubules", *Exp.Cell Res.*, vol. 275, no. 1, pp. 67-80.

Jongsma, H. J. & Wilders, R. 2000, "Gap junctions in cardiovascular disease", *Circ.Res.*, vol. 86, no. 12, pp. 1193-1197.

Jordan, K., Chodock, R., Hand, A. R., & Laird, D. W. 2001, "The origin of annular junctions: a mechanism of gap junction internalization", *J Cell Sci.*, vol. 114, no. Pt 4, pp. 763-773.

Jordan, K., Solan, J. L., Dominguez, M., Sia, M., Hand, A., Lampe, P. D., & Laird, D. W. 1999, "Trafficking, assembly, and function of a connexin43-green fluorescent protein chimera in live mammalian cells", *Mol.Biol.Cell*, vol. 10, no. 6, pp. 2033-2050.

Jung, F., Palmer, L. A., Zhou, N., & Johns, R. A. 2000, "Hypoxic regulation of inducible nitric oxide synthase via hypoxia inducible factor-1 in cardiac myocytes", *Circ.Res.*, vol. 86, no. 3, pp. 319-325.

Kaba, R. A., Coppen, S. R., Dupont, E., Skepper, J. N., Elneil, S., Haw, M. P., Pepper, J. R., Yacoub, M. H., Rothery, S., & Severs, N. J. 2001, "Comparison of connexin 43, 40 and 45 expression patterns in the developing human and mouse hearts", *Cell Commun.Adhes.*, vol. 8, no. 4-6, pp. 339-343.

Kallio, P. J., Wilson, W. J., O'Brien, S., Makino, Y., & Poellinger, L. 1999, "Regulation of the hypoxia-inducible transcription factor 1alpha by the ubiquitin-proteasome pathway", *J.Biol.Chem.*, vol. 274, no. 10, pp. 6519-6525.

Kanno, S., Kovacs, A., Yamada, K. A., & Saffitz, J. E. 2003, "Connexin43 as a determinant of myocardial infarct size following coronary occlusion in mice", *J.Am.Coll.Cardiol.*, vol. 41, no. 4, pp. 681-686.

Kaprielian, R. R., Gunning, M., Dupont, E., Sheppard, M. N., Rothery, S. M., Underwood, R., Pennell, D. J., Fox, K., Pepper, J., Poole-Wilson, P. A., & Severs, N. J. 1998, "Downregulation of immunodetectable connexin43 and decreased gap junction size in the pathogenesis of chronic hibernation in the human left ventricle", *Circulation*, vol. 97, no. 7, pp. 651-660.

Keeley, E. C., Boura, J. A., & Grines, C. L. 2003, "Primary angioplasty versus intravenous thrombolytic therapy for acute myocardial infarction: a quantitative review of 23 randomised trials", *Lancet*, vol. 361, no. 9351, pp. 13-20.

Kelsell, D. P., Dunlop, J., Stevens, H. P., Lench, N. J., Liang, J. N., Parry, G., Mueller, R. F., & Leigh, I. M. 1997, "Connexin 26 mutations in hereditary non-syndromic sensorineural deafness", *Nature*, vol. 387, no. 6628, pp. 80-83.

King, T. J. & Lampe, P. D. 2005, "Temporal regulation of connexin phosphorylation in embryonic and adult tissues", *Biochim.Biophys.Acta*, vol. 1719, no. 1-2, pp. 24-35.

Kirchhoff, F., Dringen, R., & Giaume, C. 2001, "Pathways of neuron-astrocyte interactions and their possible role in neuroprotection", *Eur.Arch.Psychiatry Clin.Neurosci.*, vol. 251, no. 4, pp. 159-169.

Kjolbye, A. L., Knudsen, C. B., Jepsen, T., Larsen, B. D., & Petersen, J. S. 2003, "Pharmacological characterization of the new stable antiarrhythmic peptide analog Ac-D-Tyr-D-Pro-D-Hyp-Gly-D-Ala-Gly-NH2 (ZP123): in vivo and in vitro studies", *J.Pharmacol.Exp.Ther.*, vol. 306, no. 3, pp. 1191-1199.

Kleber, A. G. & Rudy, Y. 2004, "Basic mechanisms of cardiac impulse propagation and associated arrhythmias", *Physiol Rev.*, vol. 84, no. 2, pp. 431-488.

Klenow, H. & Henningsen, I. 1970, "Selective elimination of the exonuclease activity of the deoxyribonucleic acid polymerase from Escherichia coli B by limited proteolysis", *Proc.Natl.Acad.Sci.U.S.A*, vol. 65, no. 1, pp. 168-175.

Ko, Y. S., Coppen, S. R., Dupont, E., Rothery, S., & Severs, N. J. 2001, "Regional differentiation of desmin, connexin43, and connexin45 expression patterns in rat aortic smooth muscle", *Arterioscler.Thromb.Vasc.Biol.*, vol. 21, no. 3, pp. 355-364.

Kohama, Y., Kawahara, Y., Okabe, M., Mimura, T., & Aonuma, S. 1985, "Determination of immunoreactive antiarrhythmic peptide (AAP) in rats", *J.Pharmacobiodyn.*, vol. 8, no. 12, pp. 1024-1031.

Kohama, Y., Okimoto, N., Mimura, T., Fukaya, C., Watanabe, M., & Yokoyama, K. 1987, "A new antiarrhythmic peptide, N-3-(4-hydroxyphenyl)propionyl Pro-Hyp-Gly-Ala-Gly", *Chem.Pharm.Bull.(Tokyo)*, vol. 35, no. 9, pp. 3928-3930.

Kondo, R. P., Wang, S. Y., John, S. A., Weiss, J. N., & Goldhaber, J. I. 2000, "Metabolic inhibition activates a non-selective current through connexin hemichannels in isolated ventricular myocytes", *J.Mol.Cell Cardiol.*, vol. 32, no. 10, pp. 1859-1872.

Kostin, S., Rieger, M., Dammer, S., Hein, S., Richter, M., Klovekorn, W. P., Bauer, E. P., & Schaper, J. 2003, "Gap junction remodeling and altered connexin43 expression in the failing human heart", *Mol.Cell Biochem.*, vol. 242, no. 1-2, pp. 135-144.

Kostin, S., Klein, G., Szalay, Z., Hein, S., Bauer, E. P., & Schaper, J. 2002, "Structural correlate of atrial fibrillation in human patients", *Cardiovasc.Res.*, vol. 54, no. 2, pp. 361-379.

Kronengold, J., Trexler, E. B., Bukauskas, F. F., Bargiello, T. A., & Verselis, V. K. 2003, "Pore-lining residues identified by single channel SCAM studies in Cx46 hemichannels", *Cell Commun.Adhes.*, vol. 10, no. 4-6, pp. 193-199.

Kronengold, J., Trexler, E. B., Bukauskas, F. F., Bargiello, T. A., & Verselis, V. K. 2003, "Single-channel SCAM identifies pore-lining residues in the first extracellular loop and first transmembrane domains of Cx46 hemichannels", *J.Gen.Physiol*, vol. 122, no. 4, pp. 389-405.

Kwak, B. R., Mulhaupt, F., Veillard, N., Gros, D. B., & Mach, F. 2002, "Altered pattern of vascular connexin expression in atherosclerotic plaques", *Arterioscler.Thromb.Vasc.Biol.*, vol. 22, no. 2, pp. 225-230.

Kwak, B. R., van Kempen, M. J., Theveniau-Ruissy, M., Gros, D. B., & Jongsma, H. J. 1999, "Connexin expression in cultured neonatal rat myocytes reflects the pattern of the intact ventricle", *Cardiovasc.Res.*, vol. 44, no. 2, pp. 370-380.

Kwak, B. R. & Jongsma, H. J. 1996, "Regulation of cardiac gap junction channel permeability and conductance by several phosphorylating conditions", *Mol.Cell Biochem.*, vol. 157, no. 1-2, pp. 93-99.

Kwak, B. R., Saez, J. C., Wilders, R., Chanson, M., Fishman, G. I., Hertzberg, E. L., Spray, D. C., & Jongsma, H. J. 1995, "Effects of cGMP-dependent phosphorylation on rat and human connexin43 gap junction channels", *Pflugers Arch.*, vol. 430, no. 5, pp. 770-778.

Kwak, B. R., van Veen, T. A., Analbers, L. J., & Jongsma, H. J. 1995, "TPA increases conductance but decreases permeability in neonatal rat cardiomyocyte gap junction channels", *Exp.Cell Res.*, vol. 220, no. 2, pp. 456-463.

Laemmli, U. K. 1970, "Cleavage of structural proteins during the assembly of the head of bacteriophage T4", *Nature*, vol. 227, no. 5259, pp. 680-685.

Lai, A., Le, D. N., Paznekas, W. A., Gifford, W. D., Jabs, E. W., & Charles, A. C. 2006, "Oculodentodigital dysplasia connexin43 mutations result in non-functional connexin hemichannels and gap junctions in C6 glioma cells", *J.Cell Sci.*, vol. 119, no. Pt 3, pp. 532-541.

Laing, J. G., Tadros, P. N., Westphale, E. M., & Beyer, E. C. 1997, "Degradation of connexin43 gap junctions involves both the proteasome and the lysosome", *Exp.Cell Res.*, vol. 236, no. 2, pp. 482-492.

Laird, D. W. 2006, "Life cycle of connexins in health and disease", *Biochem.J.*, vol. 394, no. Pt 3, pp. 527-543.

Laird, D. W. 2005, "Connexin phosphorylation as a regulatory event linked to gap junction internalization and degradation", *Biochim.Biophys.Acta*, vol. 1711, no. 2, pp. 172-182.

Laird, D. W., Castillo, M., & Kasprzak, L. 1995, "Gap junction turnover, intracellular trafficking, and phosphorylation of connexin43 in brefeldin A-treated rat mammary tumor cells", *J.Cell Biol.*, vol. 131, no. 5, pp. 1193-1203.

Laird, D. W., Puranam, K. L., & Revel, J. P. 1991, "Turnover and phosphorylation dynamics of connexin43 gap junction protein in cultured cardiac myocytes", *Biochem.J.*, vol. 273(Pt 1), pp. 67-72.

Lampe, P. D. & Lau, A. F. 2004, "The effects of connexin phosphorylation on gap junctional communication", *Int.J.Biochem.Cell Biol.*, vol. 36, no. 7, pp. 1171-1186.

Lampe, P. D. & Lau, A. F. 2000, "Regulation of gap junctions by phosphorylation of connexins", *Arch.Biochem.Biophys.*, vol. 384, no. 2, pp. 205-215.

Lampe, P. D., TenBroek, E. M., Burt, J. M., Kurata, W. E., Johnson, R. G., & Lau, A. F. 2000, "Phosphorylation of connexin43 on serine368 by protein kinase C regulates gap junctional communication", *J.Cell Biol.*, vol. 149, no. 7, pp. 1503-1512.

Lampe, P. D., Kurata, W. E., Warn-Cramer, B. J., & Lau, A. F. 1998, "Formation of a distinct connexin43 phosphoisoform in mitotic cells is dependent upon p34cdc2 kinase", *J.Cell Sci.*, vol. 111 (Pt 6), pp. 833-841.

Lau, A. F., Hatch-Pigott, V., & Crow, D. S. 1991, "Evidence that heart connexin43 is a phosphoprotein", *J.Mol.Cell Cardiol.*, vol. 23, no. 6, pp. 659-663.

Lauf, U., Giepmans, B. N., Lopez, P., Braconnot, S., Chen, S. C., & Falk, M. M. 2002, "Dynamic trafficking and delivery of connexons to the plasma membrane and accretion to gap junctions in living cells", *Proc.Natl.Acad.Sci.U.S.A*, vol. 99, no. 16, pp. 10446-10451.

Lauf, U., Lopez, P., & Falk, M. M. 2001, "Expression of fluorescently tagged connexins: a novel approach to rescue function of oligomeric DsRed-tagged proteins", *FEBS Lett.*, vol. 498, no. 1, pp. 11-15.

Lawrence, T. S., Beers, W. H., & Gilula, N. B. 1978, "Transmission of hormonal stimulation by cell-to-cell communication", *Nature*, vol. 272, no. 5653, pp. 501-506.

Lazarowski, E. R., Boucher, R. C., & Harden, T. K. 2003, "Mechanisms of release of nucleotides and integration of their action as P2X- and P2Y-receptor activating molecules", *Mol.Pharmacol.*, vol. 64, no. 4, pp. 785-795.

Lerner, D. L., Yamada, K. A., Schuessler, R. B., & Saffitz, J. E. 2000, "Accelerated onset and increased incidence of ventricular arrhythmias induced by ischemia in Cx43-deficient mice", *Circulation*, vol. 101, no. 5, pp. 547-552.

Leybaert, L., Braet, K., Vandamme, W., Cabooter, L., Martin, P. E., & Evans, W. H. 2003, "Connexin channels, connexin mimetic peptides and ATP release", *Cell Commun.Adhes.*, vol. 10, no. 4-6, pp. 251-257.

Leybaert, L. & Sanderson, M. J. 2001, "Intercellular calcium signaling and flash photolysis of caged compounds. A sensitive method to evaluate gap junctional coupling", *Methods Mol.Biol.*, vol. 154, pp. 407-430.

Li, H., Liu, T. F., Lazrak, A., Peracchia, C., Goldberg, G. S., Lampe, P. D., & Johnson, R. G. 1996, "Properties and regulation of gap junctional hemichannels in the plasma membranes of cultured cells", *J.Cell Biol.*, vol. 134, no. 4, pp. 1019-1030.

Li, W. E. & Nagy, J. I. 2000, "Connexin43 phosphorylation state and intercellular communication in cultured astrocytes following hypoxia and protein phosphatase inhibition", *Eur.J.Neurosci.*, vol. 12, no. 7, pp. 2644-2650.

Liang, G. S., de, M. M., Gomez-Hernandez, J. M., Glass, J. D., Scherer, S. S., Mintz, M., Barrio, L. C., & Fischbeck, K. H. 2005, "Severe neuropathy with leaky connexin32 hemichannels", *Ann.Neurol.*, vol. 57, no. 5, pp. 749-754.

Lin, L. C., Wu, C. C., Yeh, H. I., Lu, L. S., Liu, Y. B., Lin, S. F., & Lee, Y. T. 2005, "Downregulated myocardial connexin 43 and suppressed contractility in rabbits subjected to a cholesterol-enriched diet", *Lab Invest*, vol. 85, no. 10, pp. 1224-1237.

Lin, R., Warn-Cramer, B. J., Kurata, W. E., & Lau, A. F. 2001, "v-Src phosphorylation of connexin 43 on Tyr247 and Tyr265 disrupts gap junctional communication", *J.Cell Biol.*, vol. 154, no. 4, pp. 815-827.

Little, T. L., Beyer, E. C., & Duling, B. R. 1995, "Connexin 43 and connexin 40 gap junctional proteins are present in arteriolar smooth muscle and endothelium in vivo", *Am.J.Physiol*, vol. 268, no. 2 Pt 2, p. H729-H739.

Litvin, O., Tiunova, A., Connell-Alberts, Y., Panchin, Y., & Baranova, A. 2006, "What is hidden in the pannexin treasure trove: the sneak peek and the guesswork", *J.Cell Mol.Med.*, vol. 10, no. 3, pp. 613-634.

Locke, D., Liu, J., & Harris, A. L. 2005, "Lipid rafts prepared by different methods contain different connexin channels, but gap junctions are not lipid rafts", *Biochemistry*, vol. 44, no. 39, pp. 13027-13042.

Loddenkemper, T., Grote, K., Evers, S., Oelerich, M., & Stogbauer, F. 2002, "Neurological manifestations of the oculodentodigital dysplasia syndrome", *J.Neurol.*, vol. 249, no. 5, pp. 584-595.

Loewenstein, W. R. 1981, "Junctional intercellular communication: the cell-to-cell membrane channel", *Physiol Rev.*, vol. 61, no. 4, pp. 829-913.

Lowry, O. H., Rosebrough, N. J., Farr, A. L., & Randall, R. J. 1951, "Protein measurement with the Folin phenol reagent", *J.Biol.Chem.*, vol. 193, no. 1, pp. 265-275.

Luke, R. A. & Saffitz, J. E. 1991, "Remodeling of ventricular conduction pathways in healed canine infarct border zones", *J.Clin.Invest*, vol. 87, no. 5, pp. 1594-1602.

Makowski, L., Caspar, D. L., Phillips, W. C., & Goodenough, D. A. 1977, "Gap junction structures. II. Analysis of the x-ray diffraction data", *J.Cell Biol.*, vol. 74, no. 2, pp. 629-645.

Malchow, R. P., Qian, H., & Ripps, H. 1993, "Evidence for hemi-gap junctional channels in isolated horizontal cells of the skate retina", *J.Neurosci.Res.*, vol. 35, no. 3, pp. 237-245.

Martin, P. E. & Evans, W. H. 2004, "Incorporation of connexins into plasma membranes and gap junctions", *Cardiovasc.Res.*, vol. 62, no. 2, pp. 378-387.

Martin, P. E., Hill, N. S., Kristensen, B., Errington, R. J., & Rachael, J. T. 2004, "Ouabain exerts biphasic effects on connexin functionality and expression in vascular smooth muscle cells", *Br.J.Pharmacol.*, vol. 141, no. 2, pp. 374-384.

Martin, P. E., Blundell, G., Ahmad, S., Errington, R. J., & Evans, W. H. 2001, "Multiple pathways in the trafficking and assembly of connexin 26, 32 and 43 into gap junction intercellular communication channels", *J.Cell Sci.*, vol. 114, no. Pt 21, pp. 3845-3855.

Martin, P. E., Errington, R. J., & Evans, W. H. 2001, "Gap junction assembly: multiple connexin fluorophores identify complex trafficking pathways", *Cell Commun.Adhes.*, vol. 8, no. 4-6, pp. 243-248.

Martin, P. E., Mambetisaeva, E. T., Archer, D. A., George, C. H., & Evans, W. H. 2000, "Analysis of gap junction assembly using mutated connexins detected in Charcot-Marie-Tooth X-linked disease", *J.Neurochem.*, vol. 74, no. 2, pp. 711-720.

Martin, P. E., Steggles, J., Wilson, C., Ahmad, S., & Evans, W. H. 2000, "Targeting motifs and functional parameters governing the assembly of connexins into gap junctions", *Biochem.J.*, vol. 349, no. Pt 1, pp. 281-287.

Martin, P. E., Coleman, S. L., Casalotti, S. O., Forge, A., & Evans, W. H. 1999, "Properties of connexin26 gap junctional proteins derived from mutations associated with non-syndromal heriditary deafness", *Hum.Mol.Genet.*, vol. 8, no. 13, pp. 2369-2376.

Martin, P. E., George, C. H., Castro, C., Kendall, J. M., Capel, J., Campbell, A. K., Revilla, A., Barrio, L. C., & Evans, W. H. 1998, "Assembly of chimeric connexin-aequorin proteins into functional gap junction channels. Reporting intracellular and plasma membrane calcium environments", *J.Biol.Chem.*, vol. 273, no. 3, pp. 1719-1726.

Milks, L. C., Kumar, N. M., Houghten, R., Unwin, N., & Gilula, N. B. 1988, "Topology of the 32-kd liver gap junction protein determined by site-directed antibody localizations", *EMBO J.*, vol. 7, no. 10, pp. 2967-2975.

Mizuguchi, H. & Kay, M. A. 1998, "Efficient construction of a recombinant adenovirus vector by an improved in vitro ligation method", *Hum.Gene Ther.*, vol. 9, no. 17, pp. 2577-2583.

Moreno, A. P. 2005, "Connexin phosphorylation as a regulatory event linked to channel gating", *Biochim.Biophys.Acta*, vol. 1711, no. 2, pp. 164-171.

Moreno, A. P., Laing, J. G., Beyer, E. C., & Spray, D. C. 1995, "Properties of gap junction channels formed of connexin 45 endogenously expressed in human hepatoma (SKHep1) cells", *Am.J.Physiol*, vol. 268, no. 2 Pt 1, p. C356-C365.

Moreno, A. P., Saez, J. C., Fishman, G. I., & Spray, D. C. 1994, "Human connexin43 gap junction channels. Regulation of unitary conductances by phosphorylation", *Circ.Res.*, vol. 74, no. 6, pp. 1050-1057.

Morley, G. E., Taffet, S. M., & Delmar, M. 1996, "Intramolecular interactions mediate pH regulation of connexin43 channels", *Biophys.J.*, vol. 70, no. 3, pp. 1294-1302.

Muller, A., Gottwald, M., Tudyka, T., Linke, W., Klaus, W., & Dhein, S. 1997, "Increase in gap junction conductance by an antiarrhythmic peptide", *Eur.J.Pharmacol.*, vol. 327, no. 1, pp. 65-72.

Muller, A., Schaefer, T., Linke, W., Tudyka, T., Gottwald, M., Klaus, W., & Dhein, S. 1997, "Actions of the antiarrhythmic peptide AAP10 on intercellular coupling", *Naunyn Schmiedebergs Arch.Pharmacol.*, vol. 356, no. 1, pp. 76-82.

Munster, P. N. & Weingart, R. 1993, "Effects of phorbol ester on gap junctions of neonatal rat heart cells", *Pflugers Arch.*, vol. 423, no. 3-4, pp. 181-188.

Murphy, E. 2004, "Primary and secondary signaling pathways in early preconditioning that converge on the mitochondria to produce cardioprotection", *Circ.Res.*, vol. 94, no. 1, pp. 7-16.

Musil, L. S. & Goodenough, D. A. 1993, "Multisubunit assembly of an integral plasma membrane channel protein, gap junction connexin43, occurs after exit from the ER", *Cell*, vol. 74, no. 6, pp. 1065-1077.

Musil, L. S., Beyer, E. C., & Goodenough, D. A. 1990, "Expression of the gap junction protein connexin43 in embryonic chick lens: molecular cloning, ultrastructural localization, and post-translational phosphorylation", *J.Membr.Biol.*, vol. 116, no. 2, pp. 163-175.

Nao, T., Ohkusa, T., Hisamatsu, Y., Inoue, N., Matsumoto, T., Yamada, J., Shimizu, A., Yoshiga, Y., Yamagata, T., Kobayashi, S., Yano, M., Hamano, K., & Matsuzaki, M. 2003, "Comparison of expression of connexin in right atrial myocardium in patients with chronic atrial fibrillation versus those in sinus rhythm", *Am.J.Cardiol.*, vol. 91, no. 6, pp. 678-683.

Nelis, E., Haites, N., & Van, B. C. 1999, "Mutations in the peripheral myelin genes and associated genes in inherited peripheral neuropathies", *Hum.Mutat.*, vol. 13, no. 1, pp. 11-28.

Nicholson, B. J., Weber, P. A., Cao, F., Chang, H., Lampe, P., & Goldberg, G. 2000, "The molecular basis of selective permeability of connexins is complex and includes both size and charge", *Braz.J.Med.Biol.Res.*, vol. 33, no. 4, pp. 369-378.

Niessen, H., Harz, H., Bedner, P., Kramer, K., & Willecke, K. 2000, "Selective permeability of different connexin channels to the second messenger inositol 1,4,5-trisphosphate", *J.Cell Sci.*, vol. 113 (Pt 8), pp. 1365-1372.

Nishii, K., Kumai, M., & Shibata, Y. 2001, "Regulation of the epithelial-mesenchymal transformation through gap junction channels in heart development", *Trends Cardiovasc.Med.*, vol. 11, no. 6, pp. 213-218.

North, R. A. 2002, "Molecular physiology of P2X receptors", *Physiol Rev.*, vol. 82, no. 4, pp. 1013-1067.

Oh, S., Ri, Y., Bennett, M. V., Trexler, E. B., Verselis, V. K., & Bargiello, T. A. 1997, "Changes in permeability caused by connexin 32 mutations underlie X-linked Charcot-Marie-Tooth disease", *Neuron*, vol. 19, no. 4, pp. 927-938.

Okada, S. F., Nicholas, R. A., Kreda, S. M., Lazarowski, E. R., & Boucher, R. C. 2006, "Physiological regulation of ATP release at the apical surface of human airway epithelia", *J.Biol.Chem.*, vol. 281, no. 32, pp. 22992-23002.

Oviedo-Orta, E. & Evans, W.H. 2004, "Gap junctions and connexin-mediated communication in the immune system", *Biochim.Biophys.Acta*, vol. 1662, no. 1-2, pp. 102-112.

Paemeleire, K., Martin, P. E., Coleman, S. L., Fogarty, K. E., Carrington, W. A., Leybaert, L., Tuft, R. A., Evans, W. H., & Sanderson, M. J. 2000, "Intercellular calcium waves in HeLa cells expressing GFP-labeled connexin 43, 32, or 26", *Mol.Biol.Cell*, vol. 11, no. 5, pp. 1815-1827.

Pal, J. D., Liu, X., Mackay, D., Shiels, A., Berthoud, V. M., Beyer, E. C., & Ebihara, L. 2000, "Connexin46 mutations linked to congenital cataract show loss of gap junction channel function", *Am.J.Physiol Cell Physiol*, vol. 279, no. 3, p. C596-C602.

Parpura, V., Scemes, E., & Spray, D. C. 2004, "Mechanisms of glutamate release from astrocytes: gap junction "hemichannels", purinergic receptors and exocytotic release", *Neurochem.Int.*, vol. 45, no. 2-3, pp. 259-264.

Paul, D. L. 1986, "Molecular cloning of cDNA for rat liver gap junction protein", *J.Cell Biol.*, vol. 103, no. 1, pp. 123-134.

Paulson, A. F., Lampe, P. D., Meyer, R. A., TenBroek, E., Atkinson, M. M., Walseth, T. F., & Johnson, R. G. 2000, "Cyclic AMP and LDL trigger a rapid enhancement in gap junction assembly through a stimulation of connexin trafficking", *J.Cell Sci.*, vol. 113 (Pt 17), pp. 3037-3049.

Paznekas, W. A., Boyadjiev, S. A., Shapiro, R. E., Daniels, O., Wollnik, B., Keegan, C. E., Innis, J. W., Dinulos, M. B., Christian, C., Hannibal, M. C., & Jabs, E. W. 2003, "Connexin 43 (GJA1) mutations cause the pleiotropic phenotype of oculodentodigital dysplasia", *Am.J.Hum.Genet.*, vol. 72, no. 2, pp. 408-418.

Pearson, R. A., Dale, N., Llaudet, E., & Mobbs, P. 2005, "ATP released via gap junction hemichannels from the pigment epithelium regulates neural retinal progenitor proliferation", *Neuron*, vol. 46, no. 5, pp. 731-744.

Peracchia, C., Wang, X. G., & Peracchia, L. L. 1999, "Is the chemical gate of connexins voltage sensitive? Behavior of Cx32 wild-type and mutant channels", *Am.J.Physiol*, vol. 276, no. 6 Pt 1, p. C1361-C1373.

Perkins, G. A., Goodenough, D. A., & Sosinsky, G. E. 1998, "Formation of the gap junction intercellular channel requires a 30 degree rotation for interdigitating two apposing connexons", *J.Mol.Biol.*, vol. 277, no. 2, pp. 171-177.

Peters, N. S., Coromilas, J., Severs, N. J., & Wit, A. L. 1997, "Disturbed connexin43 gap junction distribution correlates with the location of reentrant circuits in the epicardial border zone of healing canine infarcts that cause ventricular tachycardia", *Circulation*, vol. 95, no. 4, pp. 988-996.

Peters, N. S., Severs, N. J., Rothery, S. M., Lincoln, C., Yacoub, M. H., & Green, C. R. 1994, "Spatiotemporal relation between gap junctions and fascia adherens junctions during postnatal development of human ventricular myocardium", *Circulation*, vol. 90, no. 2, pp. 713-725.

Peters, N. S., Green, C. R., Poole-Wilson, P. A., & Severs, N. J. 1993, "Reduced content of connexin43 gap junctions in ventricular myocardium from hypertrophied and ischemic human hearts", *Circulation*, vol. 88, no. 3, pp. 864-875.

Pfahnl, A. & Dahl, G. 1999, "Gating of cx46 gap junction hemichannels by calcium and voltage", *Pflugers Arch.*, vol. 437, no. 3, pp. 345-353.

Pfahnl, A. & Dahl, G. 1998, "Localization of a voltage gate in connexin46 gap junction hemichannels", *Biophys.J.*, vol. 75, no. 5, pp. 2323-2331.

Phelan, P. 2005, "Innexins: members of an evolutionarily conserved family of gap-junction proteins", *Biochim.Biophys.Acta*, vol. 1711, no. 2, pp. 225-245.

Poindexter, B. J., Smith, J. R., Buja, L. M., & Bick, R. J. 2001, "Calcium signaling mechanisms in dedifferentiated cardiac myocytes: comparison with neonatal and adult cardiomyocytes", *Cell Calcium*, vol. 30, no. 6, pp. 373-382.

Pol, A., Ortega, D., & Enrich, C. 1997, "Identification and distribution of proteins in isolated endosomal fractions of rat liver: involvement in endocytosis, recycling and transcytosis", *Biochem.J*, vol. 323 (Pt 2), pp. 435-443.

Polontchouk, L., Haefliger, J. A., Ebelt, B., Schaefer, T., Stuhlmann, D., Mehlhorn, U., Kuhn-Regnier, F., De Vivie, E. R., & Dhein, S. 2001, "Effects of chronic atrial fibrillation on gap junction distribution in human and rat atria", *J.Am.Coll.Cardiol.*, vol. 38, no. 3, pp. 883-891.

Puljung, M. C., Berthoud, V. M., Beyer, E. C., & Hanck, D. A. 2004, "Polyvalent cations constitute the voltage gating particle in human connexin37 hemichannels", *J.Gen.Physiol*, vol. 124, no. 5, pp. 587-603.

Qu, Y. & Dahl, G. 2002, "Function of the voltage gate of gap junction channels: selective exclusion of molecules", *Proc.Natl.Acad.Sci.U.S.A*, vol. 99, no. 2, pp. 697-702.

Quist, A. P., Rhee, S. K., Lin, H., & Lal, R. 2000, "Physiological role of gap-junctional hemichannels. Extracellular calcium-dependent isosmotic volume regulation", *J.Cell Biol.*, vol. 148, no. 5, pp. 1063-1074.

Rahman, S. & Evans, W. H. 1991, "Topography of connexin32 in rat liver gap junctions. Evidence for an intramolecular disulphide linkage connecting the two extracellular peptide loops", *J.Cell Sci.*, vol. 100 (Pt 3), pp. 567-578.

Reaume, A. G., De Sousa, P. A., Kulkarni, S., Langille, B. L., Zhu, D., Davies, T. C., Juneja, S. C., Kidder, G. M., & Rossant, J. 1995, "Cardiac malformation in neonatal mice lacking connexin43", *Science*, vol. 267, no. 5205, pp. 1831-1834.

Reed, K. E., Westphale, E. M., Larson, D. M., Wang, H. Z., Veenstra, R. D., & Beyer, E. C. 1993, "Molecular cloning and functional expression of human connexin37, an endothelial cell gap junction protein", *J.Clin.Invest*, vol. 91, no. 3, pp. 997-1004.

Retamal, M. A., Cortes, C. J., Reuss, L., Bennett, M. V., & Saez, J. C. 2006, "S-nitrosylation and permeation through connexin 43 hemichannels in astrocytes: induction by oxidant stress and reversal by reducing agents", *Proc.Natl.Acad.Sci.U.S.A*, vol. 103, no. 12, pp. 4475-4480.

Revel, J. P. & Karnovsky, M. J. 1967, "Hexagonal array of subunits in intercellular junctions of the mouse heart and liver", *J.Cell Biol.*, vol. 33, no. 3, p. C7-C12.

Reynhout, J. K., Lampe, P. D., & Johnson, R. G. 1992, "An activator of protein kinase C inhibits gap junction communication between cultured bovine lens cells", *Exp.Cell Res.*, vol. 198, no. 2, pp. 337-342.

Ripps, H., Qian, H., & Zakevicius, J. 2004, "Properties of connexin26 hemichannels expressed in Xenopus oocytes", *Cell Mol.Neurobiol.*, vol. 24, no. 5, pp. 647-665.

Rivard, A., Berthou-Soulie, L., Principe, N., Kearney, M., Curry, C., Branellec, D., Semenza, G. L., & Isner, J. M. 2000, "Age-dependent defect in vascular endothelial growth factor expression is associated with reduced hypoxia-inducible factor 1 activity", *J.Biol.Chem.*, vol. 275, no. 38, pp. 29643-29647.

Rivedal, E., Mollerup, S., Haugen, A., & Vikhamar, G. 1996, "Modulation of gap junctional intercellular communication by EGF in human kidney epithelial cells", *Carcinogenesis*, vol. 17, no. 11, pp. 2321-2328.

Robertson, J. D., Bodenheimer, T. S., & Stage, D. E. 1963, "The ultrastructure of Mauthner cell synapses and nodes in goldfish brains", *J.Cell Biol.*, vol. 19, pp. 159-199.

Romanello, M., Veronesi, V., & D'Andrea, P. 2003, "Mechanosensitivity and intercellular communication in HOBIT osteoblastic cells: a possible role for gap junction hemichannels", *Biorheology*, vol. 40, no. 1-3, pp. 119-121.

Rose, B. & Loewenstein, W. R. 1976, "Permeability of a cell junction and the local cytoplasmic free ionized calcium concentration: a study with aequorin", *J.Membr.Biol.*, vol. 28, no. 1, pp. 87-119.

Rudy, Y. & Shaw, R. M. 1997, "Cardiac excitation: an interactive process of ion channels and gap junctions", *Adv.Exp.Med.Biol.*, vol. 430, pp. 269-279.

Ruiz-Meana, M., Garcia-Dorado, D., Lane, S., Pina, P., Inserte, J., Mirabet, M., & Soler-Soler, J. 2001, "Persistence of gap junction communication during myocardial ischemia", *Am.J.Physiol Heart Circ.Physiol*, vol. 280, no. 6, p. H2563-H2571.

Ruiz-Meana, M., Garcia-Dorado, D., Hofstaetter, B., Piper, H. M., & Soler-Soler, J. 1999, "Propagation of cardiomyocyte hypercontracture by passage of Na(+) through gap junctions", *Circ.Res.*, vol. 85, no. 3, pp. 280-287.

Rutz, M. L. & Hulser, D. F. 2001, "Supramolecular dynamics of gap junctions", *Eur.J.Cell Biol.*, vol. 80, no. 1, pp. 20-30.

Saez, J. C., Retamal, M. A., Basilio, D., Bukauskas, F. F., & Bennett, M. V. 2005, "Connexin-based gap junction hemichannels: gating mechanisms", *Biochim.Biophys.Acta*, vol. 1711, no. 2, pp. 215-224.

Saez, J. C., Berthoud, V. M., Branes, M. C., Martinez, A. D., & Beyer, E. C. 2003, "Plasma membrane channels formed by connexins: their regulation and functions", *Physiol Rev.*, vol. 83, no. 4, pp. 1359-1400.

Saez, J. C., Martinez, A. D., Branes, M. C., & Gonzalez, H. E. 1998, "Regulation of gap junctions by protein phosphorylation", *Braz.J.Med.Biol.Res.*, vol. 31, no. 5, pp. 593-600.

Saez, J. C., Nairn, A. C., Czernik, A. J., Fishman, G. I., Spray, D. C., & Hertzberg, E. L. 1997, "Phosphorylation of connexin43 and the regulation of neonatal rat cardiac myocyte gap junctions", *J.Mol.Cell Cardiol.*, vol. 29, no. 8, pp. 2131-2145.

Saez, J. C., Nairn, A. C., Czernik, A. J., Spray, D. C., Hertzberg, E. L., Greengard, P., & Bennett, M. V. 1990, "Phosphorylation of connexin 32, a hepatocyte gap-junction protein, by cAMP-dependent protein kinase, protein kinase C and Ca2+/calmodulin-dependent protein kinase II", *Eur.J.Biochem.*, vol. 192, no. 2, pp. 263-273.

Saez, J. C., Connor, J. A., Spray, D. C., & Bennett, M. V. 1989, "Hepatocyte gap junctions are permeable to the second messenger, inositol 1,4,5-trisphosphate, and to calcium ions", *Proc.Natl.Acad.Sci.U.S.A*, vol. 86, no. 8, pp. 2708-2712.

Saffitz, J. E. 2000, "Regulation of intercellular coupling in acute and chronic heart disease", *Braz.J.Med.Biol.Res.*, vol. 33, no. 4, pp. 407-413.

Saffitz, J. E. & Yamada, K. A. 1998, "Do alterations in intercellular coupling play a role in cardiac contractile dysfunction?", *Circulation*, vol. 97, no. 7, pp. 630-632.

Saiki, R. K., Gelfand, D. H., Stoffel, S., Scharf, S. J., Higuchi, R., Horn, G. T., Mullis, K. B., & Erlich, H. A. 1988, "Primer-directed enzymatic amplification of DNA with a thermostable DNA polymerase", *Science*, vol. 239, no. 4839, pp. 487-491.

Salameh, A. & Dhein, S. 2005, "Pharmacology of gap junctions. New pharmacological targets for treatment of arrhythmia, seizure and cancer?", *Biochim.Biophys.Acta*, vol. 1719, no. 1-2, pp. 36-58.

Sala-Newby, G. B., Freeman, N. V., Skladanowski, A. C., & Newby, A. C. 2000, "Distinct roles for recombinant cytosolic 5'-nucleotidase-I and -II in AMP and IMP catabolism in COS-7 and H9c2 rat myoblast cell lines", *J.Biol.Chem.*, vol. 275, no. 16, pp. 11666-11671.

Sanderson, M. J., Charles, A. C., Boitano, S., & Dirksen, E. R. 1994, "Mechanisms and function of intercellular calcium signaling", *Mol.Cell Endocrinol.*, vol. 98, no. 2, pp. 173-187.

Schmilinsky-Fluri, G., Valiunas, V., Willi, M., & Weingart, R. 1997, "Modulation of cardiac gap junctions: the mode of action of arachidonic acid", *J.Mol.Cell Cardiol.*, vol. 29, no. 6, pp. 1703-1713.

Schulz, R. & Heusch, G. 2004, "Connexin 43 and ischemic preconditioning", *Cardiovasc.Res.*, vol. 62, no. 2, pp. 335-344.

Schwanke, U., Konietzka, I., Duschin, A., Li, X., Schulz, R., & Heusch, G. 2002, "No ischemic preconditioning in heterozygous connexin43-deficient mice", *Am.J.Physiol Heart Circ.Physiol*, vol. 283, no. 4, p. H1740-H1742.

Segal, S. S. & Duling, B. R. 1989, "Conduction of vasomotor responses in arterioles: a role for cell-to-cell coupling?", *Am.J.Physiol*, vol. 256, no. 3 Pt 2, p. H838-H845.

Semenza, G. L. 2001, "HIF-1 and mechanisms of hypoxia sensing", *Curr.Opin.Cell Biol.*, vol. 13, no. 2, pp. 167-171.

Sepp, R., Severs, N. J., & Gourdie, R. G. 1996, "Altered patterns of cardiac intercellular junction distribution in hypertrophic cardiomyopathy", *Heart*, vol. 76, no. 5, pp. 412-417.

Severs, N. J., Coppen, S. R., Dupont, E., Yeh, H. I., Ko, Y. S., & Matsushita, T. 2004, "Gap junction alterations in human cardiac disease", *Cardiovasc.Res.*, vol. 62, no. 2, pp. 368-377.

Severs, N. J. 2001, "Gap junction remodeling and cardiac arrhythmogenesis: cause or coincidence?", *J.Cell Mol.Med.*, vol. 5, no. 4, pp. 355-366.

Severs, N. J., Rothery, S., Dupont, E., Coppen, S. R., Yeh, H. I., Ko, Y. S., Matsushita, T., Kaba, R., & Halliday, D. 2001, "Immunocytochemical analysis of connexin expression in the healthy and diseased cardiovascular system", *Microsc.Res.Tech.*, vol. 52, no. 3, pp. 301-322.

Severs, N. J. 2000, "The cardiac muscle cell", *Bioessays*, vol. 22, no. 2, pp. 188-199.

Shah, M. M., Martinez, A. M., & Fletcher, W. H. 2002, "The connexin43 gap junction protein is phosphorylated by protein kinase A and protein kinase C: in vivo and in vitro studies", *Mol.Cell Biochem.*, vol. 238, no. 1-2, pp. 57-68.

Shaw, R. M. & Rudy, Y. 1997, "Ionic mechanisms of propagation in cardiac tissue. Roles of the sodium and L-type calcium currents during reduced excitability and decreased gap junction coupling", *Circ.Res.*, vol. 81, no. 5, pp. 727-741.

Simes, R. J., Topol, E. J., Holmes, D. R., Jr., White, H. D., Rutsch, W. R., Vahanian, A., Simoons, M. L., Morris, D., Betriu, A., Califf, R. M., & . 1995, "Link between the angiographic substudy and mortality outcomes in a large randomized trial of myocardial reperfusion. Importance of early and complete infarct artery reperfusion. GUSTO-I Investigators", *Circulation*, vol. 91, no. 7, pp. 1923-1928.

Skerrett, I. M., Aronowitz, J., Shin, J. H., Cymes, G., Kasperek, E., Cao, F. L., & Nicholson, B. J. 2002, "Identification of amino acid residues lining the pore of a gap junction channel", *J.Cell Biol.*, vol. 159, no. 2, pp. 349-360.

Smith, J. H., Green, C. R., Peters, N. S., Rothery, S., & Severs, N. J. 1991, "Altered patterns of gap junction distribution in ischemic heart disease. An immunohistochemical study of human myocardium using laser scanning confocal microscopy", *Am.J.Pathol.*, vol. 139, no. 4, pp. 801-821.

Smolenski, R. T., Lachno, D. R., Ledingham, S. J., & Yacoub, M. H. 1990, "Determination of sixteen nucleotides, nucleosides and bases using high-performance liquid chromatography and its application to the study of purine metabolism in hearts for transplantation", *J.Chromatogr.*, vol. 527, no. 2, pp. 414-420.

Solan, J. L. & Lampe, P. D. 2005, "Connexin phosphorylation as a regulatory event linked to gap junction channel assembly", *Biochim.Biophys.Acta*, vol. 1711, no. 2, pp. 154-163.

Somekawa, S., Fukuhara, S., Nakaoka, Y., Fujita, H., Saito, Y., & Mochizuki, N. 2005, "Enhanced functional gap junction neoformation by protein kinase A-dependent and Epac-dependent signals downstream of cAMP in cardiac myocytes", *Circ.Res.*, vol. 97, no. 7, pp. 655-662.

Sosinsky, G. E. & Nicholson, B. J. 2005, "Structural organization of gap junction channels", *Biochim.Biophys.Acta*, vol. 1711, no. 2, pp. 99-125.

Spray, D. C., Ye, Z. C., & Ransom, B. R. 2006, "Functional connexin "hemichannels": A critical appraisal", *Glia*, vol. 54, no. 7, pp. 758-773.

Spray, D. C. & Burt, J. M. 1990, "Structure-activity relations of the cardiac gap junction channel", *Am.J.Physiol*, vol. 258, no. 2 Pt 1, p. C195-C205.

Srinivas, M., Calderon, D. P., Kronengold, J., & Verselis, V. K. 2006, "Regulation of connexin hemichannels by monovalent cations", *J.Gen.Physiol*, vol. 127, no. 1, pp. 67-75.

Srinivas, M., Kronengold, J., Bukauskas, F. F., Bargiello, T. A., & Verselis, V. K. 2005, "Correlative studies of gating in Cx46 and Cx50 hemichannels and gap junction channels", *Biophys.J.*, vol. 88, no. 3, pp. 1725-1739.

Starich, T., Sheehan, M., Jadrich, J., & Shaw, J. 2001, "Innexins in C. elegans", *Cell Commun.Adhes.*, vol. 8, no. 4-6, pp. 311-314.

Stebbings, L. A., Todman, M. G., Phillips, R., Greer, C. E., Tam, J., Phelan, P., Jacobs, K., Bacon, J. P., & Davies, J. A. 2002, "Gap junctions in Drosophila: developmental expression of the entire innexin gene family", *Mech.Dev.*, vol. 113, no. 2, pp. 197-205.

Steel, K. P. & Kros, C. J. 2001, "A genetic approach to understanding auditory function", *Nat.Genet.*, vol. 27, no. 2, pp. 143-149.

Stewart, W. W. 1981, "Lucifer dyes--highly fluorescent dyes for biological tracing", *Nature*, vol. 292, no. 5818, pp. 17-21.

Stout, C., Goodenough, D. A., & Paul, D. L. 2004, "Connexins: functions without junctions", *Curr.Opin.Cell Biol.*, vol. 16, no. 5, pp. 507-512.

Stout, C. E., Costantin, J. L., Naus, C. C., & Charles, A. C. 2002, "Intercellular calcium signaling in astrocytes via ATP release through connexin hemichannels", *J.Biol.Chem.*, vol. 277, no. 12, pp. 10482-10488.

Suchyna, T. M., Xu, L. X., Gao, F., Fourtner, C. R., & Nicholson, B. J. 1993, "Identification of a proline residue as a transduction element involved in voltage gating of gap junctions", *Nature*, vol. 365, no. 6449, pp. 847-849.

Sutter, C. H., Laughner, E., & Semenza, G. L. 2000, "Hypoxia-inducible factor 1alpha protein expression is controlled by oxygen-regulated ubiquitination that is disrupted by deletions and missense mutations", *Proc.Natl.Acad.Sci.U.S.A*, vol. 97, no. 9, pp. 4748-4753.

Takens-Kwak, B. R., Jongsma, H. J., Rook, M. B., & van Ginneken, A. C. 1992, "Mechanism of heptanol-induced uncoupling of cardiac gap junctions: a perforated patch-clamp study", *Am.J.Physiol*, vol. 262, no. 6 Pt 1, p. C1531-C1538.

Tamaddon, H. S., Vaidya, D., Simon, A. M., Paul, D. L., Jalife, J., & Morley, G. E. 2000, "High-resolution optical mapping of the right bundle branch in connexin40 knockout mice reveals slow conduction in the specialized conduction system", *Circ.Res.*, vol. 87, no. 10, pp. 929-936.

Taylor, H. J., Chaytor, A. T., Edwards, D. H., & Griffith, T. M. 2001, "Gap junction-dependent increases in smooth muscle cAMP underpin the EDHF phenomenon in rabbit arteries", *Biochem.Biophys.Res.Commun.*, vol. 283, no. 3, pp. 583-589.

TenBroek, E. M., Lampe, P. D., Solan, J. L., Reynhout, J. K., & Johnson, R. G. 2001, "Ser364 of connexin43 and the upregulation of gap junction assembly by cAMP", *J.Cell Biol.*, vol. 155, no. 7, pp. 1307-1318.

Thimm, J., Mechler, A., Lin, H., Rhee, S., & Lal, R. 2005, "Calcium-dependent open/closed conformations and interfacial energy maps of reconstituted hemichannels", *J.Biol.Chem.*, vol. 280, no. 11, pp. 10646-10654.

Thompson, R. J., Zhou, N., & MacVicar, B. A. 2006, "Ischemia opens neuronal gap junction hemichannels", *Science*, vol. 312, no. 5775, pp. 924-927.

Tillman, T. S. & Cascio, M. 2003, "Effects of membrane lipids on ion channel structure and function", *Cell Biochem.Biophys.*, vol. 38, no. 2, pp. 161-190.

Torok, K., Stauffer, K., & Evans, W. H. 1997, "Connexin 32 of gap junctions contains two cytoplasmic calmodulin-binding domains", *Biochem.J.*, vol. 326 (Pt 2), pp. 479-483.

Traub, O., Look, J., Dermietzel, R., Brummer, F., Hulser, D., & Willecke, K. 1989, "Comparative characterization of the 21-kD and 26-kD gap junction proteins in murine liver and cultured hepatocytes", *J.Cell Biol.*, vol. 108, no. 3, pp. 1039-1051.

Turner, M. S., Haywood, G. A., Andreka, P., You, L., Martin, P. E., Evans, W. H., Webster, K. A., & Bishopric, N. H. 2004, "Reversible connexin 43 dephosphorylation during hypoxia and reoxygenation is linked to cellular ATP levels", *Circ.Res.*, vol. 95, no. 7, pp. 726-733.

Turner, M. S., Haywood, G. A., Evans, W. H., Discher, D. J., Webster, K. A., & Bishopric, N. H. Different regulation of connexin 43 in cardiac myocytes by hypoxia and ischemia. Circulation 104 [206 Abst]. 2001. Ref Type: Abstract

Unger, V. M., Kumar, N. M., Gilula, N. B., & Yeager, M. 1997a, "Projection structure of a gap junction membrane channel at 7 A resolution", *Nat.Struct.Biol.*, vol. 4, no. 1, pp. 39-43.

Unwin, P. N. & Ennis, P. D. 1984, "Two configurations of a channel-forming membrane protein", *Nature*, vol. 307, no. 5952, pp. 609-613.

Uzzaman, M., Honjo, H., Takagishi, Y., Emdad, L., Magee, A. I., Severs, N. J., & Kodama, I. 2000, "Remodeling of gap junctional coupling in hypertrophied right ventricles of rats with monocrotaline-induced pulmonary hypertension", *Circ.Res.*, vol. 86, no. 8, pp. 871-878.

Vaidya, D., Tamaddon, H. S., Lo, C. W., Taffet, S. M., Delmar, M., Morley, G. E., & Jalife, J. 2001, "Null mutation of connexin43 causes slow propagation of ventricular activation in the late stages of mouse embryonic development", *Circ.Res.*, vol. 88, no. 11, pp. 1196-1202.

Valiunas, V., Mui, R., McLachlan, E., Valdimarsson, G., Brink, P. R., & White, T. W. 2004, "Biophysical characterization of zebrafish connexin35 hemichannels", *Am.J.Physiol Cell Physiol*, vol. 287, no. 6, p. C1596-C1604.

Valiunas, V., Beyer, E. C., & Brink, P. R. 2002, "Cardiac gap junction channels show quantitative differences in selectivity", *Circ.Res.*, vol. 91, no. 2, pp. 104-111.

Valiunas, V. & Weingart, R. 2000, "Electrical properties of gap junction hemichannels identified in transfected HeLa cells", *Pflugers Arch.*, vol. 440, no. 3, pp. 366-379.

van der Velden, H. M., Ausma, J., Rook, M. B., Hellemons, A. J., van Veen, T. A., Allessie, M. A., & Jongsma, H. J. 2000, "Gap junctional remodeling in relation to stabilization of atrial fibrillation in the goat", *Cardiovasc.Res.*, vol. 46, no. 3, pp. 476-486.

van der Velden, H. M., van Kempen, M. J., Wijffels, M. C., van, Z. M., Groenewegen, W. A., Allessie, M. A., & Jongsma, H. J. 1998, "Altered pattern of connexin40 distribution in persistent atrial fibrillation in the goat", *J.Cardiovasc.Electrophysiol.*, vol. 9, no. 6, pp. 596-607.

van Kempen, M. J. & Jongsma, H. J. 1999, "Distribution of connexin37, connexin40 and connexin43 in the aorta and coronary artery of several mammals", *Histochem.Cell Biol.*, vol. 112, no. 6, pp. 479-486.

van Rijen, H. V., van Veen, T. A., van Kempen, M. J., Wilms-Schopman, F. J., Potse, M., Krueger, O., Willecke, K., Opthof, T., Jongsma, H. J., & de Bakker, J. M. 2001, "Impaired conduction in the bundle branches of mouse hearts lacking the gap junction protein connexin40", *Circulation*, vol. 103, no. 11, pp. 1591-1598.

van Rijen, H. V., van Veen, T. A., Hermans, M. M., & Jongsma, H. J. 2000, "Human connexin40 gap junction channels are modulated by cAMP", *Cardiovasc.Res.*, vol. 45, no. 4, pp. 941-951.

van Veen, T. A., van Rijen, H. V., & Jongsma, H. J. 2006, "Physiology of cardiovascular gap junctions", *Adv.Cardiol.*, vol. 42, pp. 18-40.

van Veen, T. A., van Rijen, H. V., & Jongsma, H. J. 2000, "Electrical conductance of mouse connexin45 gap junction channels is modulated by phosphorylation", *Cardiovasc.Res.*, vol. 46, no. 3, pp. 496-510.

Vasconcellos, J. P., Melo, M. B., Schimiti, R. B., Bressanim, N. C., Costa, F. F., & Costa, V. P. 2005, "A novel mutation in the GJA1 gene in a family with oculodentodigital dysplasia", *Arch.Ophthalmol.*, vol. 123, no. 10, pp. 1422-1426.

Verselis, V. K., Trexler, E. B., & Bukauskas, F. F. 2000, "Connexin hemichannels and cell-cell channels: comparison of properties", *Braz.J.Med.Biol.Res.*, vol. 33, no. 4, pp. 379-389.

Verselis, V. K., Ginter, C. S., & Bargiello, T. A. 1994, "Opposite voltage gating polarities of two closely related connexins", *Nature*, vol. 368, no. 6469, pp. 348-351.

Vozzi, C., Dupont, E., Coppen, S. R., Yeh, H. I., & Severs, N. J. 1999, "Chamber-related differences in connexin expression in the human heart", *J.Mol.Cell Cardiol.*, vol. 31, no. 5, pp. 991-1003.

Wagner, L. M., Saleh, S. M., Boyle, D. J., & Takemoto, D. J. 2002, "Effect of protein kinase Cgamma on gap junction disassembly in lens epithelial cells and retinal cells in culture", *Mol.Vis.*, vol. 8, pp. 59-66.

Wang, X., Li, L., Peracchia, L. L., & Peracchia, C. 1996, "Chimeric evidence for a role of the connexin cytoplasmic loop in gap junction channel gating", *Pflugers Arch.*, vol. 431, no. 6, pp. 844-852.

Wang, Y. & Ashraf, M. 1999, "Role of protein kinase C in mitochondrial KATP channel-mediated protection against Ca2+ overload injury in rat myocardium", *Circ.Res.*, vol. 84, no. 10, pp. 1156-1165.

Warn-Cramer, B. J., Lampe, P. D., Kurata, W. E., Kanemitsu, M. Y., Loo, L. W., Eckhart, W., & Lau, A. F. 1996, "Characterization of the mitogen-activated protein kinase phosphorylation sites on the connexin-43 gap junction protein", *J.Biol.Chem.*, vol. 271, no. 7, pp. 3779-3786.

Warner, A., Clements, D. K., Parikh, S., Evans, W. H., & DeHaan, R. L. 1995, "Specific motifs in the external loops of connexin proteins can determine gap junction formation between chick heart myocytes", *J.Physiol*, vol. 488 (Pt 3), pp. 721-728.

Webster, K. A., Discher, D. J., Kaiser, S., Hernandez, O., Sato, B., & Bishopric, N. H. 1999, "Hypoxia-activated apoptosis of cardiac myocytes requires reoxygenation or a pH shift and is independent of p53", *J.Clin.Invest*, vol. 104, no. 3, pp. 239-252.

Weingart, R. & Maurer, P. 1987, "Cell-to-cell coupling studied in isolated ventricular cell pairs", *Experientia*, vol. 43, no. 10, pp. 1091-1094.

Weingart, R. 1977, "The actions of ouabain on intercellular coupling and conduction velocity in mammalian ventricular muscle", *J.Physiol*, vol. 264, no. 2, pp. 341-365.

Weng, S., Lauven, M., Schaefer, T., Polontchouk, L., Grover, R., & Dhein, S. 2002, "Pharmacological modification of gap junction coupling by an antiarrhythmic peptide via protein kinase C activation", *FASEB J.*, vol. 16, no. 9, pp. 1114-1116.

White, T. W. & Paul, D. L. 1999, "Genetic diseases and gene knockouts reveal diverse connexin functions", *Annu.Rev.Physiol*, vol. 61, pp. 283-310.

White, T. W., Deans, M. R., Kelsell, D. P., & Paul, D. L. 1998, "Connexin mutations in deafness", *Nature*, vol. 394, no. 6694, pp. 630-631.

Wijffels, M. C., Kirchhof, C. J., Dorland, R., & Allessie, M. A. 1995, "Atrial fibrillation begets atrial fibrillation. A study in awake chronically instrumented goats", *Circulation*, vol. 92, no. 7, pp. 1954-1968.

Willecke, K., Eiberger, J., Degen, J., Eckardt, D., Romualdi, A., Guldenagel, M., Deutsch, U., & Sohl, G. 2002, "Structural and functional diversity of connexin genes in the mouse and human genome", *Biol.Chem.*, vol. 383, no. 5, pp. 725-737.

Willecke, K., Temme, A., Teubner, B., & Ott, T. 1999, "Characterization of targeted connexin32-deficient mice: a model for the human Charcot-Marie-Tooth (X-type) inherited disease", *Ann.N.Y.Acad.Sci.*, vol. 883, pp. 302-309.

Williams, R. S. & Benjamin, I. J. 2000, "Protective responses in the ischemic myocardium", *J.Clin.Invest*, vol. 106, no. 7, pp. 813-818.

Xing, D., Kjolbye, A. L., Nielsen, M. S., Petersen, J. S., Harlow, K. W., Holstein-Rathlou, N. H., & Martins, J. B. 2003, "ZP123 increases gap junctional conductance and prevents reentrant ventricular tachycardia during myocardial ischemia in open chest dogs", *J.Cardiovasc.Electrophysiol.*, vol. 14, no. 5, pp. 510-520.

Yasui, K., Kada, K., Hojo, M., Lee, J. K., Kamiya, K., Toyama, J., Opthof, T., & Kodama, I. 2000, "Cell-to-cell interaction prevents cell death in cultured neonatal rat ventricular myocytes", *Cardiovasc.Res.*, vol. 48, no. 1, pp. 68-76.

Ye, Z. C., Wyeth, M. S., Baltan-Tekkok, S., & Ransom, B. R. 2003, "Functional hemichannels in astrocytes: a novel mechanism of glutamate release", *J.Neurosci.*, vol. 23, no. 9, pp. 3588-3596.

Yeh, H. I., Lai, Y. J., Lee, S. H., Lee, Y. N., Ko, Y. S., Chen, S. A., Severs, N. J., & Tsai, C. H. 2001, "Heterogeneity of myocardial sleeve morphology and gap junctions in canine superior vena cava", *Circulation*, vol. 104, no. 25, pp. 3152-3157.

Yellon, D. M. & Baxter, G. F. 1999, "Reperfusion injury revisited: is there a role for growth factor signaling in limiting lethal reperfusion injury?", *Trends Cardiovasc.Med.*, vol. 9, no. 8, pp. 245-249.

Yin, X., Gu, S., & Jiang, J. X. 2001, "The development-associated cleavage of lens connexin 45.6 by caspase-3-like protease is regulated by casein kinase II-mediated phosphorylation", *J.Biol.Chem.*, vol. 276, no. 37, pp. 34567-34572.

Zeevi-Levin, N., Barac, Y. D., Reisner, Y., Reiter, I., Yaniv, G., Meiry, G., Abassi, Z., Kostin, S., Schaper, J., Rosen, M. R., Resnick, N., & Binah, O. 2005, "Gap junctional remodeling by hypoxia in cultured neonatal rat ventricular myocytes", *Cardiovasc.Res.*, vol. 66, no. 1, pp. 64-73.

Zelante, L., Gasparini, P., Estivill, X., Melchionda, S., D'Agruma, L., Govea, N. et al, 1997, "Connexin26 mutations associated with the most common form of non-syndromic neurosensory autosomal recessive deafness (DFNB1) in Mediterraneans", *Hum.Mol.Genet.*, vol. 6, no. 9, pp. 1605-1609.

Zhou, X. W., Pfahnl, A., Werner, R., Hudder, A., Llanes, A., Luebke, A., & Dahl, G. 1997, "Identification of a pore lining segment in gap junction hemichannels", *Biophys.J.*, vol. 72, no. 5, pp. 1946-1953.

Zimmer, D. B., Green, C. R., Evans, W. H., & Gilula, N. B. 1987, "Topological analysis of the major protein in isolated intact rat liver gap junctions and gap junction-derived single membrane structures", *J.Biol.Chem.*, vol. 262, no. 16, pp. 7751-7763.

Zipes, D. P. 1997, "Atrial fibrillation. A tachycardia-induced atrial cardiomyopathy", *Circulation*, vol. 95, no. 3, pp. 562-564.